ON THE CONFLATION OF CONTAMINANT BEHAVIOUR PREDICTION WITHIN WHOLE BUILDING PERFORMANCE SIMULATION

Aizaz Aamir Samuel

A Thesis Submitted to fulfil
the requirements of the
Degree of Doctor of Philosophy
in
Mechanical Engineering

Energy Systems Research Unit
University of Strathclyde
Glasgow, UK
February 2006

COPYRIGHT DECLARATION

ACKNOWLEDGEMENTS

I would like to thank everyone in ESRU for their constant support and encouragement. Special thanks goes to Dr Paul Strachan for without him this work would not have been possible. In no special order I would like to thank Professor Joe Clarke, Dr Jon Hand and Dr Iain Macdonald for seeding my mind with challenging and interesting ideas, and providing with much appreciated insight time and again.

To my dearest wife Peace who kept me going
when I would have otherwise given up and
without whose support this endeavour
not have been possible.

ABSTRACT

In recent times there has been an increase in computing speed; also the number of computational engines for the prediction of physical phenomena and engineering systems has grown. In view of these advances there seems to be a growing impetus to use simulation based tools.

With interest in an urban style of life growing, people seem to be spending more time indoors. This in turn has put a greater load on building facilities and related service providers to give better quality and convenience. Unfortunately this has not been as successful an endeavour as planned and provision of a healthy and conducive environment continues to be a challenge. Focus of building service providers and designers seems to have broadened and now provision of adequate indoor quality is also deemed as a very important requirement in addition to provision of adequate thermal comfort.

Indoor contaminant behaviour prediction methods were developed using a coupled thermal and mass flow simulation technique. Focus was maintained on approaching realistic engineering solutions and relevant implementation of theoretical developments. The developed approach was then validated against analytical, inter-model and empirical results. It was shown that results were comparable to those obtained by other methods and comparable to similar tools validated in various other exercises. It was also shown that an integrated approach to the problem was necessary because situations exist in which assessment of just one facet does not give an accurate depiction of reality.

A large number of simulation software exist that all claim to perform the same calculations and solve similar problems. Whereas buildings comprise of a large number of interacting thermodynamic domains most tools only address just one or two of these domains. This is believed to give inaccurate results. This thesis attempts to describe why it is important to take a global look at how physical systems behave and how this can be realised using an integrated approach within a building performance simulation environment.

To gain an insight into the micro-climatic behaviour of contaminants within an enclosed space, the thermally coupled mass flow network and contaminants prediction facility was integrated into computational fluid dynamics. Thus the various domains could get inputs from each other at run time, thereby ensuring a better representation of reality. This approach was compared against standalone CFD software and results were promising.

TABLE OF CONTENTS

Chapter 2 Building Simulation

Chapter 3 Modelling and Implementation

Chapter 4 Validation

Chapter 5 Integrating Network Flow Modelling and CFD

Chapter 6 Case Studies

1 INDOOR AIR POLLUTION

1.0 Introduction

Air pollutants are those chemicals that are not generally present in the atmosphere because of natural causes but are disseminated into the air by human activity (Merriam Webster 2002). A small amount of pollutants do seep in from natural causes e.g. volcanic activity but these sources are not generally considered as critical. In most parts of Europe these pollutants are principally the products of combustion from space heating, power generation, chemical industry waste or from motor vehicle traffic (McGinlay 1997). Indoor air environments contain many inorganic and organic gases and vapours typically in trace (parts-per-billion) quantities. The chemical composition of air varies widely between particular locations as well as between measurements taken at different times for the same location. The nature of these variations is such that it is difficult to definitively characterize a typical indoor air environment with respect to the specific contaminants present and concentration levels (Kingsley and Davidson 2000). A large number of air pollutants have known or suspected harmful effects that can be manifested on plant or animal life and / or the environment. Pollutants may not only prove a problem in the immediate vicinity of their emission but they can travel long distances and react with other species present in the atmosphere to produce secondary pollutants (Weschler 2004).

The major air pollution problem started after the Industrial Revolution in the nineteenth and twentieth century as fossil fuels began to be adopted as the principal energy providers. What usually resulted were high levels of smoke and sulphur dioxide from the combustion of sulphur containing fossil fuels such as coal. The most perceptible after effect of this was smog. Smog, which is a health hazard in itself, can still be seen in many parts of the developing world (EPA 1999).

In economically developed countries, however, this problem has diminished over recent decades as a result of changing fuel-use patterns, the increasing use of cleaner fuels such as natural gas, and the implementation of effective smoke and emission control policies.

In both developed and developing countries, the major threat to outdoor clean air is now posed by traffic emissions (McGinlay 1997). Petrol and diesel engine motor vehicles emit a wide variety of pollutants, principally carbon monoxide (CO), oxides of nitrogen (NO_x), volatile organic compounds (VOC), other organic compounds and particulate matter. These have an increasing impact on urban air quality.

External air quality in turn affects indoor air quality (IAQ) due to transport of air, and hence contaminants, into the built space. The built space has its own physiological contaminant issues. Many of the chemicals not present in ambient air may be produced by indoor activities. For example, natural gas cooking and heating may be the cause of indoor methane and carbon monoxide. Smoking may be the cause of Environmental Tobacco Smoke (ETS) which contains a vast number of toxic and carcinogenic agents. In addition, photochemical reactions resulting from the action of sunlight on NO_2 and VOC in the presence of ground level ozone from vehicles lead to the formation of secondary long-range pollutants, which may impact in rural areas often far from the original emission site (McGinlay 1997). Unhealthy internal humidity levels may cause the growth of fungal spores, moulds and mites. These in turn can be the initiators of asthmatic attacks, allergenic conditions or other respiratory problems in occupants.

Although IAQ standards are set in precise physical terms of concentrations of contaminants, in practice it is the level of odour by which the air quality in a space is judged. When people have control over ventilation at home, or in a room with openable windows, the decision to ventilate is usually taken because of excessive odour or moisture, or because of high temperature in the summer. In an air conditioned building, the presence of objectionable odours would certainly lead to complaints about inadequate ventilation (McIntyre 1980). There are also subjective measures for measuring perceived air quality (Fanger 1988). The olf is the emission rate of air pollutants (bio-effluents) from a standard person. Any other pollution source is quantified by the number of standard persons (olfs) required to cause the same dis-satisfaction as the actual pollution source. The decipol is the pollution caused by one standard person (one olf) ventilated by 10l/s of unpolluted air. These units can be used to identify pollution sources, calculating ventilation requirements and for the prediction and measurement of air quality. Perceived air quality is also the subject of some European guides and standards e.g. (CIBSE 1993) and (DIN 1994).

A simple and effective solution to the problem of deficient IAQ seems to be in adequate ventilation. The Victorian public reformers saw their mission as the spread of cleanliness and hygiene which included, among other things, light and air. Much of this approach was carried on into the twentieth century. In more recent times and with the advent of the 'efficient energy use' concepts, the focus seems to have shifted to airtight buildings and low levels of ventilation. This is due to the fact that as buildings become better insulated, the conduction of heat through the fabric has been reduced and so the proportion of heating and air conditioning load due to ventilation has increased and in most new building designs reducing the rate of ventilation offers the largest scope for reducing the energy demand. This in turn has a detrimental effect on IAQ because of the lack of provision for removal of indoor contaminants. On the other hand, environmental standards and expectations have risen, together with the technical ability to detect low levels of contaminants and the statistical ability to evaluate their effects through epidemiological studies (McIntyre 1980, Howieson 2005).

The purposes of ventilating a building with fresh air are:

- provision of air for respiration
- dilution of odour
- removal of excess moisture
- dilution of contaminants

- provision of air for combustion
- temperature control

If a building is either heated or cooled there will always be an energy cost to be paid for ventilation. In recent years the focus of research seems to have shifted from the energy cost consideration to the health and well being of occupants populating buildings (Molhave 2002). It will increasingly become more important that in addition to competitive energy cost, building designers of the future will also have to consider occupant health related issues. There is a WHO charter out already (see section 1.4.4) defining the right of occupants to clean air and it seems that legislation of this sort will form part of building regulations in times to come. Ventilation rates usually allow a large amount of contaminant to accumulate indoor. There have been some empirical studies (e.g. Carrer and Maroni 2002, Corsi et al 2002, Sowa 2002) and a recent simulation study (Samuel and Strachan 2005) along these lines regarding accumulation of CO_2. It was reported that empirical values as high as 4000ppm and simulated results as high as 4500ppm were obtained for a school and a public house respectively. The results may seem alarming because the ASHRAE recommended maximum level is 700ppm (ASHRAE 1992). More importantly there needs to be addressed the underlying issue of perceived air quality. Occupants will not open a window if the level of a contaminant rises above a prescribed value given in a building standard but will definitely do so if they feel hot or stuffy. Ventilation systems usually follow recommendations by guides such as those developed by ASHRAE or CIBSE. Such ventilation rates are mostly prescriptive and in most cases design conditions may be exceeded some proportion of the time. Additionally in the light of new information such ventilation rates may not be suitable for adequate indoor air quality (Samuel and Strachan 2005). Using the knowledge that such ventilation rates are not capable of sufficiently diluting indoor air it seems that the safest option is to increase the rate of ventilation.

There are a lot of issues surrounding IAQ within the building life cycle phases: building design, construction, commissioning, operation and final decommissioning and dismantling. The most important issues for building users relate to building operation because that has the longest time factor involved. However many of the decisions taken during the earlier phases of a building life have direct consequences on building operation and these may not be evident to those responsible for making those choices. The scope of this thesis includes this particular period (i.e. period of occupancy) of usage in a building's life.

1.1 Elements of Indoor Contaminant Behaviour

Assessment of contaminant behaviour, exposure and impact in residential settings requires information on the availability of the chemical(s) of concern at the point of exposure, characteristics of the building structure and micro climate and human presence within the residence. Good indoor environmental quality is one of our most fundamental needs. Poor air quality affects our health, well-being and quality of life in general. European urban and non-urban areas, in particular large cities, struggle with the problems of high levels of air pollutants. At present over 60% of the European population is living in cities (Hanssen 2004). For the next few decades it is foreseen that this percentage will increase further. The substantial growth of the urban population is associated with a further increase of the macro and micro economic activities in the cities, including progressively growing energy use and more air pollution. Regrettably, today too many occupants express annoyance or become ill in modern buildings. Terms such as sick building syndrome (SBS), tight building syndrome (TBS), building related illness (BRI), and multiple chemical sensitivity (MCS), are introduced in order to define the problems and group the different characteristics. Symptoms commonly attributed to indoor environmental quality problems include headache, fatigue, shortness of breath, sinus congestion, cough, sneezing, eye, nose, and throat irritation, skin irritation, dizziness and nausea. Several of these symptoms may occur at the same time (Hanssen 2004). Residence characteristics affect exposure in an indoor environment. Source-receptor relationships in residential exposure scenarios can be complex due to interactions among sources, and transport / transformation processes that result from chemical-specific and building-specific factors. Figure 1.1 illustrates some of the complex factors that must be considered when conducting exposure assessments in a residential setting. In addition to sources within the building, chemicals of concern may enter the indoor environment from outdoor air, soil, gas, water supply, tracked-in soil, and industrial work clothes worn by the residents. Indoor concentrations are affected by loss mechanisms, also illustrated in figure 1.1, involving chemical reactions, deposition to and re-emission from surfaces, and transport out of the building. Particle-bound chemicals can enter indoor air through resuspension. Indoor air concentrations of gas-phase organic chemicals are affected by the presence of reversible sinks formed by a wide range of indoor materials. In addition, the activity of human receptors greatly affects their exposure as they move from room to room, entering and leaving the exposure scene (Rodes et al 1991).

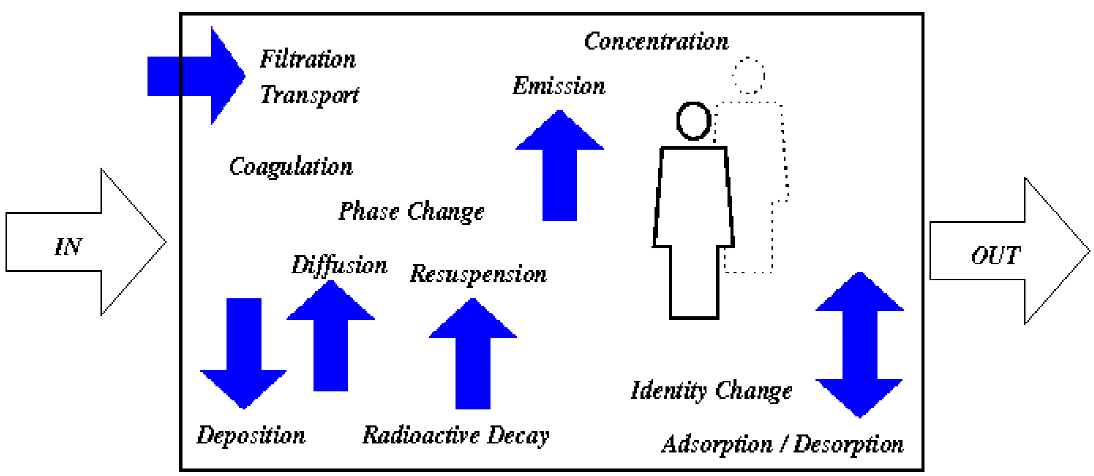

Figure 1.1 Elements of Indoor Contaminant Behaviour / Residential Exposure

The behaviour of contaminants indoors is difficult to appreciate because these may not behave similarly outdoors and indoors. Furthermore certain processes that gain relevance indoors may not be applicable outdoors e.g. the reversible sink effect which is a typical feature of carpets. Some of the more important processes that contaminants and pollutants undergo in the built space are discussed in the following sub-sections. It has been made possible to study the effect of these processes within the present research although particles are treated approximately i.e. as gases.

1.1.1 Transport

Transport may be from the outside or from connected internal spaces. Transport is heavily related to ventilation which may be intentional or inadvertent. It is not unreasonable to assume that for an example building the source of pollution is such that the air that enters into a building is fully mixed with the outdoor pollutants. It is possible that the ventilation air to the ground and topmost floor of a multi-storey building is different in composition but it should still be safe to assume that the ventilation air reaching the two spaces is homogeneous because of the turbulent nature of ambient air. Once inside, Particulate Matter (PM) tends to behave differently from gas phase pollutants. Some of the processes listed below are more suited to PM than to gases e.g. filtration. Gaseous pollutants are generally regarded to show ideal gas characteristics, the same assumption compensates prediction of PM behaviour. Furthermore gaseous pollutants are divided into non-trace and trace depending upon whether partial pressure due to them is taken or not taken into consideration. It would be somewhat difficult to justify such an approach to be suitable for PM.

1.1.2 Filtration

Transport of air indoors may be accomplished by passive or active systems (e.g. mechanical ventilation systems) or may be unintentional infiltration. For the cases where air flows in via known or intended pathways, it may be possible to filter the incoming air. Filtration is normally most effective for PM and vapours but not so effective for gases (Shaughnessy et al 1994). This is true for High Efficiency Particulate Filters (HEPA) and Sorbant Filtration Systems as well. Clausen (2004) states that within mechanically ventilated buildings the incidence of poor air quality is increased. This is due to biological contamination (bacterial and fungal agents) and chemical reactions. A small amount of ozone may be trapped within a filter. This is accompanied by the production of chemicals, some of which will desorb from the filter (Hyttinen et al 2003). There have been studies showing the importance of intake air being clean and dry (Hanssen 2004, Clausen 2004).

1.1.3 Adsorption / Desorption

Adsorption is the process in which a particle or gas can attach itself to a solid surface and desorption is the reverse process in which a particle or gas is emitted from a surface. Both these processes are active with regard to indoor air contaminants and can affect the dispersal of contaminants within buildings (Axley 1991). The lingering odours of winter clothes stored during summer with naphthalene crystals, and the odour of clothes exposed to tobacco smoke or petrol fumes that persist for days are two examples. According to Slejko (1985) adsorption may include electrostatic effects with exchange of ionic particles between adsorbate and adsorbant. The adsorption may be physical adsorption which deals with the conditions when the adsorbant is attracted due to adhesion. Otherwise there may be chemical reactions involved during the processes or binding of molecular groups without chemical transformation.

1.1.4 Diffusion

Many pollutants found in the indoor environment have a tendency to diffuse into or out of certain building materials. Diffusion is closely related to adsorption / desorption (collectively termed sorption) in that the latter two are strongly dependent on diffusion. Diffusion is one of the important parameters for models governing measurement and prediction of building material emission rates (Haghighat et al 2002). Transportation of VOC in general porous building materials is controlled by diffusion equations containing sorption effects not only on the surface of the building material but also within the building material (Murakami et al 2003). PM and VOC adsorption by indoor materials will reduce peak concentrations, and subsequent desorption will prolong the presence of a compound indoors. Diffusion within materials plays an important role in this context (Meininghaus and Uhde 2002). The indoor environment is characterized by a high surface (walls, furniture) to room volume ratio, and this consequentially increases the effect of diffusion.

1.1.5 Identity Change

Identity change is the name given to the process whereby pollutants can react amongst themselves or with air or with indoor building materials. The reactions are chemical in nature and the products of these reactions can be more harmful than the initial reactants. Chemical reactions result in a decrease in the concentration of the reactants and an increase in the concentration of the products. Reactions among indoor pollutants, apart from combustion processes, are the major source of short lived, highly reactive compounds indoors. The focus of recent research has been the reactions of ozone with organic compounds (mostly terpenes) (Wolkoff et al 2000) and nitrogen oxides (Pommer et al 2004), and the part interior surfaces play in catalysing these reactions (Weschler 2004).

1.1.6 Emission

A vast amount of work has been done regarding emission of a variety of compounds from building materials. Most of the compounds studied are VOC e.g. formaldehyde and 1,3-butadiene. VOC are of particular interest because these form the bulk of gases emitted indoors. It has been shown that wet coatings and surfaces predominantly emit vapours whereas dry coatings and surfaces emit gases (Tichenor et al 1993). Usually, simple exponential decay models are used to quantify this process but more detailed mathematical models exist (Tichenor et al 1993, Huang et al 2001). Again diffusion plays a major role and the diffusion coefficient is an important physical parameter in the models. Just as there are a large number of emissions there are a large number of emitters. Paints, PVC, wood furnishings, carpets and other floor coverings, adhesives, chip board and different upholsteries etc. have all been described as sources of indoor pollutants. Many of theses materials have the ability to act as reversible sources and sinks (Zhao et al 2002). The characteristic behaviour of these is that they behave as sources when ambient concentrations of emittant are low and behave as sinks when ambient concentrations are high.

1.1.7 Resuspension

Particles previously deposited onto indoor surfaces may become airborne again due to resuspension. Ordinary indoor activities such as walking may be the cause of this as well as the generation of new particles through abrasive wear of surfaces (Nazaroff 2004). It has been shown that coarse particles, 2.5-10 microns in size, are mainly a result of resuspension of particles resulting from personal activities (Janssen et al 2000). This is called the Personal Cloud Effect. This is dependent on a number of factors including: proximity of source, magnitude and direction of convective air movements from the source and around the body, the character of the air turbulence parcel and the presence of obstructions in the flow field (Rodes et al 1991). The Personal Cloud Effect helps explains why actual personal exposure is usually greater than indirect estimates combining indoor and outdoor concentrations and time-activity information. The increase in particle concentration as a result of a person occupying the micro-environment is usually overlooked (CEPA/FPAC 1998) in most studies.

1.1.8 Deposition

There are many mechanisms that contribute to deposition of particles and chemicals onto indoor surfaces. Particles may be swept into the boundary layer by turbulent air currents and the boundary layer characteristics then control the actual deposition. For fine particles Brownian diffusion and for coarse particles gravitational settling and inertial impaction are important mechanisms (Nazaroff 2004). For certain materials the main reason for deposition may be their chemical nature and chemisorption (superficial attachment of a chemical onto a surface because of chemical bonding between the two). This process is irreversible and is, presumably, responsible for the transport of a large variety of chemically active indoor air pollutants known to be scavenged (deposited) onto indoor surfaces. Scavenged chemicals include ozone, nitrogen monoxide, nitric acid etc. The process of deposition is approximated by the assumption that removal rates are related directly to the bulk air concentration, but mechanistic details are unclear at the moment (Axley 1993).

1.1.9 Radioactive decay

The principal problem of high indoor radiation levels is because of radon. This is a radioactive gas and comes from the radioactive decay process of naturally occurring uranium (which is found in almost all soils). The gas may rise up through the ground and enter houses through cracks and other holes in the foundation. Buildings may trap the gas inside and concentration builds up (EPA 2004a) over time. Radon decays into radioactive particles that may become trapped in the lungs. These particles breakdown further and occupants are liable to develop lung cancer.

1.1.10 Coagulation

When particles collide they may adhere to each other: possible mechanisms are adhesion, cohesion and electrostatic attraction. This process is known as coagulation. An important point to note is that particle mass concentration is not affected. Coagulation is a second order phenomenon while most other processes are first order[1]. An important consequence of this is that coagulation becomes increasingly important when concentration of particles is high, but not so important when concentration is low. The main cause for coagulation is Brownian motion (Nazaroff 2004).

1.1.11 Phase Change

It is possible for indoor chemicals to undergo a phase change from gas to vapour or gas to solid (sublimation[2]), or vice versa. Important consequences of this process can be the uptake or release of water from particles under varying humidity conditions and phase partitioning of semi volatile organic compounds between gas phase and sorbed to indoor particles. It is even possible for certain chemicals to dissociate into constituent reactants under indoor conditions (ammonia, hydrochloric acid and ammonia, nitric acid respectively (Lunden et al 2003)).

1.2 Important Air Pollutants

The European Union defines four main chemicals that have a contributing effect in the so-called greenhouse effect.

- Methane (CH_4) from energy production and use, certain forms of agriculture, landfills
- Carbon Dioxide (CO_2) from energy use, transport, industrial processes, deforestation
- Nitrous Oxide (N_2O) from fertilised soils, biomass burning, combustion of fossil fuels
- Chlorofluorocarbons (CFC) from industrial activities, refrigeration, aerosols (EU 1999).

Under the Clean Air Act, The Environmental Protection Agency EPA of the USA has defined six air pollutants for which health based standards have been set. These are:

- Carbon Monoxide (CO)
- Nitrogen Oxides (NO_x)
- Sulphur Dioxide (SO_2)
- Particulate Matter (PM^{10} and $PM^{2.5}$)
- Ozone O_3

1A first order phenomenon is one which is a linear function of contaminant concentration, whereas a second order phenomenon is a quadratic function.
2 Sublimation is the process in which a solid evaporates to the gas phase without a liquid phase. This happens when the boiling point of the substance is lower than the melting point i.e. when the pressure is not high enough to force the vapour to liquefy.

- Lead. (EPA 2004b)

Europeans spend 90% of their time indoors (EU 2003), but closed environments are not always the healthiest. Studies on human exposure to indoor pollution reveal that indoor environments pose their own threats to health and, in some cases, can be at least twice as polluting as outdoor environments. Hundreds of volatile components have been detected and some of them are toxic, mutagenic or carcinogenic. The number of potential sources is enormous. For instance, up to 20% of Europeans suffer from asthma due to substances inhaled indoors. Tobacco smoke, asbestos, radon and benzene released inside buildings are prime suspects in the increase in cancer cases in European population (EU 2003).

Some of the principal air pollutants and sources of concern that principally originate indoors are listed below.

- Environmental tobacco smoke (ETS)
- Other combustion products
- Animal dander, moulds, dust mites, other biological agents
- Volatile organic compounds (VOC)
- Heavy metals: Airborne Lead and Mercury vapours (EU 2001).

The number of actual chemicals given off from the above sources is large, and research into emissions, adsorption, chemisorption, chemical kinetics and filtration etc. is continuing. (A lot of material is available e.g. Rehwagen et al 2003, Tichenor et al 1993, Lansari et al 1996, Weschler 2000 and Axley 1993) Section 112 of the Clean Air Act (CAA) of the US Congress currently identifies some 188 pollutants as hazardous air pollutants (HAP). These are those pollutants that are known or suspected to cause serious health problems. Many of the contaminants have been identified relatively recently and information about these (source and sink models, filtration, chemical reactions etc.) is scarce. Hence it was not possible to develop source and sink models etc. On the other hand the present work focuses on providing a framework in which to incorporate new developments and not on making individual mathematical models available for use, although the latter has also been extensively applied. The list includes relatively common pollutants, such as formaldehyde, chlorine, methanol and asbestos as well as numerous less common substances (Congress 1990).

1.3 List of common Contaminants

It is considered helpful in order to understand the nature of the problem if a list of common pollutants was built. As described above the number of air pollutants is large. Furthermore many of the authoritative texts give families of chemicals e.g. CFCs as mentioned in (EU 1999). In order to work towards a list of pollutants it was considered important to focus on a limited number of chemicals. Twelve chemicals and PM were selected. These pollutants of interest were selected as follows:

- All the EU greenhouse gases (EU 1999)
- All the EPA criteria air pollutants (EPA 2004b)

An important part of the work was to divide the plethora of pollutants into workable groups. The approach used was analogous to Sofuoglu and Moschandreas (2003) who divided air pollutants in order to develop an indoor air pollutant index. Air pollutants can be divided up as:

(a) Inorganic gases

(b) Organic gases

(c) Particulate matter

(d) Biological matter

Selected contaminants contain seven inorganic gases, four organic gases, one solid and particulate matter. Biological PM exhibit markedly different characteristics than inanimate PM and are not included in the list.

For the case where a chemical family was listed, one or two chemicals from that family were considered. This selection was done on the basis of the amount of that chemical present or emitted indoors and its health hazard as detailed below. The list is not exhaustive, but is considered to be representative of common and important pollutants. Due to the extremely variegated pattern of occupancy and use of a built space it is quite difficult to define general chemicals of interest. Common pollutants is a relative term in that pollutants may vary from region to region and from one building type to another e.g. radon may be present in some buildings but not others because of its asymmetrical distribution and the choice of building materials and techniques.

Effort was made to include representative pollutants from the main three types i.e. gases, vapours and particulate matter. A brief synopsis of the different pollutants is given below. The following sections are not considered to be exhaustive and the interested reader is referred to relevant references. The pollutants considered included.

1.3.1 Carbon dioxide CO_2:

Though this gas is not a pollutant it was still considered because of its greenhouse effect. This gas is given off as a combustion and respiration by-product and is absorbed from the atmosphere by photosynthesis in green plants.

1.3.2 Nitrous oxide N_2O:

A principal use of nitrous oxide is in medical facilities as an anaesthetic. Hence the concentration of this gas may exceed safe levels in certain types of buildings (Healthy Buildings 2000).

1.3.3 Carbon monoxide CO:

Carbon monoxide is a poisonous by-product of combustion in the absence of abundant oxygen. This gas has the ability to restrict the uptake of oxygen into the bloodstream due to its preferential binding with haemoglobin and can hence prove to be lethal in minute quantities.

1.3.4 Nitrogen dioxide NO_2:

Nitrogen monoxide NO is a product of high temperature combustion of fuels as in internal combustion engines. This is readily oxidised to NO_2 in the atmosphere, NO and NO_2 (NO_x) concentrations are therefore greatest in urban areas where traffic is heaviest. Elevated levels of NO_x occur in urban environments under stable meteorological conditions, when the pollutant is unable to disperse. NO_2 is a respiratory irritant, it may exacerbate asthma and possibly increase susceptibility to infections. It is a contributor to acid rain (McGinlay 1997).

1.3.5 Sulphur dioxide SO_2:

Sulphur dioxide is a corrosive acid gas, which combines with water vapour in the atmosphere to produce acid rain. SO_2 in ambient air is also associated with asthma and chronic bronchitis. The principal source of this gas is power stations burning fossil fuels (mainly coal), which contain sulphur (McGinlay 1997).

1.3.6 Ozone O_3:

Indoor sources of ozone include appliances that generate electric discharges such as photocopiers, laser printers, ion-generating air cleaners and brush type electric motors (e.g. in a sewing machine) (Illinois Department of Public Health 2004) Ozone can irritate the eyes and air passages causing breathing difficulties and may increase susceptibility to infection. It is a highly reactive chemical, capable of attacking surfaces, fabrics and rubber materials (McGinlay 1997). Ozone reacts with other indoor pollutants and produces secondary and usually more harmful pollutants.

1.3.7 Radon Rn:

Radon is a radioactive gas. It comes from the natural decay of uranium that may be found in soil. It typically moves up through the soil and can get into buildings through cracks and other holes in the foundations. Any building can serve as a radon trap. It is a colourless and odourless gas and causes cancer (Darby et al 2001).

There are two main groups of hydrocarbons of concern: volatile organic compounds VOC and polycyclic aromatic hydrocarbons PAH. VOC and PAH are released in vehicle exhaust gases either as unburned fuels or as combustion products, and are also emitted by the evaporation of solvents and motor fuels. Indoors, VOC are present in ETS (Baek et al 2004) and may be emitted from certain building materials, products and furnishings (Park et al 2003). Benzene and 1,3-butadiene are of particular concern, as they are known carcinogens. Other VOC are important because of the role they play in the photochemical formation of ozone in the air. Toxic Organic Micro Pollutants (TOMP) are produced by the incomplete combustion of fuels. They comprise a complex range of chemicals, some of which, although they are emitted in very small quantities, are highly toxic or carcinogenic. Compounds in this category include:

- PAH (Poly Aromatic Hydrocarbons)

- PCB (Poly Chlorinated Bi phenyl)
- Dioxins
- Furans (McGinlay 1997)

1.3.8 Methane CH_4:

Methane is a colourless, odourless gas and is the primary constituent of natural gas. It can be produced as a by-product of biological degradation. It may be present indoors from leaking gas piping, faulty water heaters or other gas burning appliances. Another source could be from the P-traps in a plumbing system. If a P-trap becomes dry then methane and other sewer gases may find their way into a house.

1.3.9 Benzene C_6H_6:

Benzene is an aromatic VOC which is a minor constituent of fuel for internal combustion engines (about 2% by volume). The main sources of benzene in the atmosphere in Europe are the distribution and combustion of petrol. Household sources include ETS and paints. Benzene is a known human carcinogen (McGinlay 1997, EU 2003).

1.3.10 1,3-butadiene C_4H_6:

Like benzene this is a VOC emitted into the atmosphere principally from fuel combustion of petrol and diesel vehicles. Indoors, ETS is the primary source. 1,3-butadiene is also an important chemical in certain industrial processes, particularly the manufacture of synthetic rubber. It is also a known, potent human carcinogen (McGinlay 1997, EPA 2005).

1.3.11 Formaldehyde HCHO:

Formaldehyde is a colourless, strong smelling gas and may be present indoors from the out gassing of particle boards, paper product coatings, fibre boards and plywood. It is a suspected carcinogen. It may cause ear, nose and throat irritations and allergic reactions of the skin, eyes and respiratory tract (US Department of Labour 2002).

1.3.12 Lead Pb:

Lead is used industrially in the production of batteries, it is also used in the manufacture of some paints. Lead has been attributed to damage of the nervous system and brain tissue especially among children. A main contributor to lead pollution previously was leaded petrol but this source is now on the decline mostly due to conversion to unleaded petrol (McGinlay 1997).

1.3.13 Particulate Matter PM:

Airborne particulate matter varies widely in its physical and chemical composition, source and particle size. PM_{10}[3]

3 The fraction of particulate in air of very small size (<10 µm) are of major current concern, as they are small enough to penetrate deep into the lungs

particles as well as creating dirt, odour and visibility problems are associated with health effects including increased risk of heart and lung disease. In addition, they may carry surface absorbed carcinogenic compounds into the lungs (McGinlay 1997). The smaller particle fraction $PM_{2.5}$[4] is capable of even deeper penetration into the lungs. Scientific studies have suggested links between fine particulate matter and numerous health problems including asthma, bronchitis, acute and chronic respiratory symptoms such as shortness of breath and painful breathing, and premature death (Becker et al 2004).

1.4 Importance of studying Indoor Air Pollutants

The presence of contaminants -- intentional and unintentional – in the indoor environment, causes problems in three general areas:

- Health problems
- Productivity problems
- Comfort and odour problems

It has been confirmed that contaminant and pollution problems are a factor in the so called Sick Building Syndrome (SBS). Sick Building Syndrome is an umbrella term and some of the conditions manifested upon occupants, relevant to the scope of this document are:

- Adverse skin, eye or pharynx symptoms (Gyntelberg et al 1994, Wallace et al 1993).
- General headache or fatigue (Gyntelberg et al 1994).
- Lack of concentration (Gyntelberg et al 1994).
- Dizziness (Gyntelberg et al 1994, Wallace et al 1993).
- General feeling of malaise (Gyntelberg et al 1994).
- Sleepiness (Wallace et al 1993).
- Chills / fever (Wallace et al 1993).
- Aching muscles; back pain, shoulder / neck pain, hand / wrist pain (Wallace et al 1993).
- Problems with contact lenses (Wallace et al 1993).
- Allergies (Hedge et al 1995).
- Depression (Hedge et al 1995).
- Seasonal affective disorder[5] (Hedge et al 1995).

All of these symptoms are a subset of one or more of the previously defined problem areas i.e. health, productivity

---

and so potentially pose significant health risks.

4 The fraction of airborne particles of even smaller size (<2.5 µm). Modern research divides small PM into three categories based on size i.e. coarse (2 µm), accumulation (0.1 to 2 µm) and ultra fine (< 0.1 µm) (Nazaroff 2004).

5 Seasonal affective disorder SAD describes a pattern of sub-clinical depression symptoms which occur in the autumn / winter but not in spring / summer, Seasonal changes in light levels are thought to provoke symptoms. Workers reporting SAD are at higher risk of reporting building related symptoms (Hedge et al 1995). Association between SBS and SAD has also been reported by Burr et al (1991).

and comfort. The symptoms are experienced only after prolonged occupation of a particular building, i.e. daily or at least several times a week, and they disappear or are significantly reduced minutes or hours after leaving the building (Gyntelberg et al 1994). The symptoms are attributed to dust, bacteria, pollutant gases, mites and moulds in the indoor environment. There have been numerous studies in this area e.g. Gyntelberg et al (1994), Yu et al (1998). It is well documented that naturally ventilated buildings, compared to air-conditioned ones, are less prone to becoming sick. There is a lot of related work confirming this statement, for example Wong et al (2004), Muhic et al (2004). Muhic et al (2004) concluded that even when air quality and thermal comfort standards (ISO 7730, CEN CR 1752) were met as regards ventilation and thermal comfort, occupants expressed a relatively high degree of dissatisfaction with the air quality and thermal environment. In an earlier study (Haghighat et al 1999) it was found that meeting current air quality and ventilation standards does not ensure a reasonable level of occupant satisfaction and one of the factors with which occupants were dissatisfied was air quality. While there is clearly scope for work into the psychological and other factors regarding perceived indoor quality, it is necessary to appreciate the importance of being able to predict IAQ in terms of contaminants and their concentrations.

1.4.1 Health Problems

Indoor air is a dominant exposure for humans. Thus most illnesses related to environmental exposure stem from indoor air exposure. Poor IAQ is the cause of excessive morbidity and mortality. In developing countries unvented burning of biomass for cooking is the cause of at least 2,000,000 deaths a year (mainly women and children) (Sundell 2004), and in the developed world poor IAQ is a main cause of allergies, other hypersensitive reactions, airway infections and cancers. Cancer of the lungs is related to radon and ETS exposure. Allergies, airway infections and SBS are associated with e.g. dampness, low ventilation rates and plasticisers (Sundell 2004). All of these issues are related to the concept of contaminants in indoor air. Smith (2003) reports that burning solid fuel for cooking and heating might be responsible for nearly 4% of global diseases. In developed countries evidence is strong regarding an association between IAQ and lung cancer, allergies, other hypersensitivity reactions (e.g. SBS), multiple chemical sensitivity and respiratory infections (Sundell 1999).

There has been a shift of interest in the whole conceptualisation of indoor human comfort in recent times. Focus seems to have shifted from thermal satisfaction and odour prevention to health related and productivity issues (Samet 1993). The emergence of indoor air pollution as a unified public health concern has fostered the interdisciplinary interactions that are probably the way forward to find solutions. In 2002 an extensive literature review was carried out by eminent inter-disciplinary European scientists (Wargocki et al 2002) with expertise in medicine, epidemiology, toxicology and engineering. The group agreed that ventilation is associated with comfort in terms of perceived air quality and SBS symptoms. Furthermore they concluded there is a strong correlation between productivity and ventilation. The group found that below a fresh air supply rate of 25l/s per person it is likely that SBS symptoms are reported by occupants and that ventilation rate above 0.5ac/h in homes reduces chances of dust mite infestation. A similar assessment was carried out in 2003 (Schneider et al 2003) to determine some correlation between PM size and health issues, but no generally applicable risk indicator of health effects could be determined. This was ascribed to inadequate scientific evidence.

An earlier study (Berglund et al 1992) gave a detailed account of many different kinds of health related problems and issues that indoor air pollution causes. Samit(1993) gives a classification of adverse health problems directly related to indoor air pollution. A spectrum of health responses to indoor air pollution are identified and classification of these responses includes categories for disease, impairment, symptoms, increased risk and perceptions of general illness. The classification is as follows:

- Clinically evident diseases: Diseases for which the usual methods of clinical evaluation can establish a causal link to an indoor air pollution.
- Exacerbation of disease: The clinical status of already established disease is exacerbated by indoor air pollution.
- Increased risk for diseases: Diseases for which epidemiological or other evidence establishes increased risk in exposed individuals. However, the usual clinical methods indicative of injury typically cannot establish the causal link in an individual patient.
- Physiological impairment: Transient or persistent effects on a measure of physiological functioning which are of insufficient magnitude to cause clinical disease.
- Symptoms responses: Subjectively reported responses which can be linked to indoor pollutants or are attributed to indoor pollutants.
- Perception of unacceptable IAQ: Sensing of IAQ as uncomfortable to an unacceptable degree.
- Perception of exposure to indoor air pollutants: Awareness of exposure to one or more pollutants with an unacceptable level of concern about exposure.

In brief, there is a lot of interest in the specific area of health issues related to the indoor environment and a large amount of work is currently being done in this research field. It is not possible to list all of this, but some of the more typical and characteristic studies have been reported. It is expected that this will reflect upon the importance of the scope of the present work i.e. a way forward to predict transient contaminant behaviour within the built environment taking into account the dynamic loading factors that a building is subjected to.

1.4.2 Productivity Problems

Productivity is defined as the extent to which activities have provided performance in terms of system goals (Parsons 1993). Effects of environmental factors, namely indoor climate, accidents, human efficiency and comfort were reviewed by Wyon (1986). Wargocki et al (2000) reported that the performance of four simulated office tasks improved with increasing ventilation rates, and the effect reached formal significance in the case of text typing. On the other hand, some others reported no significant effects of productivity for short-term tests. People are highly motivated during a short-term experiment, so it may be very difficult to measure the difference in actual performance. However, it is known that productivity is reduced under poor environmental conditions in daily life. After long office hours, workers become tired with decreased performance (Tannabe 2004).

It was found that existing literature contains strong evidence that characteristics of buildings and indoor environments significantly influences rates of respiratory disease, allergy and asthma symptoms, and worker performance. Theoretical considerations, and limited empirical data, suggest that existing technologies and procedures can improve indoor environments in a manner that significantly increases health and productivity. A crude estimate of the magnitude of productivity gains that may be obtained by providing better indoor environments for the U.S. alone stands at $6-19 billion from reduced respiratory disease, $1-4 billion from reduced allergies and asthma, $10-20 billion from reduced SBS symptoms and $12-125 billion from direct improvements in worker performance that are unrelated to health. Sample calculations indicate that the potential financial benefits of improving indoor environments exceed costs by a factor of around 250% (Fisk et al 1997). The figures give an idea of both the direct cost benefits of adequate IAQ and the indirect cost benefits in terms of health. It can be seen that the potential savings to be gained from improving IAQ for productivity enhancement is not small. Wallace et al (1993) gives characteristic features of a building that had previously been suspected and was confirmed to raise health and productivity related concerns. Smoking status, type of office, time working with computers or at a copying machine, presence of new furniture or fleecy surfaces, airflow capacity, stress indices, comfort / odour factors etc. have all been implicated. In addition to these there seem to be a lot of factors that affect the well being and productivity of occupants; office refurbishments, carpets, poor ventilation, air-conditioning, presence of pollen or animal hair / dander, dust mites, mould growth, presence of excess moisture and a host of other factors have been blamed for loss of efficiency and poor health of occupants. Among the 'non-engineering' factors are some psychological factors like gender, job stress, job dissatisfaction, level of education, allergies and asthma[6]. (Mendell 1993).

Most of the information available from recent researches into the whole area of productivity is based on questionnaires handed out to occupants in commercial or industrial buildings. Where there are obvious advantages of this method, there seems to be a loss in standardisation of the procedure. Different metrics and characteristics of the occupants and conditions seem to have been measured. In spite of different methods of categorising and detailing, every research study concluded that in addition to health problems the issue of productivity loss occurs in industrial and commercial buildings with low quality of indoor air. Additionally, low attendance at schools and sick leaves in offices have been found

6 Allergies and asthma in this context relate to those conditions that are historical and not building induced for example from SBS.

to correlate to indoor environment conditions (Mendell 2005).

Although the study (Mendell 2005) focuses on schools in Northern America, the findings can be extended at a global level. Evidence is available to justify:

- immediate actions to assess and improve indoor environment quality and
- focused research to guide indoor environment quality improvements.

1.4.3 Comfort and Odour Problems

Unfortunately odour levels are neither easily quantified nor easily measured. The nose is extremely keen and olfaction is a sensitive physiological system. Humans can detect the presence of some substances at concentrations below the level at which they can be measured by the most sensitive instruments (sometimes sub parts per billion levels) (Heinsohn 1991). The intensity of perception of an odour depends in more than the concentration of the odorant. The sense of smell fatigues rapidly and consequentially the perceived strength decays quickly. Females are generally more sensitive to smell than males and acuity varies throughout the menstrual cycle (Moncrieff 1967). Odour sensitivity reduces with increased ambient temperature and also with increased humidity. Roughly, a 50% increase in odorant concentration can be counteracted by an increase in RH from 20% to 55% (McIntyre 1980).

Odours are hedonistic in that they elicit an involuntary response that pleases or offends individuals. While no two individuals are alike, groups of individuals exhibit responses that can be quantified with statistical significance. The ASHRAE (1989) guideline may be followed, and (Nielsen et al 1994) recommend ED20. This recommendation defines unobjectionable air to have a concentration of a substance at which not more than 20% of a panel deem the air to be objectionable under representative conditions of use and occupancy.

Although the presence of an odour does not in itself constitute a health hazard (Rosenkranz 2003), it can still be a contributory factor to discomfort. There have been a number of studies that have tried to formulate the extent to which people can be exposed to odours comfortably (e.g. Nielsen et al 1997) and standards exist that mandate the presence of different odour producing chemicals (WHO 1987).

1.4.4 World Health Organisation Recommendation

One of the reasons for the inadequate quality of indoor air arises from poor articulation, appreciation and understanding of basic principles underlying the policies and actions related to indoor air quality. A World Health Organisation (WHO) Working Group derived nine statements on rights to healthy indoor air. The discussions and statements are available as a WHO report (WHO 2000). It informs the individuals and groups responsible for healthy indoor air about their rights and obligations, and empowers the general public by making people familiar with those rights. One year after their publication the statements were adopted as the base for future regulation and guidance. The Board of

Directors of the International Society of Indoor Air Quality (ISIAQ) and the participants of two international conferences endorsed the use of the statements. No opposition to the statements has been registered. The statements have entered curricula of training courses and have been used in lawsuits (Molhave et al 2003).

The WHO statements read as follows:

- Under the principle of the human right to health, everyone has the right to breathe healthy indoor air.
- Under the principle of respect for autonomy (self-determination), everyone has the right to adequate information about potentially harmful exposures, and to be provided with effective means for controlling at least part of their indoor exposures.
- Under the principle of non-maleficence (doing no harm), no agent at a concentration that exposes any occupant to an unnecessary health risk should be introduced into indoor air.
- Under the principle of beneficence (doing good), all individuals, groups and organizations associated with a building, whether private, public or governmental, bear responsibility to advocate or work for acceptable air quality for the occupants.
- Under the principle of social justice, the socio-economic status of occupants should have no bearing on their access to healthy indoor air, but health status may determine special needs for some groups.
- Under the principle of accountability, all relevant organizations should establish explicit criteria for evaluating and assessing building air quality and its impacts on the health of the population and on the environment.
- Under the precautionary principle, where there is a risk of harmful indoor air exposure, the presence of uncertainty shall not be used as a reason for postponing cost-effective measures to prevent such exposure.
- Under the 'polluter pays principle', the polluter is accountable for any harm to health and for welfare resulting from unhealthy indoor air exposures. In addition, the polluter is responsible for mitigation and remediation.
- Under the principle of sustainability, health and environmental concerns cannot be separated, and the provision of healthy indoor air should not compromise global or local ecological integrity, or the rights of future generations.

The need for the above principles was felt to a large extent because of ignorance of the principles of good IAQ and lack of understanding of the underpinning important issues related to policy and action. As a result the general public is familiar neither with those principles nor their associated rights. These statements inform individuals and groups responsible for healthy indoor air about their rights and obligations, and empower the general public by making people familiar with those rights.

1.5 Summary

It was seen that air pollution is mostly caused by the human activity and resource utilisation. People remain indoors most of the time and so a study into transport, distribution and growth / decay of pollutants indoors is important. Important air pollutants of indoor and outdoor origin are described. Legislative bodies on both sides of the Atlantic have defined dangerous air pollutants and exposures have been documented. A WHO guideline, describing human rights for good IAQ, exists and it is hoped that this will raise the standard of regulations. A small number of pollutants have been chosen to form an initial list. Indoor air pollutants exhibit a number of phenomena and different mechanisms come into play for different pollutants (or for the same pollutant in different states) depending upon nature, physical state, chemical properties, air movement and a horde of other conditions and properties. It was seen that behaviour of pollutants indoors is complex and cannot be described adequately by simplistic schemes. Buildings may become sick due to contaminants and this has the effect of making the occupants sick. This is the reason for a large amount of health and comfort concerns and productivity loss. Research into this subject area is increasing and it is hoped that this trend will continue.

1.6 References

ASHRAE. 1989. *Ventilation for Acceptable Indoor Air Quality*. Atlanta, GA. American Society of Heating, Refrigeration and Air-conditioning Engineers (ASHRAE Standard 62-1989)

Axley, J. W. 1991. *Adsorption Modelling for Building Contaminant Dispersal Analysis*. Indoor Air 1991;1, 2.

Axley, J. W. 1993. *Modelling Sorption Transport in Rooms and Sorption Filtration Systems for Building Air Quality Analysis*. Indoor Air 1993;3, 3.

Baek, S. O., Jenkins, R. A. 2004. *Characterization of Trace Organic Compounds Associated with Aged and Diluted Side Stream Tobacco Smoke in a Controlled Atmosphere—Volatile Organic Compounds and Polycyclic Aromatic Hydrocarbons.* Atmospheric Environment 2004, 38.

Becker, S., Dailey, L., Soukup, J. M., Silbajoris, R., Devlin, R. B. 2004. *TLR-2 is involved in Airway Epithelial Cell Response to Air Pollution Particles*. Toxicology and Applied Pharmacology. Accepted July 2004 (Article in press at time of writing)

Berglund, B., Brunekreef, B., Knoppel, H., Lindvall, T., Maroni, M., Molhave, L., Skov, P. 1992. *Effects of Indoor Air Pollution on Human Health*. Indoor Air 1992;2, 1.

Burr, G. A., Alderfer, R. J. 1991. *NIOSH Health Hazard Evaluation Report HETA 89-065-2119.* National Institute for Occupational Safety and Health. Washington D. C., U.S.A.

Carrer, P., Maroni, M. 2002. *Allergens in indoor air: environmental assessment and health effects*. Science of the Total Environment, 2002, Vol 270.

CEPA/FPAC. 1998. *National Ambient Air Quality Objectives for Particulate Matter*. *Executive Summary*. Health Canada. Environment Canada. © Minister, Public Works and Government Services. ISBN 0-662-63486-1. http://www.hc-sc.gc.ca/hecs-sesc/air_quality/pdf/98ehd220.pdf

CIBSE 1993. *CIBSE Guide A, revision section 2 "Environmental Criteria for Design,"* Chartered Institute of Building Services Engineers, UK.

Clausen, G. 2004. *Ventilation Filters and Indoor Air Quality: A Review of Research from the International Centre for Indoor Environment and Energy*. Indoor Air 2004;14, Supplementary 7.

Congress. 1990. *Section 112. National Emissions Standards for Hazardous Air Pollutants. The Clean Air Act (Amended 1990)*. Congress of the United States of America.

Corsi, R.L., Torres, V.M., Sanders, M., Kinney, K.A. 2002. *Carbon Dioxide Levels and Dynamics in Elementary Schools: results of the TESAIS Study. Conference Proceedings,* Indoor Air 2002, The International Academy of Indoor Air Sciences, Monterey, July 2002.

Darby, S., Deo, H., Doll, R., Whitley, E. 2001. *A Parallel Analysis of Individual and Ecological Data on Residential Radon and Lung Cancer in South-West England*. Journal of the Royal Statistical Society: Series A (Statistics in Society) Volume 164, Issue 1.

DIN 1994. DIN 1946 Part 2, 1994. *"Ventilation and Air Conditioning: Technical Health Requirements."*

EPA. 1999. *Smog – Who does it hurt? EPA-452/K-99-001*. Environmental Protection Agency. Washington D. C. U.S.A.

EPA. 2001. Indoor Air Pollution. *An introduction for Health Professionals*. American Lung Association. American Medical Association, US Consumer Product Safety Commission. Environmental Protection Agency. Washington D. C. U.S.A.

EPA. 2004a. *A Citizen's Guide to Radon. The Guide to Protecting Yourself and Your Family From Radon.* Environmental Protection Agency. Washington D. C. U.S.A.

EPA. 2004b. *What are the Six Common Air Pollutants?* http://www.epa.gov/air/urbanair/6poll.html Environmental Protection Agency. Washington D. C. U.S.A.

EPA. 2005. *U.S. EPA Toxics Release Inventory: Community right to know homepage* http://www.epa.gov/tri Environmental Protection Agency. Washington D. C. U.S.A.

EU. 1999. *EU Focus on Clean Air*. European Commission. Directorate-General Environmental, Nuclear Safety and Civil Protection. Luxembourg: Office for Official Publications of the European Communities, 1999. ISBN 92-828-4803-5

EU. 2003. Rapid Press Release. *Indoor Air Pollution: New EU Research Reveals Higher Risks Than Previously Thought*. Reference IP/03/1278 of 22-09-2003

Fanger, P. O. 1988. *Introduction of the olf and the decipol Units to Quantify Air Pollution Perceived by Humans Indoors and Outdoors*. Energy and Buildings 12;1.

Fisk, W. J., Rosenfeld, A. H. 1997. *Estimates of Improved Productivity and Health from Better Indoor Environments.* Indoor Air 1992;7 , 3.

Gyntelberg, F., Suadicani, P., Nielsen, J. W., Skov, P., Valbjmn, O., Nielsen, P. A., Schneider, T., Jargensen, O., Wolkofes, P., Wilkins, C. K., Gravesed, S., Norn, S. 1994. *Dust and the Sick Building Syndrome*. Indoor Air 1994;4.

Haghighat, F., Donnini, G. 1999. *Impact of Psycho-Social Factors on Perception of the Indoor Air Environment studies in 12 Office Buildings.* Building and Environment 1999;34, 4.

Haghighat, F., Lee, C. S., Ghaly, W. S. 2002. *Measurement of Diffusion coefficients of VOCs for building materials: review and development of a Calculation Procedure*. Indoor Air 2002;12, 2.

Hanssen, S. O. 2004. *HVAC - the Importance of Clean Intake Section and Dry Air*. Indoor Air 2004;14, Supplementary 7.

Healthy Buildings. 2000. Workshop 22. *IAQ in Hospitals. Proceedings of Healthy Buildings*. August 6th - 10th, 2000. Espoo, Finland.

Hedge, A., Erickson, W. A., Rubin, G. 1995. *Individual and Occupational Correlates of the Sick Building Syndrome.* Indoor Air 1995;5, 1.

Heinsohn, R. J. 1991. *Industrial Ventilation: Engineering Principles.* John Wiley and Sons, Inc. New York.

Howieson, S. 2005. *Housing and Asthma.* Spon Press, Taylor and Francis Group.

Huang, H., Haghighat, F. 2001. eSim 2001. *The Canadian Conference on Building Energy Simulatio*n. June 13th - 14th, 2001. Ottawa, Canada.

Hyttinen, M., Pasanen, P., Salo, J. 2003. *Reactions of Ozone on Ventilation Filters.* Indoor and Built Environment 2003;12.

Illinois Department of Public Health. 2004. *Ozone. Environmental Health Fact Sheet*. Illinois Department of Public Health. Springfield, Illinois. http://www.idph.state.il.us/envhealth/factsheets/ozone.htm

Janssen, N. A. H., de Hartog, J. J., Hoek, G., Brunekreef, B., Lanki, T., Timonen, K.. Pekkanen, J. 2000. *Personal Exposure to Fine Particulate Matter in Elderly Subjects: Relation Between Personal, Indoor and Outdoor Concentrations*. Journal of Air Waste Management Association, Volume 50.

Kingsley, M., Davidson, J. 2000. *Gaseous Indoor Pollutants.* University of Minnesota

Lansari, A., Streicher, J. J., Huber, A. H., Crescenti, G. H., Zweidinger, R. B., Duncan, J. W., Weisel, C. P., Burton, R. M. 1996. *Dispersion of Automotive Alternate Fuel Vapors within a Residence and its Attached Garage*. Indoor Air 1996;6, 2.

Lunden, M. M., Revzan, K. L., Fischer, M. L., Thatcher, T. L., Littlejohn, D., Hering, S. V., Brown, N. J. 2003. *The Transformation of Outdoor Ammonium Nitrate Aerosols in Indoor Environment*. Atmospheric Environment 2003, 37

McGinlay, J. 1997. *The Chemistry of Atmospheric Pollutants.* National Environmental Technology Centre. AEA Technologies PLC UK http://www.aeat.co.uk/netcen/airqual/kinetics

McIntyre, D. A. 1980. *Indoor Climate*. Applied Science Publishers Ltd., London.

Meininghaus, R., Uhde, E. 2002. *Diffusion Studies of VOC Mixtures in a Building Material.* Indoor Air 2002;12, 4.

Mendell, M. J. 1993. *Non-Specific Symptoms in Office Workers: A Review and Summary of the Epidemiologic Literature.* Indoor Air 1993;3, 4.

Mendell, M. J., Heath, G. A. 2005. *Do Indoor Pollutants and Thermal Conditions Influence Student Performance? A Critical Review of the Literature.* Indoor Air 2005;15, 1.

Merriam Webster. 2002. *Merriam-Webster Medical Dictionary,* © 2002 Merriam-Webster, Inc. *Database*

Molhave, L., Krzyzanowski, M. 2003. *The Right to Healthy Air: status by 2002*. Indoor Air 2003;13, Supplementary 6.

Moncrieff, R. W. 1967. *The Chemical Senses.* International Textbook Co. London 2nd Edition.

Muhic, S., Butala, V. 2004. *The Influence of Indoor Environment in Office Buildings on their Occupants: expected – unexpected.* Building and Environment 2004;39, 3.

Murakami, S., Kato, S., Ito, K., Zhu, Q. 2003. *Modelling and CFD Prediction for Diffusion and Adsorption within room with various Adsorption Isotherms.* Indoor Air 2003;13, Supplementary 6.

Nazaroff, W. W. 2004. *Indoor Particle Dynamics.* Indoor Air 2004;14, Supplementary 7.

Nielsen, G. D., Hansen, L. F., Wolkoff, P. 1997. *Chemical and Biological Evaluation of Building Material Emissions. II. Approaches for Setting Indoor Air Standards or Guidelines for Chemicals.* Indoor Air 1997;7, 1.

Nielsen, P. A., Jensen, L. K., Eng, K., Bastholm, P, Hugod, C., Husemoen, T., Molhave, L., Wolkoff, P. 1994. *Health-Related Evaluation of Building Products based on Climate Chamber Tests.* Indoor Air 1994;4, 3.

Park, J. S., K. Ikeda, K. 2003. *Database system, AFoDAS/AVODAS, on Indoor Air Organic Compounds in Japan*. Indoor Air 2003;13, Supplementary 6.

Parsons, K. 1993. *Human Thermal Environment*. London, UK. Taylor and Francis.

Pommer, L., Fick, J., Nilsson, A., Barbro, A. 2004. *An Experimental Comparison of a Kinetic Model for the Reaction of Alpha Pinene and Delta 3 Carene with Ozone and Nitrogen Oxides.* Indoor Air 2004;14, Supplementary 8.

Rehwagen, M., Schlink, U., Herbarth, O. *Seasonal Cycle of VOCs in Apartments.* Indoor Air 2003;13, 3.

Rodes, C. E., Kamens, R. M., Wiener, R. W. 1991. *The Significance and Characteristics of the Personal Activity Cloud on Exposure Assessment Measurements for Indoor Contaminants*. Indoor Air 1991;1, 2.

Rosenkranz, H. S., Cunningham, A. R. 2003. *Environmental Odours and Health Hazards*. The Science of the Total Environment 2003;313, 1-3.

Samet, J. M. 1993. *Indoor Air Pollution: A Public Health Perspective.* Indoor Air 1993;3, 4.

Samuel, A. A., Strachan, P. A. 2005. *Integration of Contaminant Modelling within Whole Building Simulation.* Conference Proceedings, BS '05. The International Building Performance Simulation Association, Montreal, August 2005.

Schneider, T., Sundell, J., Bischof, W., Bohgard, M., Cherrie, J. W., Clausen, P. A., Dreborg, S., Kildeso, J., Kjaergaard, S. K., Lovik, M., Pasanen, P., Skyberg, K. 2003. '*EUROPART'. Airborne Particles in the Indoor Environment. A European Interdisciplinary review of Scientific Evidence on Associations between Exposure to Particles in Buildings and Health Effects.* Indoor Air 2003;13, 1.

Shaughnessy, R. J., Levetin, E., Blocker, J., Sublette, K. L. 1994. *Effectiveness of Portable Indoor Air Cleaners: Sensory Testing Results.* Indoor Air 1994;4, 3.

Slejko, F. L. 1985. *Adsorption Technology: A Step-by-step Approach to Process Evaluation and Application.* New York, Marcel Dekker Inc.

Smith, K. R. 2003. *The Global Burden of Disease from Unhealthy Buildings: Preliminary Results from Comparative Risk Assessment*. Proceedings of Healthy Buildings. December 7th – 11th. 2003. Singapore.

Sofuoglu, S. C., Moschandreas, D. J. 2002. *The Link Between Symptoms of Office Building Occupants and In-Office Air Pollution: the Indoor Air Pollution Index*. Indoor Air 2002;13, 4.

Sowa, J. 2002. *Air Quality and Ventilation Rates in Schools in Poland - Requirements, Reality and Possible Improvements. Conference Proceedings,* Indoor Air 2002. The International Academy of Indoor Air Sciences, Monterey, July 2002.

Sundell, J. 1999. *Indoor Environment and Health*. Stockholm, Sweden: National Institute of Public Health.

Sundell, J. 2004. *On the History of Indoor Air Quality and Health.* Indoor Air 2004;14, 1.

Tanabe, S., Nishihara, N. 2004. *Productivity and Fatigue*. Indoor Air 2004;14, Supplementary 7.

Tichenor, B. A., Guo, Z., Sparks, L. E. 1993. F*undamental Mass Transfer Model for Indoor Air Emissions from Surface Coatings.* Indoor Air 1993;3, 4.

US Department of Labour. 2002. *Formaldehyde. OSHA Factsheet. Occupational Safety and Health Administration.* US Department of Labour.

Wallace, L. A., Nelson, C. J., Highsmith, R., Dunteman, G. 1993. *Association of Personal and Workplace Characteristics with Health, Comfort and Odour: A Survey of 3948 Office Workers in Three Buildings.* Indoor Air 1993;3.

Wargocki, P., Sundell, J., Bischof, W., Brundrett, G., Fanger, P. O., Gyntelberg, F., Hanssen, S. O., Harrison, P., Pickering, A., Seppanen, O. Wouters, P. 2002. *Ventilation and Health in non-industrial Indoor Environments: report from a European Multidisciplinary Scientific Consensus Meeting (EUROVEN).* Indoor Air 2002;12, 2.

Wargocki, P., Wyon, D. P., Sundell, J., Clausen, G., Fanger, P. O. 2000. *The Effects of Outdoor Air Supply Rate in an Office on Perceived Air Quality, Sick Building Syndrome (SBS) Symptoms and Productivity*. Indoor Air 2000;10, 4

Weschler, C. J. 2000. *Ozone in Indoor Environments; Concentration and Chemistry.* Indoor Air 2000;10, 4.

Weschler, C. J. 2004. *Chemical Reactions Among Indoor Pollutants: What We've Learned in the New Millennium.* Indoor

Air 2004;14, Supplementary 7.

WHO. 1987. *Air Quality Guidelines for Europe*. Copenhagen, Denmark. WHO Regional Office for Europe (European Series No. 23).

WHO. 2000. *The Right to Healthy Indoor Air. Report of a WHO Meeting.* May 15th – 17th, 2000. Bilthoven, The Netherlands. EUR/00/5020494.E69828, Copenhagen, Denmark, WHO Regional Office for Europe.

Wolkoff, P., Clausen, P. A., Wilkins, C. K., Nielsen, G. D. 2000. *Formation of Strong Airway Irritants in Terpene/Ozone Mixtures.* Indoor Air 2000;10, 2.

Wong, N. H., Huang, B. 2004. *Comparative Study of the Indoor Air Quality of Naturally Ventilated and Air-Consitioned Bedrooms of Residential Buildings in Singapore*. Building and Environment 2004;39, 9.

Wyon, D. P. 1986. *The Effects of Indoor Climate on Productivity and Performance: a review.* WS and Energi, Productivity, Thermal Environment.

Yu, C., Crump, D. 1998. *A Review of the Emission of VOCs from Polymeric Materials used in Buildings.* Building and Environment 1998;33, 6.

Zhao, D., Little, J. C., Hodgson, A. T. 2002. *Modelling the Reversible, Diffusive Sink Effect in Response to Transient Contaminant Sources.* Indoor Air 2002;12, 3.

2 BUILDING SIMULATION

2.1 Recent Historical Review

The built environment is a complex set of numerous thermodynamic domains across the boundaries of which various transfers and interactions of heat, mass and momentum take place. These transfers interact dynamically under the action of occupant and system control. The problem of representing such time varying interactions in a manner suitable for prediction and evaluation of alternative designs has been addressed by many researchers (Macdonald 2002).

2.1.1 Early Building Performance Prediction Tools

Up until the mid 1960s only simple hand-calculation methods were available for estimating energy usage in buildings. The degree day method was commonly used to calculate heating energy requirements. The more detailed bin method was used for both heating and cooling analyses. Degree days, a measure of a climate's severity, are calculated by integrating over the year the daily-averaged outdoor-air temperature relative to a fixed base (often 15.5^{0}C). Degree days for various locations are tabulated, published and used in conjunction with the steady-state peak heating load and a fixed heating-system efficiency to estimate the usage of heating fuel over the year. Although it was useful at the time, the degree day method neglected or oversimplified many significant factors, such as transient thermal storage in building materials, solar gains, internal gains, variations in outdoor-air ventilation and infiltration rates, and the non-steady operation of heating equipment. As with the degree day approach, the bin method treats outdoor air temperature as the independent variable in the analysis. The analysis period — usually a year — is sorted into "bins" according to the outdoor temperature. Each bin thus contains the number of occurrences (usually measured in hours) within its range of outdoor temperatures (typically 3^{0}C wide). The energy consumption of each bin is determined (independently) using simplified steady-state approaches much like those of the degree day method. The predictions from all bins are then summed, yielding an estimate of the building's heating and cooling energy consumption. Compared to the degree day approach, the bin method allows some assumptions about fixed conditions to be dropped: infiltration rates and cooling system efficiencies can vary with indoor-outdoor temperature difference, for example. However, the bin method implicitly assumes that energy flows within the building are exclusively a function of indoor-outdoor temperature difference; therefore the timing (even day versus night) of solar and internal gains, and transient indoor conditions cannot be explicitly considered. Although more resolved binning approaches have been introduced in an attempt to address this fundamental shortcoming, the unifying characteristic of all bin methods is that time has been eliminated as a variable in the analysis (Beausoleil-Morrison 2000).

2.1.2 Building Simulation

The first true simulation methods (in the sense that they treated time as the independent variable) appeared after the mid 1960s (GATC 1967). At that time computing resources were limited and slow. Consequentially it became necessary to divide the problem domain. The three main division were loads, systems and plant. The building's thermal loads were calculated first for the whole year with an assumed set of indoor conditions. These loads were then used as the input to the next domain i.e. systems (fans, heating devices, cooling devices, diffusers etc.). This second simulation gave the demand placed on the plant's energy conversion systems e.g. boilers, chillers etc. In the third and final step, simulation of energy conversion and related systems was carried out using the outputs of the second step as the input. Obviously the sequential nature of the approach eliminates appreciation of interactions between the three domains. Furthermore if there is strong coupling between the steps (e.g. the impact of air handling unit on infiltration or the impact of room temperature on occupant behaviour) then this cannot be adequately treated.

Many of these early methods incorporated simple approaches for modelling various loads and demands. One such approach is the time-averaging approach in which the heat gains are smeared out over a period of time and this roughly approximated transient thermal storage, radiation and convection processes in an effort to emulate reality. The response factor method (Stephenson and Mitalas 1967) was a major breakthrough that significantly advanced the modelling of transient heat transfer through the opaque fabric and the heat transfer between internal surfaces and the room air. The method uses the superposition principle to decompose the complex non-linear heat transfer system into a summation of responses of the component parts. This allows, for example, lighting gains to be modelled with a simple algebraic summation using weighting factors which relate the convection of heat to room air to the solar radiation absorbed by the internal surfaces at the previous periods of time. Heat transfer through the walls is calculated by another summation operating on the time series history of wall surface temperatures and associated physical parameters of the wall. This is in effect solving the decoupled thermodynamic domains.

2.1.3 The Heat Balance Approach

In the 1970s the heat balance approach was introduced (e.g. Kusuda 1970). This enabled a more rigorous approach to the treatment of building loads. The approach did away with the concept of weighting factors and replaced it with heat balances to characterise the thermal response of the room air to solar insolation, internal gains, heat transfer through the fabric, longwave radiation exchange between internal surfaces and convection of indoor air. In effect this approach considers all the important energy flow paths. The heat balances are formed and solved each time step to estimate surface and room air temperatures and heat flows. This approach is more resource intensive with regards to computational requirements but it allows significant assumptions of linearity to be dropped. For example heat transfer coefficients can respond to the thermal state of the interior environment rather than being constant. Although weighting factors are dropped a response factor was still used to calculate heat transmission through opaque surfaces.

Clarke (1977) stated that numerical discretisation and simultaneous solution techniques were superior to the response factor methods. This approach essentially extends the concept of the heat balance methodology to all relevant building and plant components. A finite volume or finite difference discretisation approach to the conservation of energy is employed to represent the opaque and transparent surfaces, internal air spaces and plant components. This approach does not demand linearity and allows material properties to vary with temperature and time. It also gives the flexibility of allowing a user specified time step.

2.1.4 Plant and Airflow Modelling

The modelling of HVAC systems was improved upon in the 1980s. Transient models and more fundamental approaches were developed (e.g. Lebrun 1982) as alternatives to the traditional approach which performed mass and energy balances on pre-configured templates of common HVAC systems, the components of which were represented by overall efficiency values. One big step forward was the integration of simulation of building and plant (e.g. McLean 1982, Clarke 1982, Tang 1985).

The modelling of airflow was also developed. Methods for estimating wind and buoyancy driven infiltration were pioneered (e.g. Sherman and Grimsrud 1980) and on a higher resolution platform, computational fluid dynamics (CFD) approaches were being used to study airflows (Nielsen 1974). The multi-zone airflow network model was developed for simulating both infiltration and ventilation (Jackman 1970, Sander 1974). This method treats air flow at a macroscopic level and represents large air volumes (e.g. rooms) by single nodes and predicts flow through discrete paths.

In the mid 1980s the thermal and airflow simulations were integrated (Walton 1983, Maver and Clarke 1984). This resulted in a coupling between the multi-zone airflow network model and thermal model. This was also the time when the first pollutant dispersal analyses were made possible. Until this time thermal simulation tools focused mainly on energy processes and airflow was not simulated but rather merely its impact considered in the thermal simulation. As a result configurations in which heat and air flow were strongly coupled e.g. naturally ventilated buildings, could not be simulated accurately.

2.1.5 Further Advances in Building Modelling

Further to these fundamental methodological developments, more rigorous, accurate and resolved methods have been developed for many of the significant heat transfer paths. The science of the various building processes is being developed, such as: longwave radiation from external surfaces to the sky with varying sky temperatures; inter-surface radiation exchange using ray tracing facilities to calculate view factors in conjunction with radiosity models; transient heat exchange with the ground using transient heat storage of soil and three-dimensional heat conduction physics. The scope of building simulation has now been extended and efforts have been made to integrate related domains such as illumination, electric power flow, occupant comfort, inter-fabric moisture flow, mould growth, pollutant transport and dispersal. This continual evolution toward higher resolution and integrated approach is driven by a need to address the complex nature of real world design and analysis problems and various demands placed on buildings. Exponentially increasing computing power and decreasing cost provide the pivot for escalating usage, requirement and significance. Legislative bodies now seem to be getting interested in the science and so are providers of building services. The simulation industry appears to be set for a boom.

2.1.6 Computational Fluid Dynamics (CFD)

CFD has been widely and successfully applied in the prediction of room air motion for a quarter of a century. Whittle (1986), Nielsen (1989), and Jones and Whittle (1992) provide a thorough review of the applications. Due to high computational requirements analysis is usually restricted to single rooms or spaces within buildings. Prediction accuracy is — as with all modelling techniques — highly sensitive to the boundary conditions supplied (assumed) by the user (e.g. Awbi 1998; Emmerich 1997; Xu and Chen 1998). Essentially, the flow inside the CFD solution domain (i.e. a room) is driven by the boundary conditions. The importance of boundary conditions is underlined by Versteeg and Malalasekera (1995) who describe a CFD solution as nothing more than the extrapolation of boundary conditions into the domain interior.

The application of boundary conditions with whole building thermal and airflow simulation is relatively straightforward. The model boundary is usually placed at the exterior of the building fabric. Thus boundary conditions can be established, with a great degree of confidence, from prevailing climatic conditions. This is usually done with the help of an appropriate weather data file that holds parameters like dry bulb temperature, humidity, wind speed and direction, solar radiation etc. However in modelling a room with CFD the model boundary is located within the building fabric and the user must supply boundary conditions in the form of surface temperatures or heat fluxes, air flows entering and leaving the room, pollutant fluxes etc. The fundamental problem is clear. Whereas climatic conditions can be considered to be independent of the building, boundary conditions for the room are a function of it. The room is not independent of the building and so inherently affects its own boundary conditions. Air flow through the openings and wall conditions are dynamically varying parameters depending upon states prevailing throughout the rest of the building and the local climate. CFD researchers address this issue usually by integrating dynamic fabric models and inter-surface radiation models into the source code (Holmes et al 1990, Moser et al 1995, Schild 1997). This allows room air flow to be calculated by prescribing boundary conditions external to the building or in adjoining spaces rather than within the room.

This concept was extended by (Negrao 1995) who introduced a conflationary mechanism between a CFD code and the building performance simulation software ESP-r (ESRU 2005). The two modelling domains operate in tandem with mutual feedback between the two at each time step. The coupled thermal and airflow simulations performed by the 'conventional' building simulator *bps* provide realistic and dynamic boundary conditions to the CFD solver *dfs* which passes back information to correct the original inputs to *bps*. CFD has the potential to predict the details of flow and temperature fields within particular zones of interest. This mutual cooperation thus enables flow visualisation, studies of pollutant behaviour patterns and localised thermal comfort assessments to name a few applications. Two flow responsive modelling techniques were devised and implemented by Beausoleil-Morrison (2000) within the ESP-r simulation program. A turbulent model was developed which hopes to enhance the thermal domain by dynamically controlling the simulation of internal surface convection.

2.2 User perspective

Usage of simulation by the design profession is growing. Clients are now becoming aware of the possibilities available to them by using simulation and in a large part to the convincing evidence that the effective application of simulation can lead to more energy efficient, comfortable and healthier buildings. Building simulation has been considered to become part of legislation and some rely on it in order to demonstrate compliance (NRC 1997, CEC 1999, EU 2002). with the likelihood is that in the future it will be an essential part. Moreover, simulation tools form a key component of some government and utility energy efficiency programmes (NRCan 1999). As a result of this growing demand, building designers and analysts will continue to call for models that more closely resemble reality, necessitating continual refinement in the treatment of the relevant physical processes. Notwithstanding the growth in simulation usage, many significant barriers — in addition to the need for more refined models — remain. For example, many users (and potential users) perceive that the learning curve for simulation is too steep; that user interfaces are too cumbersome; and that data gathering and input time is too onerous. There are also liability concerns over design decisions derived from simulation-based analyses, and questions regarding the credibility of results. Initiatives are under way to address these barriers. These range from creating user interfaces that are responsive to the iterative and evolving nature of the building design process (Hand 1998); to enabling the use of simulation at the conceptual design stage (Papamichael 1999); to allowing simulation programs to share data models with other tools such as CAD drawing packages (Bazjanac and Crawley 1997; Clarke et al 1995). The delivery of training and the production of learning materials (e.g. Hand et al 1998) is also receiving increasing attention. Additionally, many validation exercises have been conducted (e.g. Judkoff and Neymark 1995; Lomas et al 1994; Jensen 1993) and test procedures developed (e.g. ASHRAE 1998) to assess, improve, and demonstrate the integrity of simulation tools. Without doubt, removing barriers to the use of simulation by the design professions will continue to be a focus in the building simulation field for years to come.

2.3 Integrated Contaminant Simulation

The major part of contaminant simulation has to do with prediction of contaminant concentrations within the indoor environment and this fact effectively puts contaminant simulation within the domain of air flow simulation. Other enhancements to this fundamental model may then be made. These additions e.g. source and sink models, filters etc. increase the resolution of the model and bring it closer to reality. The state of the art in standalone contaminant simulation tools may be divided into three categories:

- Network model based
- CFD based
- Zone based

The network based tools first solve a mass flow nodal network (Hensen 1991, Walton 1988) and then compute contaminant concentrations for mass flow nodes as scalars. The contaminant analysis may be based (employing contaminant mass conservation) on simultaneous solution of contaminant flow equations. Temperature may be defined via schedules. An example of this type of tool is CONTAM (Dols and Walton 2002). CFD based tools employ mass, momentum and energy conservation principles to obtain, among other results, micro-climatic contaminant concentrations. An example of such a tool is FLUENT (FLUENT 2003). Some researchers (Huang et al 2002, Stewart and Ren 2003) have tried to marry the two concepts into what is called the zonal approach in which a room is divided into a number of airflow network nodes and mass balance employed. This is similar to a coarse CFD grid with only continuity switched on.

The developed approach in this thesis is based on the network flow and CFD approaches but, instead of using fixed temperatures, a fully integrated approach is adopted. Contaminant concentrations are still post-processed after running the mass flow solver but by including other building performance domains such as lighting, thermal and plant domains for the mass flow solution, results will take into account these interactions and hence be more representative of reality. The contaminant transport model assumes that ambient contaminant concentration are known and that the mass of contaminant transported indoors / outdoors is a linear function of the air mass flow rate obtained from the network airflow model. Hence the contaminant mass flows are in effect directly proportional to the air mass flow rates. Contaminant prediction facilities exist at the CFD level and the coarser network mass flow level. These can be used either in conjunction or separately depending upon the level of detail and / or relevant available information.

It has been shown by previous research studies that not taking into account dynamic temperature differences has a considerable impact on predicted air flows and contaminant transport (Bossaer et al 1999). This was confirmed in the present work. This brings in question the relevance and reliability of standalone airflow prediction tools. Although some work has been reported on linking contaminant prediction into thermal modelling (Weber et al 2003) no applications have been presented.

2.3.1 Domain Integration

Buildings and related energy systems can easily have tens of principal parameters (insulation level, capacity position, ventilation rate, glazing area, glazing type, lighting load, fuel type and so on) and the permutations available for the domain configuration are very large (SESG 1999). Within ESP-r a building comprises a collection of interacting technical domains, the properties of which and associated processes for which are well understood. Each domain is solved by exploiting the specific nature of the underlying physics and mathematical theories (Clarke and Tang 2004).

Two approaches can be adopted to integrate the different domains: internal coupling and external coupling. Internal coupling can be seen as a form of program extension and essentially expands the capabilities of existing software by adding new modules into an existing program. External coupling on the other hand makes use of existing packages in different domains (for example thermal building simulation for the thermal domain and CFD for the flow domain) and provides a mechanism for these programs to communicate. External coupling is defined as a runtime communication of two separate programs. ESP-r is especially suited to internal coupling i.e. within its different modules e.g. building thermal and air flow because of its modular nature and because much of the common information between two domains need not be written out twice. Information would need to be written twice (i.e. once in each tool) for the case of two unique simulation tools. Two otherwise independent ESP-r modules can write to and read from the same FORTRAN common block and this can thus provide a simple and effective mechanism of communication. Communication between two independent tools would have to take place at a system level i.e. external to the tools themselves.

Internal coupling can either be sequential or simultaneous. In the sequential approach the first module solves, results from it are input into the second module, then the second module solves and simulation progresses to the next time step. In the simultaneous approach the two domains keep on passing information back and forth until some mutual convergence criterion is satisfied. The simultaneous approach can thus be much more computationally intensive, but it has been shown to be more accurate than the sequential approach for certain design configurations (Hensen 1995).

The approach adopted in this thesis looks at using some mechanism of integrating contaminant prediction facilities using the mass flow network algorithm into main stream building thermal simulation. Prediction of contaminant concentrations can then be passed on to a CFD solver as the boundary conditions of a CFD domain. Finally there could be dynamic (at run time) passage of information between the different modules in order to make the simulation more realistic so as to give a more accurate depiction of reality. Two way conflation is developed as compared with one way conflation as reported by Djunaedy et al (2005). Two way conflation makes sure that the two conflated domains converge to a solution that is acceptable to all such domains before simulation progresses to the next time step whereas for one way conflation output from one module is taken as input to another without any feedback. More is said about this in chapter 5.

2.3.2 Domain Integration for Contaminant Modelling

Contaminant transport and distribution within the built space depends mainly on air flow patterns. Flow of air from one room to another may be approximated by bulk flow models like the network flow model but whereas network flow models can predict inter-zone air distributions they cannot predict intra-zone air flow conditions. It may be of importance to have detailed knowledge of contaminant concentrations within a space e.g. to provide personalised ventilation. Domain integration is very important when appraising a parameter that is inherently dependent on other parameters that are presently computed using more than one solution technique and boundary condition definitions. A good example of this is contaminant concentration. The solution procedure for prediction of contaminant concentration as implemented in the present research follows three solution procedures. It depends on the setting up and solution of contaminant distribution and transport equations which is a sparse linear system. It also depends upon setting up and solution of air flow equations which is a non-linear system. Thirdly it depends upon setting up and solution of building thermal equations which is again a non-linear system that is also sparse. To simplify the whole procedure the thermal model can be disregarded (as in standalone network flow solvers) but this has implications regarding accuracy of the approach and may cause misleading results. One candidate for appraising detailed air flow pattern, temperature, relative humidity and contaminant concentration is computational fluid dynamics or CFD. One the problems faced by a designer when setting up a CFD model is the definition of boundary conditions because for most flow configurations if the boundary conditions have been well specified the results will be correct.

Within ESP-r air flow networks comprise nodes, components and connections. Nodes are of two types, internal and external. The internal nodes usually have unknown pressure and are representative of air within a space (it is usual to represent the air within a room as an airflow node although higher and lower resolutions are also frequently used). The external nodes have pressure that is calculated from prevailing wind conditions. Air flow nodes are connected together by components. These are flow paths through which air can flow e.g. windows, doors, fans etc. Components are considered to have a well defined mass flow rate which is a function of pressure difference across the flow path. Finally the connections list is a list holding information as to how the nodes and components are connected (e.g. node room1 is connected to node hall via component big_fan).

The whole concept of conflation of the different domains is shown in figure 2.1 where the building thermal and air flow network domains provide boundary conditions to CFD and also provide mass flows rates to contaminant modelling. This is shown schematically in the diagram by the arrows pointing from building thermal etc. to CFD and contaminant modelling respectively. Contaminant modelling also provides boundary conditions to the CFD as shown by the arrow from contaminants to CFD. The CFD domain thus suitably initialised can now provide detailed and accurate air flows and contaminant concentrations. The arrow pointing from CFD to building thermal and mass flow represents two way conflation between CFD and mass flow network (the topic covered in chapter 5) and adaptive conflation between CFD and building thermal domain (Beausoleil-Morrison 2000).

Whereas imposing realistic boundary conditions taken from prevailing climatic conditions onto a thermal model is relatively straightforward, determining boundary conditions for a CFD study of a part of a building or associated energy

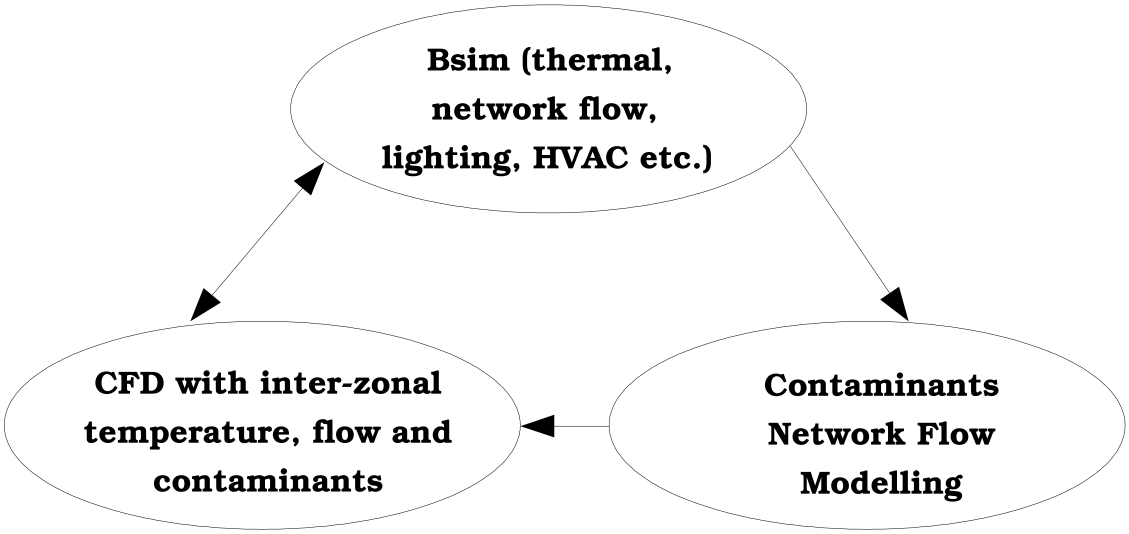

Figure 2.1 Schematic representation of domain integration

system requires more thought. The importance of boundary conditions is expounded upon in Versteeg and Malalasekera (1995) who state that flows inside the CFD solution domain are driven by the boundary conditions. In a sense the process of solving a CFD problem is nothing more than the extrapolation of a set of data defined on a boundary contour or surface into the domain interior. De Gids (1989) cites combining CFD and multi zone models as one of the most pressing research activities. Armstrong et al (2001) state that integration of CFD with building thermal and mass flow simulation can yield information useful to new advances in building operation, such as continuous commissioning, optimal control, fault detection and diagnosis, and other intelligent building functions. It is therefore important that the boundary conditions imposed onto a CFD problem are physically realistic and well posed, otherwise difficulties may arise in obtaining an accurate solution.

2.3.3 Domain Integration within ESP-r

Within ESP-r the external coupling approach is extensively used to impose communication between the different building simulation domains. The different interacting technical domains are solved by exploiting individual specific properties and nature of the underlying theory and physical principles (e.g. linear / non-linear, sparse / compact etc.). Important couplings include:

- building thermal processes – natural illuminance distribution
- building thermal / plant processes – distributed fluid (usually air and / or water) flow
- building thermal processes – intra room air flow
- electrical demand profiles – integrated embedded generation
- building thermal processes – moisture flow

Clarke and Tang (2004) define conflation of the different domains as the coordinated solution of the domain equations under control action that links certain model critical parameters (e.g. room air temperature to the mass flow rate induced by a fan). All the couplings within the different domains of integrated simulation take place by passing this critical information between themselves. Figure 2.2a summarises the ESP-r procedure which is based on the iteration of nested domains. The building side capacitances are generally greater than plant or air flow side capacitances, so it is possible to run plant and / or electrical and / or flow networks at a higher frequency than building thermal simulation. Contaminant flow because of its inherent dependence on flow parameters thus needs to be run at a higher frequency as well.

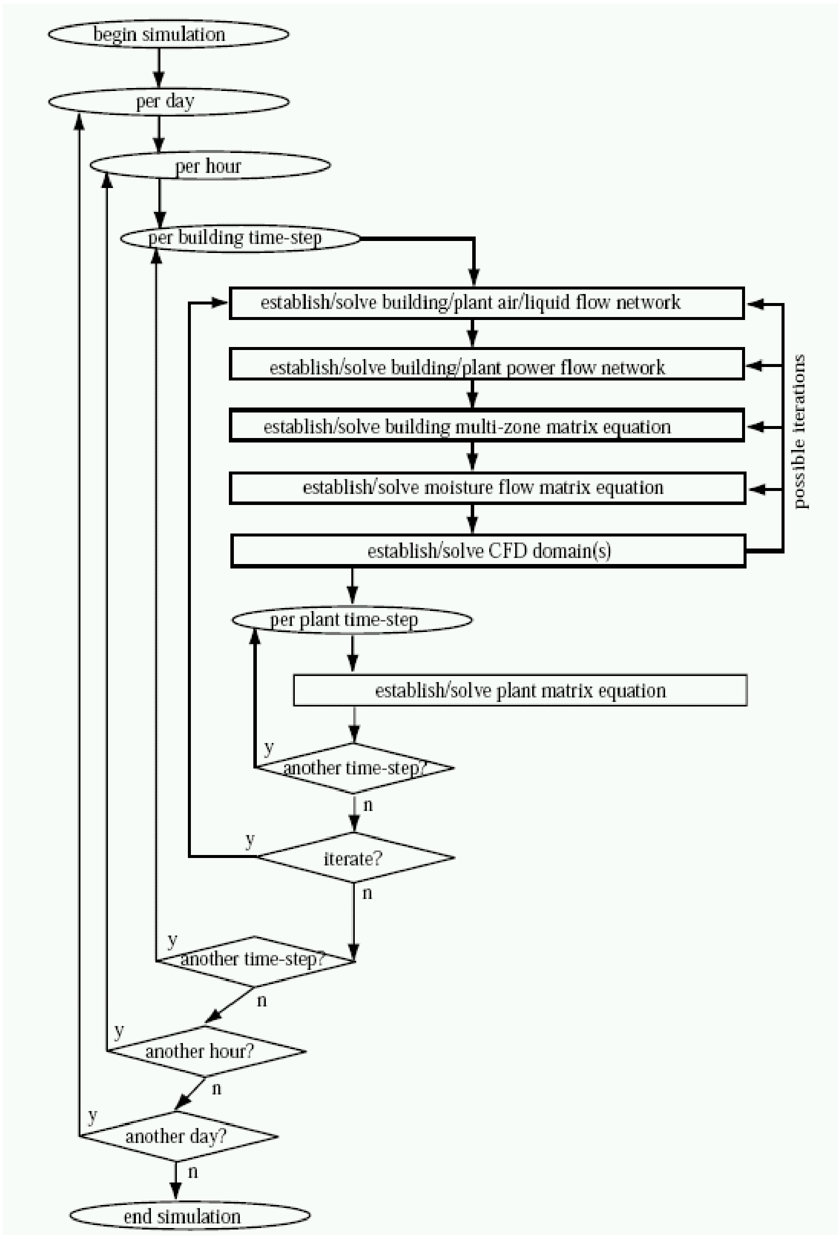

Figure 2.2a Iterative Solution of Nested Domains (Clarke and Tang 2004)

The CFD model is set up with the building side temperatures (or heat fluxes), air flow rates from integrated flow modelling and contaminant mass injections from the combined knowledge of air flow rates and contaminant concentration from the contaminant network model. The CFD and flow domains may run a number of times in order to reach mutual convergence. Mutual convergence is defined as the state of two coupled domains when the change in either is negligible under the particular set of parameters that they pass between themselves. To control the process, domain aware conflation controllers are imposed. For example an adaptive conflation controller is imposed upon the building thermal and CFD domain that dynamically ensures that the CFD model is appropriately configured.

2.4 Integration within Thermally Conflated Mass Flow and CFD domains

With energy and mass prediction systems as complicated as building thermal simulation and network mass flow many different methods of integration exist. These methods have their own advantages and disadvantages some of which are discussed later in this chapter. There is the concept that because CFD takes into account possible mechanisms of heat and mass transfer within a fluid it may be used as a standalone solver for building simulation problems. Furthermore one may argue that a CFD program can be extended to solve heat transfer in solid materials, such as building walls, with an appropriate radiation model. This is the conjugate heat transfer method and many applications are available (Holmes et al 1990, Chen et al 1995, Moser et al 1995 and Schild 1997). With an energy model for the HVAC systems and plant, the CFD can include the function of building simulation. This method sounds powerful but it is computationally expensive (Chen et al 1995). The reason for this is twofold. First, when the CFD calculates the heat transfer in solid materials, the equation set becomes stiffer and the computing time goes up dramatically (Thompson and Leaf 1988). Room air has a characteristic time constant of a few minutes at most while for the building envelope it is a few hours. CFD simulation must be performed over a long period for the thermal performance of the building envelope, but it must use a small time-step to account for the room air characteristics. Secondly, the computing time grows exponentially with building size. Hence, the conjugate heat transfer method is not practical for immediate use in a design context with current computer capabilities and speed (Zhai et al 2002).

The solution to this problem lies within domain integration. External and internal approaches. The external approach is coupling within different programs using a few critical parameters to pass information. Examples of such coupling are TRNFLOW (Weber et al 2003) and that between COMIS and Energy Plus. An example of internal coupling is *mfs* and *dfs* within the present research. There are other reasons why coupling is preferred. Code improvements in one module can be immediately used within the coupled program and there is no time delay for updating a computer tool. Additionally the processes some of these domains emulate are well understood and so it is easier to track how solution takes place. If all solution parameters are built up into one super equation set involving various complex interactions it progressively gets more difficult to understand how the computer code is behaving.

Hensen (1995) describes two algorithms for external coupling. The “ping pong” or sequential approach in which one way transfer of information takes place every time step and the “onion” or simultaneous approach in which two way transfer takes place (see figure 2.2b). In the sequential approach the domains solve independently and pass information to each other after convergence. Though this method is attractive from a computational point of view, it has the drawback that at any given time step the domain that solves first does not have up to date information from the domain that solves second but has previous time row values. It is not hard to imagine this could give significant error in a problem where due to wind effects flow through an airflow network connection or branch changes direction from one time step to the next. The second of Hensen's (1995) approaches is the simultaneous approach in which two domains solve simultaneously (not necessarily at the same time but rather at the same time step) and there is exchange of information between the two before simulation proceeds to the next time step. This approach shows greater promise of accuracy than the sequential approach because changes in one domain have a direct bearing on the other domain. (A classic problem illustrating this can be quoted. Consider a stack ventilated naturally cooled room. The hotter the room the greater the stack pressure and air flow. The greater the airflow the cooler the room.)

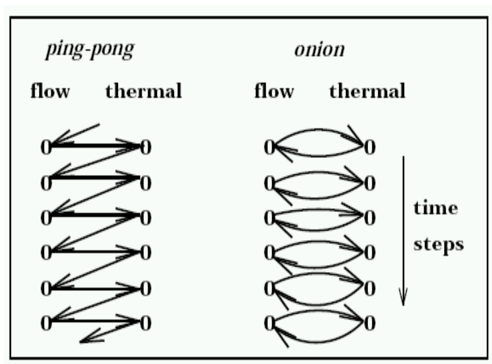

Figure 2.2b Onion and Ping-Pong approaches (Hensen 1995)

Zhai et al (2002) list a number of coupling approaches with energy simulation (ES) and CFD (see figure 2.2c). Although the particular coupling for their research was building thermal (temperature and heat flux calculations) and CFD the concepts developed in their work can be extended to understand mass flow and CFD conflation. Their first method i.e. static coupling (one step) is similar to Hensen's (1995) sequential coupling in which one way transfer of information takes place and there is no way for the second domain to impose its findings onto the first domain. Zhai et al (2002) go on to make this into a two step process in order to overcome this shortcoming, but even now there is no guarantee that both solution mechanisms will converge to the same unique solution.

Under dynamic coupling they describe “One-Time-Step Dynamic Coupling”. This coupling is invoked for one particular time step. It works by allowing both domains to run sequentially a number of times passing back and forth relevant parameter values. The solution is thought to be obtained when both the domains converge according to their respective convergence criteria. In cases when it is not possible to predict the same parameters from each domain, the difference of the present and previous run values can provide an indication of convergence. The "Quasi-dynamic coupling" algorithm is also similar to the "One-time-step-dynamic-coupling" but repeats the coupling after every n time steps. Such an approach may be useful when one of the domains runs at a smaller time step than the other one and parameters do not change much over the course of one time step. The default method used in the present work is "full dynamic coupling" in which thermal simulation and CFD run iteratively passing critical parameters between them until both converge to the same solution. "Virtual dynamic coupling" is purely a thermal conflation algorithm in which

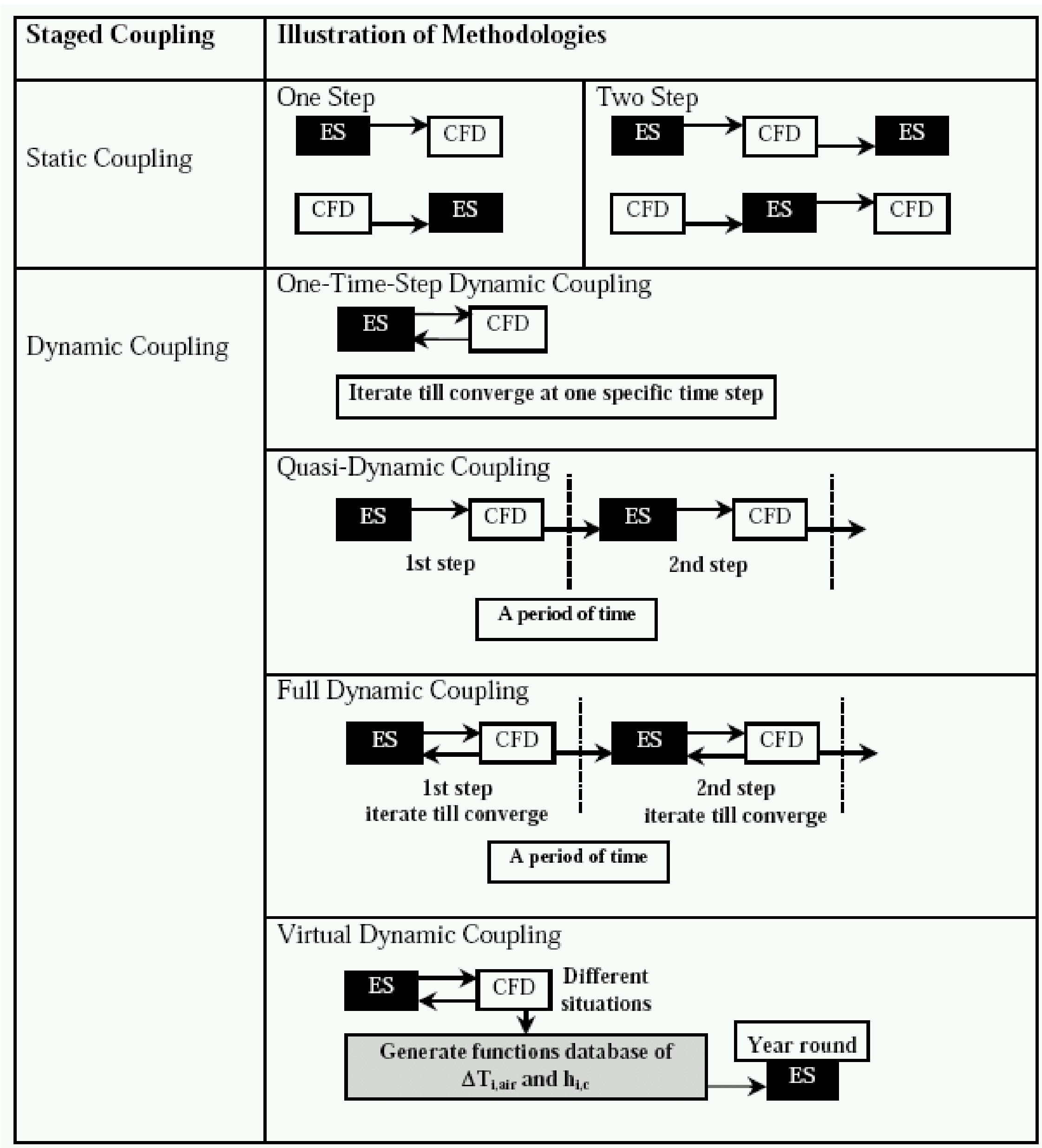

Figure 2.2c Coupling strategies as detailed by Zhai et al (2002)

temperatures and heat transfer coefficients are calculated by CFD as functions of heating / cooling load. At each time step thermal simulation interpolates CFD results to get predicted conditions. Such an approach would be useful in buildings that do not undergo a large change in temperature (e.g. hospital wards etc.).

In addition to these conflation approaches other approaches exist in which one or more parameters have been chosen to be scheduled or approximated by functions generated empirically. Srebric et al (2000) report using a CFD solver thermally coupled to a quasi steady state thermal solver. Heat injections were taken from ASHRAE methods (ASHRAE 1997) and time invariant air flow was assumed.

Conflation of building thermal and air flow processes within ESP-r's CFD is described by (Negrao 1995 and 1998) who worked on the interactions of building thermal and CFD domains interfaces, namely zone surfaces and zone openings. Thermal boundary conditions for the CFD domain are taken from building thermal simulation results for zone surfaces and zone openings are considered to be air flow boundary conditions with source / sink of thermal energy because of air flow.

In recent years there have been further advances in the coupling of building thermal processes and CFD. Notably Beausoleil-Morrison (2000, 2001 and 2002) has described an adaptive coupling algorithm that intelligently configures which turbulence model to use at run time. Zhai and Chen (2003) showed that the solution set of a coupled thermal and CFD problem is real and unique. They further state that for the purposes of integrated building performance appraisal there are three types of boundary conditions relevant for the CFD specification: the Dirichlet condition in which only surface temperature is specified; the Newmann condition in which surface convective heat flux is specified and the Robbins condition in which a relationship between the two is specified. These three conditions are the boundary specification mechanisms that Beausoleil-Morrison (2000) used in his adaptive conflation.

Integrating contaminant prediction capability within CFD inherently demands conflation of mass flow network with CFD. This is because of the complete dependence of contaminant prediction upon the mass flow rates predicted from the mass flow network solution. Therefore treatment is required for the conflation between CFD and mass flow solution and once this is achieved the contaminants model can be thought to be completely integrated within the CFD. In literature one such conflation mechanism between an air flow network and a CFD domain is that given by Negrao (1995). He replaced the node representative of the CFD domain by the CFD domain within the flow network (figure 2.3). Negrao himself states that the algorithm is unstable and implementation was problematic. The need then is to identify and develop a more robust algorithm that satisfactorily conflates the two domains and is ideally independent of building thermal and CFD conflation so as to make the couplings flexible to apply. Once realised the conflation mechanism will allow appraisal of contaminant distributions in terms of species concentration using intelligently configured boundary conditions predicted from network mass flow that will be continually corrected by iterating at a time step before going on to the next time step. The solution procedure using the conflationary approach will allow study of bulk contaminant flow patterns in the whole

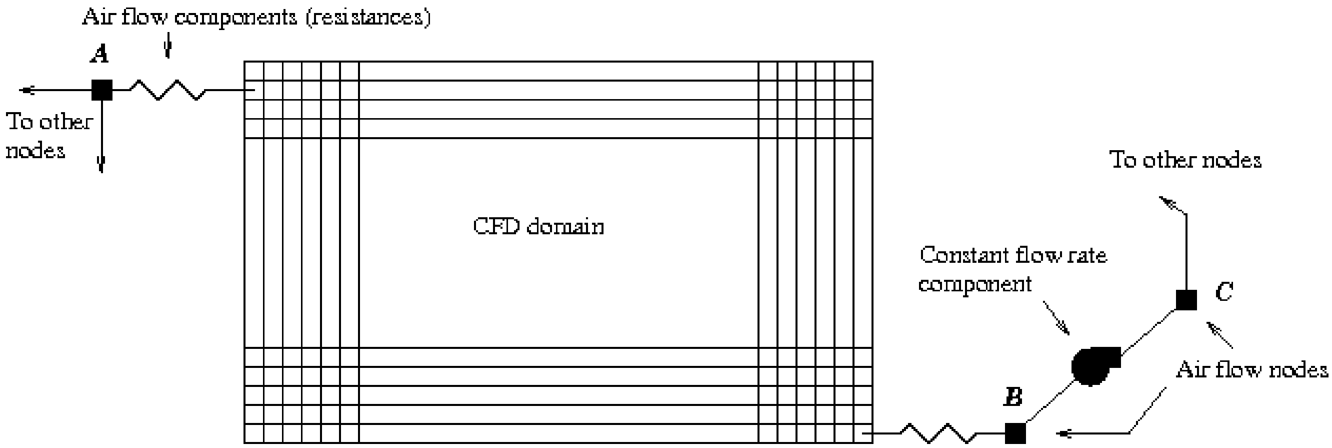

Figure 2.3 Network with constant mass flow type component

building and detailed contaminant flow characteristics of a much smaller space (say a room) simultaneously.

The algorithm used by Negrao is shown schematically in figure 2.4. In order to understand his approach one needs to know the various ESP-r modules (and associated solvers). This information is provided in table 2.1.

Module name	***Description***
mfs	Mass flow network module and solver
bps	Integrated building and plant thermal solver *(bld)* and mass flow network solver *(mfs)*
dfs	CFD module and solver
ctm	Contaminant module and solver

Table 2.1 Summary of some of ESP-r's modules

A closer look at figure 2.4 and relevant ESP-r source code makes clear the following points:

- *mfs* is called every *dfs* iteration (called sweep in the figure)
- *mfs* either passes mass flow rates or pressures as boundary conditions to *dfs*
- *dfs* passes both pressures and mass flow rates to *mfs*; these are imposed as boundary conditions.

It is clear that there is passage of information between the two modules before *dfs* has had a chance to converge although *mfs* converges before passing back information. If this be the case then information passed on from an unconverged *dfs* will most probably not be correct and possibly will be quite different from the solution. Therefore it would be correct for the two modules to call each other only when each has converged. *mfs* uses standard mass flow network theory (Hensen 1991) in which each pathway is defined using mass flow as a function of pressure difference across that pathway. The network is solved by applying mass balance and using climatic wind data as boundary conditions until mass residuals decrease below some pre-set tolerance. Fixing both mass flow and pressure in such a network is analogous to setting up a problem in which the solution has already been imposed. In a sense *mfs* does not feed any information back to *dfs* but only accepts *dfs* calculated mass flows and pressures and imposes them onto the remainder of

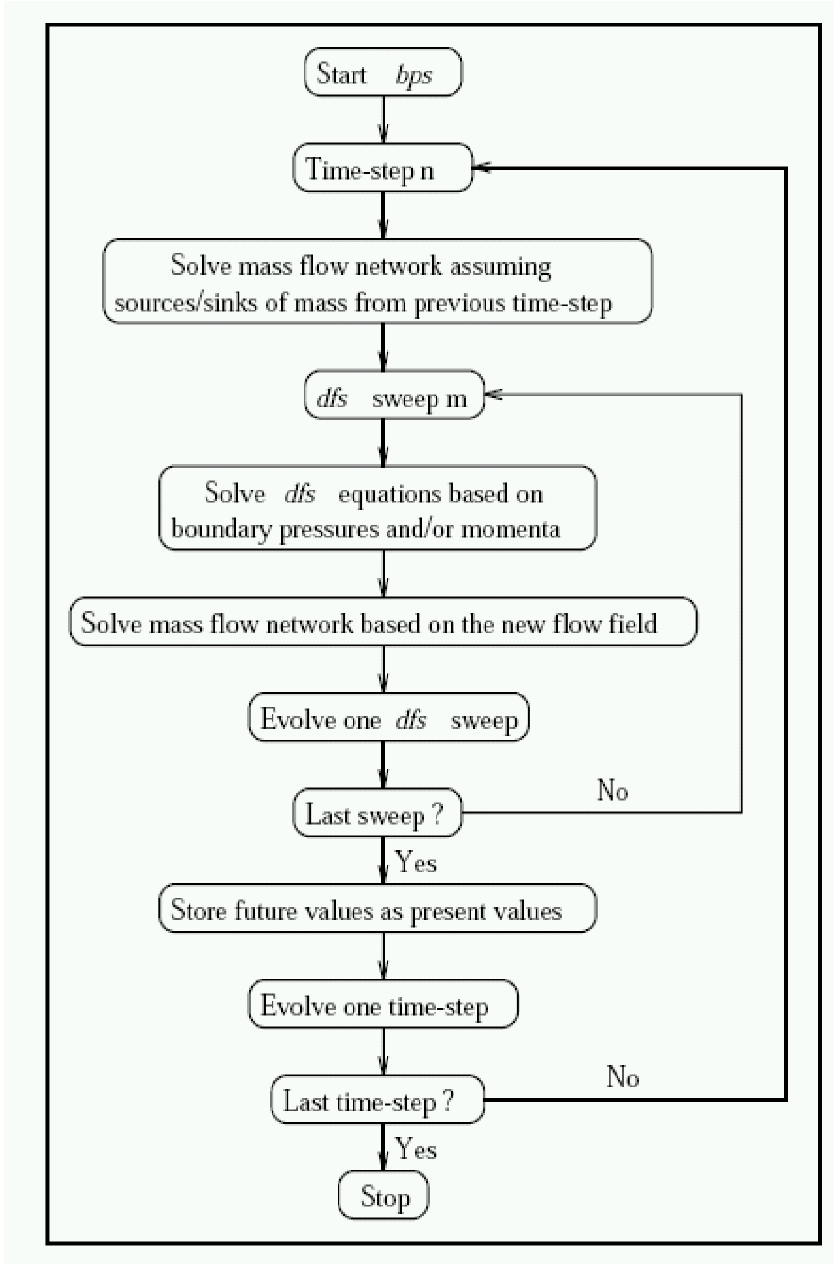

Figure 2.4 mfs-dfs Conflation Algorithm (Negrao 1995)

the network (and *dfs* at the next iteration). Probably for this reason information is passed back every *dfs* sweep because after one complete CFD convergence there is no new information available to be passed to *mfs*. This mechanism thus makes this approach inherently unstable.

Furthermore this algorithm cannot be used for a CFD domain with just two openings. This would cause mass imbalance. This will happen because the convergence criteria for mass flow networks is generally more relaxed than that for CFD (i.e. whereas a mass flow network is considered to be converged when the maximum residual is less than 10^{-2}kg (say) a CFD solver is much stricter when checking for convergence and may typically have a tolerance set at one tenth of this value or less). Therefore when imposing mass flow network predicted mass flow rates onto a CFD domain one has to normalise the flow rates so that they total zero exactly (or are within the CFD tolerance if known). This sort of a conflation mechanism can not handle two openings within a CFD domain firstly because there is no normalisation within the imposition of the mass flow type boundary condition (called velocity type boundary condition in ESP-r). Secondly if mass flows are passed to CFD (in terms of flow velocity and area) there will be no new information passed back when CFD converges because these mass flow rates however specified will be the boundary conditions which are of course invariant. Even if normalisation is introduced the CFD algorithm does not change velocity type inlet boundary condition but just changes all other cell pressures. This reason for this is that the pressure field obtained by solving the pressure correction equation does not give absolute pressures (Patankar 1980). The algorithm in ESP-r sets the pressure correction for the first velocity type opening to zero and corrects all other cell pressures. Hence if only pressure is fixed for the next *mfs* run the mass flow 'in' to the CFD domain will be the same whereas mass flow 'out' would have changed due to pressure correction.

This is illustrated with a hypothetical example. Consider the flow network of figure 2.5a. Suppose that node B is to be represented by a CFD domain as shown in figure 2.5b. In order to do this a conflated mass flow network is set up that defines air flow nodes for all openings in the CFD domain and replaces the original node representative of the CFD domain by the CFD domain itself. Figure 2.5a shows the original mass flow network and figure 2.5b and 2.5c show the conflated network. More detail of the method is given in Negrao (1995). The values of pressure at the nodes and the flow rates have already been determined by *mfs*. Now when the CFD solution proceeds the pressure of the first air flow opening type boundary condition is set to zero and all other cell and other boundary conditions pressures are computed from that datum. Supposing the opening on the left was initialised to zero, the opening on the right will be at a different (lower for this case) pressure. The CFD pressure datum is different from mfs datum so the CFD pressures (shown in blue in figure 2.5b) need to be corrected. The CFD pressures should now be corrected to *mfs* pressures which is a simple matter of adding the original node pressure (5Pa) to both the opening pressures. When the CFD has converged the final adjusted pressures of 5Pa and 4.5Pa will be passed back to *mfs* (figure 2.5c) which will now solve mass flows as function of pressure difference. This has the consequence that mass flow rate for the first opening is unaltered because its pressure is unaltered but pressure at the other opening has changed so a different mass flow rate will be calculated. It can be argued that the pressure drops are expected because of resistance of the room to air flow, but for a two opening only CFD domain, the mass flowing in must be equal to the mass flowing out which is not possible as shown in this example.

Due to this, there is no better way of knowing what the correct mass flow is apart from the original mass flow network that provides a value approximated because of not considering conditions within the CFD domain, this being the first set of boundary conditions passed to *dfs* which in turn provides pressures.

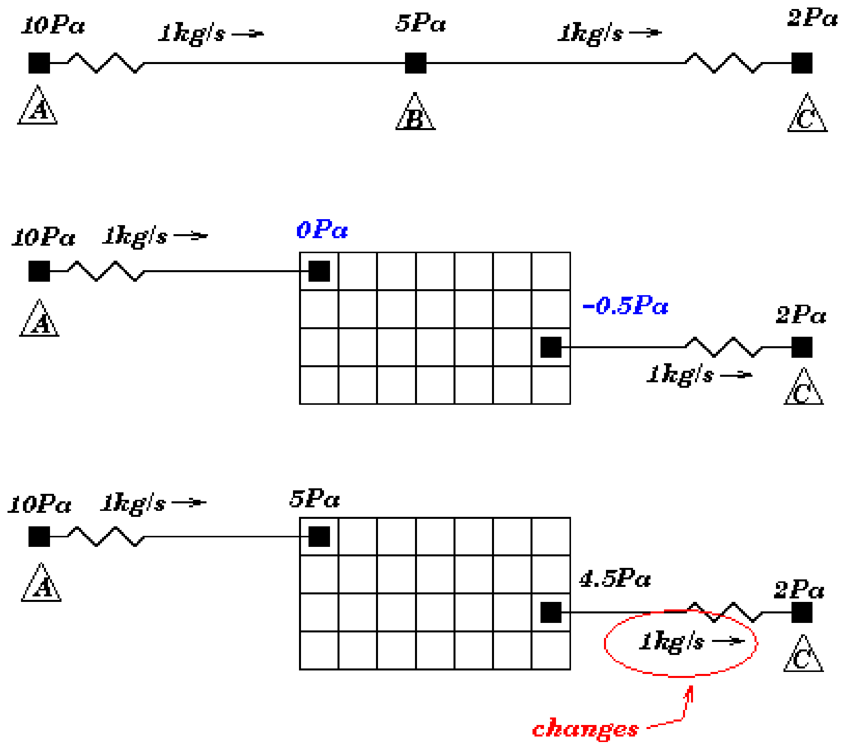

Figure 2.5a (top) shows the mass flow network with nodes A,B and C with hypothetical pressures and mass flow rates. This is replaced by the conflated network of figure 2.5b (middle): the pressures defined from the CFD datum are shown in blue. When the CFD defined pressures are brought up to the mfs datum, as shown in figure 2.5c (bottom), there is a pressure loss for the second opening and the circled mass flow rate changes.

The algorithm of figure 2.4 would also fail if there is a constant mass flow type air flow component down stream or upstream of the CFD domain. Such a network is shown in figure 2.3. It is possible that in such a network *dfs* calculates mass flow in one direction and *mfs* calculates a different mass flow in another direction or even different flow in the same direction, because the mass flow calculated by *mfs* will be independent of pressure for the constant mass flow type air component. Suppose that at a particular iteration *dfs* is in such a state that it predicts pressures corresponding to an air flow rate from node A to the CFD domain of 1kg/s. Because of mass conservation it is expected the same mass flow goes out of the domain to node B. Suppose further that node B is only connected to node C in the air flow network via a constant mass flow rate component which is different from 1kg/s. *mfs* would not be able to converge if the flow rate of this component is other than 1kg/s. One possible way around the problem is to connect nodes B and C via another connection albeit at the cost of accuracy. In more complicated networks it may be difficult and time consuming to detect where the problematic connection is located.

2.5 Research Objectives

The need then is to provide practitioners with the means to address contaminant behaviour within the built environment at an appropriate level of confidence. To achieve this suitable methods have to be identified and implemented.

This work aims to:

- develop a robust mechanism to integrate thermal and airflow simulation with contaminant modelling;
- validate this approach in order to gain confidence in the method used;
- apply this approach to real world problems and provide solutions for the provision of good indoor air quality;
- investigate control and ventilation options for contaminants;
- integrate airflow and CFD domains in order to appreciate intra-room distribution of contaminants under dynamic boundary conditions;

The objectives, if realised, will allow modellers to:

- improve contaminant behaviour predictions by including dynamic thermal effects;
- investigate design options, controls and optimisations based on thermal comfort requirements and indoor contaminant concentration levels;
- base more confidence in results from CFD contaminant appraisals;
- give designers the information needed for them to design better buildings.

2.6 References

Armstrong, P. R., Stenner, R. D., Hadley, D. L., Janus, M. C. 2001. *Whole Building Airflow Network Characterisation by a Many-Pressure-States (MPS) Technique.* ASHRAE Transactions 2001, Volume 107 Part II.

ASHRAE. 1997. *1997 ASHRAE Handbook – Fundamentals.* Atlanta: American Society of Heating, Refrigeration and Air-Conditioning Engineers, Inc.

ASHRAE. 1998. *Standard Method of Test for the Evaluation of Building Energy Analysis Computer Programs: ASHRAE Standard 140P*. Working Draft 98/2, American Society of Heating, Refrigerating, and Air-Conditioning Engineers, Atlanta USA.

Awbi H. B. 1998. *Calculation of Convective Heat Transfer Coefficients of Room Surfaces for Natural Convection.* Energy and Buildings 28.

Bazjanac V,Crawley D B. 1997. *The Implementation of Industry Foundation Classes in Simulation Tools for the Building Industry,* Proceedings. Building Simulation 1997, (1). International Building Performance Simulation Association, Prague Czech Republic.

Beausoleil-Morrison, I. 2000. *The Adaptive Coupling of Heat and Air Flow Modelling within Dynamic Whole-Building Simulation.* PhD Thesis, University of Strathclyde, Glasgow, UK.

Beausoleil-Morrison, I. 2001. *An Algorithm for Calculating Convective Coefficients for Internal Building Surfaces for the case of Mixed Flow in Rooms.* Energy and Buildings 33(4).

Beausoleil-Morrison, I. 2002. *The Adaptive Coupling of Heat and Air Flow Modelling within Dynamic Whole-Building Simulation.* PhD Thesis. ESRU. University of Strathclyde, UK.

Bossaer, A., Ducarme, D., Wouters, P., Vandaele, L. 1999. *An Example of Model Evaluation by Experimental Comparison: Pollutant Spread in an Apartment.* Energy and Buildings 30 (1999) 53-59.

CEC. 1999. *Energy Efficiency Standards for Residential and Non-residential Buildings*, P400-98-001, California Energy Commission, Sacramento USA.

Chen, Q., Peng, X., van Paassen, A. 1995. *Prediction of room thermal response by CFD technique with conjugate heat transfer and radiation models*. ASHRAE Transactions 3884:50–60.

Clarke J. A. 1977. *Environmental Systems Performance.* PhD Thesis, University of Strathclyde, UK.

Clarke J. A. 1982. *Dynamic Energy Simulation: the Integration of Building and Plant.* Proceedings. International Conference on System Simulation in Buildings. Commission of the European Communities, Liege, Belgium.

Clarke J. A., Hand J. W., Strachan P. A., MacRandal D. F. 1995. *The Development of an Intelligent, Integrated Building Design System Within the European COMBINE Project*, Proceedings. Building Simulation '95. International Building Performance Simulation Association, Madison USA.

Clarke J. A., Tang D. 2004. *A Co-operative Solver Approach to Building Simulation*. Proceedings. Esim Conference, Vancouver, Canada.

de Gids, W. F. 1989. *A perspective on the AIVC. Progress and Trends in Air Infiltration and Ventilation Research.* 10th AIVC Conference, Espoo, Finland.

Djunaedy E., Hensen J. L. M., Loomans M. 2005. *External Coupling between CFD and Energy Simulation: Implementation and Validation*. ASHRAE Transactions Vol 111(1).

Dols, W. S., Walton, G. N. 2002. *CONTAMW 2.0 User Manual.* National Institute of Standards and Technology, Gaithersburg, U.S.A.

Emmerich S. J. 1997. *Use of Computational Fluid Dynamics to Analyse Indoor Air Quality Issues,* National Institute of Standards and Technology report NISTIR 5997, USA.

ESRU. 2005. *The ESP-r System for Building Energy Simulation. User Guide Version 10 Series.* http://www.esru.strath.ac.uk

EU. 2002. *Directive 2002/91/EC of the European Parliament and of the Council on the Energy Performance of Buildings.* Official Journal of the European Communities.

FLUENT. 2003. *FLUENT User's Manual.* Fluent Inc. http://www.fluent.com

GATC. 1967. *Computer Program for Analysis of Energy Utilization in Postal Facilities: Volume 1 User' s Manual*, General American Transportation Corporation, Niles USA.

Hand J. W. 1998. *Removing Barriers to the Use of Simulation in the Building Design Professions,* PhD Thesis, ESRU, University of Strathclyde, UK.

Hand J. W., Irving S. J., Lomas K. J., McElroy L. B., Parand F., Robinson D., Strachan P. 1998, *CIBSE Application Manual AM11 Building Energy and Environmental Modelling*, Chartered Institute of Building Services Engineers, London UK.

Hensen J. 1995. *Modelling Coupled Heat and Air Flow: Ping-Pong vs Onions*. Proceedings. 16th AIVC Conference. Palm Springs. September 1995.

Hensen, J. 1991. *On the Thermal Interaction of Building Structure and Heating and Ventilating System.* PhD Thesis, Eindhoven University of Technology. The Netherlands.

Holmes, M. J., Lam, J. K. W., Ruddick, K. G., Whittle, G. E. 1990, *Computation of Conduction, Convection, and Radiation in the Perimeter Zone of an Office Space,* Proceedings. ROOMVENT '90 , Oslo Norway.

Huang H., Haghighat F., Wurtz E. 2002. *An Integrated Zonal Model for Predicting Transient VOC Distribution in a Ventilated Room.* Proceedings Esim Conference, Rochelle, France.

Jackman J. 1970, *A Study of Natural Ventilation of Tall Office Buildings,* J. Inst. Heat. Vent. Eng., 38.

Jensen S. O. 1993. *Validation of Building Energy Simulation Programs, Part I and II,* Research Report PASSYS Subgroup Model Validation and Development, CEC, Brussels, EUR 15115 EN.

Jones P. J., Whittle G. E. 1992. *Computational Fluid Dynamics for Building Air Flow Prediction— Current Status and Capabilities,* Building and Environment, 27 (3).

Judkoff R., Neymark J. 1995. *International Energy Agency Building Energy Simulation Test (BESTEST) and Diagnostic Method.* IEA Energy Conservation in Buildings and Community Systems Programme Annex 21 Subtask C and IEA Solar Heating and Cooling Programme Task 12 Subtask B.

Kusuda T, 1976. *NBSLD: The Computer Program for Heating and Cooling Loads in Buildings,* NBS Building Science Series No. 69, National Bureau of Standards, Washington USA.

Lebrun J. 1982. *Proceedings International Conference on System Simulation in Buildings,* Commission of the European Communities, Liege, Belgium.

Lomas K. J., Eppel H., Martin C., Bloomfield D. 1994. *Empirical Validation of Thermal Building Simulation Programs Using Test Room Data, Volume 1: Final Report.* IEA Energy Conservation in Buildings and Community Systems Programme Annex 21 and IEA Solar Heating and Cooling Programme Task 12.

Macdonald I. 2002. *Quantifying the Effects of Uncertainty in Building Simulation.* PhD Thesis. ESRU, University of Strathclyde, UK.

Maver T. W., Clarke J. A. 1984. *Major Extensions to the ESP System.* Final Report for Science and Engineering Research

Council Grant GR/C/2283.7, University of Strathclyde, UK.

McLean D. J. 1982. *The Simulation of Solar Energy Systems.* PhD Thesis, University of Strathclyde, UK.

Moser A., Schalin A., Off F., Yuan X. 1995. *Numerical Modelling of Heat Transfer by Radiation and Convection in an Atrium with Thermal Inertia,* ASHRAE Transactions , SD-95-14-4.

Negrao C. 1995. *Conflation of Computational Fluid Dynamics and Building Thermal Simulation.* PhD Thesis, ESRU, University of Strathclyde, UK.

Negrao, C. 1998. *Integration of Computational Fluid Dynamics with Building Thermal and Mass Flow Simulation.* Energy and Buildings 27(2).

Nielsen P. V. 1974. *Flow in Air Conditioned Rooms.* PhD Thesis, Technical University of Denmark, Denmark.

Nielsen P. V. 1989. *Airflow Simulation Techniques – Progress and Trends. Proceedings.* 10th AIVC Conference (1).

NRC. 1997. *Model National Energy Code of Canada for Buildings.* National Research Council of Canada, Ottawa.

NRCan. 1999. *Commercial Building Incentive Program for Energy-Efficient New Construction: Technical Guide for Office Buildings,* M92-157-4-1999E, Natural Resources Canada, Ottawa.

Papamichael K. 1999. *Application of Information Technologies in Building Design Decisions.* Building Research and Information, 27 (1).

Patankar, S. 1980. *Numerical Heat Transfer and Fluid Flow.* Hemisphere Publishing Corporation, Taylor and Francis Group, New York, USA.

Sander D. M. 1974. *FORTRAN IV Program to Calculate Air Infiltration in Buildings, DBR Computer Program No. 37*, National Research Council Canada, Ottawa.

Schild P. 1997. *Accurate Prediction of Indoor Climate in Glazed Enclosures.* PhD Thesis, Norwegian University of Science and Technology, Norway.

SESG. 1999. *Hotnews.* Official Newsletter of the Scottish Energy Systems Group. (1) May 1999.

Sherman M. H., Grimsrud D. T. 1980. *Infiltration-Pressurization Correlation: Simplified Physical Model.* ASHRAE Transactions , 86 (2).

Srebric, J., Chen, Q., Glicksman, L. 2000. *A Coupled Airflow and Energy Simulation Program for Indoor Thermal Environmental Studies.* ASHRAE Transactions 106(1).

Stephenson D. C., Mitalas G. P. 1967. *Cooling Load Calculations by Thermal Response Factor Method.* ASHRAE Transactions 73 (1).

Stewart J., Ren Z. 2003. *Prediction of Indoor Gaseous Pollutant Dispersal by Nesting sub-zones within a Multi-zone Model.* Energy and Buildings 38.

Tang D. 1985. *Modelling of Heating and Air Conditioning Systems*. PhD Thesis, University of Strathclyde, UK.

Thompson, C., Leaf, G. 1988. *Application of a Multi-grid Method to a Buoyancy-Induced Flow Problem. In: McCormick SF, editor. Multi-grid Methods–Theory, Applications and Supercomputing.* New York: Marcel Dekker Inc.

Versteeg H. K., Malalasekera W. 1995. *An Introduction to Computational Fluid Dynamics: The Finite Volume Method.* Longman Group.

Walton G. N. 1983. *Thermal Analysis Research Program Reference Manual.* NBSIR 83-2655, National Bureau of Standards, Washington USA.

Walton, G. N. 1988. *Airflow Network Models for Element-Based Building Airflow Modelling.* Technical Report, National Institute of Standards and Technology, Gaithersburg, U.S.A.

Weber, A., Koschenz1, M., Dorer, V., Hiller, M., Holst, S. 2003. *TRNFLOW, A new tool for the modelling of heat, air and pollutant transport in buildings within TRNSYS.* 8th International Building Performance Simulation Association IBPSA Conference, Eindhoven, The Netherlands.

Whittle G. E. 1986. *Computation of Air Movement and Convective Heat Transfer Within Buildings.* International Journal of Ambient Energy , 7 (3).

Xu W., Chen Q. 1998. *Numerical Simulation of Air flow in a Room with Differentially Heated Vertical Walls,* ASHRAE Transactions , 104 (1).

Zhai, Z., Chen, Q. 2003. *Solution Characters of Iterative Coupling between Energy Simulation and CFD Programs.* Building and Environment 35(5).

Zhai, Z., Chen, Q., Haves, P., Klems, J. 2002. *On the Approaches to Couple Energy Simulation and Computational Fluid Dynamics Programs.* Building and Environment 37(8-9).

3 Modelling & implementation

This chapter deals with theoretical aspects of the contaminant model developed within whole building simulation. The approach coupled with the network mass flow algorithm is examined in detail and justifications for such an approach are given. The solution mechanism for the resulting set of equations is also discussed and so is the actual implementation of the mathematical model into computer source code. Capabilities of the implementation are also described and so are some limitations of the model.

The model is based on calculation of concentrations assumed from mass conservation of contaminants. Contaminant is assumed to be fully mixed within the air and therefore contaminant transport is directly proportional to air flow between nodes. The airflow network solves first and the airflows are then used to calculate contaminant flow. The air flows can also be used as input data for more detailed analysis (e.g. CFD) which may have superior techniques for PM and fluid treatment.

3.1 Mathematical Analysis

In order to analyse the distribution and transport of contaminants in the indoor environment it is important to recognise that the single most important vector is ventilation air. It has been realised that in order to model contaminant behaviour indoors the underlying airflow patterns need to be understood (Axley 1987, Feustel and Rayner-Hooson 1990). If contaminant spread is assumed to be directly proportional to air flow the mathematical model is simplified and for contaminant gases this assumption is thought to be valid. In fact two of the major standalone contaminant prediction engines, COMIS and CONTAM, are based on this assumption. PM behaves differently from gases but these differences are neglected as a first approximation . (Some typical PM characteristics were expounded in Chapter 1). As a first approximation PM can be modelled as gases. Fundamental theory for contaminant modelling outlined below is adapted from CONTAM (Dols & Walton 2002) who use the theory in stand alone air flow and contaminant prediction software, but further developments are also described.

Consider a zone i , where the mass of air is m_i and the mass of contaminant α is $m_{\alpha i}$. The concentration of α will be given by:

$$C_{\alpha i} = \frac{m_{\alpha i}}{m_i} \tag{3-1}$$

For the purposes of modelling, a zone can be thought of as a single room, a part of a single room or a number of well mixed rooms. Equation (3-1) can be resolved for any number of zones. For simultaneous solution of contaminant concentration in all the zones it has to be replaced by equation (3-2) which is the matrix equivalent of equation (3-1). In equation (3-2) Q is a vector holding contaminant mass (kg) in a zone and X is the vector holding contaminant concentration for each zone (kg/kg). The matrix M is the zone air mass matrix and holds the mass of air (kg) for each zone on the principal diagonal and all other entries are zero.

$$Q=MX \tag{3-2}$$

This steady state equation can be used to calculate contaminant concentration at any time during a simulation. Contaminant is added to a zone by one of the following mechanisms:

1. Inward airflows from adjoining zones j and from the outside air. The air may be filtered at an efficiency of $\eta_{\alpha ji}$ where filter efficiency is the fraction of pollutant that the filter removes from inlet air.
2. Generation of contaminant within the zone because of sources $G_{\alpha i}$ (kg/s)
3. Production of contaminant due to chemical reactions of other contaminants.

Removal of contaminant from a zone can be accomplished by one or more of the following:

1. Outward airflows to adjoining zones and to the ambient at the rate of $\sum_j F_{ij} C_{\alpha i}$ where F_{ij} is the mass flow rate of air from zone i to zone j
2. Removal of contaminant within the zone because of sinks $G_{\alpha i}$ (kg/s)
3. Chemical reaction of contaminant to form other compounds that are also considered to be contaminants.

Consider a second contaminant β that can react with contaminant α. Assuming the reaction is a first order chemical reaction then if $K_{\alpha\beta}$ is the chemical reaction rate constant (/s), the rate of loss of mass of α will be given by $m_i K_{\alpha\beta} C_{\beta i}$. Assuming that the mass of any contaminant in a zone is negligible compared to the mass of air then the following differential equation can be set up.

$$\frac{dm_{\alpha i}}{dt}=-\sum_j F_{ij} C_{\alpha i}+\sum_j F_{ji}(1-\eta_{\alpha ji})C_{\alpha j}+m_i\sum_\beta K_{\alpha\beta}C_{\beta i}+G_{\alpha i} \tag{3-3}$$

This differential equation is approximated by the following difference equation:

$$m^*_{\alpha i}=m_{\alpha i}+\Delta T\left[\sum_j F_{ji}(1-\eta_{\alpha ji})C_{\alpha j}+m_i\sum_\beta K_{\alpha\beta}C_{\beta i}+G_{\alpha i}-\sum_j F_{ij}C_{\alpha i}\right] \tag{3-4}$$

Here $m^*_{\alpha i}$ is the future value of contaminant mass and ΔT is the time step. This difference equation which is a statement of conservation of contaminant mass is used to predict contaminant mass and hence concentration for all internal zones. Boundary conditions for this equation are imposed from ambient contaminant concentrations which may be constant or varying in time.

3.1.1 Matrix Implementation

Equation (3-4) can be written in vector form as shown below. Let $Q*$ represent future time row contaminant mass (kg) and Q^0 represent total flow rate of contaminant into or out of a zone and total mass of contaminant lost or gained due to chemical reactions or sources / sinks (kg/s). then $Q*$ will be given by equation (3-5).

$$Q^* = Q + Q^0 \Delta T \tag{3-5}$$

The problem then simplifies to calculating Q^0

3.1.2 Weighting of present and future time row values

Equation (3-5) in its present form can be solved to give an explicit solution for future contaminant concentration. The right hand side of the equation only contains values at the previous time row so the left hand side can be calculated by forward marching in time. It can be shown that such a scheme may be unstable (Gerald and Wheatley 1984). In order to overcome this problem averaging of future and present time row values was incorporated. Equation (3-6) shows this.

$$Q^* = Q + (1 - \zeta) Q^0 \Delta T + \zeta Q^{0*} \Delta T \tag{3-6}$$

Here Q^{0*} is the future total flow rate of contaminant into or out of the zone. ζ may be thought of as a weighting factor between the future and present concentration. The value of ζ was chosen to be 0.5 by default but it is possible to set it to any user specified value. Different values of ζ correspond to different solution mechanisms as follows:

$\zeta = 0$	(Fully explicit)
$\zeta = 1/2$	(Crank Nicolson)
$\zeta = 2/3$	(Galerkin)
$\zeta = 1$	(Fully implicit)

Values of ζ of ½ or above guarantee unconditional stability. Similar averaging is done within the CONTAM solution process and it has been reported that values above 0.75 reduce oscillations (Dols & Walton 2002).

3.1.3 Airflow mass matrix K

As described above the bulk of the problem is calculating Q^0 . The vector Q^0 is described so as to take in to account all the different parameters of equation (3-4). The vector is defined as:

$$Q^0 = KX + G \tag{3-7}$$

G is the source / sink contaminant mass rate vector. In practice source and sink terms can be functions of one or more physical parameters in a zone. It is often the case that such models depend on contaminant concentration. A correct route to solution of the problem then would be to include G in the equation as an unknown term. The different source / sink algorithms may further be dissimilar functions (i.e. one source / sink function may be polynomial another exponential and another trigonometric). It is assumed that contaminant concentration over the course of a time step varies such that the source / sink function remains continuous and finite. This assumption is a reasonable one in that for a five minute (typical) time step one would not expectoscillations in contaminant concentrations for a room and if rapid fluctuations in a contaminant source were experienced then this can be accommodated by decreasing the simulation time step. For example Ekberg (1994) reports a test chamber study using N_2O and concentrations changed by about 250ppm in 100 minutes. Using this assumption previous time row values are used for calculating source and sink terms that depend upon contaminant concentrations. For scheduled concentrations the value of course does not depend upon previous concentrations.

The air flow rate mass matrix K is defined using air flow rates into and out of a zone and chemical reaction rate constants. The matrix is built up with total air leaving a zone on the principal diagonal; it has chemical reaction rate constants along adjacent diagonals. All the information in this matrix is thus known (mass flow rates from a previously solved flow network and chemical reaction information from user input). The arrangement gives $2(N-1)$ diagonals for N contaminants exclusively for inputting chemical reaction information. The other elements in the matrix are either zeroes or air flows in to the zones from different flow paths. Figure 3.1 shows the matrix for a five node problem with 3 contaminants. For this problem it was assumed that the nodes are all internal.

In general the following rules are followed to order the elements of the air flow mass matrix:

$$k_{ij} = -\Sigma F_n \qquad [i=j]$$

$$[N(n-1)+1 \le i \le Nn]$$

$$k_{ij} = K \qquad [i \ne j]$$

$$[N(n-1) < j \le Nn]$$

$$[N(n-1) < i \le Nn]$$

$$k_{ij} = F_{mn} \qquad [i \ne j]$$

$$[j = N(m-1)+p]$$

$$K_{ij} = 0 \qquad [i \ne j]$$

$$[j \ne N(m-1)+p]$$

$-\Sigma F_1$	K_{12}	K_{13}	F_{21}	0	0	F_{31}	0	0	F_{41}	0	0	F_{51}	0	0
K_{21}	$-\Sigma F_1$	K_{23}	0	F_{21}	0	0	F_{31}	0	0	F_{41}	0	0	F_{51}	0
K_{31}	K_{32}	$-\Sigma F_1$	0	0	F_{21}	0	0	F_{31}	0	0	F_{41}	0	0	F_{51}
F_{12}	0	0	$-\Sigma F_2$	K_{12}	K_{13}	F_{32}	0	0	F_{42}	0	0	F_{52}	0	0
0	F_{12}	0	K_{21}	$-\Sigma F_2$	K_{23}	0	F_{32}	0	0	F_{42}	0	0	F_{52}	0
0	0	F_{12}	K_{31}	K_{32}	$-\Sigma F_2$	0	0	F_{32}	0	0	F_{42}	0	0	F_{52}
F_{13}	0	0	F_{23}	0	0	$-\Sigma F_3$	K_{12}	K_{13}	F_{43}	0	0	F_{53}	0	0
0	F_{13}	0	0	F_{23}	0	K_{21}	$-\Sigma F_3$	K_{23}	0	F_{43}	0	0	F_{53}	0
0	0	F_{13}	0	0	F_{23}	K_{31}	K_{32}	$-\Sigma F_3$	0	0	F_{43}	0	0	F_{53}
F_{14}	0	0	F_{24}	0	0	F_{34}	0	0	$-\Sigma F_4$	K_{12}	K_{13}	F_{54}	0	0
0	F_{14}	0	0	F_{24}	0	0	F_{34}	0	K_{21}	$-\Sigma F_4$	K_{23}	0	F_{43}	0
0	0	F_{14}	0	0	F_{24}	0	0	F_{34}	K_{31}	K_{32}	$-\Sigma F_4$	0	0	F_{43}
F_{15}	0	0	F_{25}	0	0	F_{35}	0	0	F_{45}	0	0	$-\Sigma F_5$	K_{12}	K_{13}
0	F_{15}	0	0	F_{25}	0	0	F_{35}	0	0	F_{45}	0	K_{21}	$-\Sigma F_5$	K_{23}
0	0	F_{15}	0	0	F_{25}	0	0	F_{35}	0	0	F_{45}	K_{31}	K_{32}	$-\Sigma F_5$

Figure 3.1 Air flow mass matrix for 5 node and 3 contaminants problem. ΣF_i *represents total flow out from node* i $K_{\alpha\beta}$ *is the rate constant between contaminants* α *and* β , F_{ij} *is the air flow from node* i *to node* j

In the above equation N is the total number of contaminants and n goes from 1 to the total number of nodes in the system. p is the contaminant number in the problem and m is the node of interest. For a problem with N contaminants and n nodes $N \times n$ equations will result and the corresponding air flow mass matrix K will be of order $N \times n$. For a large problem K is sparse. At run time the chemical rate constants are multiplied with node air mass in order to homogenise units for the matrix and exert proper implementation of equation (3-4). Equation (3-7) thus encapsulates all aspects of equation (3-4) and needs to be solved with equation (3-6) to describe contaminant behaviour.

For the network problem of figure 3.2 the matrix that would be formulated would exclude boundary nodes that have ambient concentration of contaminant, which is a known value. Furthermore suppose for some reason a user intends to keep the contaminant concentration at a known constant value for a zone (nodes representing such zones are called 'internal known nodes'). This is a similar case to having known boundary conditions for the problem. Hence for the problem of figure 3.2, the preconditioned matrix of figure 3.3 would be used.

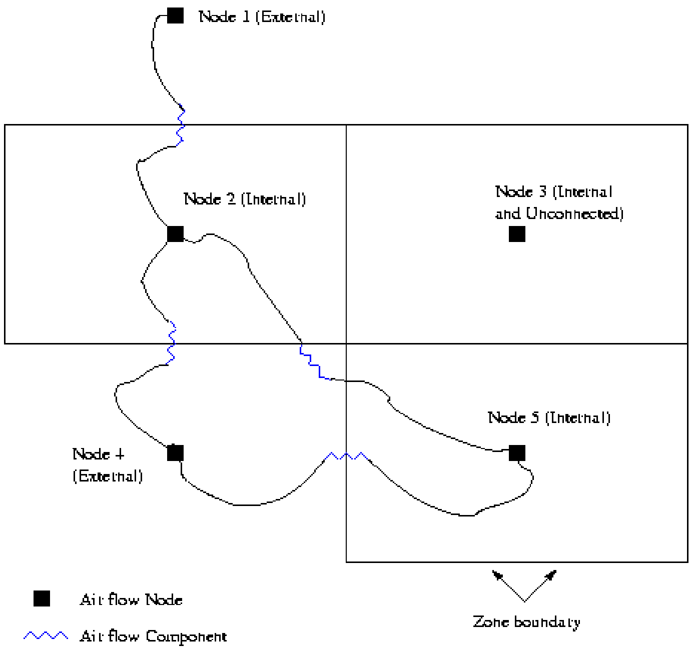

Figure 3.2 Example air flow network problem for matrix of figure 3.1

$-\Sigma F_2$	K_{12}	K_{13}	F_{52}	0	0
K_{21}	$-\Sigma F_2$	K_{23}	0	F_{52}	0
K_{31}	K_{32}	$-\Sigma F_2$	0	0	F_{52}
F_{25}	0	0	$-\Sigma F_5$	K_{12}	K_{13}
0	F_{25}	0	K_{21}	$-\Sigma F_5$	K_{23}
0	0	F_{25}	K_{31}	K_{32}	$-\Sigma F_5$

Figure 3.3 Preconditioned air flow mass matrix K^p for problem of figure 3.2

3.1.4 Calculation of Contaminant Concentration

Putting equations (3-2) and (3-7) in equation (3-6) gives:

$$MX^{*}=MX+(1-\zeta)\Delta T(KX+G)+\zeta\Delta T(KX^{*}+G) \quad (3\text{-}8)$$

After some rearrangement this equation becomes;

$$(M-\zeta\Delta TK)X^{*}=MX+(1-\zeta)\Delta T(KX+G)+\zeta\Delta TG \quad (3\text{-}9)$$

In this form the equation is solvable (after preconditioning) for X^* which is the future time row vector for contaminant concentrations using linear algebra solution techniques (see equation 3-10).

$$X^{*}=\left(M-\zeta\Delta TK\right)^{-1}\left(MX+(1-\zeta)\Delta T(KX+G)+\zeta\Delta TG\right) \quad (3\text{-}10)$$

3.1.5 Solution Procedure

Equation (3-10) is solved using Gaussian elimination with back substitution and no pivoting (Nyhoff and Leestma 1995). The matrix $(M - \zeta K \Delta T)^{-1}$ is forward reduced halfway, to a matrix whose components on the diagonal and above remain non-trivial. The solution vector $X*$ is then generated through back substitution of the known right hand side vector. It is likely that for large networks the matrix K^p will be sparse and this method of solution will not be optimal for speed. For such cases other solution techniques such as direct skyline algorithm, the iterative bi-conjugate gradient (BCG) algorithm or iterative successive over-relaxation (SOR) algorithm could be used. Such approaches have been reported in Dols & Walton (2002) and seem to give faster solution in some cases. For all the examples and problems in this thesis using Gaussian elimination, it was found that a solution could be obtained in a reasonable time (for example less than one minute[7] for a network with 15 nodes and 14 connections, using a Pentium III processor for one day simulation using five minute contaminant domain time steps and one hour building thermal domain and flow network domain time steps). This was considered to be satisfactory performance and other solution mechanisms were therefore not considered.

3.2 Assumptions built into the mathematical model

Within thermal modelling it is common to refer to zones. These can be thought of as room(s) although it is not infrequent to have a thermal zone comprising more than one room or a thermal zone made from part of a room. For the purposes of mass flow analysis a zone may be represented by one or more nodes. Boundary nodes are also defined and these are usually external to the building where boundary pressures can be calculated from wind and building facade data. Contaminant concentrations at these boundary nodes will also be known values.

The contaminant model can at best be as accurate as the airflow network model it is based on and all assumptions used for solution of the air flow network are implied for the contaminant model. The airflow network model is well established and understood. There is much documentation available (Lorenzetti 2002a, Hensen 1991, Walton 1988) and exhaustive explanation of assumptions have been reviewed. Some of the principal assumptions and limitations in this model are given below.

Assumptions regarding air flow network:

- Mass flow is a function of pressure and temperature difference.
- Air is incompressible.
- Pressure of air at a node is taken to be a single value at a particular time (similar assumption holds for density).
- Air and contaminants in a thermal zone are fully mixed so intra-zone contaminant distribution cannot be appraised.

7The time mentioned includes time for building thermal simulation and network air flow iterations as well.

Assumptions regarding contaminant prediction model:

- There are no contaminant transportation delays.
- Particulate matter is treated just like gas, and there is no mechanism to address processes like deposition (possibly gravitational settling), coagulation etc.
- In some cases propagation rate of contaminants may be overestimated or underestimated for poorly mixed zones.

The flow solver components produce a symmetric Jacobian matrix. At each time step, *mfs* (ESP-r network mass flow solver) repeatedly calculates and factors new Jacobian matrices. During this process it extracts trial solutions for the network using the Newton - Raphson method. A symmetric matrix requires only about half the storage capacity and may be factored in about half the time as a full matrix (Dennis and Schnabel 1996). The solution mechanism is accelerated within *mfs* by adopting an approach similar to Steffenson iteration (Clarke 2001). The efficiency gains are important because matrix factorisation dominates the solution time for the non-linear system. Another characteristic of the Jacobian matrix is that it is positive definite; this property guarantees existence of a unique solution (Lorenzetti 2002a). One assumption this leads to is that flow rate increases with pressure difference so as to ensure a positive rate of change. Another requirement is that each node connects directly or indirectly to a boundary node. Most flow components satisfy the first criterion. The second requirement is a function of mass flow network topology rather than flow components (Lorenzetti 2002b).

The flow network approach does not allow the study of momentum because a steady state flow based on pressure differences is calculated. Another potential problem could be delays associated with pollutant transport in flow paths. Dealing with this aspect would require accounting for both the pollutant mass stored in the flow paths and the time needed to carry it between nodes. Modelling all transport as instantaneous simplifies the assembly of the defining equations, but over-predicts the speed at which pollutant spreads through the building. One possible way around the problem could be that the addition of contaminant mass is delayed to the node it is travelling to for one or more time steps. This delay could be some function of the flow path the contaminants are taking. Transport delays were not implemented and are left as a recommendation for future work.

The airflow network solves before or after thermal solution as explained in (Clarke and Tang 2004). Although iterations at one time step are possible, this may not be usual simulation practice. Not iterating between thermal and mass flow simulations may cause some loss of accuracy.

3.3 Capabilities of the Contaminant Model

The developed approach is capable of modelling different source / sink algorithms, filter efficiencies, first order chemical equations, contaminant based air flow control and temporally varying ambient concentrations. Much of the theoretical background can be obtained from Axley (1995). There have been studies to quantify the various parameters involved in determining the behaviour of contaminants and some notable ones are studies involving emission rates (Persily et al 2002) and source strengths (Persily and Musser 2002). Whereas detailed models for the different physical processes were readily available, quantitative physical parameters to populate these models were not available for a majority of contaminants. This lack of information issue was faced time and again throughout the course of this research.

3.3.1 Source and Sink Algorithms

In the indoor environment, processes such as exhalation, emission of VOC from carpets, emission of formaldehyde from chipboard surfaces and radon decay are similar in that they are all sources of contaminant or other gases into the indoor air. There may be sinks in the indoor environment especially for those materials that can be adsorbed onto interior surfaces. For the present work a number of source / sink algorithms have been adapted for modelling such contaminant behaviour. Indoor contaminant sources from materials, furnishings, equipment and activities have been studied extensively, though much work remains before comprehensive databases are available. Much of this source data has been obtained through measurements in environmental chambers (ASTM 1997; Matthews 1987; Tucker 1991), and some of these measurements have been used to develop source models (Guo 1993). In terms of materials and furnishings much of the attention has focused on volatile organic compounds and on office buildings (Brown 1999a; Daisey et al 1994; Hodgson 1999; Hodgson et al 2000; Levin 1987). Particular attention has also been given to surface coatings (Salthammer 1997; Tichenor et al 1993), wood stains (Chang and Guo 1994), paint (Clausen 1994), adhesives (Girman et al 1986 and Nagda et al 1995), household cleaners and other products (Colombo et al 1991), floor coverings (Clausen et al 1993; Lundgren et al 1999), contaminated water (Little 1992; Andelman et al 1986; Keating et al 1997; Moya et al 1999; Howard-Reed et al 1999; Howard and Corsi 1996 and 1998) and office equipment (Brown 1999b; Wolkoff et al 1993). Building HVAC systems have also been investigated as contaminant sources (Batterman and Burge 1995). In addition to VOCs, some data are available for indoor sources of moisture (Christian 1993 and 1994), radon (Colle et al 1981, ECA 1995; Gadgil 1992; Revzan and Fisk 1992), combustion products from a range of appliances (Girman et al 1982; Mueller 1989; Nabinger et al1995; Traynor 1989; Traynor et al 1989) and from cigarette smoke (Daisey et al 1991). Contaminant entry associated with outdoor air can be another significant source, with much attention focused on ozone (Cano-Ruiz et al 1992) and particles (Weschler et al 1990). The issue of ambient contaminant concentrations is addressed later in section 3.3.5. However, when modelling entry of contaminants from outdoor air, one must account for the “efficiency” of penetration of these contaminants. Less than complete penetration is mostly an issue for particles, ozone and various reactive contaminants, and some data are available in this area (Weschler et al 1990). Contaminant loss due to surface deposition and reversible adsorption has received some attention, but again no comprehensive database is available for use in modelling. Most of the research to date has focused on model development (Axley 1994a) and experimental studies (Colombo et al 1994; Matthews et al 1987; Nazaroff et al 1993; Neretnieks et al 1993). There has been some model development in the area of water vapour storage on interior materials and furnishings (Jones 1993 and 1995; Kerestecioglu et al 1990), but data do not exist for the generalized application of such models.

A number of source and sink algorithms have been implemented for modelling contaminant behaviour and these are described in the following sections.

3.3.1.1 Constant Coefficient Source

If a source generates a constant mass of contaminant G_α at all times, the source term S_α is given by the following equation:

$$S_\alpha = G_\alpha \tag{3-11}$$

The term G_α can be thought of as the source strength of the source and the units are kg/s.

3.3.1.2 Cut-off Concentration Source

This source term is especially useful for certain volatile organic compounds. The initial contaminant source strength is G_α^0 and the generation of contaminant decreases as its concentration (C_α) increases until at a critical or cut-off concentration $(C_{\alpha co})$ the source ceases to produce any more contaminant. The expression used is as follows:

$$S_\alpha = G_\alpha^0 \left(1 - \frac{C_\alpha}{C_{\alpha co}} \right) \tag{3-12}$$

3.3.1.3 Exponential Decay and Generation

For some type of sources or sinks the concentration may change in proportion to the amount directly present. This model may be used for radioactive materials (e.g. radon) and for the decay of some volatile organic compounds. Equation (3-13) is used to calculate transient source / sink strength of the contaminant. In this equation G_α^0 is the strength (kg/s) at time t_0 , t is elapsed time and τ is the contaminant decay / generation time constant.

$$S_\alpha = G_\alpha^0 e^{\frac{\pm(t-t_0)}{\tau}} \tag{3-13}$$

3.3.1.4 Boundary Layer Diffusion Model

This is a reversible source / sink model that is used for modelling the absorption of volatile organic compounds in carpets etc. when concentration is high and desorption when concentration is low. The model is described in detail by Axley (1991). The following two equations completely describe the implementation:

$$m_s = \hat{m} A \tag{3-14}$$

$$S_\alpha = -h\rho A\left(C_{\alpha a} - \frac{C_{\alpha A}}{K}\right) \tag{3-15}$$

In the equations;

m_s = Mass of adsorbant (kg)

$\hat{m}$ = Mass of adsorbant per unit area of emitting / absorbing surface (kg/m^2)

A = Area of emitting / absorbing surface (m^2)

S_α = Source / sink strength (kg/s)

h = Average film mass transfer coefficient (m/s)

ρ = Film density of air (kg/m^3)

$C_{\alpha a}$ = Concentration of contaminant in air film (kg/kg)

$C_{\alpha A}$ = Concentration of contaminant in adsorbant (kg/kg)

K = Partition coefficient (dimensionless)

The partition coefficient describes the relationship between the concentration in the gas phase and the concentration in the material phase. It is a material property and is obtained experimentally (Huang and Haghighat 2001).

3.3.1.5 Time Dependent Constant Mass

This source / sink term is very similar to the constant coefficient source. The same equation is used but with the times of operation of this source / sink scheduled.

3.3.1.6 Personal Carbon dioxide Emission

This is a special source term used for modelling generation of carbon dioxide from occupants. Generation rates of carbon dioxide depend upon the metabolic rate of the occupants. Metabolic heat gain information may already be present in the thermal model. For the developed implementation using the ESP-r dynamic building simulation program, metabolic rates are an input to the thermal model and are provided in what are called zone operations files. These metabolic rates are obtained from the operations files by the contaminant source model and CO_2 source strength calculated as a linear function of occupants metabolic rate (adapted from Liddament 2004). The volume flow rate is then converted to mass flow rate by using density of CO_2 at that temperature. The density of CO_2 at that temperature is calculated using cubic interpolation using least squares (Monro 1982) from known values of density at different temperatures (Lide 2003).

An alternative approach is also possible in which metabolic rates are not taken from the operations file but are input manually. These are processed in a way that is similar to that described above.

3.3.2 Source and Sink Linkages with Contaminants and Nodes

Once sources and sinks have been defined the model has to link the contaminant with the appropriate source / sink model. Similarly the location of the source / sink has to be defined, i.e. which node is it associated with? This is accomplished by defining linkages between source / sink and contaminant, and between source / sink and node. In practice these are held as two, two dimensional arrays. At simulation time information for node and contaminant is read. Then if a source / sink is linked to a particular node and a particular contaminant, mass gained or lost due to it is computed and added to the total mass of contaminant in that node.

3.3.3 Filter Efficiencies

It is possible to place a filter in any airflow path or duct element to account for the removal of contaminants by filtration or gaseous air cleaning devices or by losses associated with air leakage paths. Within the airflow network airflow paths are represented by what are called components (ESRU 2001). The data needed to define a filter is a value from 0 to 1 which is the filter efficiency, and the contaminant for which that filter efficiency is to be used. This value is unique to a particular flow path or component. It is possible to define different filter efficiencies for different contaminants for the same component. Some efficiency data may be available from manufacturers and some data is available from literature, but there is no comprehensive database from which to draw efficiencies for different filter types. It is because of this reason that filter models have not been incorporated in the present work but facility for inputting of the actual filter efficiency values has been provided. Filtration characteristics are expected to be of greater importance to PM because of more information available. Some information is available for MERV[8] filters in ANSI / ASHRAE Standard 52.2-1999. Gaseous filter efficiencies are less widely available than particulate filter efficiencies. Although work has been done e.g. Persily and Ivy (2001), more work remains before efficiency data are widely available. A number of research papers have been written on the subject of gaseous air cleaning, some of which report measured efficiencies (Axley 1994b, Iwashita and Kimura 1994, VanOsdell and Sparks 1995).

3.3.4 First Order Chemical Reactions

A first order chemical reaction is one for which the rate of reaction and hence the concentration of a product is directly proportional to the first power of concentration of a reacting species. The way in which the matrices are formulated suggests that modelling of such reactions is quite easy because of linear dependence. The contaminant model allows reaction rate to be defined for two contaminants and then calculates the loss of one and the gain of the other as simulation proceeds. Second order and complex reactions can also be modelled but this was not attempted. It is mentioned as a recommendation for further work in this topic area.

For the first order reaction:

8 Minimum Efficiency Reporting Value

$$Contaminant\ \beta \rightarrow Contaminant\ \alpha$$

The generation of contaminant β is given by the product of concentration of contaminant α and the rate constant. Hence it shows that not only is contaminant β increasing but also that contaminant α is decreasing. The following relationship holds:

$$K_{\alpha\beta} = \frac{C_\alpha}{C_\beta}$$

The chemical reaction in a sense is a source or the product of the reaction and a sink of the reactant. In order to model this behaviour the source term for α is given by $m_i K_{\alpha\beta} C_{\beta i}$ kg/s.

3.3.5 Temporally varying Ambient Concentrations

Several studies (e.g. Zhang and Lioy 1994, Lawrence et al 2004) have shown that ambient concentrations of contaminants vary quite dramatically from one time to another. In view of this, a facility was added to define time varying ambient concentrations for contaminants. This facility allows the user to specify ambient contaminant concentration to either be constant or use a set of 24 hourly concentration values over a day. It is possible to increase the resolution of this data by using ESP-r's temporal definition facility but it has not been implemented.

3.4 Information Handling

3.4.1 Contaminants Definition File (*.ctm)

The ESP-r system uses a number of text based files to hold information. One such file is the airflow network file *.afn). A single file is used for the whole model and it holds information about air flow nodes, components and connections between the different nodes using components. Details of the file structure are given in e.g. (Hensen 1991, ESRU 2001). The contaminants definition file (*.ctm) is based on the airflow network file. Again one file is used to hold information about the whole model. The file is divided into seven sections. It also contains the name of the associated airflow network file. This is a quality control feature and users are warned if the airflow network file is changed. The various sections and their contents are described in table 3.1 and an example contaminants file is included in appendix CTM.

Section	***Comments***
1	Section 1 holds information about the total number of contaminants and the contaminant time step. The contaminant time step is the time step at which contaminant calculation runs. More is said about the contaminant time step in § 3.5.

Section	***Comments***
2	Section 2 holds contaminant names and ambient concentrations. Ambient concentrations are a list of 24 hourly values (which will be the same for constant ambient concentration contaminants). The number of source / sink models linked with the contaminants are also listed.
3	Section 3 holds information about chemical reactions. It holds chemical reaction rate constants for the reaction between contaminants. The user needs to define just one reaction rate and the model calculates the reaction rate of the reverse reaction and uses both at simulation time.
4	Section 4 holds node based information for the contaminants. Initial concentrations are held for all internal nodes (external nodes concentrations are taken to be equal to ambient). This is just an initialisation mechanism for contaminant calculations and it was shown that for a sufficiently large simulation (in terms of number of time steps) the effect of initial concentrations is negligible.
5	Section 5 holds component based information, specifically filter efficiencies of the flow component. Different efficiencies for different contaminants and the same component may be defined. Within the present implementation of the airflow network within ESP-r it is possible to use the same component in more than one connection. It can be thought of as different instances of the same calculation mechanism of that particular flow component. Filter information within the contaminants definition file is held at connection level and not at a component level so there is no need to define component based efficiencies.
6	Sections 6 and 7 hold source and sink information. Section 6 holds the number of source and sink models defined and also supplementary data items describing source / sink identity and other parameters describing these quantitatively.
7	Section 7 holds linkages information as to which source / sink is linked to which node and contaminant.

Table 3.1 Description of the contents of ESP-r contaminants network file.

3.4.2 Information I/O

During running of *prj* (standard ESP-r interface) information is read into common blocks. When the user exits from the contaminant definition menu, an option is given to the user to save contaminant information. It is at that point that file writing (to the *.ctm file) takes place. A previously defined contaminant file (if present) is read in when the contaminant option is selected within *prj*. At this time all contaminant common block elements are filled with requisite information from the contaminant file. For the case that such a file does not exist one is created when contaminants are defined.

3.5 Choosing a Suitable Time Step

It is important to choose a suitable time step and the following example illustrates this. Suppose there is a constant ambient concentration of contaminant α of 0. In the single zone example of figure 3.4 let initial contaminant concentration in the internal node be C_α. Suppose that a chemical reaction for contaminant β (ambient and internal concentration at C_β) has been defined in the contaminant model. The rate constant for the reaction is $K_{\alpha\beta}$. Then the only mechanism of addition of contaminant α to the zone will be chemical reaction of β and the only mechanism of removal of α from the zone is via ventilation to the ambient at the rate of $\dot{m}$ kg/s.

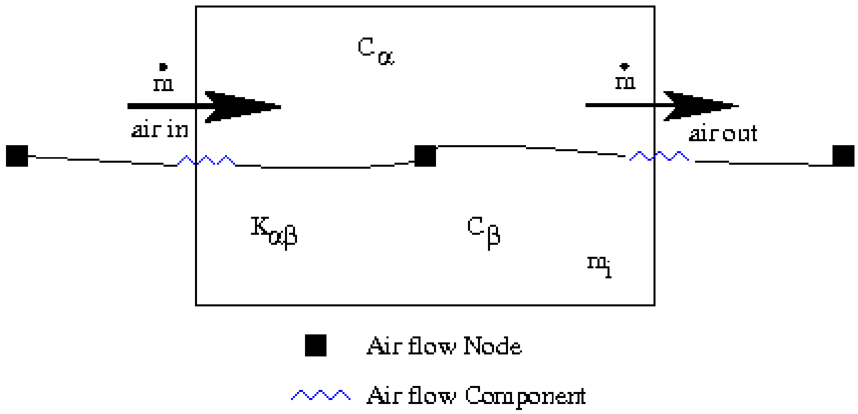

Figure 3.4 Example to illustrate proper time step selection

Let m_i be the mass of air inside the zone and ΔT be the time step then equation (3-4) becomes:

$$m_\alpha^* = m_i C_\alpha + \Delta T [m_i K_{\alpha\beta} C_\beta - \dot{m} C_\alpha] \tag{3-16}$$

The future mass of contaminant within a zone may not be negative although a zero value would be acceptable. This can be used to define an upper limit for simulation time step. This is shown below:

$$\Delta T \leqslant \frac{m_i C_\alpha}{\dot{m} C_\alpha - m_i K_{\alpha\beta} C_\beta} \tag{3-17}$$

This inequality suggests that for time step to be positive the following is true:

$$\dot{m} C_\alpha > m_i K_{\alpha\beta} C_\beta \tag{3-18}$$

Although this sets a limit to concentrations within a zone, in practice there seems to be no problem with this expression because typical reaction rates are many orders lower than typical indoor concentrations of contaminants (Weschler 2000). It may still be an important consideration where concentrations of chemicals are extremely low and initial and ambient concentrations are set to zero.

For a similar problem but with no generation of contaminant within the space inequality (3-17) reduces to:

$$\Delta T \leqslant \frac{m_i}{\dot{m}} \tag{3-19}$$

The expression on the right side is the room time constant τ and it is important in analytical calculations (as shown in appendices AS1, AS2 and AS3). Its reciprocal gives k, the room constant. In general terms the contaminant simulation time step should not be greater than the room time constant otherwise in certain cases it may result in the production of negative mass of contaminant in a room. For example the time constant for a room with x number of air changes per hour will be 1/x hours and therefore the contaminant simulation should be done at no less than x time steps per hour. For example the room time constant of room 3 in the model considered in test 2 (§ 4.3.2) is 12 minutes[9] therefore a simulation time step of 5 minutes is used. As an added quality control feature there is provision in the model to reset any non-positive concentration values to zero with a warning to the user to decrease the time step.

3.6 Contaminant Based Control

It has been shown in § 1.0 that providing adequate ventilation has an energy overhead. Building regulations define minimum ventilation levels for different kinds of spaces but these may not be optimum for good air quality. Control of ventilation air by sensing indoor contaminant conditions becomes quite relevant with reference to the background of varying patterns of ventilation requirements driven by energy considerations and requirement for good indoor air quality. Noting the inadequacy of prescriptive ventilation rates and the need to ventilate a space based on knowledge of acceptable levels of contaminant such a facility was incorporated into the contaminant model. The existing ESP-r control data structure was used and a contaminant sensor added. There is now the capability to control any air flow connection by sensing contaminant concentration at a node. The concept of control comprises the presence of the sensor in some part of the building that senses contaminant concentration. Based on the concentration being above or below a set point a decision is made for the operation of one or more air flow paths or components. The generic control features for ESP-r are retained. These include simple on/off controller, proportional controller (with or without hysteresis), range based controller and multi-sensor controller.

The on/off controller can be used with any mass flow component in order to open or shut it. Sensing of contaminant concentration can be used in a direct or inverse relation. The proportional controller is a linear hysteresis model that uses information about lower and upper contaminant concentration, relative position of the controlled variable at these values and the change in concentration needed in order to overcome hysteresis. The range based controller acts as a multi range controller with a high, mid and low set point for concentration. These set points yield four ranges with low range below the low set point, default range between low and mid set points, mid range between mid and high set points and high range above the high set point. The controller acts by increasing or decreasing the rate of flow or area of air flow components. The multi-sensor controller attempts to bring concentration of the associated node to the highest/lowest/mean/weighted value of the auxiliary sensors (ESRU 2001).

9 Room volume of $36m^3$ is roughly equivalent to 43kg of air. Dividing this with the air flow rate into the room (0.06kg/s) gives time constant.

3.7 Summary

The underlying theory of the zonal contaminant model was presented and its integration into the thermal and network flow domains developed. This was then derived into a form in which it was possible to form a network which can be solved by the simultaneous solution of system equations. An example illustrating how different matrices are set up was shown. Assumptions upon which the model is based were also examined and some justification of these given. The capabilities of the model were then described and so were some of the features unique to the implementation. The important advancement being domain integration implemented for thermal and contaminant prediction module within the broader air flow network module. There is some explanation of how data structures were manipulated and used during the definition stage within the user interface. An upper limit to the simulation time step was derived. Finally the importance of contaminant based control was emphasised.

3.8 References

Andelman, J. B., Couch, A., Thurston, W. W. 1986. *Inhalation Exposures in Indoor Air to Trichloroethylene from Shower Water*. Environmental Epidemiology, Lewis Publishers, Inc.

ASHRAE. 1992. *Standard 62-1992, Ventilation for Acceptable Indoor Air Quality*, American Society of Heating, Refrigeration, and Air Conditioning Engineers, 1992.

ASTM. 1997. *D5159-90, Standard Guide for Small Scale Environmental Chamber Determinations of Organic Emissions from Indoor Materials/Products*. American Society for Testing and Materials, USA.

Axley, J. W. 1987. *Indoor Air Quality Modelling Phase II Report. NBSIR 87-3661*. National Bureau of Standards. USA.

Axley, J. W. 1988. *Progress Toward a General Analytical Method for Predicting Indoor Air Pollution in Buildings, Indoor Air Quality Modelling Phase III Report. NBSIR 88-3814.* National Bureau of Standards. USA.

Axley, J. W. 1991. *Adsorption Modelling for Building Contaminant Dispersal Analysis.* Indoor Air 1991:1, 2.

Axley, J. W. 1994a. *Modelling Sorption Transport in Rooms and Sorption Filtration Systems for Building Air Quality Analysis*. Indoor Air 4 (1).

Axley, J. W. 1994b. *Tools for the Analysis of Gas Phase Air Cleaning Systems in Buildings.* ASHRAE Transactions 1994, Volume 100 Part 2. American Society of Heating, Refrigeration and Air Conditioning Engineers. USA.

Axley, J. W. 1995. *New Mass Transport Elements and Components for the NIST IAQ Model.* Indoor Air Quality and Ventilation Group. NIST 95-676. National Institute of Standards and Technology, USA.

Batterman, S., Burge, H. 1995. *HVAC Systems as Emission Sources Affecting Indoor Air Quality: A Critical Review.* HVAC&R Research 1 (1).

Brown, S. K. 1999a. *Chamber Assessment of Formaldehyde and VOC Emissions from Wood Based Panels.* Indoor Air, 9

(3).

Brown, S. K. 1999b. *Assessment of Pollutant Emissions from Dry Process Photocopiers.* Indoor Air 9 (4).

Cano-Ruiz, J. A., Modera, M. P., Nazaroff, W. W. 1992. *Indoor Ozone Concentrations: Ventilation Rate Impacts and Mechanisms of Outdoor Concentration Attenuation.* 13th AIVC Conference Ventilation for Energy Efficiency and Optimum Indoor Air Quality.

Chang, J. C. S., Guo, Z. 1994. *Modelling of Alkane Emissions from a Wood Stain.* Indoor Air 4 (1).

Christian, J. E. 1993. *A Search for Moisture Sources. Bugs, Mould & Rot II.*

Christian, J. E. 1994. *Moisture Sources. Manual on Moisture Control in Buildings*, MNL 18, 176-182. American Society for Testing and Materials.

Clarke, J. A. 2001. *Energy Simulation in Building Design.* Butterworth Heinemann. UK.

Clarke, J. A., Tang, D. 2004. *A Co-operating Solver Approach to Building Simulation.* Conference Proceedings. ESim 2004, The International Building Performance Simulation Association – Canada , Vancouver, June 2004.

Clausen, P. A., Laursen, B., Wolkoff, P., Rasmusen, E., Nielsen, P. A. 1993. *Emission of Volatile Organic Compounds from a Vinyl Floor Covering. Modelling of Indoor Air Quality and Exposure, ASTM STP 1205.* American Society for Testing and Materials, 3-13.

Clausen, P. A. 1994. *Emission of Volatile and Semivolatile Organic Compounds from Water Borne Paints – The Effect of the Film Thickness.* Indoor Air 4 (1).

Colle, R., Rubin, R. J., Knab, L. I., Hutchinson, J. M. R. 1981. *Radon Transport Through and Exhalation from Building Materials: A Review and Assessment.* National Bureau of Standards, Technical Note 1139.

Colombo, A., DeBortoli, M., Knoppel, H., Pecchio, E., Vissers, H. 1994. *Adsorption of Selected Volatile Organic Compounds on a Carpet, a Wall Coating, and a Gypsum Board in a Test Chamber*. Indoor Air 4 (1).

Colombo, A., DeBortoli, M., Knoppel, H., Schauenburg, H., Vissers, H. 1991. *Small Chamber Tests and Head space Analysis of Volatile Organic Compounds Emitted from Household Products.* Indoor Air 1(1).

Daisey, J. M., Gadgil, A., Hodgson, A. T. 1991. *Model Estimates of the Contributions of Environmental Tobacco Smoke to Volatile Organic Compound Exposures in Office Buildings.* Indoor Air 1 (1).

Daisey, J. M., Hodgson, A. T., Fisk, W. J., Mendell, M. J., Brinks, J. T. 1994. *Volatile Organic Compounds in Twelve California Office Buildings: Classes, Concentrations, Sources.* Atmospheric Environment 28 (22).

Dennis, J. E., Schnabel, R. B. 1996. *Numerical Methods for Unconstrained Optimisation and Non-linear Equations.* Society for Industrial and Applied Mathematics.

Dols, W. S., Walton, G. N. 2002. *CONTAMW 2.0 User manual. Multizone Airflow and Contaminant Transport Analysis Software.* NIST. USA.

ECA. 1995. *Radon in Indoor Air. European Collaborative Action, Brussels, Indoor Air Quality & Its Impact on Man,* Report No. 15.

Ekberg, L. E. 1994. *Outdoor Air Contaminants and Indoor Air Quality under Transient Conditions.* Indoor Air 1994;4, 2.

ESRU. 2001. *Data Model Summary ESP-r Version 9 Series.* University of Strathclyde, Glasgow, UK.

Feustel, H. E., Rayner-Hooson, A. (Editors). 1990. *COMIS Fundamentals.* Lawrence Berkeley Laboratory. Report LBL-28560. USA.

Gadgil. A.J. 1992. *Models of Radon Entry.* Radiation Protection Dosimetry 45 (1/4).

Gerald, C. F., Wheatley, P. O. 1984. *Applied Numerical Analysis, (3rd Edition).* Addison-Wesley Publishing Company.

Girman, J. R., Apte, M. G., Traynor, G. W., Allen J. R., Hollowell, C. D. 1982. *Pollutant Emission Rates from Indoor Combustion Appliances and Side stream Cigarette Smoke.* Environment International 8.

Girman, J. R., Hodgson, A. T., Newton, A. S., Winkes, A. W. 1986. *Emissions of Volatile Organic Compounds from Adhesives with Indoor Applications.* Environment International 12.

Guo, Z. 1993. *On Validation of Source and Sink Models: Problems and Possible Solutions. In Modelling of Indoor Air Quality and Exposure, ASTM STP 1205,* American Society for Testing and Materials, USA.

Hensen, J. L. M. 1991. *On the Thermal Interaction of Building Structure and Heating and Ventilating System*. PhD Thesis, Eindhoven University of Technology.

Hodgson, A. T. 1999. *Common Sources of Volatile Organic Compounds: Emission Rates and Techniques for Reducing Consumer Exposures.* California Environmental Protection Agency, Air Resources Board. CARB Contract No. 95-302.

Hodgson, A. T., Rudd, A. F., Beal, D., Chandra, S. 2000. *Volatile Organic Compound Concentrations and Emission Rates in New Manufactured and Site Built Houses.* Indoor Air 10 (3).

Howard-Reed, C., Moya, J., Corsi, R. L. 1999. *Mass Transfer of Volatile Organic Compounds from Drinking Water to Indoor Air: The Role of Residential Dishwashers.* Environment Science and Technology 33 (13).

Howard, C., Corsi, R. L. 1996. *Volatilisation of Chemicals from Drinking Water to Indoor Air: The role of the Kitchen Sink.* Journal of the Air and Waste Management Association 46.

Howard, C., Corsi, R. L. 1998. *Volatilisation of Chemicals from Drinking Water to Indoor Air: The role of residential Washing Machines.* Journal of the Air and Waste Management Association 48.

Huang, H., Haghighat, F. 2001. *Modelling of Volatile Organic Compounds from Dry Building Materials.* Proceedings ESim 2001 Ottawa, Canada.

Iwashita, G., Kimura, K. 1994. *Method for Evaluating Efficiency in Removing Perceived Air Pollutants by Air Cleaners.* Indoor Air 4 (1).

Jones, R. 1993. *Modelling Water Vapour Conditions in Buildings.* Building Services Engineering Research and Technology 14 (3).

Jones, R. 1995. I*ndoor Humidity Calculation Procedures.* Building Services Engineering Research and Technology 16 (3).

Keating, G. A., McKone, T. E., Gillett, J. W. 1997. *Measured and Estimated Air Concentrations of Chloroform in Showers: Effects of Water Temperature and Aerosols.* Atmospheric Environment 31 (2).

Kerestecioglu, A., Swami, M., Kamel, A. 1990. *Theoretical and Computational Investigation of Simultaneous Heat and Moisture Transfer in Buildings: "Effective Penetration Depth" Theory.* ASHRAE Transactions 96 (1).

Lawrence, A. J., Masih, A., Taneja, A. 2004. *Indoor / Outdoor Relationships of Carbon Monoxide and Oxides of Nitrogen in Domestic Homes with Roadside, Urban and Rural locations in a Central Indian Region.* Indoor Air 15 (1).

Levin, H. 1987. *The Evaluation of Building Materials and Furnishings for a New Office Building.* IAQ 1987 Practical Control of Indoor Air Problems.

Liddament, M. 2004. *Why CO_2? Air Infiltration Review, Volume 18, No 1, December 1996,* World Wide Web Edition © Oscar Faber PLC on behalf of the International Energy Agency, 1996. http://www.aivc.org/air/18_1/mwlco2.html

Lide, D. R. 2003. *CRC Handbook of Chemistry and Physics. 84th Edition.* CRC Press. ISBN 0-8493-0484-9

Little, J. C. 1992. *Applying the Two Resistance Theory to Contaminant Volatilisation in Showers.* Environmental Science and Technology 26 (7).

Lorenzetti, D. M. 2002a. *Computational Aspects of Nodal Multizone Airflow Systems.* Building and Environment 37 (2002).

Lorenzetti, D. M. 2002b. *Assessing Multizone Airflow Simulation Software.* Conference Proceedings, Indoor Air 2002, The International Academy of Indoor Air Sciences, Monterey, July 2002.

Lundgren, B., Jonsson, B., Ek-Olausson, B. 1999. *Material Emissions of Chemicals – PVC Flooring Materials.* Indoor Air 9 (3).

Matthews, G. 1987. *Environmental Chamber Test Methodology for Characterising Organic Vapours from Solid Emission Sources.* Atmospheric Environment 46 (3).

Matthews, T. G., Hawthorne, A. R., Thompson, C. V. 1987. *Formaldehyde Sorption and Desorption Characteristics of Gypsum Wall board.* Environmental Science and Technology 21 (7).

Monro, D. M. 1982. *FORTRAN 77.* Edward Arnold, London, UK. ISBN 0-7131-2794-5

Moya, J., Howard-Reed, C., Corsi, R. L. 1999. *Volatilisation of Chemicals from Tap Water to Indoor Air from Contaminated Water Used for Showering.* Environment Science and Technology 33 (14).

Mueller. E. A. 1989. *Indoor Air Quality Environmental Information Handbook: Combustion Sources. 1989 Update.* U.S. Department of Energy, DOE/EH/79079-H1.

Nabinger, S. J., Persily, A. K., Sharpless, K. S., Wise, S. A. 1995. *Measurements of Indoor Pollutant Emissions from EPA Phase II Wood Stoves.* National Institute of Standards and Technology, NISTIR 5575.

Nagada, N. L., Koontz, M. D., Kennedy, P. W. 1995. *Small Chamber and Research House Testing of Tile Adhesive Emissions.* Indoor Air 5.

Nazaroff, W. W., Gadgil, A. J., Weschler, C. J. 1993. *Critique of the Use of Deposition Velocity in Modelling Indoor Air Quality. In Modelling of Indoor Air Quality and Exposure, ASTM STP 1205*, N. L. Nagda. American Society for Testing and Materials.

Neretnieks, I., Christiansson, J., Romero, L., Dagerholt, L., Yu, J. W. 1993. *Modelling of Emission and Re-emission of Volatile Organic Compounds from Building Materials with Indoor Air Applications.* Indoor Air 3 (1).

Nyhoff, L., Leestma, S. 1995. *FORTRAN 77 and Numerical Methods for Engineers and Scientists*. Prentice Hall, NJ, USA.

Persily, A. K, Ivy, E. M. 2001. *Input Data for Multi-Zone Airflow and Indoor Air Quality Analysis.* http://www.bfrl.nist.gov/IAQanalysis/docs/NISTIR6585.pdf

Persily, A., Howard-Reed, C., Nabinger, J. 2002. *Transient Analysis of VOC Concentrations for Estimating Emission Rates.* Proceedings Indoor Air 2002. Monterey, California, USA.

Persily, A., Musser, A. 2002. *Multizone Modelling Approaches to Contaminant Based Design. ASHRAE Transactions 2002, Volume 108, Part 2*. American Society of Heating, Refrigeration and Air Conditioning Engineers. USA.

Revzan, K. L., Fisk, W. J. 1992. *Modelling Radon Entry into Houses with Basements: The Influence of Structural Factors*. Indoor Air 2.

Salthammer, T. 1997. *Emission of Volatile Organic Compounds from Furniture Coatings.* Indoor Air 7 (3).

Tichenor, B. A., Guo, Z., Sparks, L. E. 1993. *Fundamental Mass Transfer Model for Indoor Air Emissions from Surface Coatings*. Indoor Air 3 (4).

Traynor, G. W. 1989. *Selected Protocols for Conducting Field Surveys of Residential Indoor Air Pollution Due to Combustion-Related Sources. In Design and Protocol for Monitoring Indoor Air Quality, ASTM STP 1002, N.L. Nagda and J.P. Harper.* American Society for Testing and Materials. 166-177.

Traynor, G. W., Aceti, J. C., Apte, M. G., Smith, B. V., Green, L. L., Smith-Reiser, A., Novak, K. M., Moses, D. O. 1989. *Macro-model for Assessing Residential Concentrations of Combustion-Generated Pollutants: Model Development and Preliminary Predictions for CO, NO2, and Respirable Suspended Particles.* Lawrence Berkeley Laboratory, Berkeley, CA, LBL-25211.

Tucker, G. 1991. *Emission of Organic Substances from Indoor Surface Materials.* Environment International 17 (3).

VanOsdell, D., Sparks, L. 1995. *Carbon Adsorption for Indoor Air Cleaning. ASHRAE Journal 37 (2).* American Society of Heating, Refrigeration and Air Conditioning Engineers. USA.

Walton, G. N. 1988. *Airflow Network Models for Element-Based Building Airflow Modelling. Technical Report,* National Institute of Standards and Technology, Gaithersburg, USA.

Weschler, C. J. 2000. *Ozone in Indoor Environments: Concentration and Chemistry.* Indoor Air 2000;10, 3.

Weschler. C. J., Shields, H. C., Kelty, S. P., Psota-Kelty, L. A., Sinclair, J. D. 1990. *Comparison of Effects of Ventilation, Filtration, and Outdoor Air on Indoor Air at Telephone Office Buildings: A Case Study. Design and Protocol for Monitoring Indoor Air Quality, ASTM STP 1002, N. L. Nagda and J. P. Harper.* American Society for Testing and Materials.

Wolkoff, P., Wilkins, C. K., Clausen, P. A., Larsen, K. 1993. *Comparison of Volatile Organic Compounds from Processed Paper and Toners from Office Copiers and Printers: Methods, Emission Rates, and Modelled Concentrations.* Indoor Air 3 (2).

Zhang, J., Lioy, P. J. 1994. *Ozone in Residential Air: Concentrations, I/O Ratios, Indoor Chemistry and Exposures.* Indoor Air 1994;4, 2.

4 VALIDATION OF NETWORK MODEL

Validation is undertaken by first defining the validation methodology. Different validation exercises are then detailed and finally conclusions related to the validation studies are given. Validation methodology used by Jensen (1993) was adopted. The validation methodology comprises five components, not all of which need to be applied in a given context. In brief the methodology can be explained as in table 4.1:

Component	***Synopsis***	***Application***
Theory Checking	Theory of the developed computer model is examined to confirm that the theory is appropriate in terms of its application and scope.	This aspect is dealt with in Chapter 3 where theory for contaminant modelling is developed into a form that can be modelled.
Source code inspection	The code is checked to ensure that the selected algorithms are correctly implemented.	Structured programming and documentation ease this process (code checking tools (for syntax errors) and debugging tools (for logic errors) have been used).
Analytical verification	The output of the whole package or part of it is compared with the analytical solution for relatively simple contaminant distribution problems.	This chapter deals with these three aspects of program validation and each of these will be elucidated in the pages that follow.
Inter-program comparisons	The calculated results from the developed scheme is compared with other schemes within the program itself, or other programs which are considered to be better validated.	
Empirical validation	The output of the program is compared with monitored results from a real structure such as test cells.	

Table 4.1 Various components of the Validation Methodology

4.1 Validation Standard

Although IAQ models have been in use for quite some time, there is little guidance in the technical literature on the evaluation of such tools and ad-hoc procedures are employed in most instances. To provide quantitative evaluation of the contaminant model the ASTM standard D5157-97(2003) Standard Guide for Statistical Evaluation of Indoor Air Quality

Models was employed. The evaluation principles in the ASTM guide are drawn from past efforts related to outdoor air quality or meteorological models, which have objectives similar to those for IAQ models and a history of evaluation literature (Hanna 1988). This standard provides information on establishing evaluation objectives, choosing data sets for evaluation, statistical tools for assessing model performance and considerations in applying the statistical tools. The standard gives three statistical metrics for assessing accuracy and two additional metrics for assessing bias. Emmerich (2001) mentions that the ASTM D5157 standard has not been used effectively in previous validation studies and only a few ever use statistical techniques. Results from inter-model and empirical validation exercises are therefore compared based on the ASTM standard. Comments on the standard are also made in the light of the present research and the few others that have used this standard.

4.2 Summary of Validation Models

A number of ESP-r project models were developed to test the contaminant prediction tool. Subtle permutations on a basic model were also tested. In all, four basic test models were made and various aspects of contaminant simulation studied. These models were called test1, test2 and so on. In addition to these an ESP-r project model called namur was created. This model is representative of a flat near Namur, Belgium and was used in validation of contaminant prediction against empirical data collected in IEA Task 23 (IEA 1999). Table 4.2 gives a brief description of the various test models used for validation:

Model name	***Validation technique***	***Synopsis***
test1	Analytical	Single zone, three node model to study contaminant transport and generation/decay.
test2	Analytical	A more complicated network flow model to study transport of moisture.
test3	Analytical	A four node model to check convergence, consistence and stability of the proposed approach as the time step is decreased.
test4	Inter-program comparison (against CONTAM) and analytical	Similar to test2, this model simulated two contaminants. Source/sink models were studied along with filter efficiencies.
namur	Inter-program comparison (against COMIS) and empirical data	A seven zone model was built and simulated. This model represents an apartment that was previously modelled using COMIS and compared with empirical data.

Table 4.2 Summary of different validation studies

4.3 Analytical Validation

For the purpose of analytical validation a number of hypothetical test cells were created within ESP-r and contaminant simulations run against steady state boundary conditions to obtain contaminant concentration values. The results were then compared against analytical solutions. Tests 1, 2 and 3 below give the details for comparisons against the various analytical solutions.

4.3.1 Test 1

A single zone test cell model was made and a three node airflow network associated with it as shown in figure 4.1. At first only one contaminant (CO_2) was considered but then this number was increased to two. The ambient concentration of CO_2 was assumed to be constant at 4.6×10^{-4}kg/kg air. The change of CO_2 concentration within this zone was then compared with the analytical solution (appendix AS1); an example of a typical comparison is shown in figure 4.2. Heinsohn (1991) defines a room time constant (-1/*k*) such that at time *t* the contaminant concentration increases at the rate exp(-*kt*). A simulation time step of the order of the time constant or less is considered to give results that are reasonably accurate. Due to the very simple configuration of this model the simulation time step was chosen to be 60 minutes although a time step of the order of the room time constant (around 5 minutes) would have been more suitable in another circumstance (see section 3.3.5 for limits on time steps). It was found that such a time step did not adversely affect the comparison for the simple configuration of test1.

This test was done with the following variants:

Test 1-1: Initial contaminant concentration was zero and no generation/decay rate or filters were considered. The increase in contaminant concentration within the internal space, because of transport from outside air, was evaluated and compared with analytical results as given in appendix AS1.

Test 1-2: Initial internal and ambient concentration were both put equal at 4.6×10^{-4}kg/kg air, and an ideal filter was used to bring air into the room. No source/sink was present. The decay of contaminant in the room, because of transport to the outside, was compared with analytical results as given in appendix AS1.

Test 1-3: Initial internal concentration was assumed to be zero and an ideal filter was used for the air inlet. A constant coefficient source model of contaminant was used to generate the same amount as was brought in the room by test 1-2.

Figure 4.2 shows a typical result from test1-1. For the other tests of this series similar results were obtained but are not shown in the interest of brevity. On average a deviation of 0.01% or less was observed for all the simulated results.

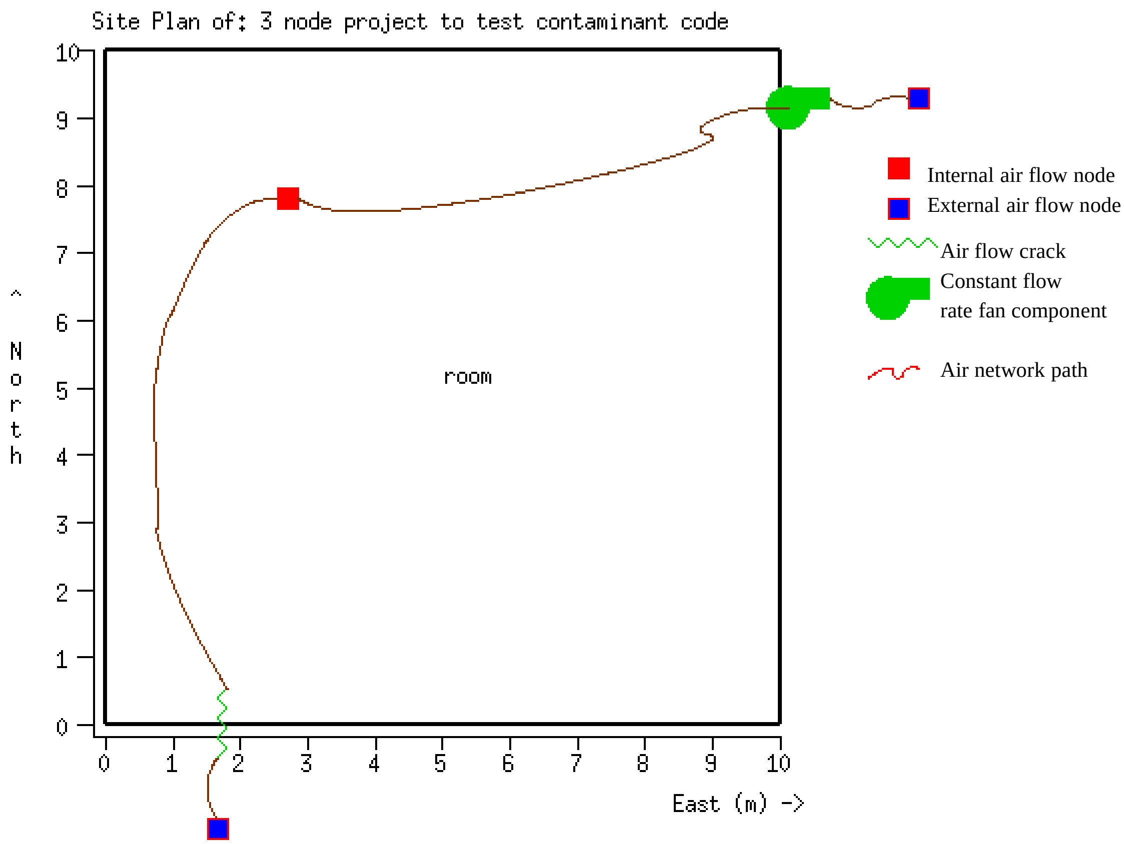

Figure 4.1 Plan of project model for test1 and associated flow network

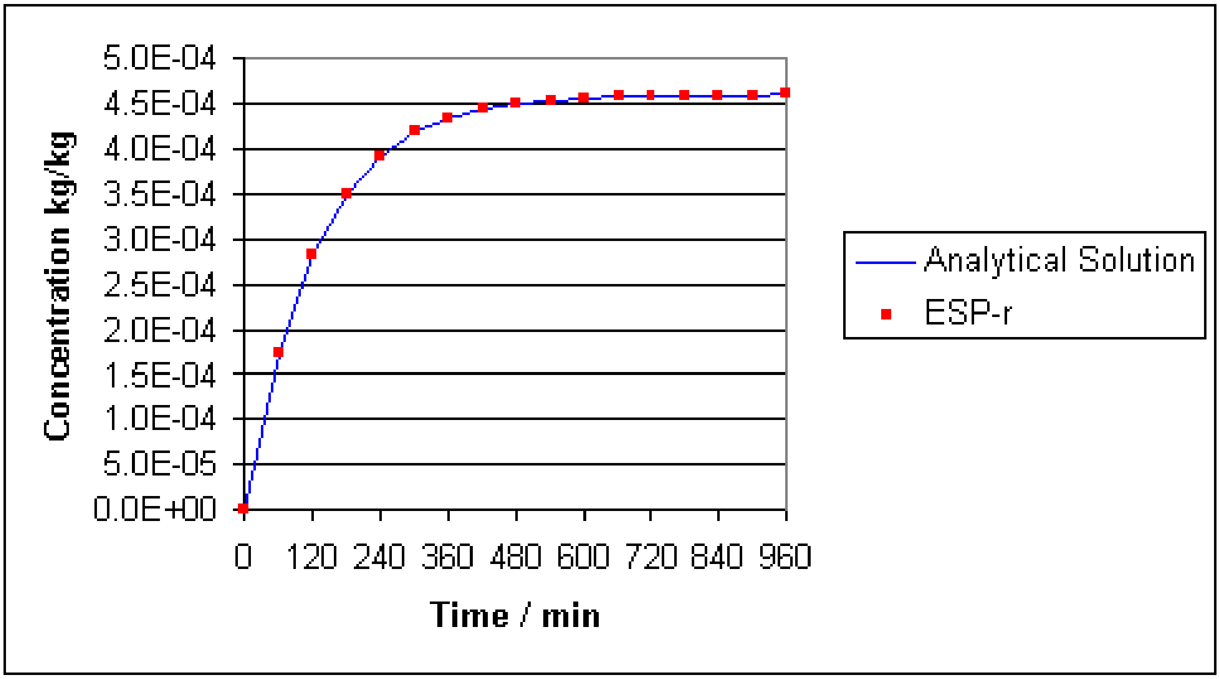

Figure 4.2 Typical result for test1-1

4.3.2 Test 2

A slightly more complicated model was chosen for this test. The simulation time step was decreased to five minutes. The objectives of this test were twofold: firstly to study the contaminant prediction model in a bigger and more complicated network and secondly to check the approach used to deal with unconnected nodes[10]. An isometric view of the model and associated airflow network are shown in figure 4.3. The contaminant chosen this time was water vapour (strictly not a contaminant, it can be simulated in the same way). An external concentration of 0.002173kg/kg was chosen: this corresponds to a relative humidity of 50% at 2^{0}C and 1.01325bar atmospheric pressure (Rogers and Mayhew 1995). Initial internal conditions were assumed to be perfectly dry i.e. with no moisture. Increase in moisture content (kg/kg) was predicted from the simulations and this was compared with the analytical solution for the model (appendix AS2). Results for the three zones are shown in figure 4.4. These show good agreement between the ESP-r contaminant model and analytical solutions (Appendix AS2).

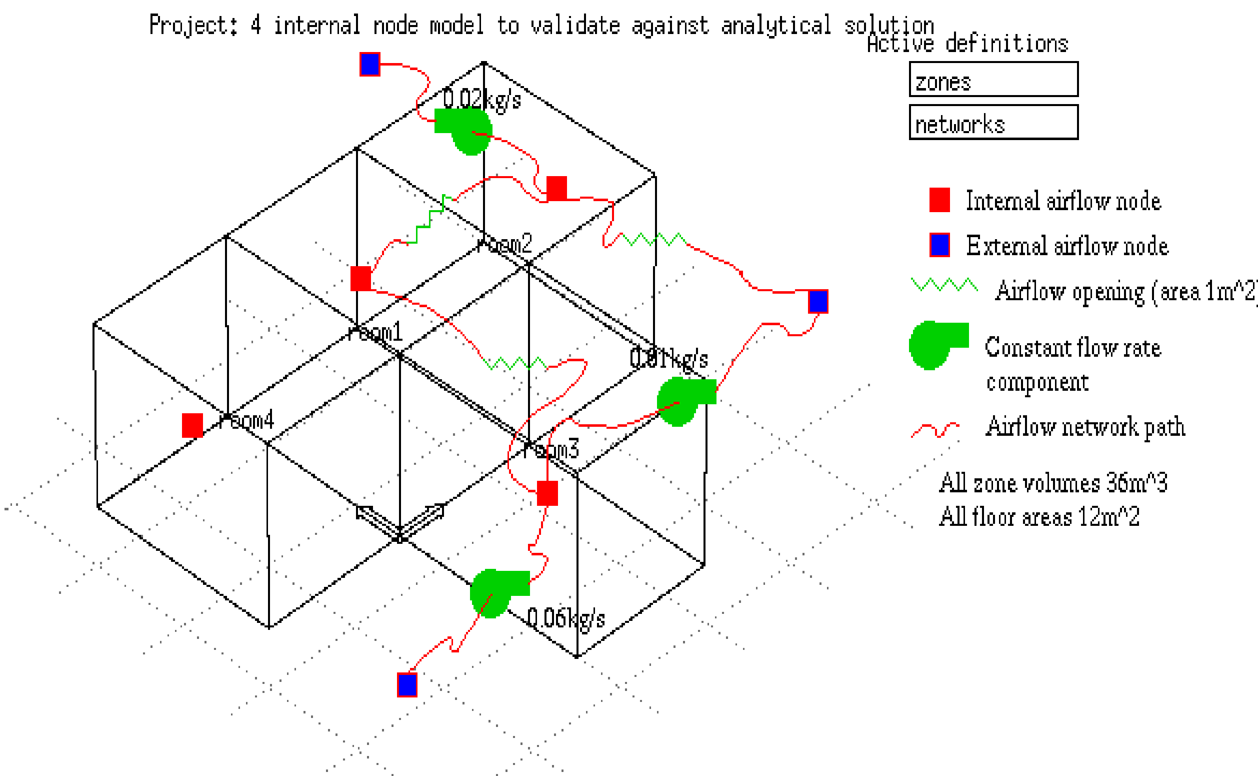

Figure 4.3 Isometric view of model for test2 and associated airflow network

10Unconnected nodes may cause a problem in the matrix setup for contaminant analysis. Because the flow rates for unconnected nodes is zero, one or more rows with zero elements may be obtained if unconnected nodes are included in the analysis. This causes problems during solution. A facility was provided to exclude unconnected nodes from the analysis but at the same time allowing them to be defined in the airflow network.

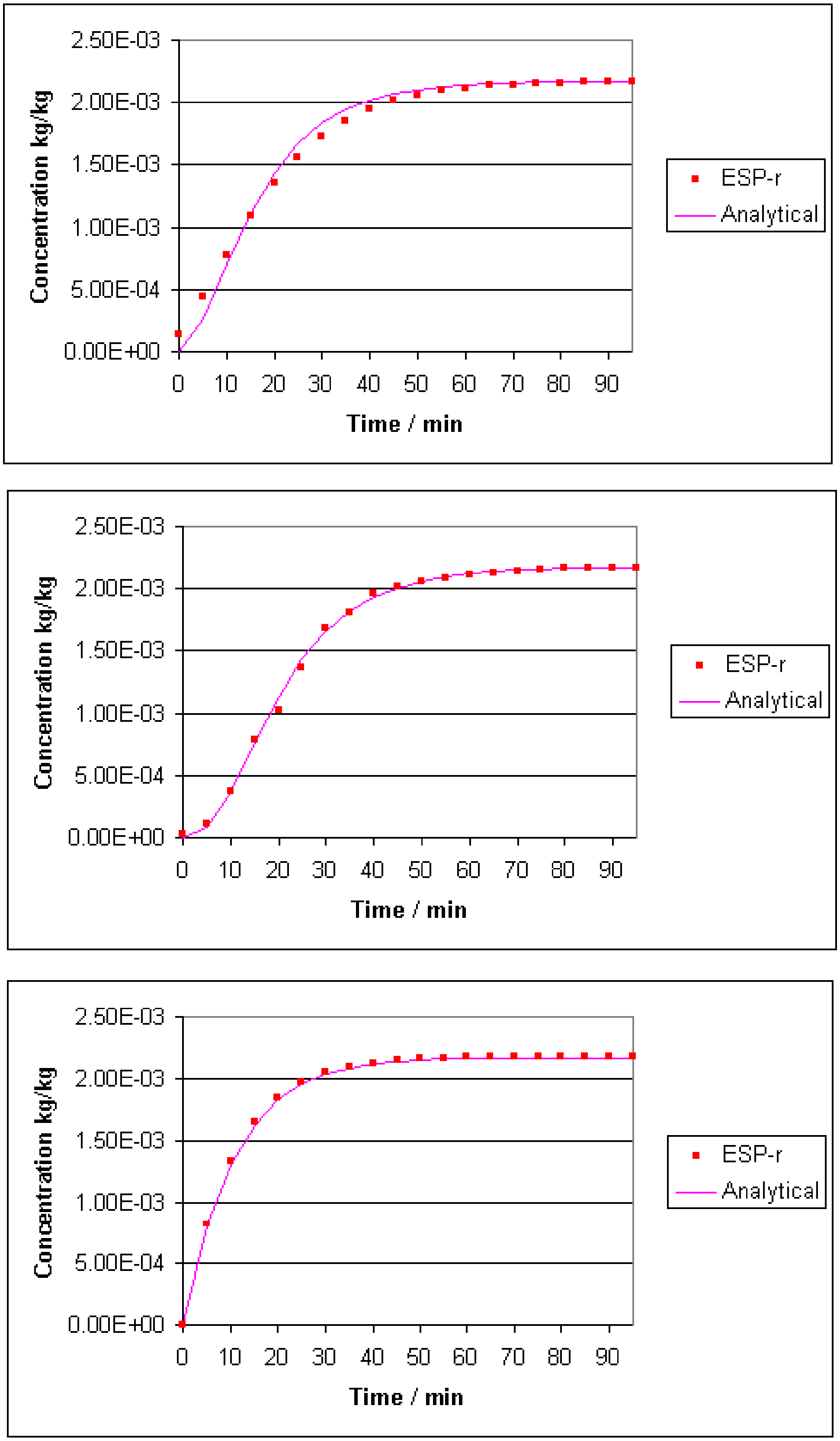

Figure 4.4 Moisture content results for room1 (top), room2 (middle) and room3 (bottom)

4.3.3 Test 3

The model for this test consisted of two zones and four air flow nodes. Details of the model are given in figure 4.5 and an analytical and numerical solution for contaminant concentration is given in appendix AS3. This test was designed to investigate how the code responded in terms of convergence, consistency and stability. These three mathematical concepts are defined in Versteeg and Malalasekera (1995 pp. 6) and are useful in determining the success or otherwise of a numerical solution algorithm. Convergence is defined as the property of a numerical method to produce a solution which approaches the exact solution as the discretization parameters of the numerical solution are reduced towards zero. Consistent numerical schemes produce systems of algebraic equations which can be demonstrated to be equivalent to the original governing equations as the discretization parameters approach zero. Stability is associated with damping of errors as the numerical method proceeds. If a technique is not stable, even round off errors in the initial data can cause wild oscillations or divergence. The discretization parameter in the contaminant model is time and this test compared results as the time step was reduced. As the time step was decreased from 10 minutes to 1 minute the error was seen to decease (figure 4.6). This indicated that the code converged to the analytical solution as the time step (t) approached zero. Consistency of the numerical equations was checked against analytically generated ones and it was found that as time step approached zero numerical solution approached the analytical solution. Stability of the numerical method can be demonstrated from the graph of figure 4.6 in that no oscillations are seen.

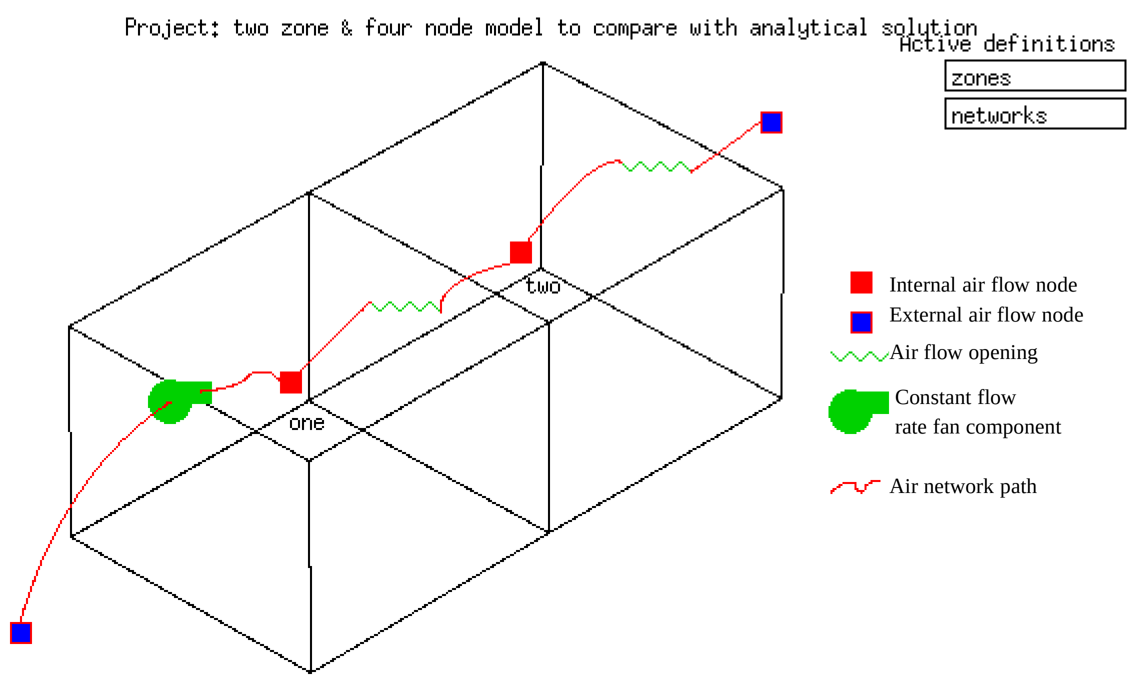

Figure 4.5 Model details for test3

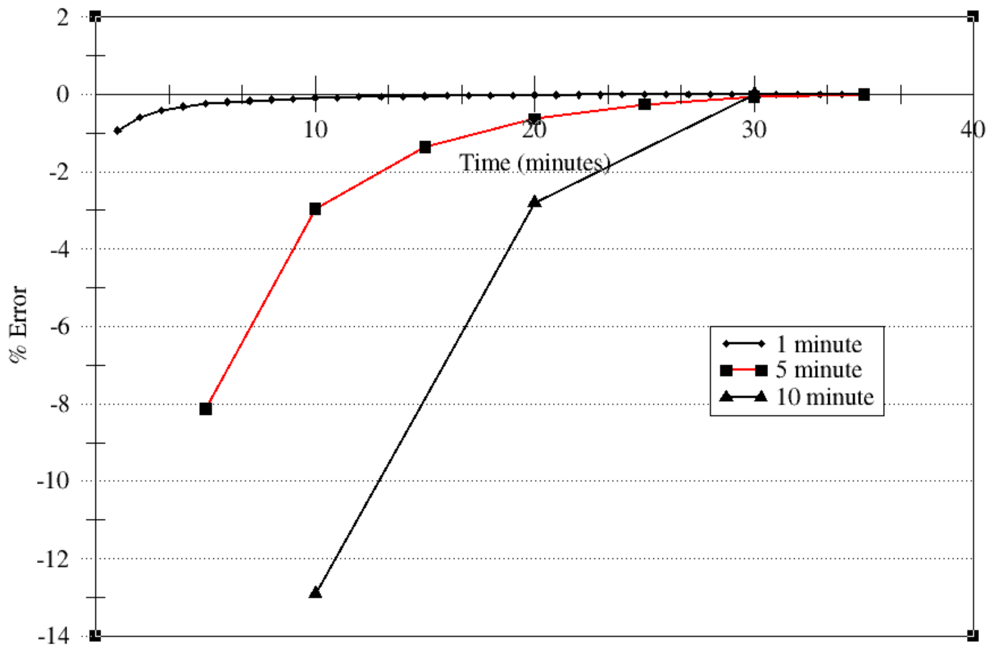

Figure 4.6 Effect of reducing time step on results accuracy

4.4 Inter-program comparisons

The NIST software CONTAM 2.0 (Dols and Walton 2002) was chosen for validation. CONTAM is a multi-zone indoor air quality program which resembles the standalone mass flow solver *mfs* within ESP-r. CONTAM can furthermore solve for contaminant concentrations as scalar quantities by assuming contaminant mass flow to be directly proportional to the air mass flow rate. It assumes well mixed zones and can provide for non-trace contaminants (i.e. the density of air changes depending upon the type and amount of contaminant). It is not integrated with thermal simulation but takes temperature variations into account by schedules. This software was chosen because of availability, comprehensive documentation and the presence of a support group.

4.4.1 Test 4

The model considered was similar to the one used for test2. A steady state climate of 20^0C dry bulb temperature and zero wind speed was chosen. The model as it appears on the CONTAM sketchpad is shown in figure 4.7. It was also possible to formulate an analytical solution to the problem details of which can be found in appendix AS4. Results were also compared according to ASTM D5157. ASTM D5157 defines six parameters and requires that values of these be within certain ranges: details of these can be found in table 4.3. The parameters were calculated for both ESP-r and CONTAM and both programs show good agreement when compared with the analytical solutions. One reason for this may be that the standard is meant for comparison when airflow rates are also computed by the program and in this test airflow rates were carefully maintained by constant flow rate components.

There were three permutations of a basic model:

Test 4-1: Two contaminants, contaminant1 and contaminant2 were considered. Both had ambient concentrations of 0.0008kg/kg. Initial concentration of contaminant1 was zero in all three zones but contaminant2 had concentrations of 0.0020, 0.0016 and 0.0012kg/kg in zones one, two and three respectively.

Test 4-2: This test was similar to test 4-1 but with the addition of a constant coefficient source of 0.005kg/s in zone two and a cut-off concentration source of 0.005kg/s in zone three with a cut-off concentration of 0.2kg/kg. Both sources were for contaminant 1.

Test 4-3: This was similar to test 4-2 but with a filter (13% efficient) for air entering zone one and a chemical reaction between the two contaminants.

Results for test 4-1 are displayed in table 4.4. Results for the other tests were quite similar. Graphical results from test 4-2 are shown in figure 4.8. It can be seen that ESP-r gives better agreement than CONTAM. This could be because of better configuration of the problem, quicker response time and absence of pointer algebra within ESP-r. The solution techniques for the two tools are also different. Results for test 4-3 were similar to the other two tests and are not shown.

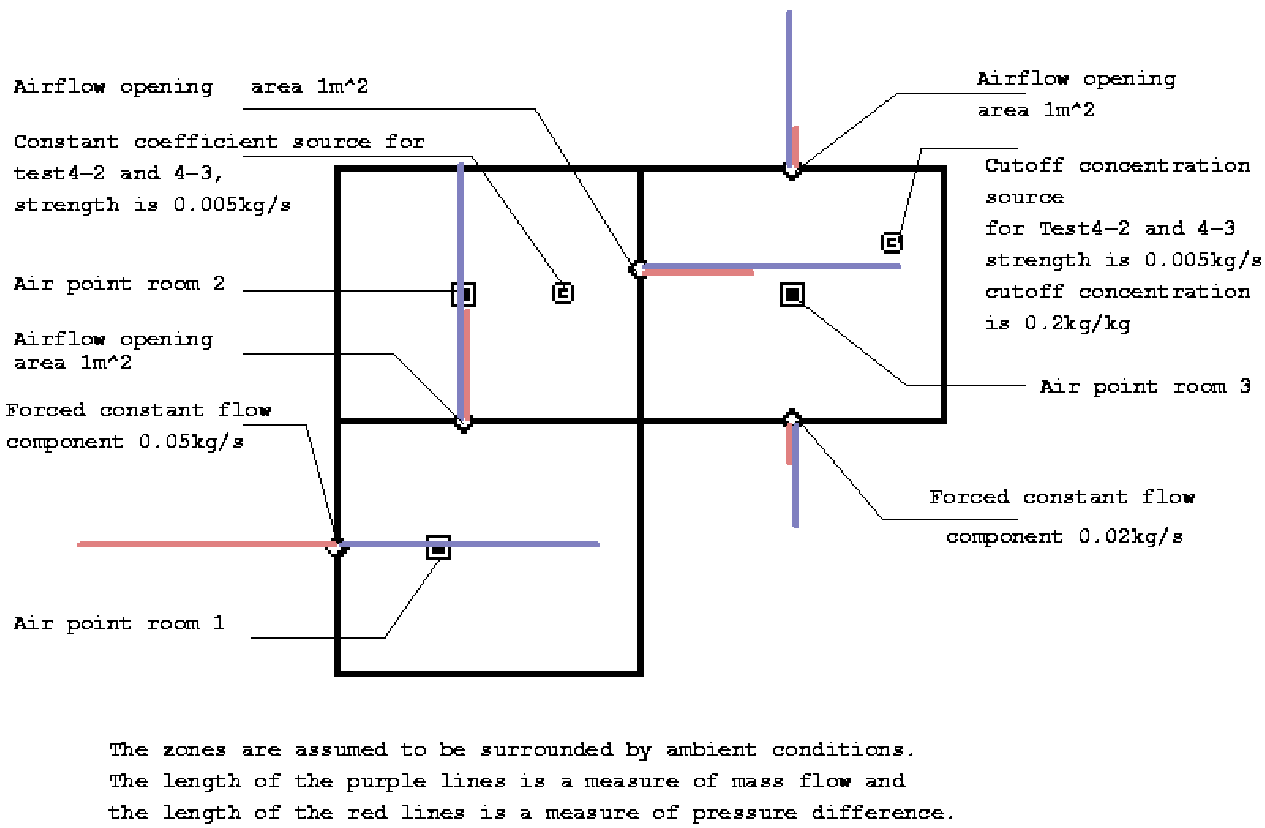

Figure 4.7 CONTAM sketchpad for test4

Parameter	***Synopsis***	***Prescribed Range***
r	Correlation coefficient	0.9 to 1.0 or -0.9 to -1.0
b	Slope of line of regression	Between 0.75 and 1.25
a	Intercept on vertical axis of line of regression	25% or less of average measured concentration
NMSE	Normalized mean square error	0.25 or lower
FB	Normalized or fractional bias	0.25 or lower
FS	Similar index of bias based on variance	0.5 or lower

Table 4.3 ASTM D5157 criteria for statistical evaluation of IAQ models

	Zone one		***Zone two***		***Zone three***	
	Contaminant 1					
	CONTAM	***ESP-r***	***CONTAM***	***ESP-r***	***CONTAM***	***ESP-r***
r	1.00	1.00	1.00	1.00	1.00	1.00
b	1.00	0.99	0.98	0.99	0.96	0.99
a	-2.5×10^{-5}	4.3×10^{-6}	1.2×10^{-6}	1.3×10^{-6}	6.1×10^{-6}	3.6×10^{-6}
NMSE	7.5×10^{-4}	8.5×10^{-5}	1.1×10^{-3}	4.5×10^{-5}	1.8×10^{-3}	5.0×10^{-5}
FB	0.0210	0.0072	-0.0260	0.0046	-0.0280	0.0039
FS	0.0440	-0.0240	-0.0450	0.0140	-0.0900	-0.0083
	Contaminant 2					
r	1.00	1.00	1.00	1.00	1.00	1.00
b	1.01	0.99	1.00	1.00	1.00	1.00
a	-4.1×10^{-5}	1.9×10^{-6}	-2.0×10^{-5}	-6.5×10^{-6}	-1.3×10^{-5}	-1.2×10^{-6}
NMSE	8.0×10^{-4}	9.6×10^{-5}	4.9×10^{-4}	4.3×10^{-5}	5.1×10^{-4}	5.6×10^{-5}
FB	0.0210	-0.0086	0.0130	-0.0042	0.0044	0.0021
FS	0.0450	0.0120	-0.0850	0.0340	0.0210	0.0650

Table 4.4 ASTM D5157 results for test4-1

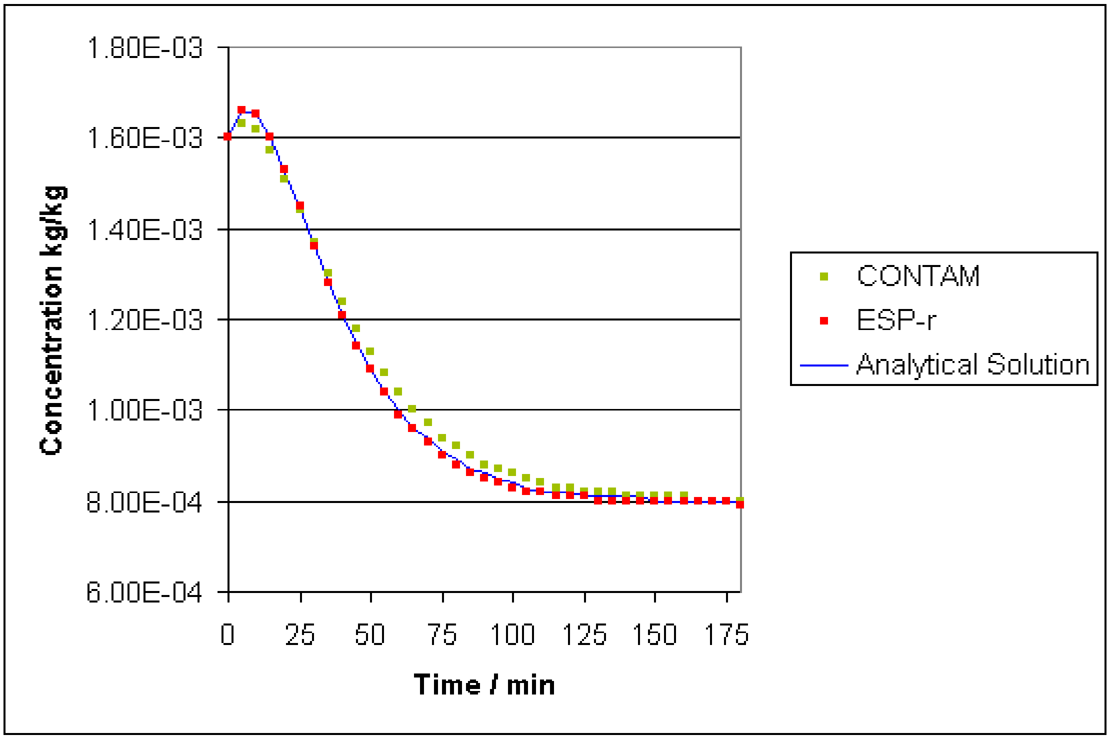

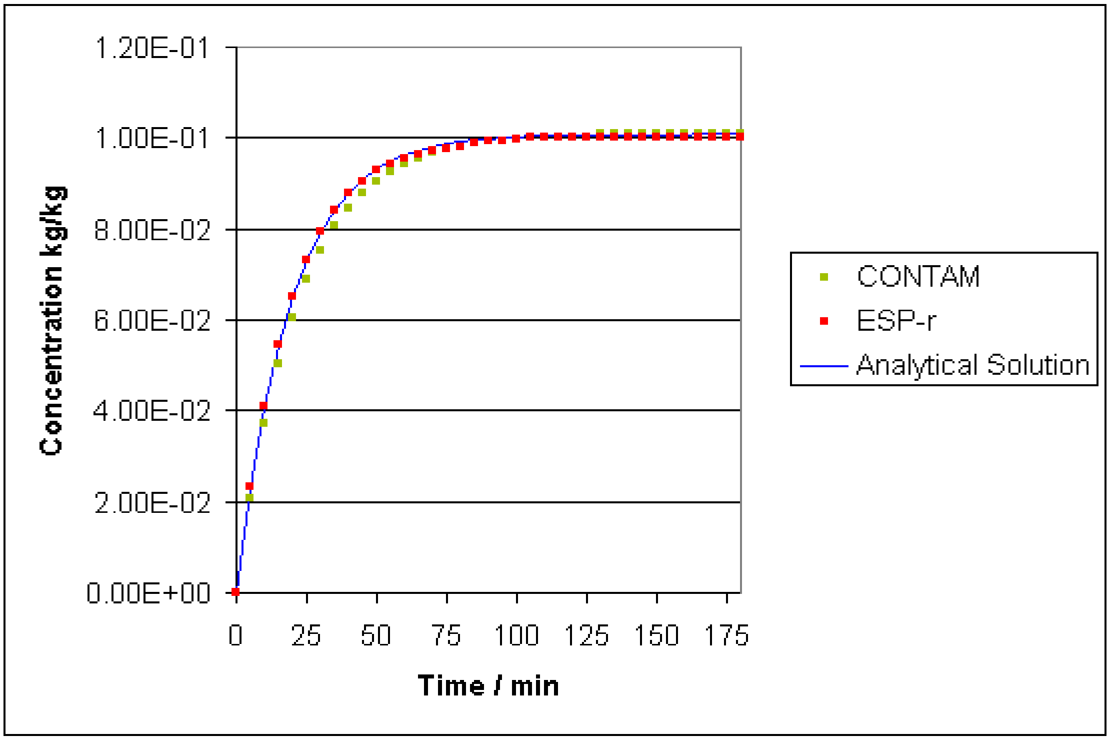

Figure 4.8 Contaminant 1 concentrations for test 4-1, zone two (above) and contaminant 2 concentrations for test 4-2, zone two (below). Note that with the presence of a source term the concentration now becomes constant at a value greater than ambient.

4.5 Empirical Validation

The contaminant flow model was validated against a previous study (Bossaer et al 1999) that evaluated a COMIS model by experimental comparison. The ESP-r model was built according to the COMIS model and spread of contaminant in the built space was studied.

4.5.1 Model detail

The model consists of a flat in a suburban area in Namur in Belgium. The building has nine storeys, each with four apartments. Measurements had been made in an unoccupied flat on the ground floor. Figure 4.9 shows the plan of the flat as built in ESP-r. It consists of seven zones: LIV (living room), KIT (kitchen), BED1, BED2 (bedrooms), HALL, BATH (bathroom) and TOIL (toilet). The airflows into the apartment are from LIV, BED1, BED2, HALL and KIT. Air flows out of the apartment via ducts from KIT, BATH and TOIL. The airflow network as modelled in ESP-r is also shown in figure 4.9.

Contaminant (CO_2) was injected into BED2 at the rate of 14ml/s for two hours and the concentrations of the gas were simultaneously measured in BED2 and all other zones. Measurements were performed at several places within one zone and the results averaged. This was thought to be representative of the concentration of CO_2 in that zone.

Flows due to wind were measured in the original study by tracer gas techniques and the measured flow rates were imposed by the use of forced airflow components, with temporally defined flow rates, in the model. The components used included:

1. Door components to model bi-directional flow; the dimensions of the door were 0.85m by 2m and the coefficient of discharge was 0.6.
2. Cracks to model the exit of air from KIT, BATH and TOIL. The crack dimensions in the original study could not be determined and a number of simulations were carried out to determine how the final results were affected by it. There appeared to be a large deviation when choosing different crack dimensions. Results for typical crack dimensions that gave the best correlation for airflow rates are reported.
3. Forced airflow components with temporally defined flow rates were used to model wind effect on the different inlets. The flow rates changed over time and average flow rate per hour was used.

The original study reported that temperature differences within the different rooms were a major contributor to the associated airflows and therefore to the concentrations of contaminants therein. Temperature was thus carefully controlled to the nearest 0.1^0C. It was confirmed in this study that temperature differences indeed did contribute remarkably to the airflow. Airflow results, quite different from the measured values, were obtained until the measured temperatures were incorporated into the model. Ambient temperature was taken to be the average of the temperatures of KIT, TOIL and

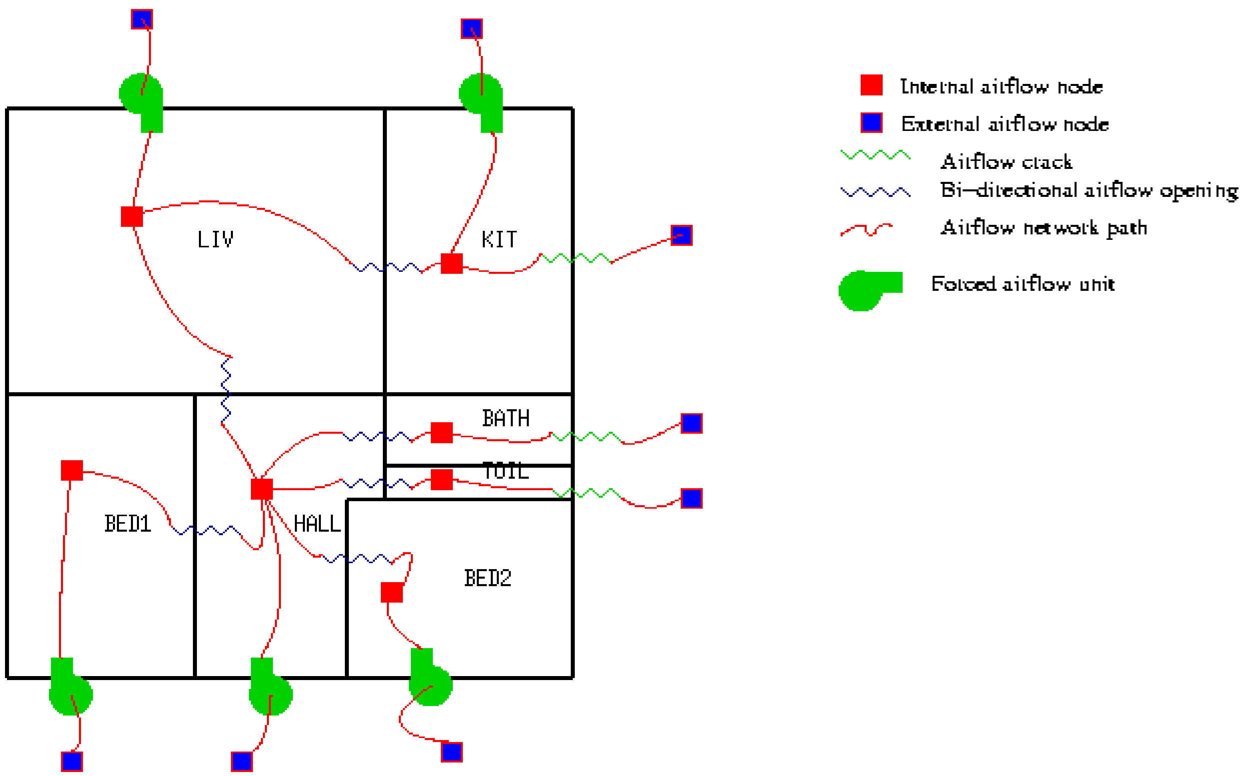

Figure 4.9 Plan and airflow network for Namur flat, as modelled in ESP-r

BATH because temperature in the other zones do not affect the airflow which is regulated by known forced flow components.

4.5.2 Simulation

The model was simulated using *bps* (standard ESP-r building and plant simulation engine). This simulation engine has a fully integrated thermal and airflow computation facility. The contaminant injection was modelled by a uniform source term for BED2 that came on during the two hours of injection. Results were obtained for the concentration of CO_2 in the various zones.

4.5.3 Results

Figure 4.10 shows the transient concentrations of the contaminant in all the zones. There is a fair degree of agreement between COMIS, ESP-r and the experimental observations for the zones. ASTM D5157 parameters for this study were evaluated and results for two of the zones are shown in table 4.5. A complete list is given in Appendix CAS.

It can be seen that both COMIS and ESP-r do not fully satisfy ASTM D5157-97 criteria. For BED1 the NMSE is out with prescribed results and for BED2 the intercept for regression line (*a*) is somewhat different for ESP-r. Nevertheless correlation between these is high as can be seen by the high value of correlation coefficient (*r*). Furthermore the results do show that the integrated contaminant model shows appreciably close agreement with COMIS predictions and with the experimental data.

There are some important factors to consider before drawing conclusions as to COMIS and ESP-r modelling capability from this test. Emmerich and Nabringer (2001) discussed that absolute validation of a complex building thermal and airflow model is impossible, because the user can create an infinite variety of models. However one important reason to perform experimental validation is to identify and hopefully eliminate large errors (Emmerich and Nabringer 2003). For the situations modelled in this study no large errors (more than 10%) in the ESP-r model were identified.

	BED1		***Prescribed results***
	COMIS	***ESP-r***	
r	0.97	0.98	0.9 or more
a	-96	-53	±52 or less
b	1.51	1.08	0.75 to 1.25
NMSE	0.83	0.24	0.25 or less
FB	0.05	-0.20	0.25 or less
FS	0.20	0.09	0.5 or less
	BED2		
r	0.99	0.99	0.9 or more
a	29	-120	±108or less
b	1.29	1.25	0.75 to 1.25
NMSE	0.14	0.21	0.25 or less
FB	0.31	-0.03	0.25 or less
FS	0.53	0.46	0.5 or less

Table 4.5 ASTM D5157 criteria for BED1 and BED2 for Namur flat

It is also important to remember that the ASTM D5157 guide is a guideline not an ultimate arbiter of model accuracy. Rather than the specific parameters and criteria, its primary value may be to move model validation beyond the all too common and oversimplified analysis of “the measurements and predictions differed by X %” and towards useful statistical analysis of model validation results.

Additionally, some of the discrepancies between model predictions and experimental measurements are due to experimental limitations instead of deficiencies in the models. For example, this effort involved a comprehensive data set in terms of number of variables monitored and spatial and temporal detail. Still, after completing the simulation effort additional measurements can be identified that would have been desirable. Specifically the three cracks in the model provide the prime pathways for contaminant transport and air flowing out of the system – having the exact dimensions and flow characteristics of these important components would have been desirable. This is possibly the largest source of

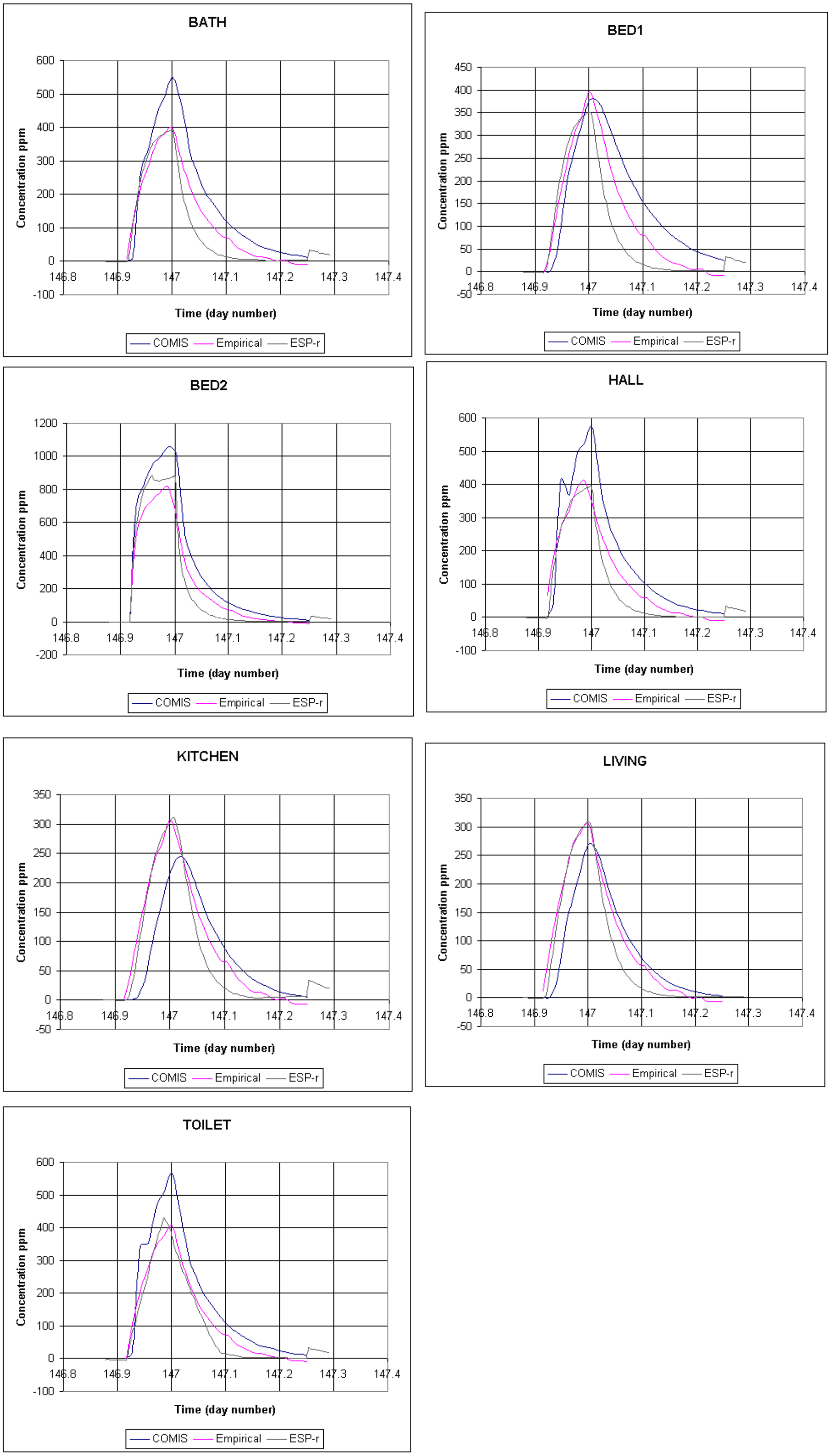

Figure 4.10 Results for CO2 concentration for Namur flat

uncertainty of input parameters in this study and consequentially has bearing on the final comparison. Also, inaccuracies in experimental measurements include much more than simply the instrument accuracy. All concentration measurements reported are values over the whole rooms averaged to be representative of the air space. The ability of such a procedure to represent the room is certainly questionable, especially shortly after a major perturbation (i.e. a quick injection of a large amount of contaminant) or in the presence of continuous local disruption (i.e. location of a sensor in the path of ventilation supply air).

Another factor of interest could be that due to the different approach used to convert wind velocity from the meteorological station to building height. In ESP-r, a wind speed reduction factor (which accounts for the difference between reported velocity and wind speed at building height) was input directly to keep the sets of input data identical. But in COMIS, such an option is not available and the program uses the given wind speed at the meteorological site and calculates the speed at 60m high (or higher if the meteorological station or the building is in rough terrain and wind speed profile exponent is greater than 0.34; in this condition, COMIS program calculates the height of boundary layer). This speed at 60 m (or higher) is assumed to be equal to the wind speed at the same height above the building. The velocity at the building reference height is calculated using this boundary layer profile (Feustel and Smith 1997). Therefore, it is impossible in COMIS to get the same wind velocity at building height as that in ESP-r. It was possible to output the wind as calculated by COMIS and impose on the ESP-r model (or the other way around) but only results from the original model were available the model itself was not. This caused different input wind pressures and consequently resulted in different performance of the programs.

4.6 References

ASTM. 2003. D5157-97 (Re approved 2003). *Standard Guide for Statistical Evaluation of Indoor Air Quality Models.* American Society for Testing and Materials.

Bossaer A., Ducarme D., Wouters P., Vandaele L. 1999. *An example of model evaluation by experimental comparison: pollutant spread in an apartment.* Energy and Buildings 30, 1999.

Dols W. S., Walton G. N. 2002. *CONTAMW 2.0 User Manual Multizone Airflow and Contaminant Transport Analysis Software.* Building and Fire Research Laboratory. National Institute of Standards and Technology. U.S. Department of Commerce

Emmerich S. J. 2001. *Validation of Multizone IAQ Modelling of Residential-Scale Buildings: A Review.* National Institute of Standards and Technology, Gaithersburg, MD. ASHRAE Transactions 2001, V. 107, Pt. 2. CI-01-8-1;

Emmerich S. J., Nabinger S. J. 2001. *Measurements and Simulation of the IAQ Impact of Particle Air Cleaners in a Single-Zone Building.* International Journal of HVAC&R Research Vol.1, No. 7, ASHRAE.

Emmerich S. J., Nabinger S. J. 2003. *Validation of CONTAMW Predictions for Trace Gas in a Town house.* 8th International Building Performance Simulation Association IBPSA Conference. Eindhoven, The Netherlands.

Feustel H., Smith B. V. 1997. *COMIS 3.0 – User's Guide*. Lawrence Berkeley National Laboratory. U. S.

Hanna S. R. 1988. *Air Quality Model Evaluation and Uncertainty*. Journal of Air Pollution Control Association, Volume 38, 1988.

Heinsohn R. J. 1991. *Industrial Ventilation: Engineering Principles.* John Wiley and Sons, Inc.

International Energy Agency. 1999. *Annex23 Multizone Air Flow Modelling (Sub-task 2&3) Final Report. Evaluation of COMIS*. Tome 1

Jensen S. O. 1993. *The PASSYS Project: Subgroup Model Validation and Development*, Brussels. Final Report, Part I and II 1986-1992. Commission of the European Communities. DGX1I, EUR 15115 EN.

Rogers G. F. C., Mayhew Y. R. 1995. *Thermodynamic and Transport Properties of Fluids (SI Units) Fifth Edition.* Basil Blackwell Ltd.

Versteeg H. K., Malalasekera W. 1995. *An Introduction to Computational Fluid Dynamics. The Finite Volume Method.* Prentice Hall.

5 INTEGRATING NETWORK FLOW MODELLING AND CFD

5.0 Introduction

This chapter begins with an introduction to conflation of ESP-r's fluid mass flow network solver *mfs* and domain flow (CFD) solver *dfs*. The idea of conflation is based on a fluid flow network defined independent of a CFD domain. The CFD domain takes its boundary conditions regarding mass input and outlet from the fluid flow solver and feeds back information to the fluid flow solver. Both solvers are then run iteratively until some mutual convergence criteria are met. It is assumed that such an approach leads to more accurate solution than using just one solver. A number of different conflation mechanisms are possible.

From a number of possible conflation types the most prominent conflation type is then discussed first. This is called the Known Pressure Node Type Conflation or Principal Conflation Technique. This technique is the most accurate and robust technique from a number of possible conflation techniques. The technique bases itself on ownership and exchange of information between network mass flow and CFD. Network flow owns overall mass flows, pressures and momenta whereas CFD owns the same at the intra-room resolution and information from network flow model can be passed as source terms for mass, momentum and species. Run time mutual convergence using respective convergence criteria is obtained by passage of information between the two solution techniques. Where there is a mismatch between the configuration of the problem for the two domains in terms of the network components used and the actual size of the openings a special technique is used to resolve this (Bartak et al 2002, Clarke 2001, Denev 1995). Assuming arbitrary initial values network mass flow converges and then passes mass flow rate information to CFD. CFD takes this as boundary conditions and source terms for mass, momentum and species mass. This allows CFD to predict more accurately as the boundary conditions are taken from dynamic integrated thermal and flow modelling instead of static or scheduled values. After convergence CFD passes back pressures to network flow in order to correct flow predictions. This process repeats until both CFD and network flow results are within some tolerance. Lesser conflation techniques are also detailed followed by a discussion of their shortcomings.

Conflation of air flow prediction facilities is important because contaminant prediction is inherently dependant on air flow prediction. This is true because contaminant flow depends largely on air flow and for this research it is assumed that contaminant flow rate is directly proportional to air flow rate. Hence once air flow rates are accurately known contaminant flow rates and concentrations can be calculated as scalar quantities. Whereas air flow conflation depends upon definition of CFD boundary condition specification and iterative correction, contaminant transport integration depends upon CFD source term definition. It is assumed that a contaminant flow network has been defined. Translation to the CFD domain is realised by the definition of contaminant sources within the CFD grid. These are representative of contaminant sources / sinks defined in the contaminant flow network. Furthermore any contaminant addition / subtraction from the CFD domain due to conflated mass flow network and CFD is realised by defining virtual sources and sinks within the CFD grid. These virtual sources and sinks are representative of contaminant mass injection / rejection as predicted from air flowing in to or out of the CFD domain.

The chapter concludes by describing a validation study for the developed conflation approach. The validation exercise comprises of three models that were compared. The base case was considered to be a thermally conflated network mass flow model. The conflated approach and a stand alone CFD solution were compared against this model.

5.1 Conflation of *mfs* and *dfs*

The present concept of *mfs* and *dfs* conflation is built on that proposed by Negrao (1995 and 1998). As briefly stated in Chapter 2 the airflow network node representative of the CFD domain is replaced by the CFD domain (the node representative of the CFD domain is termed dom_nod). This means that all connections from dom_nod are removed. One air flow node is created for every opening type boundary condition within the CFD domain (the opening nodes are called opn_nod). Finally these nodes are connected to the nodes dom_nod was originally connected to (the nodes external to the CFD domain which are called ext_nod) and using the same components. The same procedure is followed for all the different conflation types described shortly. Figure 5.1 shows how the flow network is modified. There are three types of air flow nodes identifiable for the following discussion and illustrated in figure 5.1. The first is dom_nod which is the air flow node representative of the CFD domain. Secondly ext_nod can be defined as the nodes that are linked to dom_nod. Finally opn_nod can be defined as new air flow nodes that are defined for the conflated network. These are representative of the air flow openings in the CFD domain.

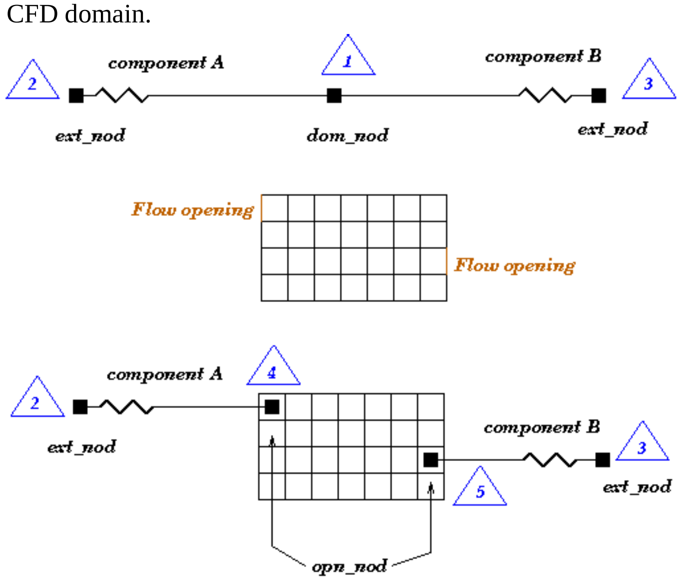

Figure 5.1a (above) original mass flow network where dom_nod is to be represented by a CFD domain with two flow openings (shown in figure 5.1b (middle)). Figure 5.1c (below) conflated mass flow network for simple three node configuration (Node numbers shown in blue triangles and air flow openings for CFD domain shown in brown)

The connections between dom_nod and opn_nod and the nature of opn_node (fixed pressure or unknown pressure) are the parameters that vary for the various conflation types which are discussed in the following sections. This corresponds to the parameters that *mfs* and *dfs* pass between each other when conflated. The parameters are mass flow rate and pressure. Both domains can pass either mass flow rate or pressure and accept either mass flow rate or pressure but mass flow rates cannot be passed as output by both modules because then no new information is passed on. This is shown in table 5.1.

Another possible option was also studied. This is the constant pressure difference feedback type conflation (Type D). The various conflation mechanisms are described in figure 5.2 to provide an overview of the discussion so far. Individual conflation types A, B, C and D are discussed in the following paragraphs.

Number	***mfs output / dfs input***	***dfs output / mfs input***	***Comments***	***Name***
1	**mass flow rate**	**pressure**	**Allowed**	**Type A**
3	pressure	mass flow rate	Allowed	Type B
2	pressure	pressure	Allowed	Type C
4	mass flow rate	mass flow rate	Not allowed	

Table 5.1 Various conflation mechanisms for dfs and mfs. The ***Principal Conflation Technique*** *is shown in* ***bold.***

Wang and Chen (2005) have attempted to conflate stand alone network mass flow and CFD. They report three mechanisms for it. These mechanisms essentially differ in the boundary conditions they pass back and forth. The pressure

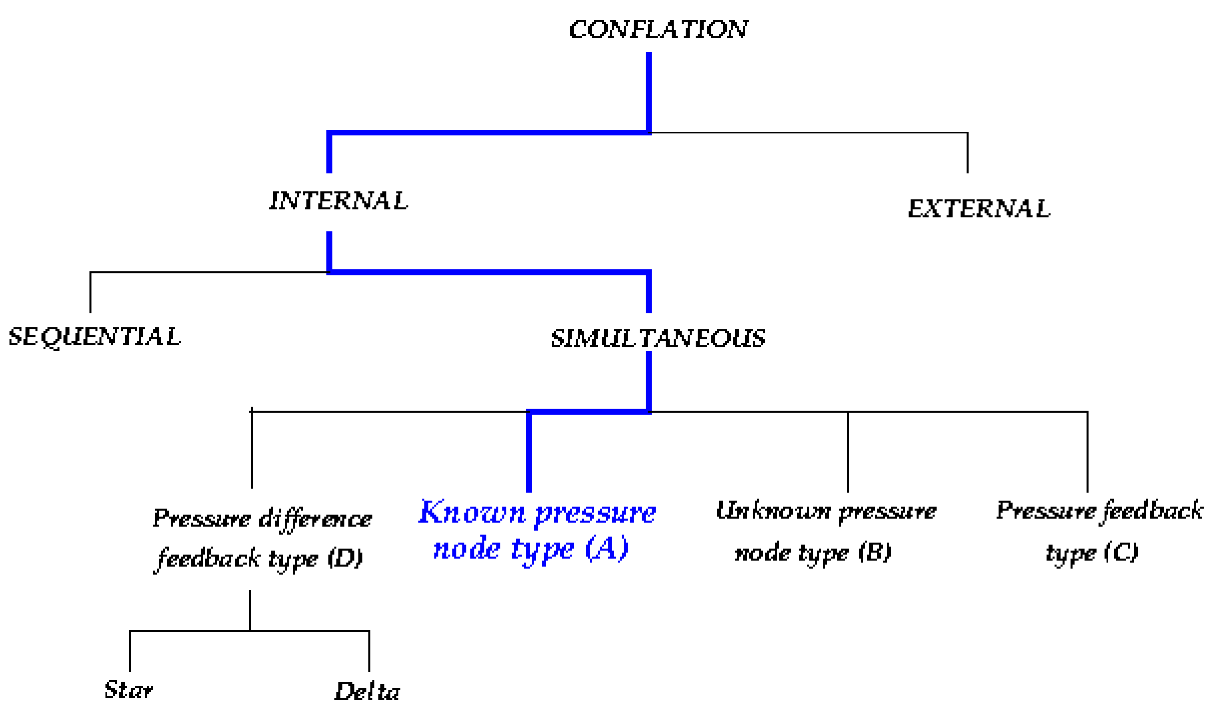

Figure 5.2 Various conflation types (Principal technique shown in blue)

– pressure type conflation (type C) exchanges only pressures between the domains. The mass – pressure type conflations work with one domain (either CFD or mass flow) passing mass flow rate as the boundary condition and the other domain passing pressure (types A and B). Wang and Chen (2005) state that the mutual iterative method basically tries to obtain a Gauss-Seidel solution. It was shown by them that the pressure – pressure type conflation is unconditionally stable whereas mass – pressure type conflation is conditionally stable if the Gauss-Seidel analogy is assumed to be valid. They used the Scarborough criterion (Scarborough 1966) to judge stability. It was shown that all three conflation types (A, B and C) give similar results for a well posed problem. In practice one would not expect change within a flow network if a CFD domain is incorporated into it (because the air flow resistance of a CFD domain will be negligible) and using any of the conflation mechanisms will give the same results. This finding was reported by Wang and Chen (2005) as well. Therefore any one of the conflation types can be considered to give accurate results and under normal building conditions choosing type C over A or B would not give any additional benefits.

We can divide the conflationary mechanisms into two classes the first comprising type D with the other three belonging to the second class. The distinction is that for conflation type D new connections are defined between nodes representative of the openings (the CFD domain node may or may not be connected depending upon conflation type -- to be discussed later) whereas no such requirement is made for the other three conflation types.

In both of these classes information computed from *mfs* is fed back to *dfs* and it is ensured that each module runs such that no information is exchanged whilst a solver is still unconverged. The approach used for conflation of ESP-r's CFD module *dfs* and *mfs* (integrated within *bps)*, is such that two way conflation (sharing of information) and mutual convergence every time step is built in as the default conflation mechanism. If *dfs* does not converge for a particular time step the coupling mechanism automatically falls back to one way conflation and results from a failed *dfs* are not used in the solution. Similarly if *mfs* fails to converge then *dfs* does not take up those results. As a safety measure the *dfs* file holds some velocity type boundary condition information that is used in *dfs* standalone mode. The air flow coupling is independent of any type of thermal coupling mechanism which gives flexibility to the user to describe any type of thermal conflation if at all.

5.2 Known Pressure Node Type Conflation (Type A)

(The Principal Conflation Technique)

For this type of conflation the CFD domain is considered to be a replacement of the dom_nod and associated connections. The original network of figure 5.1a is replaced by the conflated network of figure 5.1c. The dom_nod is not included in the conflated network but all opn_nod are defined to be constant pressure type air flow nodes. These nodes are similar to internal nodes but with the property that any amount of mass can be added to or subtracted from them without loss of pressure at the node. All opn_nod are connected to ext_nod using the same air flow components hence maintaining network similarity. During integrated simulation the algorithm of figure 5.3 is implemented.

As shown in figure 5.3 the original network is solved, the conflated network is activated and pressures at all opn_nod (nodes 4 and 5 in the example of figure 5.1) are initialised to the pressure of dom_nod. The conflated network at this point is exactly similar to the original network i.e. it gives the same solution. Now the stack pressures are calculated based on previous flow direction or direction definition if this is the first time step. Mass flows are then imposed onto the CFD domain as velocity type boundary conditions. This is done by first determining each connection between ext_nod and opn_nod and flow direction (to or away from CFD domain). Flow velocity is determined by dividing mass flow by the opening area and density of air. For air flows going into the domain the temperature is set from either the previous time step temperature of the adjoining zone or the ambient depending upon the origin of air. The flow rates are then normalised as in conflation type D so that the residual from *mfs* convergence is not carried on into the CFD solution.

The CFD module *dfs* is then allowed to run using *mfs* defined boundary conditions. Now the average pressure in the CFD domain is determined and is used to calculate the pressure correction factor. The method is similar to that used for conflation type D. The pressure correction factor is the difference of the *mfs* determined pressure of dom_nod and the average CFD domain pressure. This pressure correction factor is then used to correct the pressure of each opn_nod. This is important because the CFD code does not use absolute pressures as does *mfs*. As explained previously pressure correction between *mfs* and *dfs* sets the two domains on the same pressure datum. The pressure predicted at the cells representative of opn_nod are then imposed onto the constant pressure type opn_nod. The conflated network is solved again and if the mass flows and pressures of the present run are within a certain tolerance of the previous run values it is assumed that both domains have converged mutually. If convergence has not been achieved the program runs through the mutual iteration loop again. This is repeated until convergence has been achieved or the maximum number of mutual iterations has been reached. If convergence is not achieved the program deactivates the conflated network and activates the original network. The original boundary conditions for the CFD domain are also reimposed.

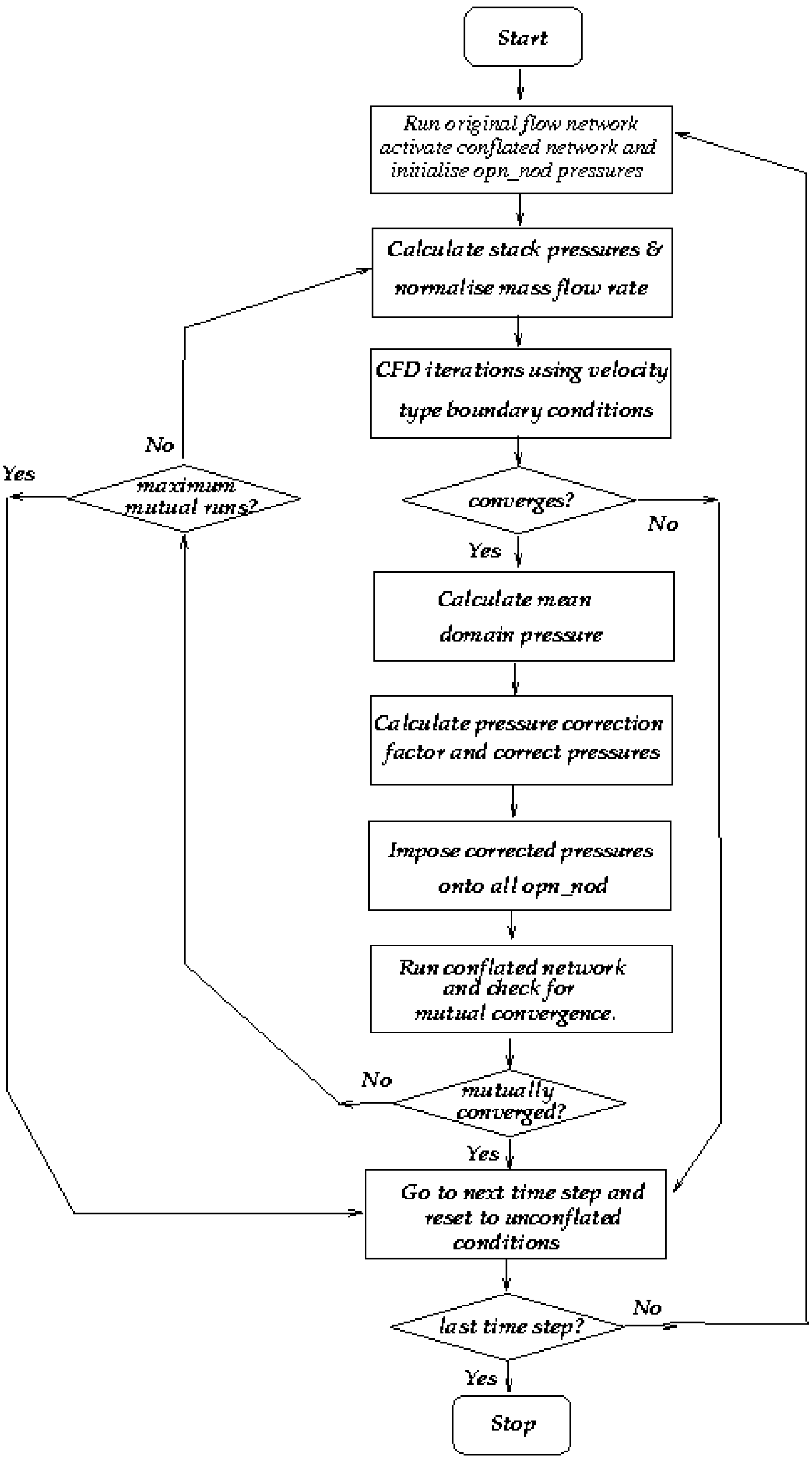

Figure 5.3 Conflation algorithm for type A

5.3 Pressure Difference Feedback Type Conflation (Type D)

Consider the original mass flow network of figure 5.1a. It consists of one internal and two external nodes. The pressures of the external nodes are derived from prevailing wind conditions by using information about the building facade and exposure (Clarke 2001). The internal node pressure is calculated by imposing a mass balance upon the network. A CFD domain is defined so as to be representative of the space that the internal node (dom_nod) represents. Hence the problem specification includes an air flow network (which is referred to as the original *mfs*), the CFD domain and the conflated network. The conflated network is obtained by connecting the two ext_nod either directly or through the dom_nod. It does not make a difference how they are connected for a CFD domain with just two openings because the mass flow through each connection is the same. If the number of openings is more then interconnections of the opn_nod can be complex and connecting the dom_nod can change results. This is discussed later in this section.

Nodes representative of openings in the CFD domain (called opn_nod) relevant for air flow network purposes are also defined within the conflated network. These nodes are then connected to nodes originally connected to dom_nod (these nodes are called ext_nod) using the original components. The algorithm of figure 5.4 can now be used to conflate the two modules. Initially the original network is run just as it would have been run if there were no conflation. Then connections between the opn_nod and dom_nod (connections 5 and 6) are defined. All connections are made using a simple air flow opening which requires area of the opening as the only parameter. The mass flow rate through this component is defined from the following equation:

$$\dot{m} = C_d A \sqrt{2 \rho \, \Delta P} \qquad (5\text{-}1)$$

Here C_d is the discharge coefficient which is usually taken to be 0.65 (Hensen 1991). The area *A* is not defined at this stage but is calculated after *dfs* has run and converged. The mass flows rates though are set equal to the original run values (i.e. m_{21} in figure 5.1a is set equal to m_{24} in figure 5.1c and m_{31} in figure 5.1a is set equal to m_{35}[11] in figure 5.1c).

Next stack pressures are calculated. Then total mass into the CFD domain is normalised with total mass flowing out. This is done by calculating the difference of the total mass flowing into the domain and out of it. This difference is less than the tolerance of *dfs* because the results are taken from a converged *mfs.* This difference is then added to the first opening type boundary condition to ensure mass balance when *dfs* runs. Then all mass flows to and from the domain are converted to velocity type boundary conditions. Using *mfs* defined boundary conditions *dfs* starts to iterate and hopefully converges. In the case that it does not converge it is deemed that further information cannot be extracted from the data set and everything is reset to the original conditions. After the CFD simulation has converged the mean domain pressure is calculated; this is the average pressure of all the CFD grid cells. From here the pressure correction is calculated which is

11Here m_{ab} represents the mass flow rate of air from node a to node b

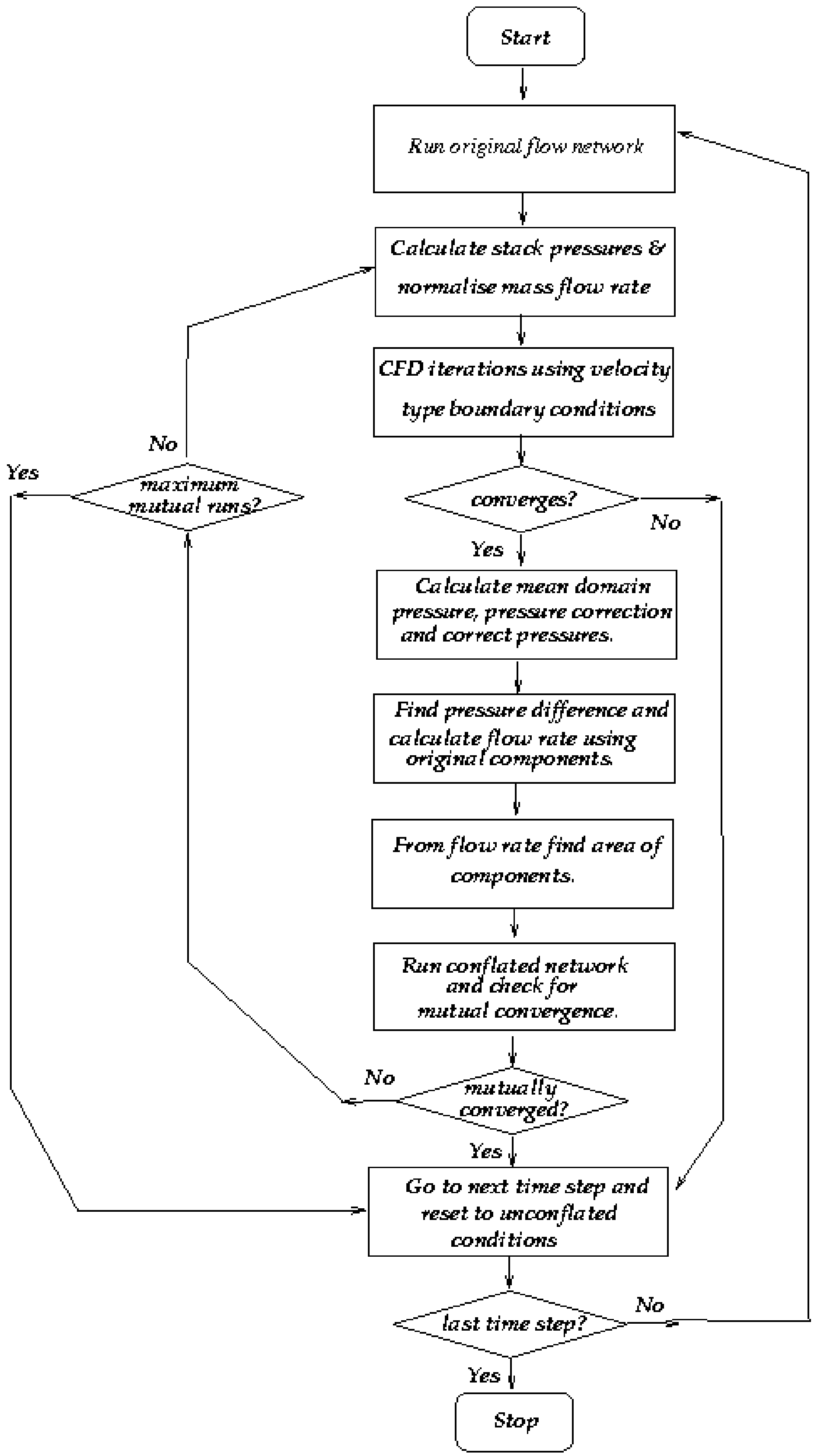

Figure 5.4 Conflation algorithm for type D

the difference between the absolute dom_nod pressure and the CFD mean pressure. This term is now used to correct the pressures of all the opn_nod present in the CFD domain. Then for each opening, pressure difference of ext_nod and opn_nod is calculated and used to find the mass flow using components from the original network. This mass flow is then used to calculate area in equation (5-1) where ΔP for each opn_nod and dom_nod is used. The solution to equation (5-1) effectively gives the air flow resistance of that particular path. The conflated network is run and solved and if the previously calculated values of flow rates and pressures are within a predefined tolerance to the present ones mutual convergence is achieved. If mutual convergence is achieved then the original mass flow network is re-established and original CFD boundary conditions are assumed. If mutual convergence is not achieved the algorithm loops back and increments counter for mutual runs, this goes on for maximum allowed number of runs and if convergence is not achieved even then, the whole process is aborted and simulation goes on to the next time step after resetting original conditions. In practice this was never observed for any configuration i.e. *mfs* always converges if *dfs* converges. Figure 5.5 shows how the mass flow rate converges to a stable value as *dfs* and *mfs* are run using type D conflation. A two opening model room with free floating control and wind induced boundary pressures is simulated.

Attractive as it seems there are a few drawbacks in this approach. Firstly it is possible to get anomalous results if a pressure difference used in equation (5-1) is of an opposite sign to that expected or close to zero because then the equation would predict a very large opening area or become undefined. One possible solution to this problem is to have some

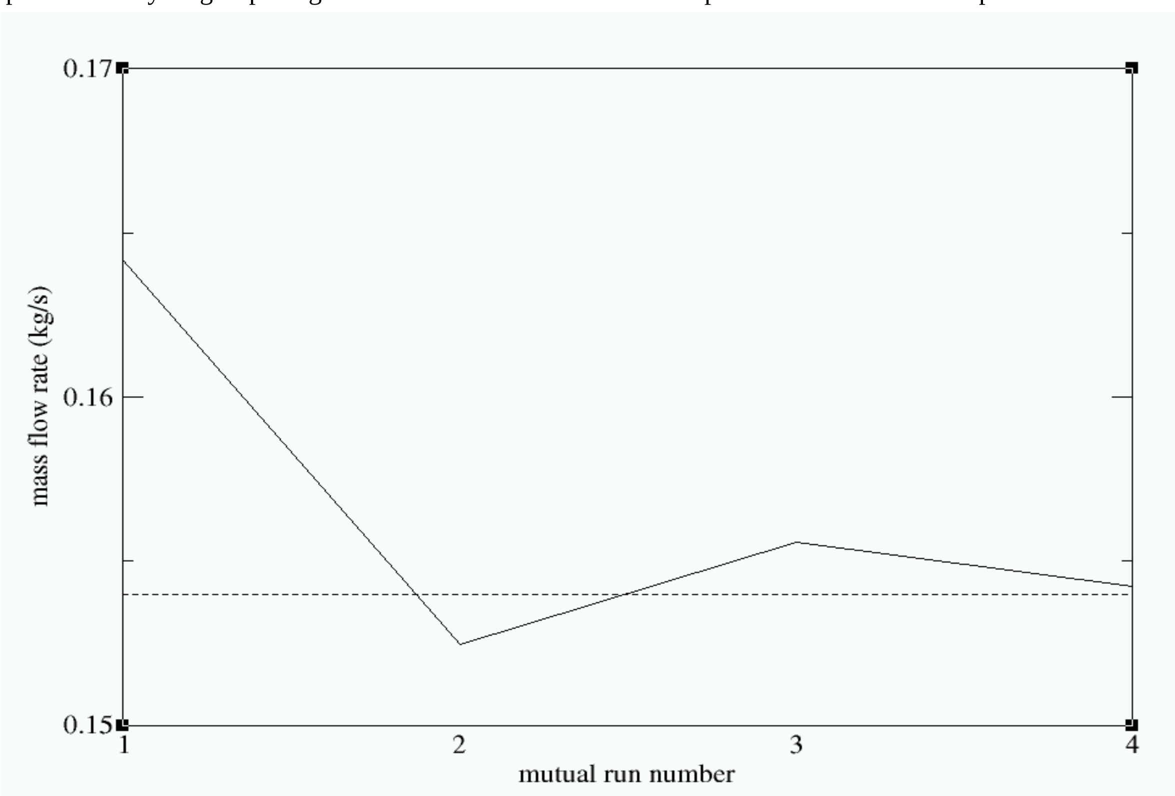

Figure 5.5 Convergence of conflation algorithm

maximum large value (e.g. 10m^2) used for the area in such situations.

Secondly the situation gets complicated when there are more than two openings in the CFD domain. For a CFD domain with three opening type boundary conditions there exist two ways in which the three opening nodes can be connected, termed star type connections and delta type connections. These two possible connection configurations are shown in figure 5.6. The star type connections assume a central node (the CFD domain node) and connects this central node to all the opening nodes. The star type connections have the advantage that the number of connections does not get very large as the number of openings is increased (there are the same number of connections as openings). For the delta type, flow connections are made from one opening node to all other opening nodes. This results in more connections than openings ($n(n-1)/2$ connections for n openings). This has the advantage that the flow paths are maintained without any central air flow node and this can be thought of as the approach that is closer to reality. The problem that both of these approaches do not address is that there is no way of explicitly defining the opening parameters in the mass flow network i.e. one set of data (mass flow rates and pressure differences from the CFD solution) is used to define the openings independent of the whole mass flow network. If the network is solved for the opening parameters assuming known mass flow rates (from *dfs*) then there is no way of ensuring that the calculated parameters are realistic. This shortcoming of this type of conflation is not evident in a CFD domain with just two openings because there is no ambiguity about mass flow

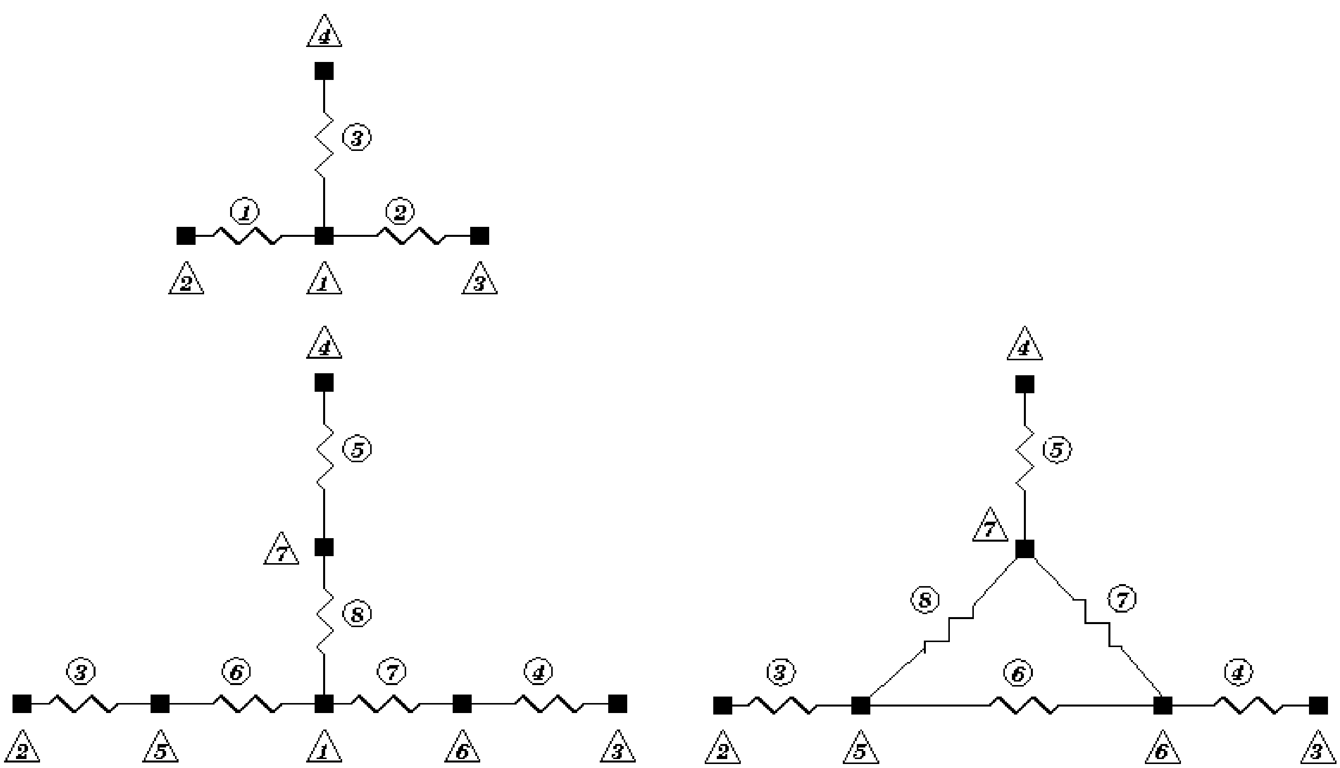

Figure 5.6 Different conflated network arrangements for a three opening CFD domain, node numbers are given in triangles and connection numbers are given in circles. Top left is the original network, bottom left is the star type connection and bottom right is the delta type connection.

rates and internal connections (i.e. star and delta configuration are similar for this case).

Figure 5.7 shows a CFD domain with three openings. This model was built within ESP-r and cold air was made to flow through one of the low level openings. It is expected that most of the cold air would flow out from the second low level opening and a small amount would escape from the opening in the ceiling. Though the airflow network solution would not be able to predict this, the CFD solution includes the effect of momentum and thus predicts more air flowing out of the lower opening than the ceiling opening. Results from using pressure difference feedback type conflation show that *mfs* is not able to discern this even with *dfs* predicting correct mass flow rates. The reason ascribed to this could be that the opening parameters of the new connections defined for the CFD domain are not realistic for more than two openings. The areas seem to be very large for the predicted mass flows and do not impose enough resistance on the mass flow network to cause a change in flow rates corresponding to predictions from *dfs*. Therefore an alternate approach is required.

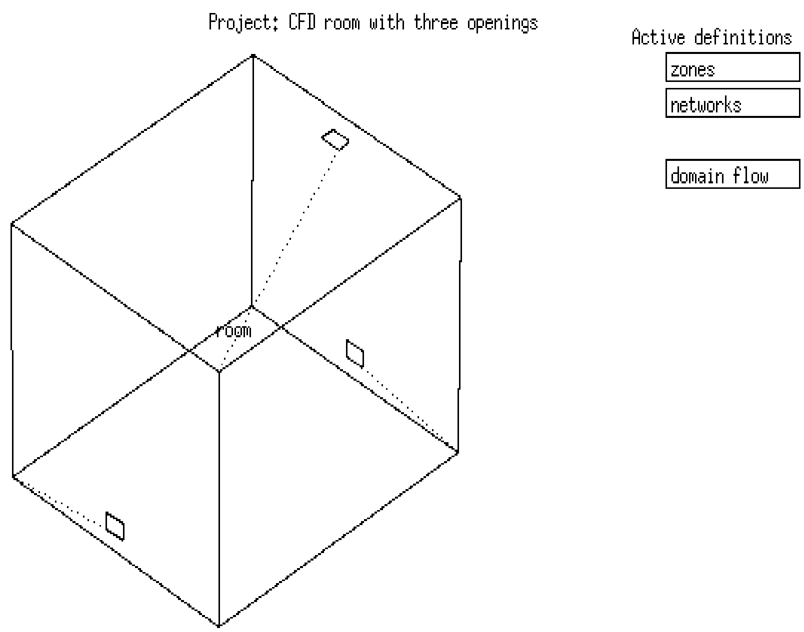

Figure 5.7 CFD domain with three air flow openings

5.4 Unknown Pressure Node Type Conflation (Type B)

The difference between this type of conflation and known pressure node type conflation (type A) is in the parameter passing between *dfs* and *mfs*. In type A *mfs* passes mass flow rates as velocity type boundary condition and *dfs* passes pressure. In type B *dfs* passes mass flow rates and *mfs* passes pressure as pressure type boundary condition. The pressure at opn_nod when it has converged need not be known when mass flow rates are passed to it, hence the name unknown pressure node type conflation. The algorithm implemented for this type of conflation is shown in figure 5.8.

The original mass flow network is solved. The conflated network is activated and node pressures for all opn_nod

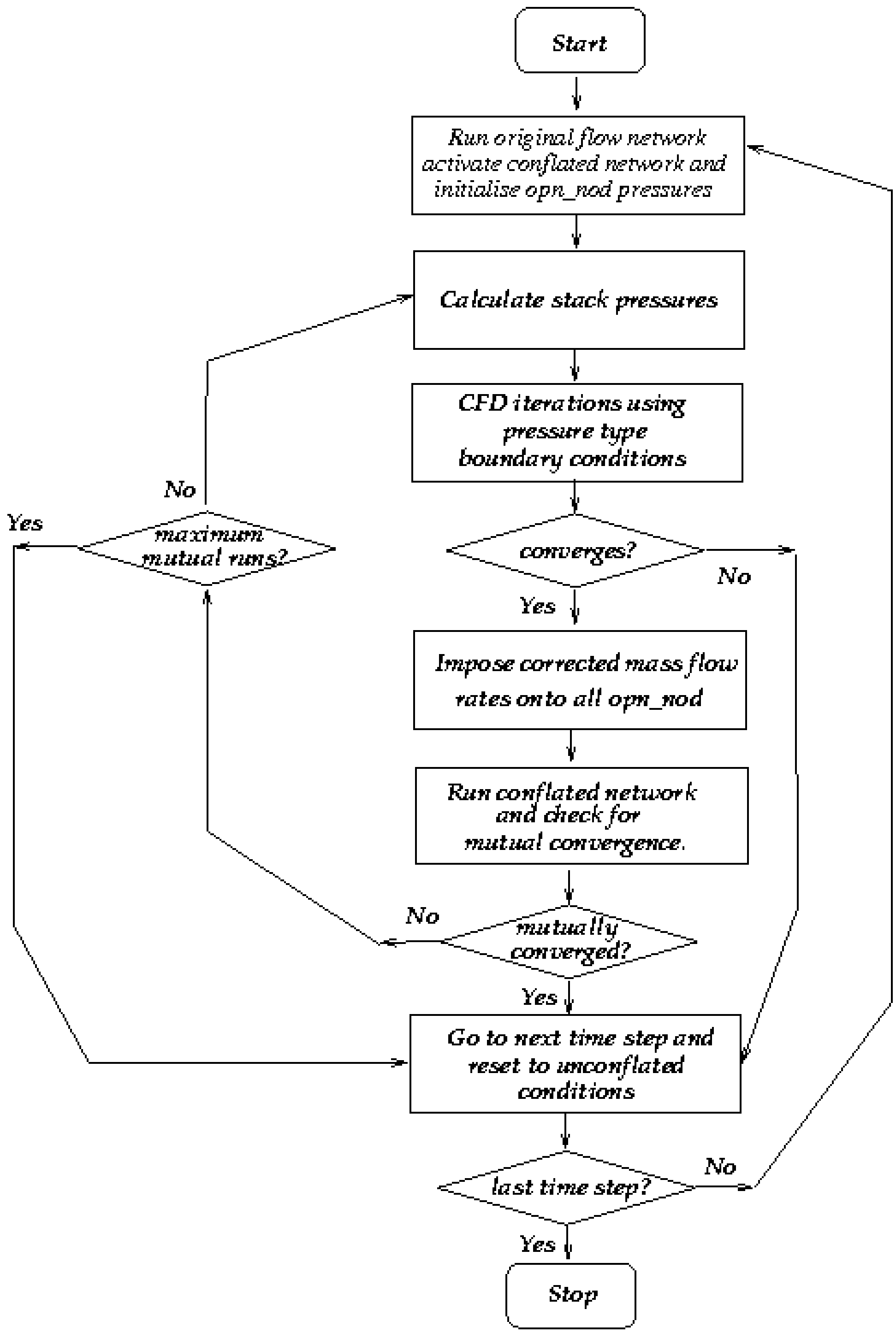

Figure 5.8 Conflation algorithm for type B

are initialised as in the previous conflation type. The stack pressures are then recalculated. The CFD domain openings are defined as pressure type openings and are passed pressure as calculated by *mfs*. The CFD module *dfs* is now called and CFD solution is started. The solution may or may not converge. If the solution does not converge it is rerun and this is repeated until the solution has converged or the maximum number of times it can run has been exceeded in which case the original mass flow network and CFD boundary conditions are reinstated. If the solution converges the *dfs* computed mass flows are reimposed onto *mfs*. The conflated network is rerun and if pressures and mass flow rates from this run are similar to those computed from the previous run it is assumed that mutual convergence of the two has been obtained.

5.5 Pressure Feedback Type Conflation (Type C)

Conflation type C is again very similar to types A and B. The only difference is the parameters passed between the two domains. Both *mfs* and *dfs* pass pressures between themselves. This can seem a bit paradoxical in the sense that if pressure is passed as a boundary condition how can it be calculated? This is resolved by passing the upwind pressure to *dfs* and returning the downwind pressure from *dfs*. The upwind and downwind pressures are defined for the relevant mass flow network component. This can be illustrated if figure 2.4 is considered again (This is shown here as figure 5.9). In figure 5.9b for the opn_nod connected to node A the pressure is defined as 10Pa and for the opn_node connected to node C the pressure is defined as 2Pa. Now *dfs* is run and the pressures are reimposed onto the original mass flow network.

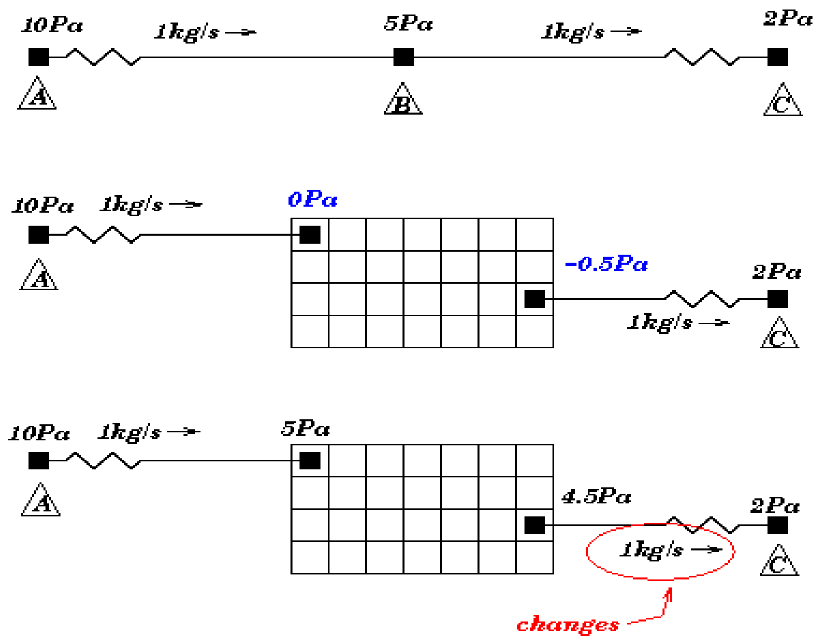

Figure 5.9a (top) shows the mass flow network with nodes A,B and C with hypothetical pressures and mass flow rates. This is replaced by the conflated network of figure 5.9b (middle): the pressures defined from the CFD datum are shown in blue. When the CFD defined pressures are brought up to the mfs datum, as shown in figure 5.9c (bottom), there is a pressure loss for the second opening and the circled mass flow rate changes.

This can be illustrated by figure 5.10. The original flow network is solved. The conflated network is activated and initialised to the values calculated by the original network. Stack pressures are calculated and the pressures for the opn_nod are passed as boundary conditions to *dfs*. After that CFD iterations are run and if the CFD solution converges the

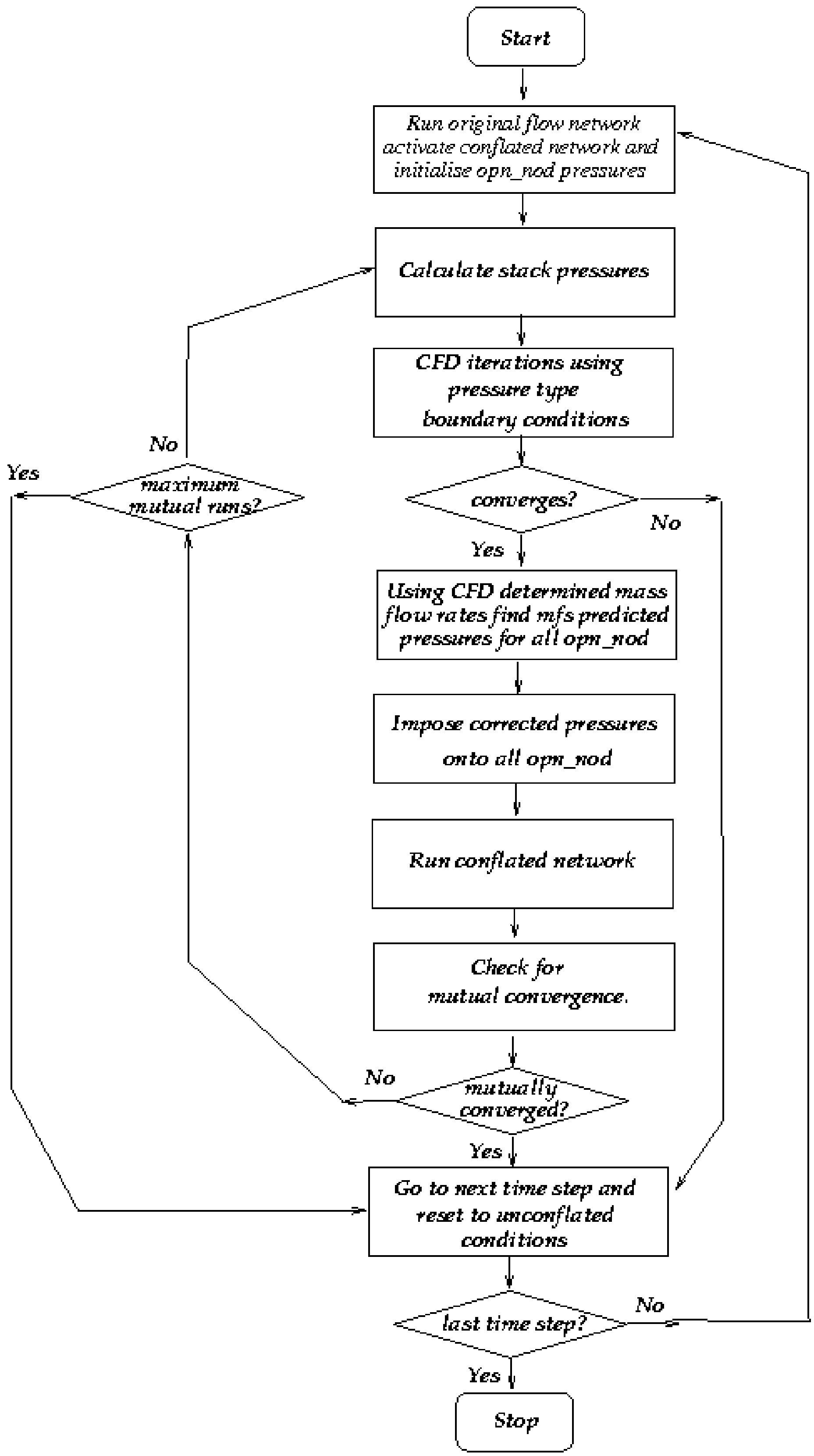

Figure 5.10 Conflation algorithm for type C

CFD determined mass flow rates are imposed on the connections connecting opn_nod to ext_nod (node 1 to 4 and node 3 to 5 in figure 5.1c). The mass flow rate and pressure difference equations that are representative of the various components used in these connections when solved in this way give the pressure differences. Assuming that the ext_nod is at the original boundary pressure the corrected pressure of the opn_nod can be determined. In the context of figure 5.9b, *dfs* is passed the pressures 10Pa and 2Pa as boundary conditions. Once *dfs* has converged the mass flow rates for the two openings (into and out of the domain) are known. Using these mass flow rates and the governing equations for the connections (where mass flow rate is given as a function of pressure difference) the pressure difference is calculated. This pressure difference can then be used to calculate the pressures at all opn_nod assuming that the ext_nod are at the pressures of 10Pa and 2Pa.

After this the conflated network can be solved and assumed to converge if similar criteria are met as in the previous conflations. Similarly if the CFD solution does not converge or if mutual convergence is not obtained steps similar to the previous conflation types are taken.

Although Wang and Chen (2005) report that pressure feedback type conflation (type C) is the most stable of types A, B and C. This method is not implemented within the current research because of a particular problem. If the flow network contains a component that allows only a fixed amount of mass to flow through per unit time i.e. a constant mass flow rate component and if this is the <u>only</u> connection to the CFD domain either directly or indirectly then the mass flow rate from the CFD cannot be imposed on the mass flow network. This is equivalent to stating that mass flow rate is not a function of pressure difference for such a component and this is one of the underlying assumptions of conflation type C. For the same reason conflation type B is also not recommended. This problem is illustrated in figure 5.11 where air flow node B is connected to the CFD domain and also to node C via a constant flow rate component. Now supposing CFD predicts a mass flow rate different from that imposed by the constant flow rate component, the solution for *mfs* will not be achieved because mass conservation would be violated in the sense that different masses would be flowing along the same

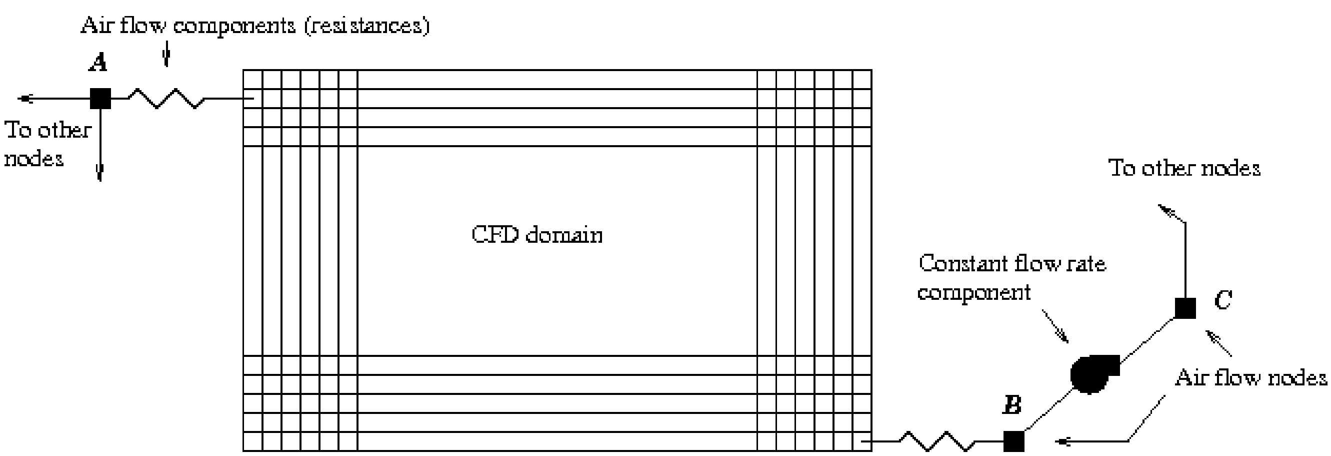

Figure 5.11 Network with constant mass flow type component

flow path at the same time. Hence the known pressure node type conflation (A) is recommended and is the conflation method implemented. Furthermore Wang and Chen (2005) report that the results from the three conflation types they had implemented were similar so for practical purposes it can be safely assumed that the three methods will give similar results provided constant mass flow rate components are not used.

A further benefit of passing mass flow rates to the CFD domain is that momentum effects can also be considered. Negrao (1995) states that boundary types come into play when the flow may or may not be momentum governed. He prescribes velocity type boundary conditions when flow is dominantly dependent upon momentum and prescribes pressure type boundary conditions when it is not.

Results from the three types of conflation mechanisms have been reported to show no perceptible difference (Wang and Chen 2005). Hence conflation type A is retained as default with provision to switch to conflation type B or C. It is believed that for a well posed and realistic problem both *mfs* and *dfs* will not behave badly and give mutual convergence problems because the parameters passed will not differ significantly with each mutual iteration. One exception to this is given as a case study in Chapter 6. Here the mass flow direction was quite sensitive to the temperature indoors and direction changed quite rapidly. This resulted in both *mfs* and *dfs* predicting flows in opposite direction each subsequent mutual run. It was therefore not possible to get mutual convergence for *dfs* and *mfs* so the time step had to be decreased to ensure that both modules solved to give flows in the same direction.

5.6 Contaminant Prediction Integration

The integration of mass flow network and CFD paves the way for accurate contaminant prediction capabilities. It has been shown that contaminant distribution depends upon air flow hence the importance of coupled air flow predictions from network and CFD approaches. Within this approach the CFD domain and mass flow solver are integrated with the thermal solution so as to impose realistic heat and mass (and therefore contaminant) transfer conditions. For contaminant prediction the zone openings are considered to be the only mechanism of interaction of contaminant mass between the various domains. Ambient or internal contaminant concentration is again considered to govern contaminant mass injection / rejection for the CFD domain where average concentrations are calculated using weighted average of contaminant mass in the CFD grid cells. This is based on the assumption that contaminant is mixed homogeneously in the air and contaminant mass transfer is directly proportional to air mass transfer. The homogeneity assumption is considered to be valid for the whole air within a room represented by a mass flow node and a whole grid cell within a CFD domain.

Contaminant integration within CFD is achieved by allowing definition of source and sink terms within the CFD domain. These sources and sinks are dynamically configured depending upon the network mass flow predictions and the contaminants network model. The definition of source and sink type boundary conditions and interlinking with mass and contaminant flow networks is kept semi-automatic with the user providing essential details only.

The contaminant model in order to run needs information from the air flow network model. Once this is obtained as described in chapter 3 it then determines contaminant mass flows assuming them to be proportional to the air flows as predicted from the flow domain. Within ESP-r it is possible to run the standalone mass flow solver *mfs* or the integrated thermal and mass flow solver *bps*. Hence integrating contaminant capability within ESP-r automatically integrates this capability with thermal and mass flow solution. The user of course has the option to invoke standalone or thermally integrated air flow simulation and hence similar contaminant modelling.

5.7 Validation

Validation of the conflation approach was considered necessary in order to achieve confidence in the results. The preferred method was inter-model comparison because analytical solutions are not possible. One important application of the developed approach is the mutual convergence of mass flow network and CFD and to do this it is important that there be more than two openings in the CFD domain. Otherwise the flow in and flow out of the domain would be completely defined and no new information would be passed between the mass flow solver and the CFD solver. One may argue that the CFD domain itself offers some resistance to air flow and hence acts as a resistive term in a detailed flow network but the flow resistance is small for most flow geometries and the decrease in mass flow although perceptible is of the order of the expected error. This was evident from runs made using type A conflation using a two opening variant of the model shown in figure 5.7 (remember that a flow connection was made between the two openings and its flow resistance computed). This flow resistance was representative of the CFD domain. The results were similar to a standalone mass flow network solution and addition of the CFD domain did not appreciably change the total mass flow.

Validation was therefore carried out against a FLUENT (FLUENT 2003) model. The ESP-r model of figure 5.7 is reproduced in figure 5.12a along with geometrical detail. Figure 5.12b shows details of CFD gridding and operating conditions. The ESP-r model was set up to keep the walls of the domain at a constant temperature of 20^0C. External temperature was defined to be the same to ensure that the air that entered the CFD domain was the same temperature as the indoors. The only driver for air flow within the domain was wind pressure. Both the ESP-r and FLUENT models consist of 1080 hexahedral grid cells. This was the smallest number of grid cells that gave acceptable results as was shown from a parametric study. It was considered acceptable because the present work is a validation study and it is expected that in a real world model a larger number of grid cells would be used. The models consist of nine boundary conditions: six of these are representative of the solid walls and the other three are the air flow openings (EFGH, KLMN and TUVW). The walls were named north, south, east and west assuming north to be in the direction of positive y axis. The horizontal surface at the top was called roof and the one at the base was called floor. The air flow opening in west was called west_out, the one in east was called east_out and the one in the roof was called top_out. These nine boundary conditions and gridding similar to the ESP-r model form the complete description of the CFD model. The wall type boundary conditions were set to have a

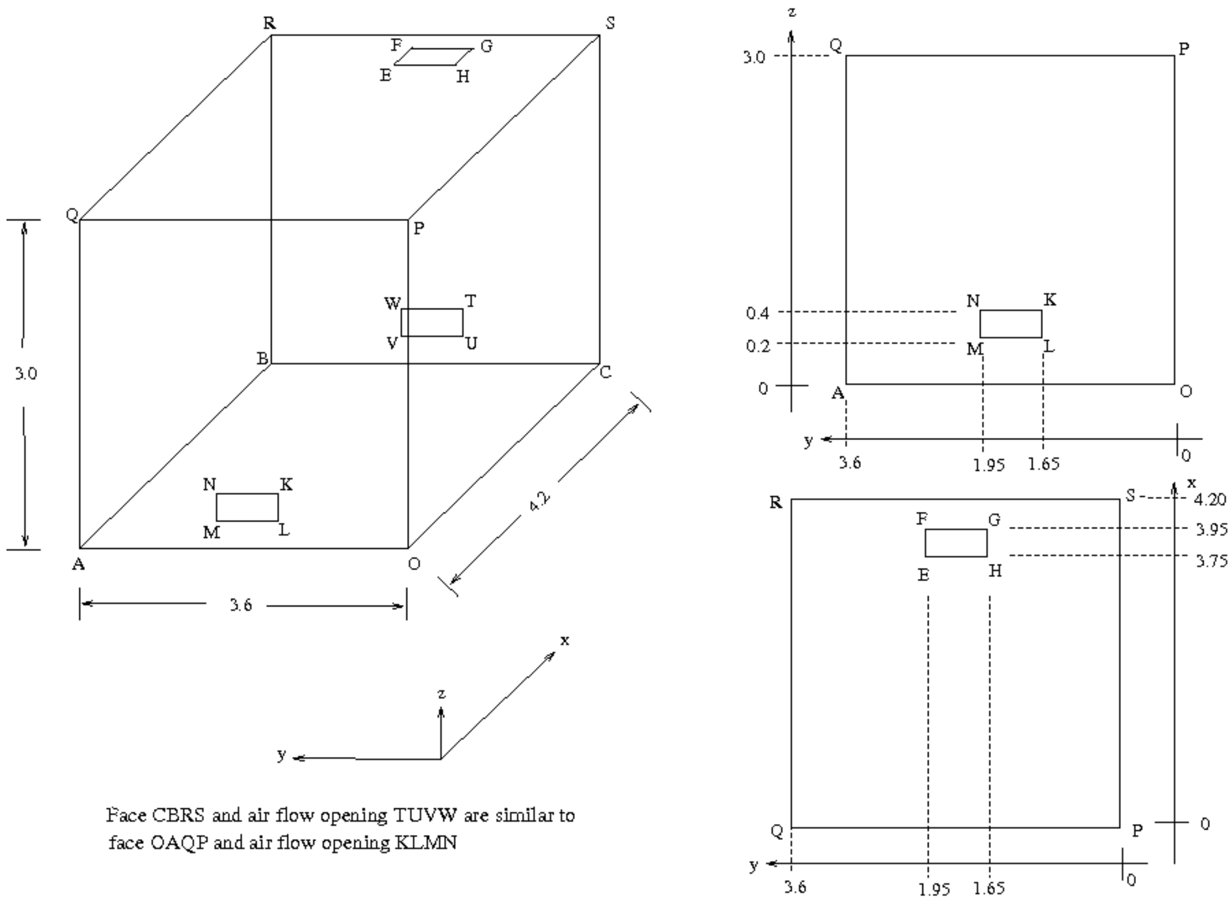

Figure 5.12a Geometrical details of model for inter-model comparison (all dimensions in metres)

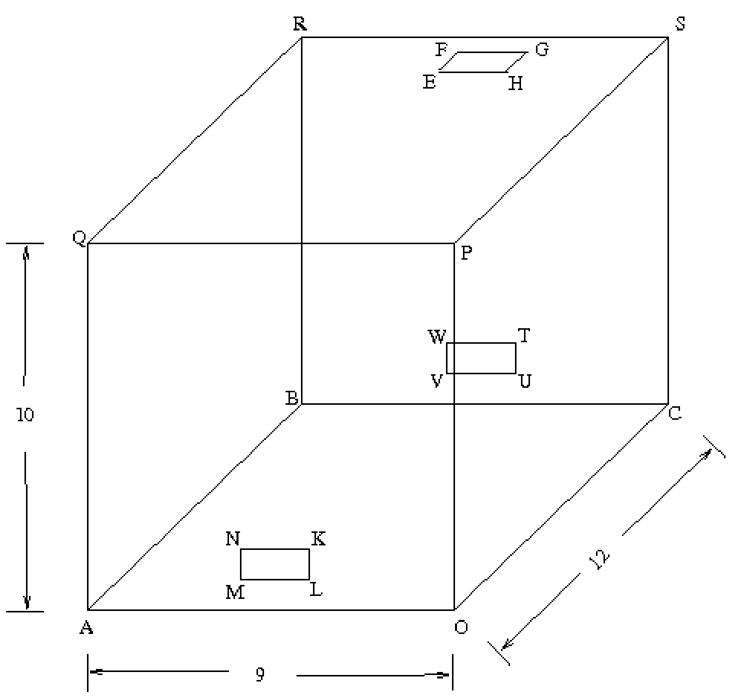

The number of cells along each axis are shown in the figure. A total of 1080 CFD grid cells were used.
Cell dimensions are
0.35m along x–axis
0.40m along y–axis
0.3m along z–axis

Operating conditions:
Pressure = 1.01325 bar
Temperature = 293K
Gravity = 9.81m/s^2
Density of air = 1.225kg/m^3

Figure 5.12b Gridding detail

constant temperature of 20^0C. The air flow openings were defined to be constant pressure type boundary conditions for the FLUENT model and these were taken from the ESP-r model. Knowing prevailing wind direction and speed (held in an ESP-r climate file) it is possible to calculate the pressure that will be exerted onto a building surface if the orientation of that surface is known. This method is given in detail in (Clarke 2001) and is briefly explained here. A dimensionless pressure coefficient is defined:

$$C_p = P_d \div \left(\frac{1}{2} \rho V_r^{\,2} \right) \tag{5-2}$$

where C_p is the pressure coefficient for wind direction d, P_d is the surface pressure (Pa), ρ is the density of air (kg/m³) and v_r is some wind speed (m/s) corresponding to that wind direction. A pressure coefficient set typically consists of 16 compass values offset at 22.5^0 intervals. Computing wind pressure at any surface is then a matter of putting the values of the various climate parameters (wind speed and air density) and building orientation functions (relevant pressure coefficient values for surface direction) into equation (5-2). The ESP-r model was simulated and pressures at each of the boundary nodes were exported to the FLUENT model as the three opening type boundary conditions were defined as constant pressure type boundary conditions. Doing so ensures that the two models are equivalent even though they may have different types of air flow boundary conditions.

Both the models were allowed to solve and converge. The results predicted from both were then compared. The mass flow network used, along with predicted pressures, is shown in figure 5.13. The mass flow rates shown on the figure

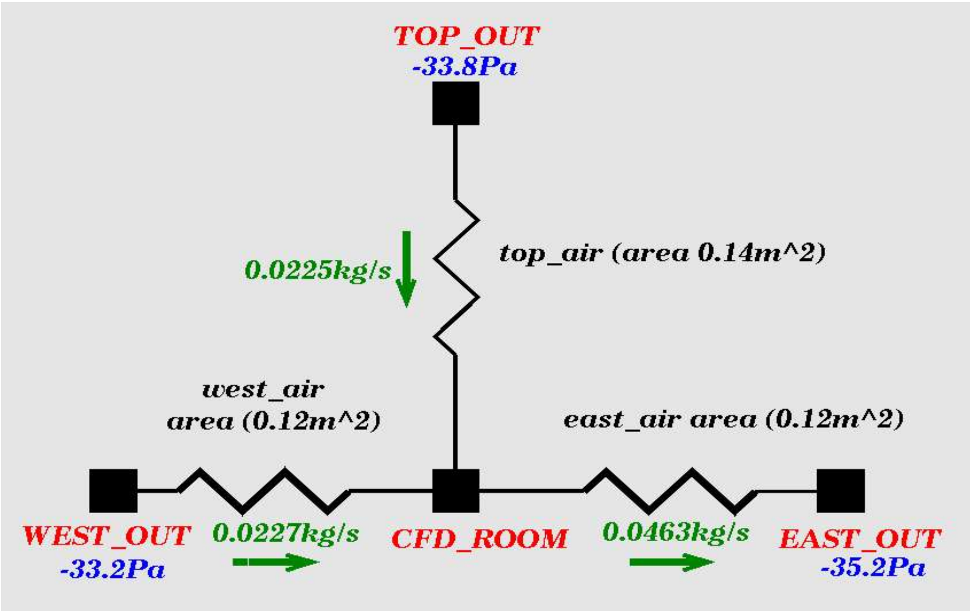

Figure 5.13 Air flow network for the ESP-r model. Node and connection names are in UPPER CASE RED and lower case black respectively. Pressures are shown in blue and mass flow rates predicted from thermally coupled mass flow network in green.

are those from thermally coupled mass flow solver and do not include CFD data. Similar results were obtained for 24 hourly values using a constant ambient and internal temperature and only varying wind pressure. The mass flow solver was then coupled with CFD using Yuan wall functions (Yuan et al 1993) to treat near wall conditions and a standard $k-\epsilon$ turbulence model using the known pressure node conflation mechanism (type B1) and a corrected version of the mass flows and internal pressures was obtained. Finally the FLUENT model was simulated using similar wall functions, turbulence model and pressure boundary conditions taken from the ESP-r model. Different grid sizes were used to ascertain that the results were grid independent. The models that were compared were thus three namely: thermally integrated mass flow network (model 1), thermally integrated mass flow network conflated with a CFD domain (model 2) and standalone CFD (model 3). The conflation type used for model 2 was type B1 and corresponding air flow openings within the CFD were defined using that conflation method. The air flow openings in model 3 were defined as constant pressure type boundary conditions as described above. The three models, although defined in different ways, were considered to be equivalent as far as bulk air flow was concerned. The two models 2 and 3 were considered to be equivalent on the scale of detailed air movement as well. Contaminant prediction for the models is calculated as a scalar therefore it was considered appropriate that only air flow rates were compared. All contaminant concentrations would by default be directly proportional to the air flow rates and hence relative errors would be identical.

The results from all three types of simulation for one time step are given in Appendix CCS. An elementary analysis computing relative differences shown as a histogram showing percent deviation from thermally conflated *mfs* is shown in figure 5.14. It can be seen that the conflated approach (model 2) is very close to the thermally coupled *mfs* (model 1). The difference in the FLUENT results (model 3) can be ascribed chiefly to the choice of flow coefficient within the flow network which governed mass flow in the conflated approach but not the FLUENT standalone CFD.

The flow coefficient determines mass flow rate through the opening defined in the mass flow network. The governing equation (Hensen 1991) is equation (5-3)

$$\dot{m}=C_d A\sqrt{2\rho\Delta P} \qquad (5\text{-}3)$$

Where $\dot{m}$ is mass flow rate, C_d is the discharge coefficient, A is the area of orifice, ρ is the density of air and ΔP is the pressure difference across the orifice.

Karava et al (2004) suggest that assuming a constant 'text book' value of the discharge coefficient is sufficient for all configurations of shape and location in the facade, wind angle and Reynolds number is questionable as a simplification. The best method for determination of discharge coefficient is wind tunnel experiments taking into consideration scaling, upstream flow conditions, internal partitions and the assumptions of turbulent flow. A less resource intensive course was taken for the determination of the discharge coefficient in this study.

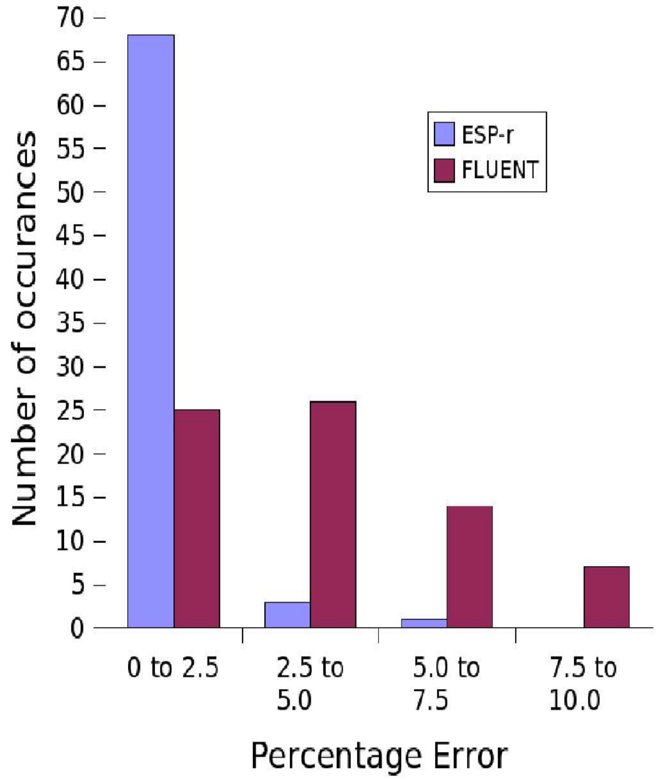

Figure 5.14 Comparison of conflated and standalone CFD against bps

It was seen that varying the discharge coefficient did change flow rate significantly and there needed to be some way in which the discharge coefficient could be determined. In order to determine the discharge coefficient, arbitrarily chosen boundary pressures were imposed and the value of discharge coefficient within ESP-r was varied. Flow rates from the ESP-r model were compared with those predicted by FLUENT and that value of discharge coefficient was chosen that gave best overall agreement for the arbitrarily chosen flow field. Another flow condition was then chosen and the validity of the coefficient was confirmed. This mechanism although quite unorthodox provides results for which two thirds are within 5% of those predicted by ESP-r and a fifth are within 7½%. No more than 10% error was reported for any flow rate. Another possible reason for the difference within the results is the convergence criteria used. Convergence criterion for the conflated approach and the standalone CFD solver was kept such that the solution was considered to converge when the maximum residual was 0.001kg in any cell. This is comparable to the error in the flow rates obtained as detailed in Appendix CCS and could be the cause of some discrepancy. Figure 5.15a shows the results from the model 2 simulation. The 2D slice shown is the central East West section. The image shows that most of the room air is stagnant with some air flow into the domain from west_out and top_out. The overall flow pattern is similar to that predicted by FLUENT (figure 5.15b). Direction of flow was similar for the two models and can be seen in figure 5.16.

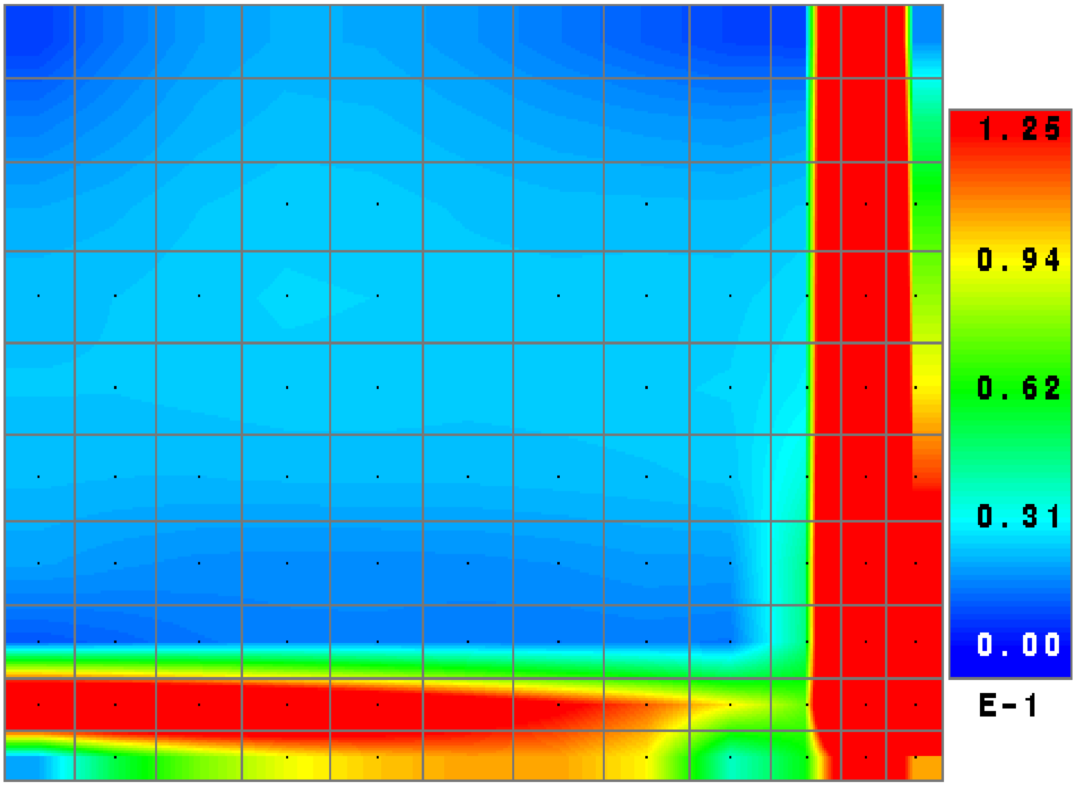

Figure 5.15a Conflated ESP-r predicted air speed at central East - West section of CFD domain (units m/s)

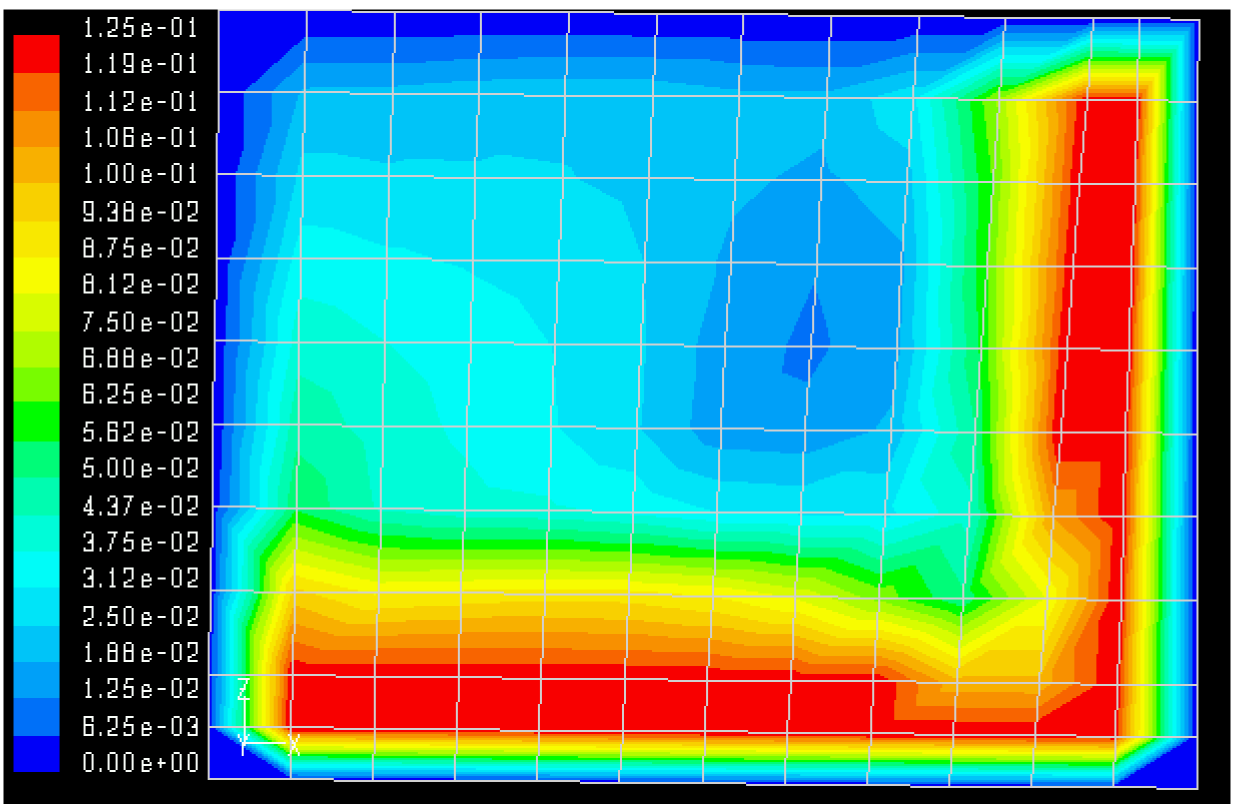

Figure 5.15b FLUENT predicted air speed at central East -West section of CFD domain (units m/s)

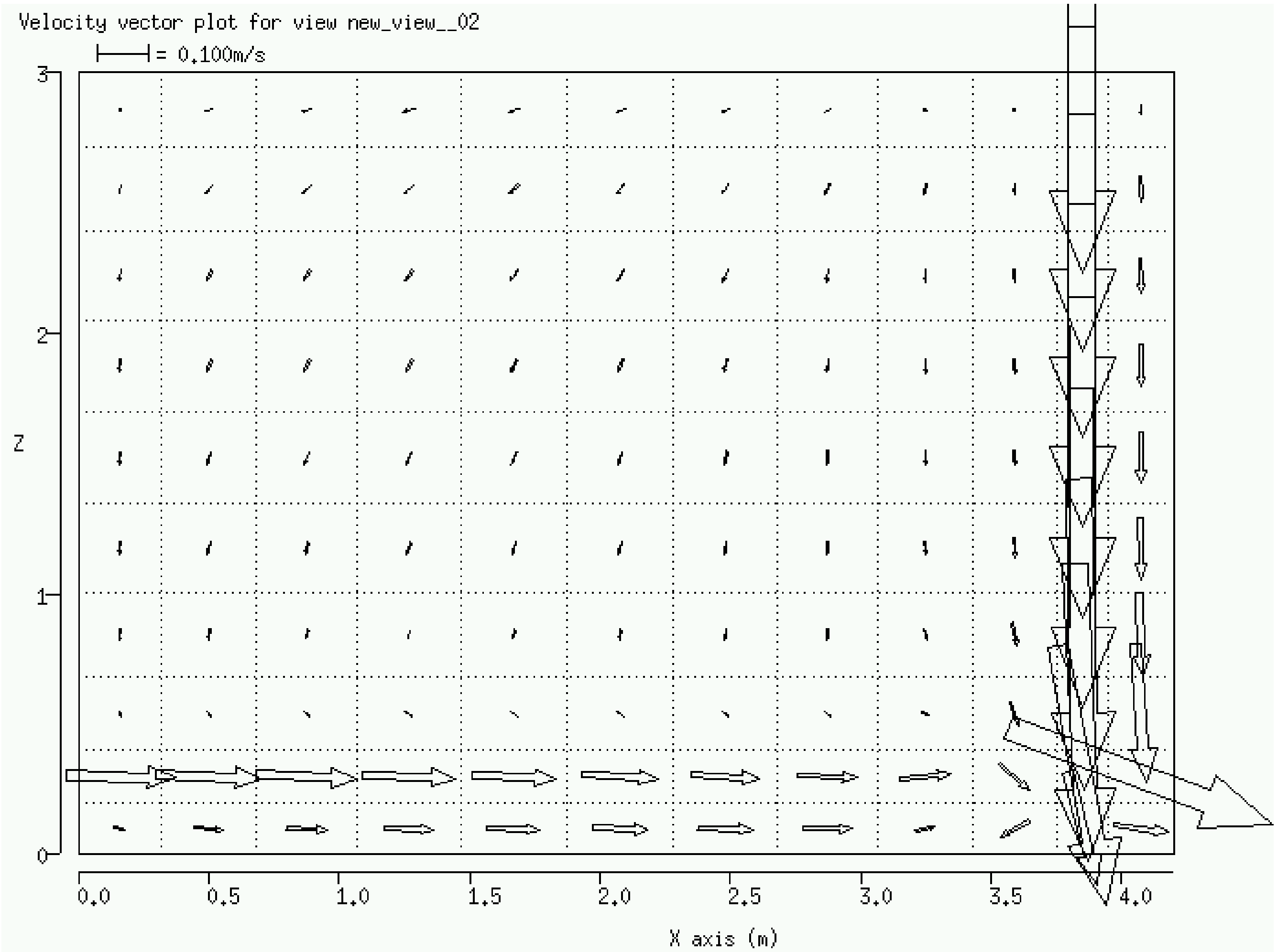

Figure 5.16 Flow directions for the CFD validation model

5.8 Summary

In order to model contaminants rigorously i.e. within buildings using a bulk contaminant flow model and in greater detail within one part of a building (e.g. a room) it was important to conflate mass flow network with CFD. This conflation is in addition to the conflation between thermal simulation and mass flow network and thermal simulation and CFD. Hence the solution process occurs with simultaneous solution of all the different domains exchanging information amongst themselves and thereby converging onto a more accurate solution than if these modules were solved in isolation. The importance of generic domain integration cannot be stressed enough within building simulation. Individual domains e.g. building thermal, HVAC, lighting etc. are well developed and well understood and have reasonably well developed and tested solution methods. The need is to conflate these different domains using critical parameters for passing information amongst them. The specific problem of integration of mass flow network and CFD modelling has been addressed in this chapter. While some approaches for conflation exist they are still mostly theoretical and have not been implemented and applied widely. Different possible approaches have been examined in detail and so are the advantages and disadvantages.

The known pressure node conflation (type B1) is implemented as default by using constant pressure type air flow network nodes. This approach is then validated using a conflated CFD model with three mass flow type boundary conditions against a standalone CFD model using the same configuration but with the mass flow boundary conditions being dictated by wind pressures. A thermally integrated mass flow network was also solved and compared with the two solution methods. The conflated CFD domain had no information regarding wind but was passed this information via the coupled mass flow network in the form of velocity type boundary conditions. Validation results seem to be promising. The next chapter illustrates the approach using case studies.

5.9 References

Bartak, M. Beausoleil-Morrison, I. Clarke, J. A. Denev, J. Drkal, F. Lain, M. Macdonald, I. A. Melikov, A. Popiolek, Z. Stankov, P..2002. *Integrating CFD and Building Simulation*, Building and Environment**,** 37(8-9).

Clarke, J. 2001. *Energy Simulation in Building Design*. Butterworth-Heinemann, Oxford, UK. ISBN 0-7506-5082-6

Denev, J. A. 1995. *Boundary conditions related to near-inlet regions and furniture in ventilated rooms.* Proceedings of Application of Mathematics in Engineering and Business, Institute of Applied Mathematics and Informatics, Technical University, Sofia.

FLUENT. 2003. *FLUENT User's Manual.* Fluent Inc. http://www.fluent.com

Hensen, J. 1991. *On the Thermal Interaction of Building Structure and Heating and Ventilation System.* PhD Thesis, Technische Universiteit Eindhoven, The Netherlands.

Karava, P., Stathopoulos, T., Athienitis, A. K. 2004. *Wind Driven Flow Through Openings – A Review of Discharge Coefficients.* International Journal of Ventilation, Volume 3, (3).

Negrao, C. 1995. *Conflation of Computational Fluid Dynamics and Building Thermal Simulation*. PhD Thesis, University of Strathclyde, Glasgow, UK.

Negrao, C. 1998. *Integration of Computational Fluid Dynamics with Building Thermal and Mass Flow Simulation*. Energy and Buildings 27(2).

Scarborough, J. 1966. *Numerical Mathematical Analysis*. 6th Edition, The John Hopkins Press, Baltimore, USA.

Thompson, C., Leaf, G. 1988. *Application of a Multi-grid Method to a Buoyancy-Induced Flow Problem. In: McCormick SF, editor. Multi-grid Methods–Theory, Applications and Supercomputing.* New York: Marcel Dekker Inc.

Wang, L. L., Chen, Q. 2005. *On Solution Characteristics of Multi-zone and CFD programs in Building Air Distribution Simulation.* Proceedings of 9th IBPSA Conference, 2005, Montreal, Canada.

Yuan, X., Moser, A., Suter, P. 1993. *Wall Functions for Numerical Simulation of Turbulent Natural Convection Along Vertical Plates.* International Journal of Heat and Mass Transfer, 36 (18).

6 CASE STUDIES

6.0 Introduction

Integration of the contaminant prediction facility using a contaminants network within the context of whole building simulation has been achieved successfully. The contaminants network facility allows bulk flow of contaminants to be studied by modelling the contaminant flow calculated from the bulk flow of air from one building section to another. The mass flow network that is employed to solve for air mass flow rates is integrated thermally with energy simulation of the building and associated energy systems. This provides a more accurate picture of the bulk air flow and contaminant fields. Contaminants can also be studied at the much finer intra-room level using CFD. The network mass flow approach was conflated with CFD and validated in chapter 5. It is now possible to look at bulk transport of contaminants within a building and also to look at detailed contaminant distribution within a part of the building

This chapter describes a number of case studies that demonstrate how the contaminant prediction facility can be used to give results that can be used in a design context to provide detailed contaminant flow characteristics. This provides designers and other interested parties with a tool to assess indoor air quality in terms of species concentration and then to base decisions on such findings.

6.1 Public House in England (IAQ vs Energy)

6.1.1 Model Description and Operating Conditions

Figure 6.1 shows a public house in England which was studied to show how CO_2 and CO from smoking varied within occupied hours. The model consists of five zones named public, lounge, bar, conser and conser_sun. The model

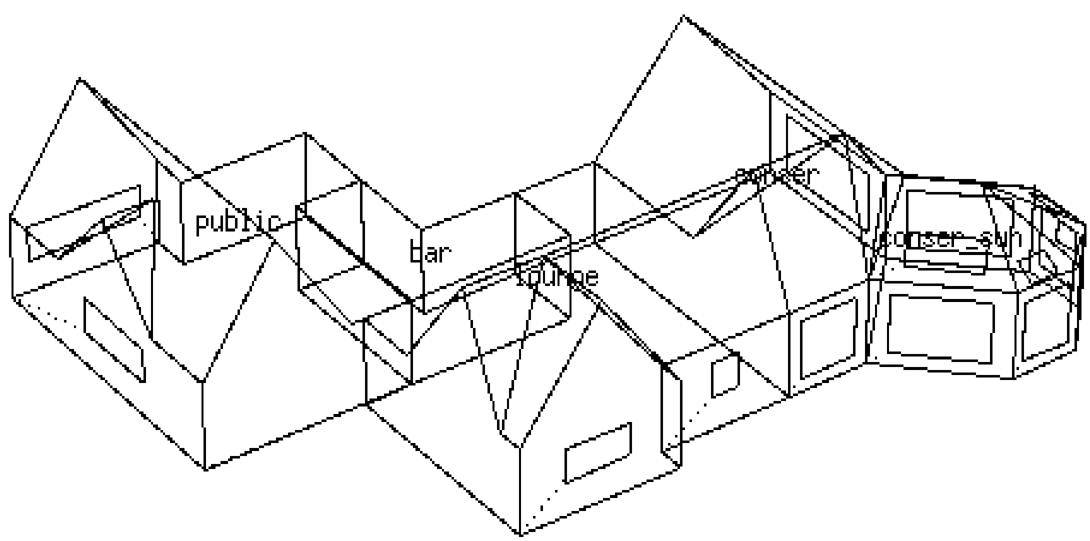

Figure 6.1 George and Dragon Holmes Chapel (public house in England)

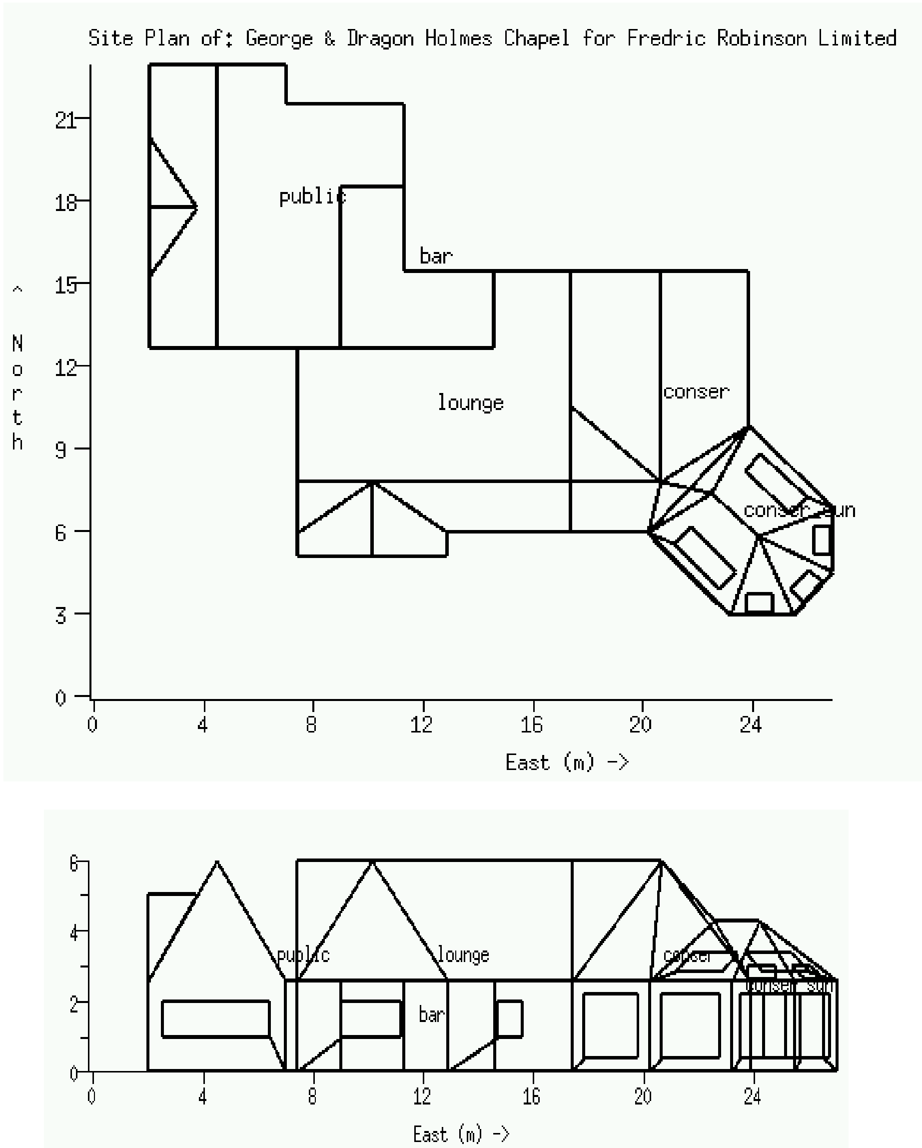

Figure 6.2 Plan and South Elevation of Public House

was built to study thermally induced effects on the air flow (and hence on the contaminants transfer) of a new conservatory that was to be built on the south side of the public house. This conservatory was modelled by the two zones conser and conser_sun. This study also investigated the opposing demands made by the requirement of provision of adequate air quality and the requirement of provision of adequate thermal comfort on the HVAC system. As a worst case scenario simulations were carried out in winter in order to exacerbate the contrast between energy provision for heating and IAQ. This was hoped to provide information that might lead to understanding of the important point that increasing ventilation rate provides better IAQ but increases energy demands for heating at the same time. Furthermore one section of the building (the public bar represented as zone 'public') was designed to be a smoking area, hence aggravating the problem of providing adequate indoor air quality.

Design air temperature for the winter time was 21^0C for all parts of the building except the bar which had a design air temperature of 18^0C. The occupancy was modelled as 160 people between 1200-1400 and again between 1900-2400. Between the hours 1400-1900 it was assumed that the building operated with reduced occupancy of 32 people. This occupancy was divided among the various zones comprising the building in rough proportion to floor areas so as to give an even (and realistic) spread of occupant casual gains and CO_2 emissions. Occupants were assumed to be the only sources of CO_2. The occupants were further assumed to be generating heat at the rate of 140W per person. This metabolic rate corresponds to 5.6×10^{-3} l/s of CO_2 (Liddament 2004). Ambient concentration of CO_2 was assumed to be constant at 4.6×10^{-6} kg/kg. Occupant smoking was modelled using carbon monoxide CO (although tobacco smoke contains numerous chemicals only one is modelled in order to simplify the problem; furthermore it is assumed that the path taken by one chemical from tobacco smoke will be similar to the path taken by other chemicals of the same origin). The amount of CO given out from one cigarette is 58.5mg (ARBSSD 2005). It was assumed that 75% of occupants in the smoking area were smoking at any given time and that one cigarette lasted 5 minutes.

Figure 6.2 shows model detail where a plan view and south elevation of the building divided up into thermal zones is drawn. The bulk of the simulated space is the occupied space which can be divided up into three principal regions: the public space where the main entrance is located which is also the smoking area within the building, the lounge which is a non smoking space which also has an entrance and is similar in occupancy patterns to the public bar and the conservatory which is a non-smoking space. The south eastern section of the conservatory is the conservatory proper i.e. with most of the wall area comprising transparent construction. For this reason it is modelled as a separate thermal zone. The simulated space consists of around $250m^2$ of floor area occupying a space of more than $1000m^3$. Built with typical construction materials the public house has brick walls with glass wool and air insulation for walls. The roof is light mix concrete with roofing felt, glass wool insulation and plaster board finish. The floor is common earth packed and gravel based with heavy mix concrete followed by glass wool insulation, chipboard and carpet.

A detailed mass flow model comprising five internal, two ventilation system and fourteen external nodes was built to describe various forced and unforced air flows. This is shown in figure 6.3. A balanced HVAC system was used to define intentional air flows for the building. Fresh air is introduced in the region above the bar i.e. in the thermal zone called bar. This air is then assumed to flow to the public and lounge spaces. Additional ventilation air inlets are provided in the zone conser. Air is extracted from public, lounge and conser. Airflows between the zones were modelled using door type air flow components that allow bi-directional flow. Unintentional flows through small openings around windows and other openings to the ambient were modelled using crack type components. Effort was made to account for all flow paths in the building. Ventilation rate for the building was taken to be at 8l/s per person and this was maintained even when the

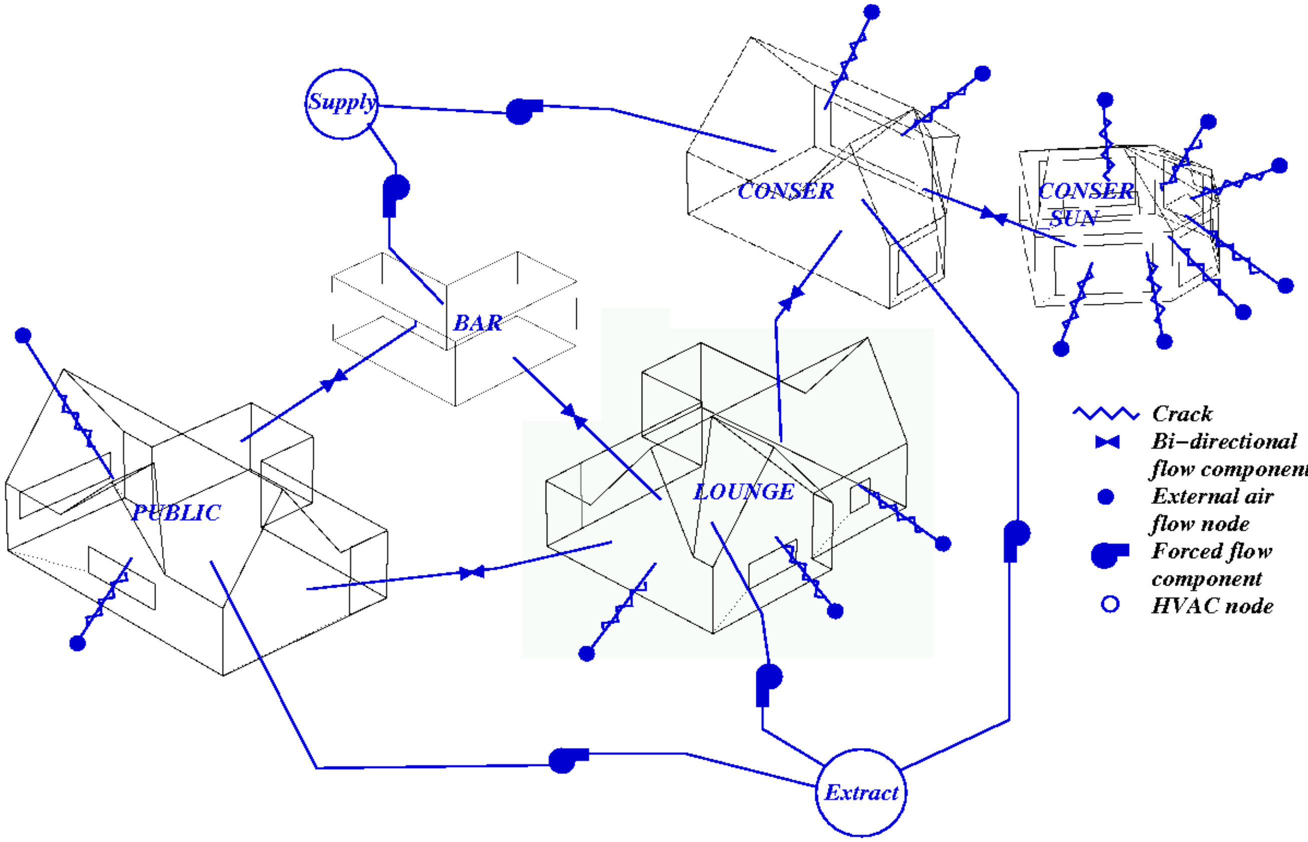

Figure 6.3 Air Flow Network for Public House

building was operating at less than design occupancy. Heating was achieved by heat input directly to the room and all fresh incoming air was considered to be at ambient temperature. This model supplied an opportunity to study the effects of providing enough air for dilution of contaminants against space heating energy requirements.

Detailed simulations were carried out for one winter day i.e. 8th January. The contaminants simulated in this study were CO_2 and CO. CO_2 is used as an indicator for indoor air quality because of its relative inertness in the indoor environment, homogeneity and ease of measurement. Therefore CO_2 was used as the contaminant of choice in this study. The ventilation system was designed to maintain a lower pressure in the smoking parts of the building (thermal zone public); this in turn could cause CO_2 to accumulate there. CO is used as an indicative contaminant that indicated how the contaminants generated by smoking would be distributed and to make sure that contaminant levels in both the smoking and non-smoking spaces were acceptable.

Flow control was also defined in the model. The windows in the model were opened when the CO_2 levels in that zone were above some threshold value. An alternative thermal control was also defined in which case windows were opened when temperature in the zone rose above some threshold value. At any given time either contaminant based control or temperature based control could be employed.

6.1.2 Ventilation Flow Variations Investigated

Two different ventilation schemes were studied in order to provide the best air quality in terms of thermal comfort and contaminant levels. The study was originally done as a commercial project and the clients did not want any air flow equipment (duct and diffusers etc.) within the conservatory region conser_sun. Thus the only connection that conser_sun had with the rest of the building was through the door to zone conser as shown in figure 6.3. It was thought at the start of the simulation that this would cause poor air quality and a better way to provide adequate air quality would be to have air extracted from conser_sun instead of conser. This was the second design variant and this is not shown graphically in the interests of brevity. Suffice to say that the connection from conser to extract in figure 6.3 was replaced by a connection from conser_sun to the extract using the same component.

6.1.3 Results Analysis

It was found that if control was kept limited to temperature sensing only, the heating requirements for all spaces was 540kWh without any form of ventilation based control for 1200-2400. This gave high CO_2 concentrations in some parts of the building. This is shown in figure 6.4. It can be seen that concentration in most parts of the building is relatively low except the zone conser_sun which does not have any extract. In the original study it was supposed that due

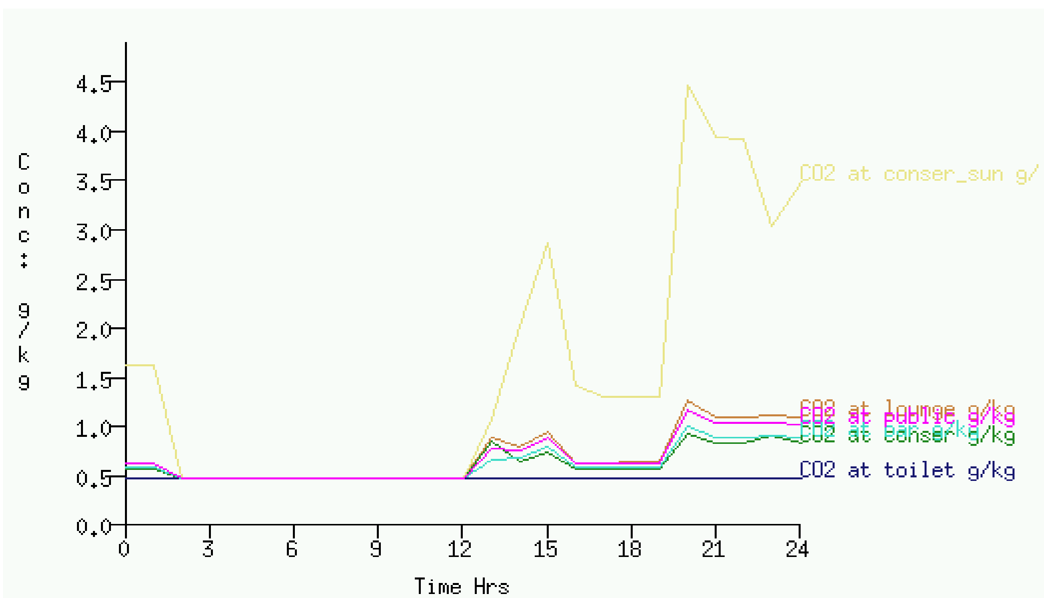

Figure 6.4 Concentration profile with temperature based control

to the construction of this particular zone (timber and glass) it would not be aesthetically appropriate to place HVAC equipment in that zone. Later on this supposition was dropped in favour of good IAQ. Aesthetics were thought to be recovered by employing a false ceiling. It can be stated that all zones show poor air quality in terms of contaminant concentration because the generally accepted level of CO_2 is around 1000ppm or 1.0g/kg (Sundell 1982).

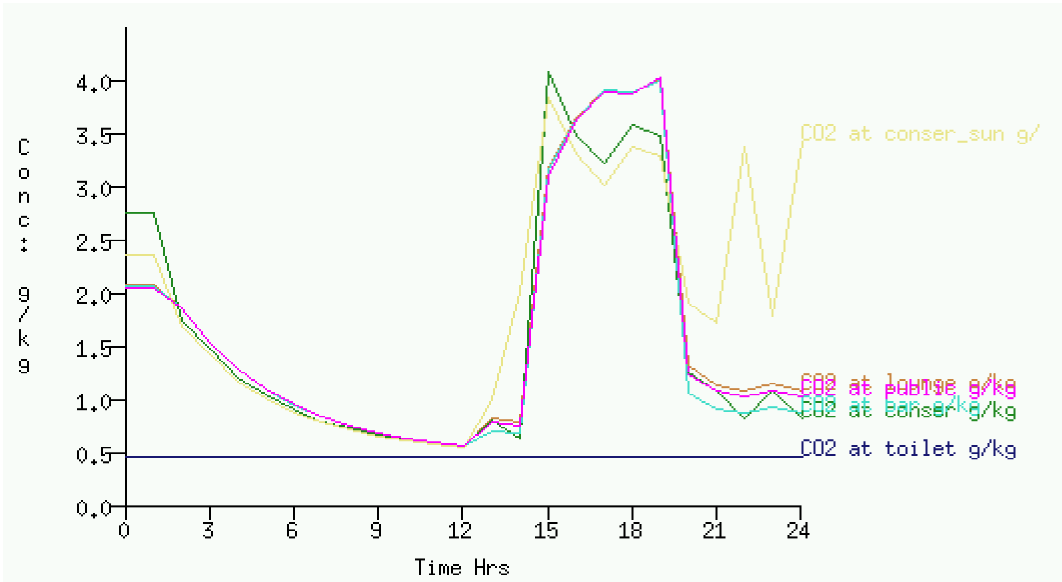

Figure 6.5 Concentration profile with occupancy based control

Temperature based control was dropped in favour of occupancy based control because of lower energy consumption. It was assumed that occupancy would be reduced to 20% in the quieter afternoon hours of 1400-1900. Correspondingly ventilation rates were lowered to 20% during that time. It was found that although the heating energy

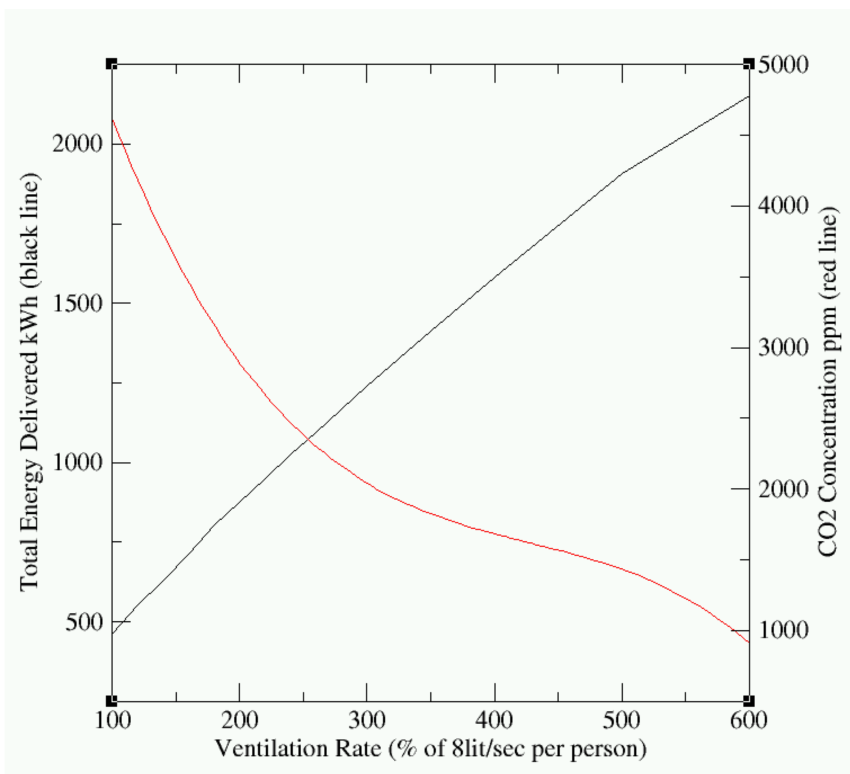

Figure 6.6 Effect of increasing ventilation on heating requirement and concentration

requirement dropped by about 50% to 274kWh CO_2 concentration rose dramatically in all zones. This is shown in figure 6.5. If this was a study of just space heating requirements and energy efficiency such a control may have been reported as a possible solution.

The maximum concentration was approximately 4100ppm in the zone conser for this type of ventilation control. To get a better picture this simulation was repeated a number of times with increased ventilation up to a maximum of 600%. Figure 6.6 shows heating energy results from the various simulations and maximum CO_2 concentration.

Being able to provide suitable air quality with 600% recommended ventilation plant size and more than four times more energy is clearly not the optimal solution. Problems in the original design and implemented control was then sought and possible solutions explored. One of the obvious problems with the ventilation system was improper air extraction from the zone conser. The air introduced in that zone was based on the combined load of that zone and conser_sun and there was no mechanism for extract from conser_sun. Air was therefore extracted from conser_sun. This improved both energy requirements and contaminant concentration. It was found that restricting CO_2 levels to slightly more than 1000ppm could be achieved by increasing ventilation by a factor of 2. This corresponded with a heating energy requirement of 880kWh.

CO tracking for the building shows that the zone public has the highest concentration of CO as expected but the ventilation system seems to be providing adequate ventilation air and the maximum concentration is 220ppm. Although there is no safe level for CO this concentration is below typical concentrations within smoking spaces (ARBSSD 2005). Figure 6.7 shows how CO varied for the different zones.

This case study provides an illustration of how indoor air quality can be compromised because of energy

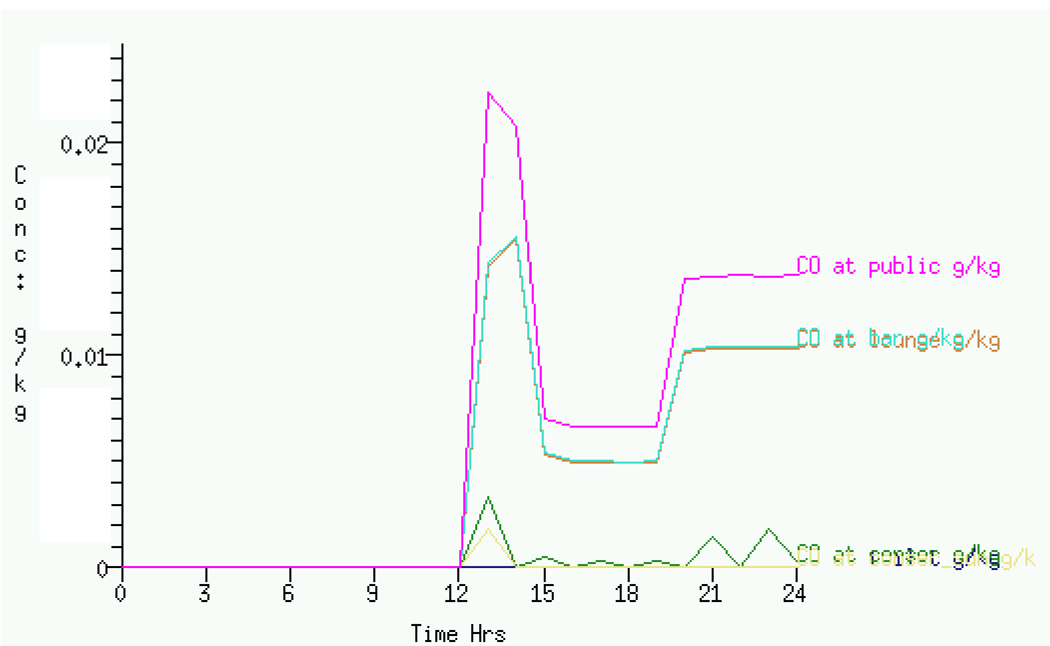

Figure 6.7 CO concentration pattern for public house

conservation considerations. It is not meant to understate the importance of good energy economy and efficiency measures but to imply that good air quality is also an important issue to consider when appraising energy conservation measures in order to ensure well being of inhabitants. Furthermore good design of a ventilation system can lower energy requirements for a space and at the same time alleviate poor air quality problems. It can be concluded that with an energy overhead of 60% CO_2 levels fell from 4500ppm to little above 1000ppm.

The work done in this research of integrating contaminant prediction and thermally integrated air flow modelling has made it possible to study contaminant behaviour and transport within the built space with a greater accuracy than by using standalone (i.e. not thermally coupled) network air flow and contaminant prediction tools. This is because temperatures are predicted dynamically and the program does not rely on predefined schedules. Consequentially air flow rates between the different areas of a building are more realistic and the contaminant flow rates which depend on air flow rates are therefore more realistic. It is hard to imagine a similar thermal, airflow and contaminant study, using control and design variants, to be undertaken by using one or more standalone tools.

6.2 Manager's Office (CO_2 Based Control)

6.2.1 Introduction

A hypothetical office in a building is simulated in this case study. The purpose of the study is to show how when design conditions of occupancy are not maintained there can be an air quality problem. The study also shows how CO_2 based ventilation control can be a means to overcome this problem. The model consists of two offices and a corridor. One of the offices is used to offer a base case scenario in which a manager works from 9am to 5pm with a lunch break at noon. The situation in this office (thermal zone manager_b) does not change but when an all day meeting takes place in the other office (thermal zone manager_a) the CO_2 levels of the two provide a stark contrast. Finally the situation is resolved by increasing the ventilation supply from 8l/s per person to the higher value of 48l/s per person and CO_2 based control is invoked to set this higher rate ventilation.

6.2.2 Model Detail

Figure 6.8 shows the model detail. As can be seen, the model consists of two offices on the same side of a corridor. These offices are part of a longer line of offices in the middle of a building. The zone of interest manager_a is a typical office with about 14m^2 floor area, and glazed area a little less than 40% of floor area. In addition to one occupant it has lighting at 10W/m^2 and one computer in the room. Double glazing is used and most walls of the room are internal, exceptions being the south facing walls which are external. The building was modelled with climate for Kew (ESRU 2005) from 9th January to 15th January. The building is located in London and has typical external concentration of CO_2 of

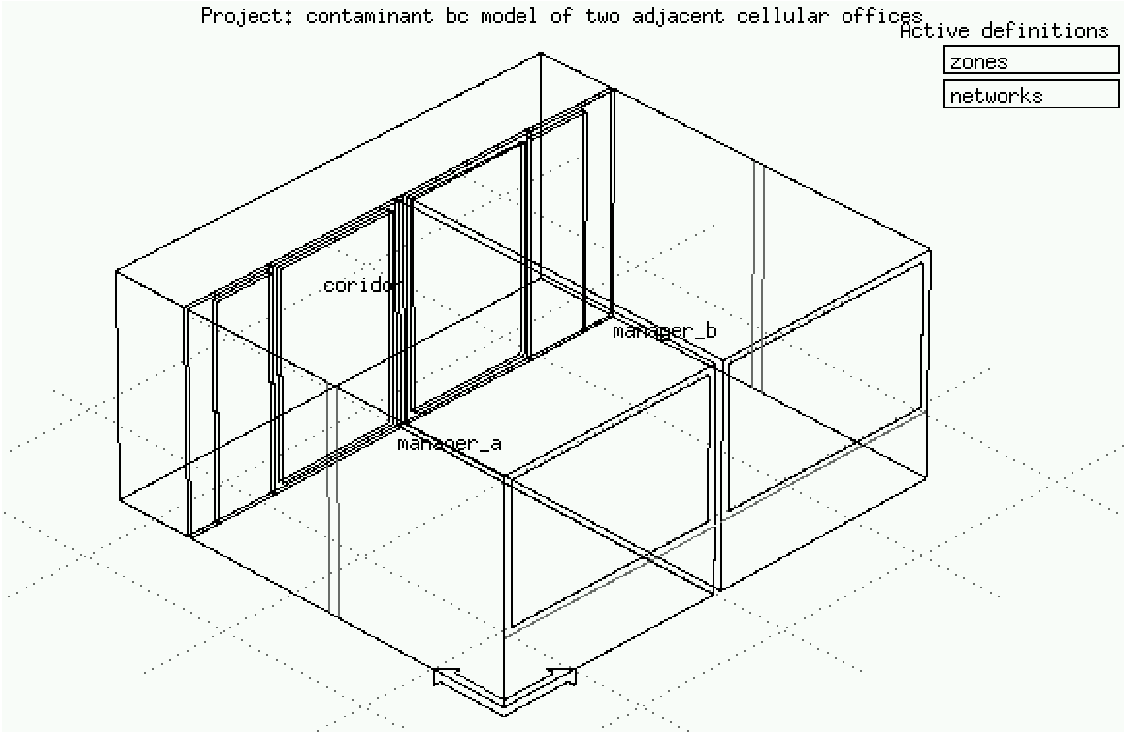

Figure 6.8 Model detail for cellular offices

4.6×10^{-4} kg/kg. Typical constructions were used with gypsum plaster board internal partitions, double glazed windows, false ceilings and a suspended floor. The building is thought to be a high rise building and consequentially the external walls of this building are modelled as walls fully exposed to the wind. To model the air flow for the rooms an air flow network was used.

Figure 6.9 shows the air flow network used to model the cellular offices. The network consists of six nodes, three of which are boundary and the other three represent the building spaces. There are only two components in the base case network model: these are the air flow crack and opening. The air flow crack allows air to flow through it following equation (6-1) and the opening allows air to flow through it as defined in equation (6-2)

$$\dot{m}=\rho k \Delta P^{x} \tag{6-1}$$

$$\dot{m}=C_d A\sqrt{2\rho \Delta P} \tag{6-2}$$

where $\dot{m}$ is mass flow rate (kg/s), ρ is density (kg/m^3), ΔP is pressure difference (Pa), C_d is discharge coefficient, A is area of opening (m^2), $x=0.5+0.5\exp(-500W)$ and $k=L9.7(0.0092)^x/1000$ where L (m) and W (m) are crack length and width respectively (Hensen 1991). For the air flow crack a length of 2.0m and width of 0.015m was chosen and for the air flow opening an area of 0.25m^2 was chosen.

In addition to the base case model two more air flow models were investigated. The first variant were built by replacing the opening connecting the nodes manager_a and manager_b to south_ext by one 8l/s fan each. For the second variant a 48l/s fan was put in place of the crack joining manager_a to south_ext. Hence the base case was purely naturally ventilated whereas the other two models were not. For the mechanically ventilated models design air flow rates were 8l/s. For the second mechanically ventilated flow network the 48l/s fan came on when CO_2 levels in the space rose past the set point of 1000ppm. This is a typical example of contaminant based control.

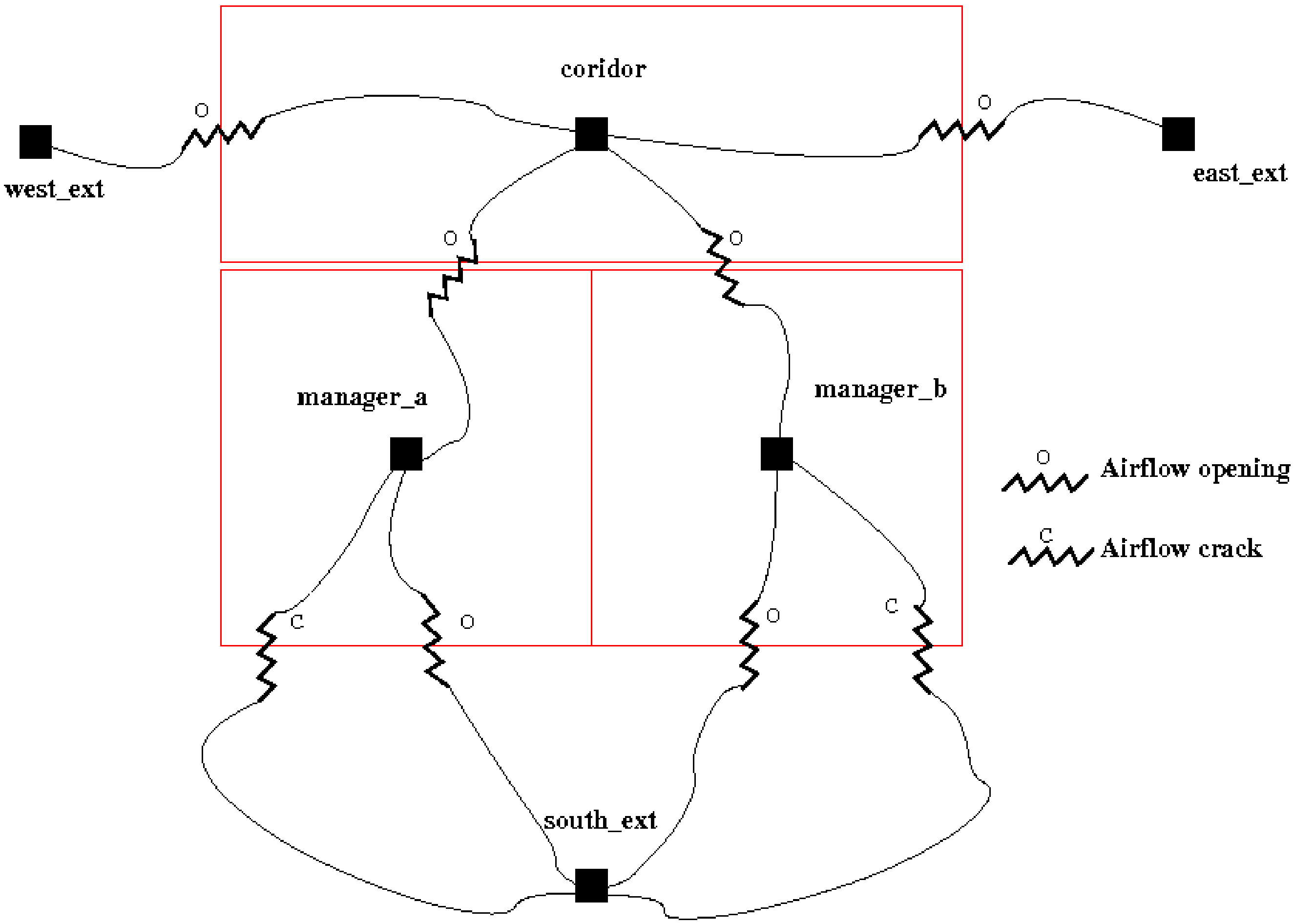

Figure 6.9 Air flow network for cellular offices

6.2.3 Simulation and Results

Simulations were carried out with natural ventilation for design occupancy and higher occupancy. Figure 6.10 shows results obtained for design conditions for one week. The fluctuations in the graph can be attributed to time varying wind speed and direction. As can be seen CO_2 levels do not rise above 1000ppm. This condition is changed when a meeting in manager_a draws a total of six people (for this example it is assumed that the meeting lasts for the whole day for six days). Figure 6.11 shows contaminant concentrations which are much in excess of the recommended value of 1000ppm. It can be concluded that even if natural ventilation is sufficient for design conditions there needs to be some

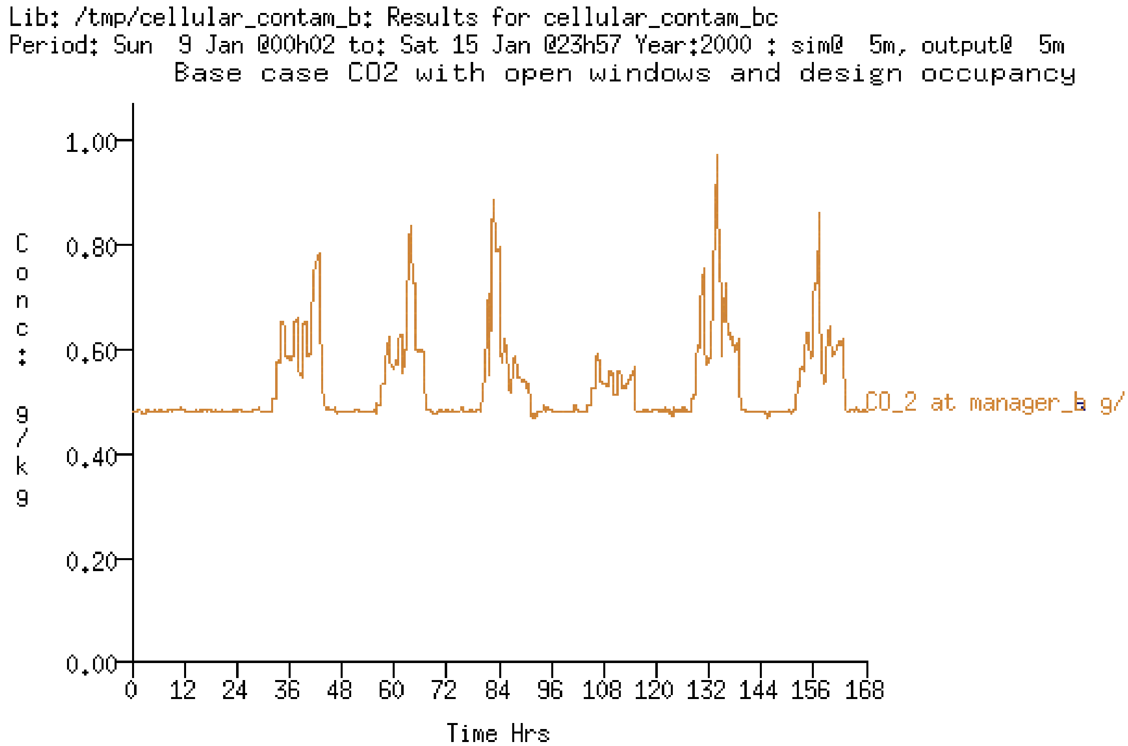

Figure 6.10 Concentrations with design occupancy for manager_a and manager_b (both offices show similar profile)

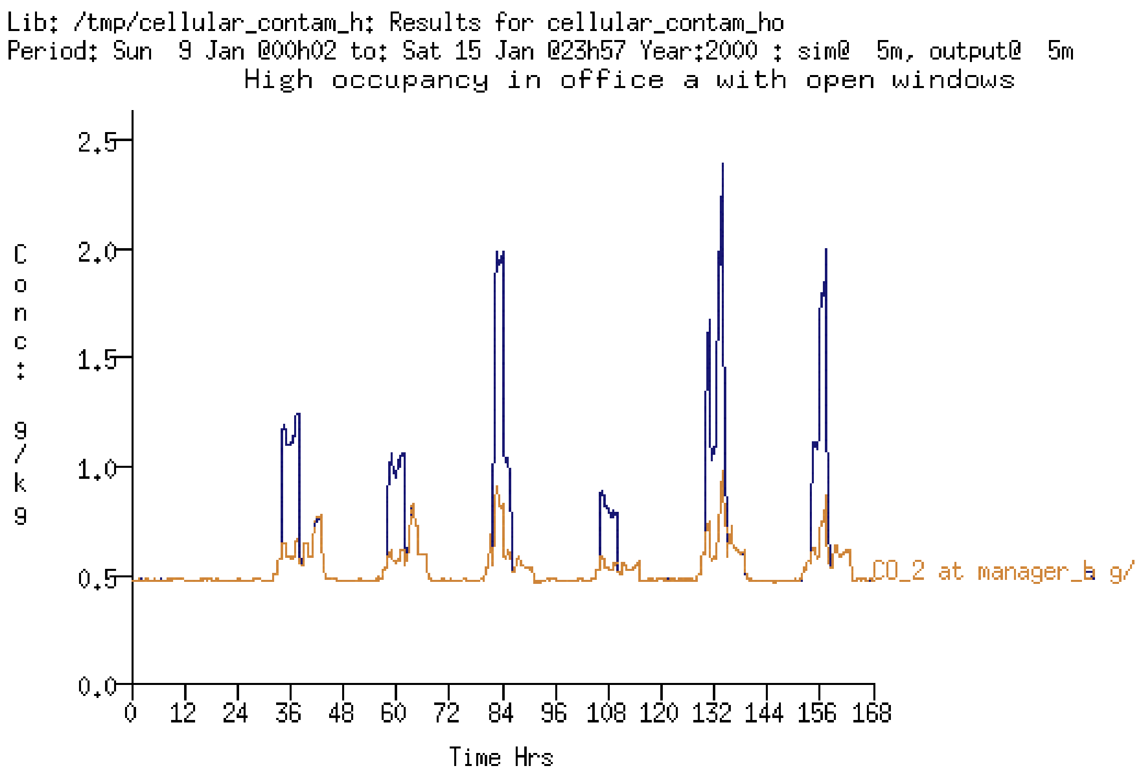

Figure 6.11 High occupancy with natural ventilation. Concentration in manager_a is shown in blue and in manager b it is shown as orange.

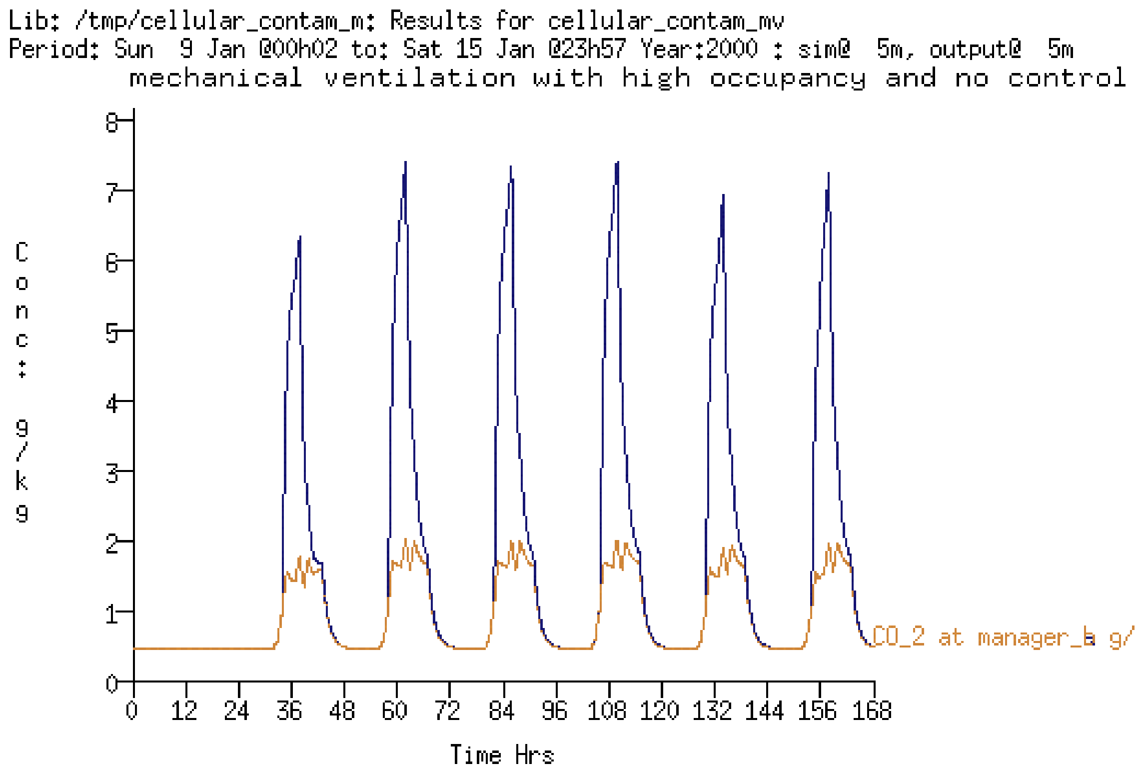

Figure 6.12 Increased occupancy in manager_a with no control and design ventilation levels. Concentration in manager_a is shown in blue and in manager b it is shown as orange.

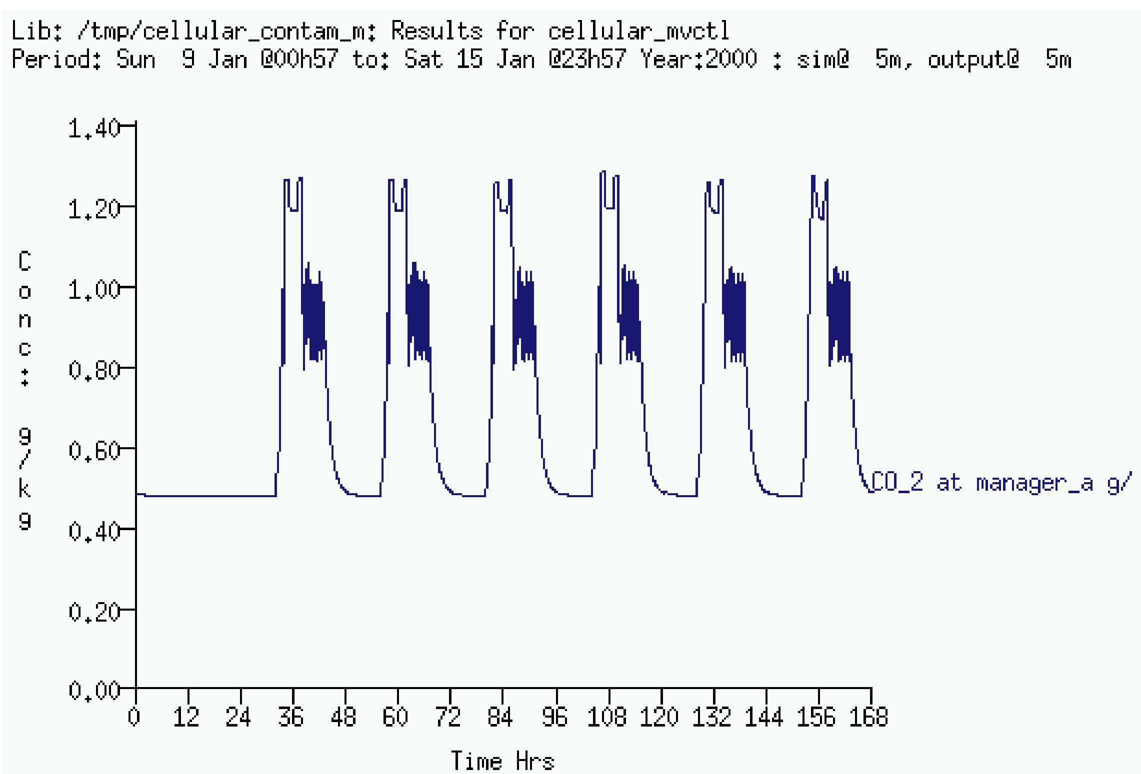

Figure 6.13 Controlling IAQ by better ventilation and control

mechanical ventilation for periods of high occupancy in the offices.

This situation would worsen in the presence of mechanical ventilation designed to provide for the needs of one manager in the office. Mechanical ventilation was modelled by modifying the network of figure 6.8. The air flow opening joining manager_a to the external node south_ext was deleted and another connection was made between the nodes using a fan represented by a constant flow rate component. The simulation was repeated and results are shown in figure 6.12. As can be seen concentrations as high as 7000ppm were obtained when the office is occupied by six people. This is clearly not acceptable.

The problem is alleviated by introducing a bigger fan (represented by a constant flow rate component again) and controlling it using a CO_2 sensor. Simulation results are shown in figure 6.13. It can be seen that once CO_2 control starts, after an initial surge of high concentration, the contaminant level is strictly controlled to within permissible limits.

This study has demonstrated how the new facility of contaminant prediction can be used to study ventilation and contaminant problems in an integrated manner and it is now possible to model the well being of occupants . The effects of wind speed and direction, internal occupants, heat gains from equipment, internal and external temperature difference, network mass flow, radiant and convective heat exchange etc. have all been taken into account in order to calculate bulk transport and distribution of contaminants. Such appraisals had not been possible previously.

6.3 Balancing of Energy Consumption and Good IAQ by using CO_2 Control

The use of CO_2 control was investigated to study the balance between energy requirements and good indoor air quality. The model used was the English public house and details are given earlier in section 6.1. CO_2 control was imposed on the different fan components in the flow network. Direct control was imposed i.e. if the CO_2 concentration rose above 1000ppm the ventilation fans started operation. It was found that with a bigger heating plant capacity, energy demands did not increase as they did when ventilation was increased (figure 6.6). Instead energy consumption reached a fairly constant value with increase in ventilation capacity. This corresponds to roughly the same amount of air being introduced within the space over a long period of time (one day). In the case of a smaller plant, ventilation comes on in longer bursts and in the case of a larger plant, ventilation comes on in shorter bursts but with the net effect of delivering the same amount of air. Table 6.1 shows how heating requirement changes with bigger capacity plant (100% ventilation is equivalent to 8l/s per person).

It was also found that the distribution of contaminant was more uniform in the whole space i.e. over all the zones with CO_2 based control and this was true for all concentrations whether above the permissible limit or below it. This was because of providing fresh air on a demand basis and not on static assumptions e.g. floor area or projected occupancy etc.

In summary it can be said that a higher capacity ventilation system would be better suited to provide energy conservation and at the same time better air quality. This would be possible only if contaminant based ventilation control is used. It was concluded that bigger plant should be used which gives the best efficiency for building design and operating conditions. The only other limiting factor would be the capital investment and logistics for operation and commissioning required for the bigger plant. Again integrated simulation can be seen as a tool that helps in intelligent design decisions to be made early in a project and thus saves time and money and provides for better planning.

Ventilation Rate	100%	200%	400%	600%	800%	1000%
Energy kWh	339	475	528	667	665	669

Table 6.1 Change of energy consumption with progressive increase in ventilation capacity using CO_2 control

6.4 Canadian Conference Building with Atrium

6.4.1 Model Detail

This model was originally studied by Hand and Strachan (2002): the design of the building ventilation system was novel and not energy intensive. It involved a displacement ventilation system driven by occupant, lighting and small power gains within the building and linked to an atrium which is comfort conditioned. The idea was to naturally ventilate the conference rooms of figure 6.14 from the atrium. The driving forces behind this ventilation would be stack effect enhanced by thermal gains within the rooms. In a sense ventilation would be driven by heat gains from the rooms because when there would be no heat gains in the rooms (probably in the absence of occupants) the stack effect would diminish and so would the ventilation rate.

The original study reported several design options in detail. It also identified that a solution with greater resolution would be required in a building that was so sensitively balanced in terms of ventilation and thermal performance. Such a solution was not possible at the time the original study took place but can now be obtained and studied using the developed approach of conflation of mass flow network with CFD as explained in chapter 5. This case study looks at this aspect of air flow appraisal and the associated contaminant distribution patterns. This model was suited for a conflation study because among other things the original study included assessment of sensitivity of the design to:

- placement of inlets (side vents vs floor vents)
- use of common vs separate risers for each occupied floor
- effect of depth of room on ventilation, mixing and contaminant distribution
- full conditioning of the atrium vs opportunistic use of ambient air
- constant atrium temperatures vs use of night flushing
- different occupancy and gains levels

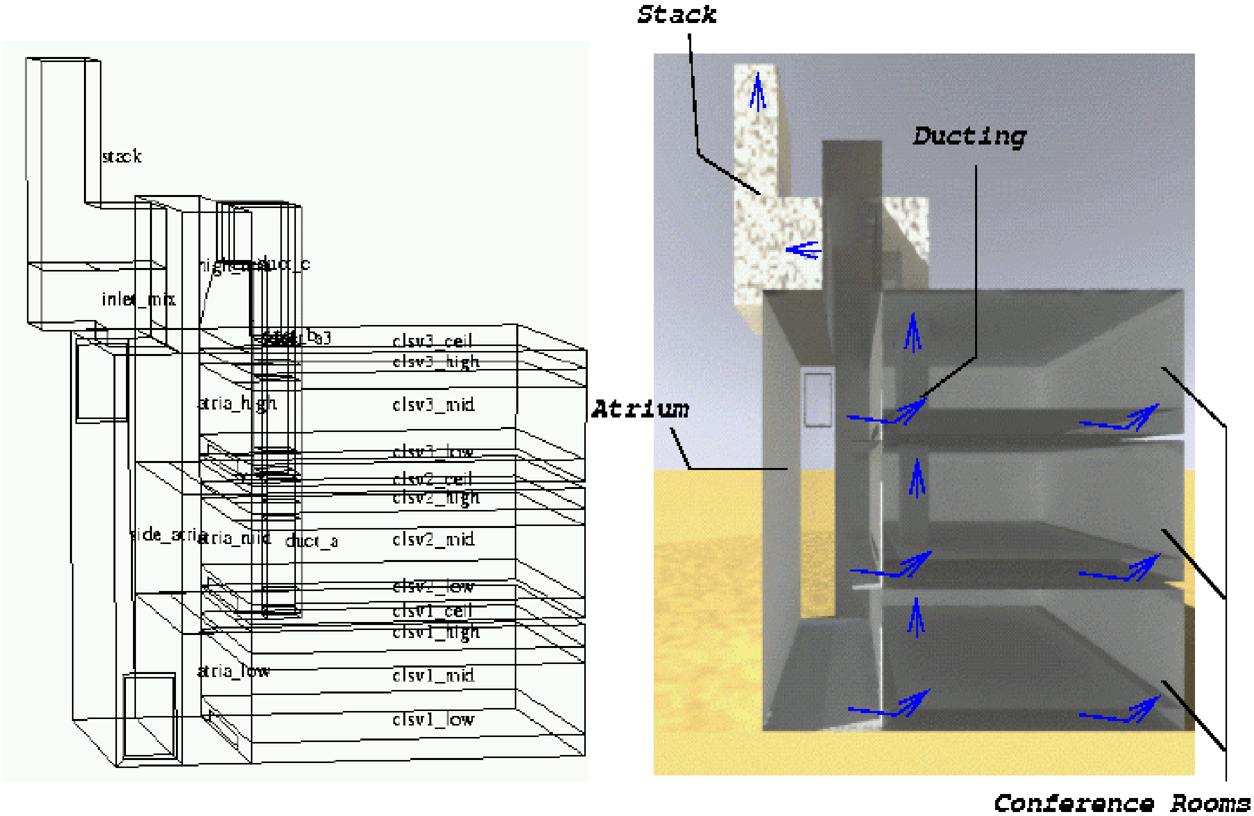

Figure 6.14a (left) ESP-r and figure 6.14b (right) RADIANCE images.
Blue arrows indicate intended air flows. (Adapted from Hand and Strachan (2002))

The dependence of air flow on internal temperature distributions, ambient temperature, geometry and configuration of non-adventitious openings made it important that a thermally coupled mass flow network be used and greater detail obtained from dynamic boundary condition specification used for detailed fluid flow analysis. The model is shown in figure 6.14 where the ESP-r model and RADIANCE (LBNL 2003) rendered images are shown.

The ground level conference room was defined to be represented by a CFD domain and the boundary conditions were defined from thermal simulation for the solid boundaries. The airflow boundaries were defined from the conflated CFD and mass flow network approach of chapter 5. In addition to enhanced resolution it was also hoped that more confidence would be put into the conflation approach by solving a complicated flow network. The flow network used for this model was based on the flow pattern as shown in figure 6.14b. Outside air is allowed to enter the atrium. This air then flows into each of the conference rooms through underfloor vents on both sides of the rooms. (Due to the lack of mechanical ventilation air flow rates to each level may be quite different because of the prevalence of buoyancy effects.) Once inside the rooms, the air is heated by occupancy and equipment gains and rises. Temperature stratification typically around 4-6^{0}C is established and flow rates of 0.4-0.55m^3/s are obtained. Outside occupied periods temperature stratification drops to ~1^{0}C and flow rate to ~0.2m^3/s. Air from the rooms exits the building via individual risers that lead into the stack and from there on to the outside.

6.4.2 Findings from Detailed Fluid Flow (CFD) Analysis

In the original study it had been troublesome to study detailed flow restrictions and patterns in the room when air

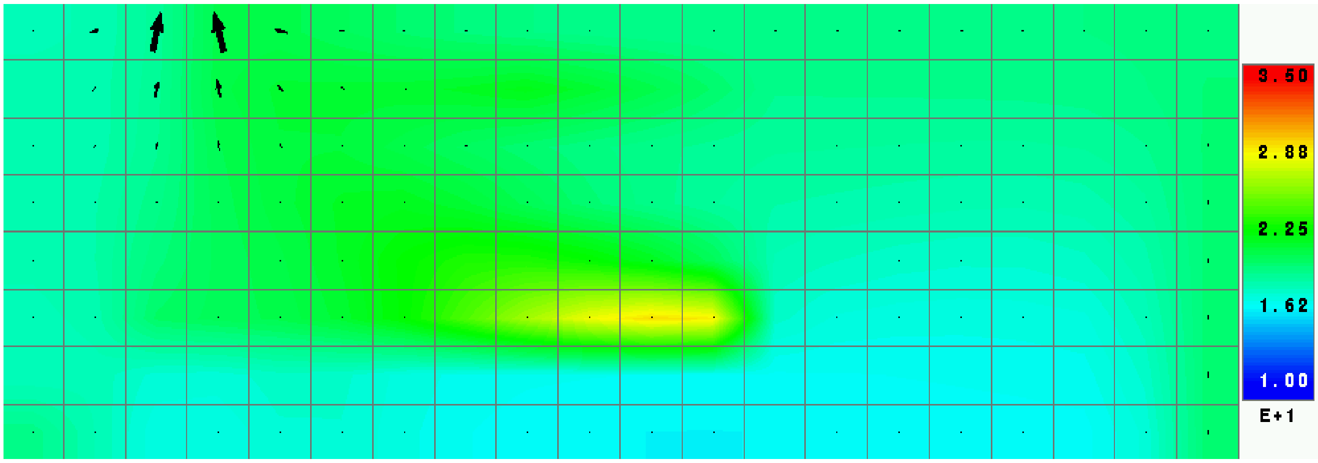

Figure 6.15 Temperature distribution in ground level room (atrium is to the left)

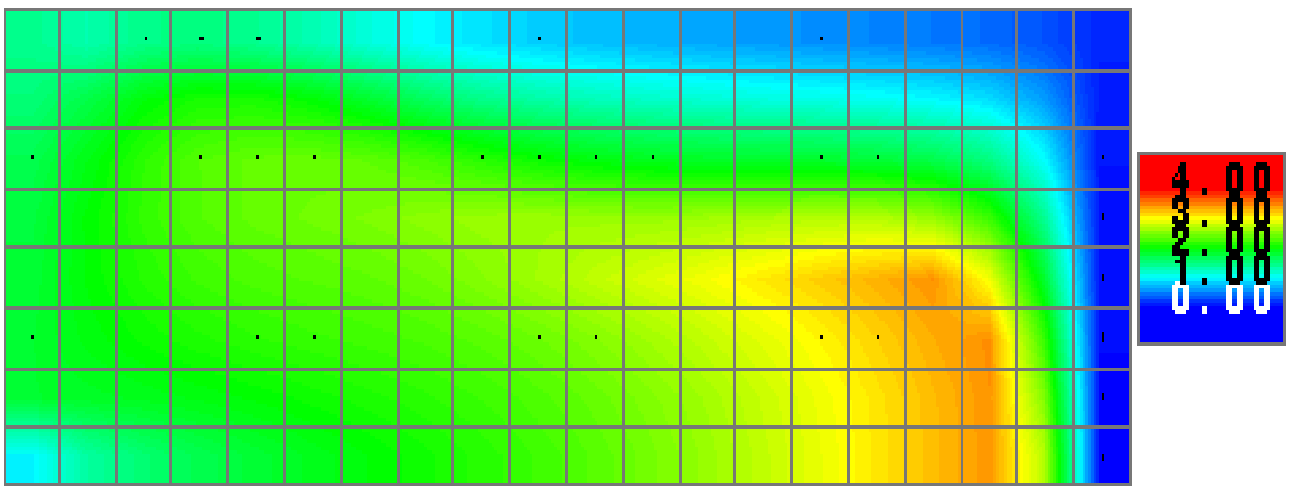

Figure 6.16 Local mean age of air distribution in ground level room

was introduced through the wall grills as compared to when it was introduced through the floor grills. Although bulk air movement predictions suggested that using floor grills to introduce air from the atrium raised floor level temperatures and provided slightly lower temperatures, this was demonstrated conclusively in the conflated CFD study (figure 6.15 shows temperature distribution for underfloor air inlet). Similarly it was difficult to study the effect of displacement of air by using wall mounted grills. With the low pressures and velocities that were typical of this project it was difficult to analyse contaminant concentration distributions and age of air. The solution came from the conflated simulation which suggested that depth of penetration is sufficient but the region between the two inlets at the near and far side of the room is poorly ventilated. Consequentially local mean age of air was highest in that part of the room (figure 6.16). Figure 6.15 shows results for one particular time in the morning (0906) using floor grills to provide fresh air. Complete results from one of

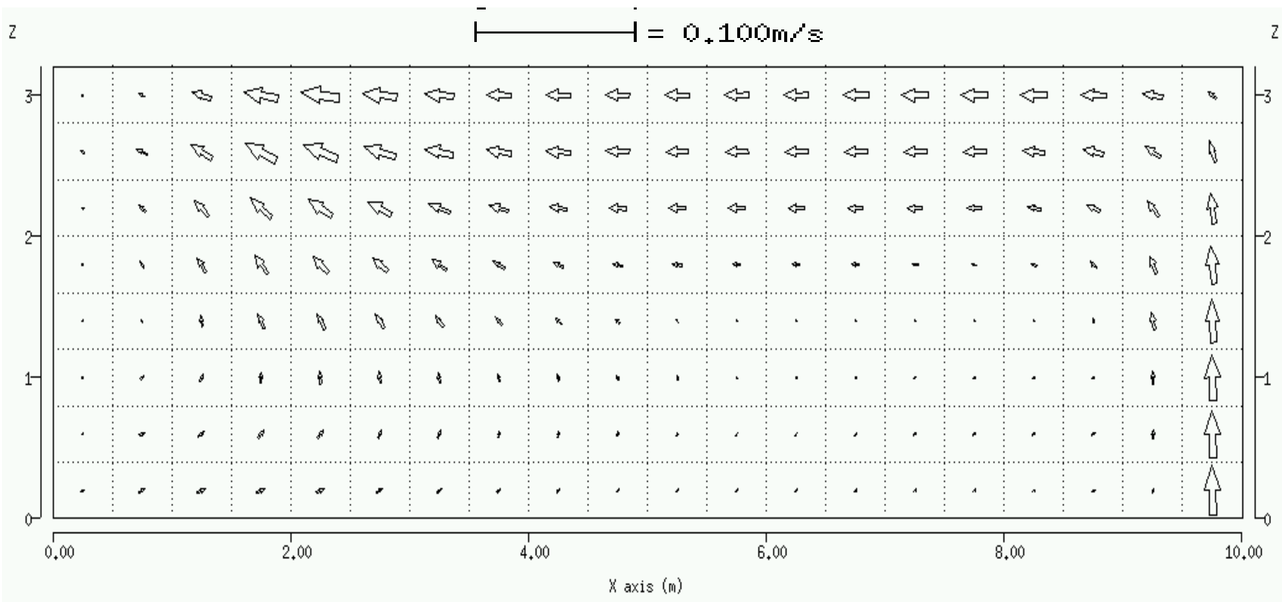

Figure 6.17 Air velocity distribution in ground level room

the CFD studies is given in appendix ATR. The figure shows that fresh and cool air is rising from the floor into a warmer surrounding. The air temperature before this snapshot was considerably higher but this high temperature drove the ventilation system to higher mass flow which resulted in cooling of this space. Temperatures after 0906 seemed to stabilise with a high temperature patch near equipment in the room.

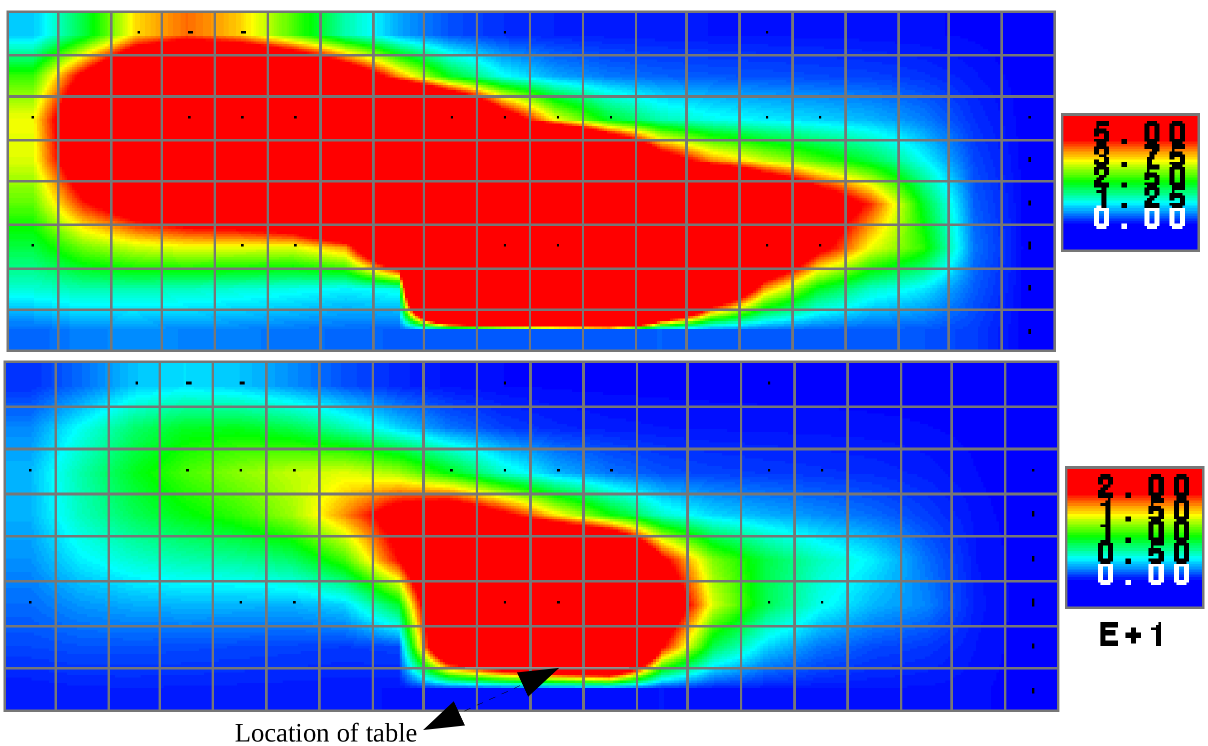

Figure 6.18 TVOC concentration for ground level room

Figure 6.16 shows CFD results for the computation of local mean age of air within the space and figure 6.17 shows the velocity of the rising air. Both results are for 1000 hours. It can be seen that the fresh air provided from the floor grills tends to accumulate towards the right wall in the image and there is some stratification between the two grills. It can now be recommended that if the grill design was changed such that the ventilation air initially flowed parallel to the floor, air freshness would be better distributed within the room.

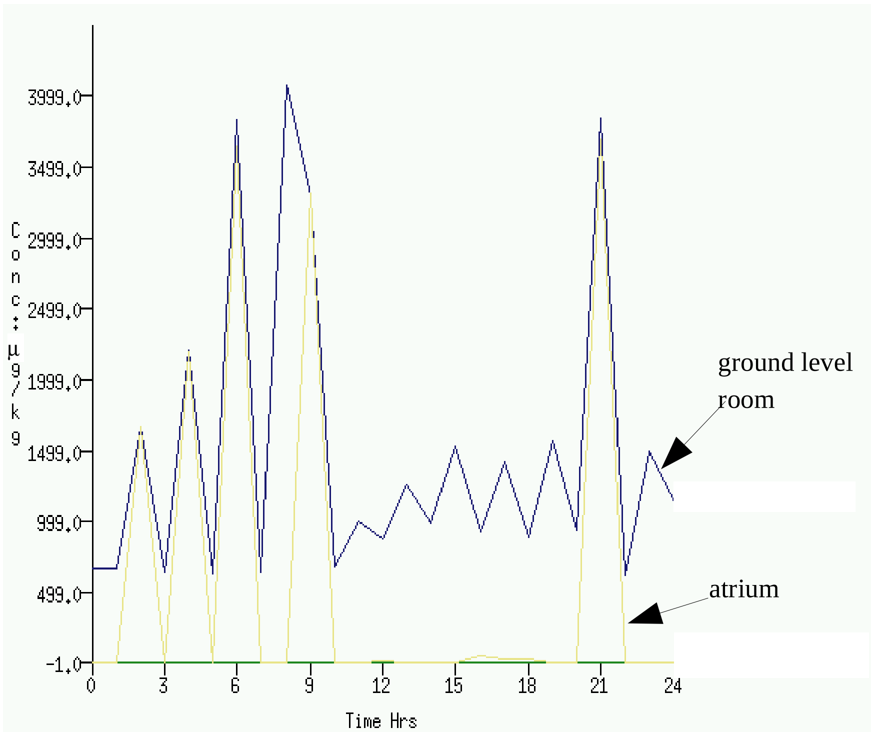

Figure 6.19 TVOC concentration in ground level room and atrium

Further simulations were then done to determine contaminant movement within the space. It was assumed that the room had a new table and this was a source of VOC in the space. One particular VOC was not considered but instead the total VOC (TVOC) concentration was simulated. It was assumed that the table was a constant source of TVOC with a strength of 20µg/m²s. The permissible level of TVOC was taken to be 200µg/m³ (Awbi 2003). The area of the table was 4m² and so the TVOC strength was 80µg/s.

TVOC concentration was tracked for this simulation. Figure 6.18 shows how TVOC concentration varied within the space at 1000. TVOC from the table top migrate towards the extract duct which is located towards the top right side of the room. Figure 6.18a shows the resolution of VOC concentrations (measured in mg/kg) in the less polluted regions of the room and figure 6.18b shows the resolution in more polluted regions. It can be seen that the region on the far right of the room has the best ventilation air even though it is furthest from the atrium whereas the region just near the exhaust duct is the most polluted after the table top itself.

It is also possible to look at TVOC levels in the atrium. So it is possible to study contaminants originating from a thermally and air flow network integrated CFD domain. The contaminant levels in the atrium can be seen in figure 6.19 that show that even though there is no source of TVOC in the atrium and the ambient concentration is zero there is some concentration of TVOC in the atrium. The effect of emissions from the table in the ground level room can similarly be investigated for the other rooms. This case study shows that using the developed approach it is possible to study contaminant transport and distribution at an inter-zone level using network mass flow and at an intra-zone level using CFD. The two being predicted within a fully integrated environment where it is ensured that solutions from the different domains are consistent with each other.

6.5 Summary

Three case studies have been presented and it is hoped that these illustrate the different aspects of the developed contaminant prediction facility. Some of the features such as filter efficiencies and chemical reactions have not been studied in the case studies but have nonetheless been tested within the validation section. More emphasis in the case studies has been placed on some of the more environmentally, academically and commercially important issues such as contaminant based control and micro-climatic appraisal of concentrations. In the first case study it was shown that energy efficient ventilation is best achieved when it is governed by contaminant based control to give good indoor air quality simultaneously. The second case study dealt with how a larger ventilation system is better suited to provide adequate air quality when design conditions are exceeded. The third case study showed how the conflated approach is better suited to study a problem delicately balanced between occupant gains and ventilation air supply. Contaminant prediction is also possible for other regions of the model such as the atrium. This is an example of how contaminants defined in the CFD domain would also be automatically defined (and modelled) in the mass flow network.

In the broader context it is believed that the developed approach has been adequately demonstrated to be applicable in a design context. The approach used is a fully integrated appraisal of contaminants taking into consideration air mass flow and building thermal processes. These provide the inputs to a CFD model and use two way conflation (CFD and network mass flow) and adaptive conflation (CFD and thermal simulation if required) where applicable. Such an approach can give more accurate answers to design questions than those obtained by using modules and software that address one or two of these issues without regard to other thermodynamic processes or overly simplify the processes by using scheduling of critical parameters.

6.6 References

ARBSSD. 2005. *Proposed Identification of Environmental Tobacco Smoke as a Toxic Air Contaminant.* California Environmental Protection Agency. Air Resources Board Stationary Source Division (ARBSSD), Air Quality Measure Branch.

Awbi, H. 2003. *Ventilation of Buildings 2nd Edition.* Spon Press, London and New York.

ESRU. 2005. *ESP-r System Version 10.10 Building Performance Simulation Environment.* University of Strathclyde, http://www.esru.strath.ac.uk Glasgow, UK.

Hand, J., Strachan, P. 2002. *Passive Displacement Ventilation Study, ESRU Report*. Private Communication.

Hensen, J. 1991. *On the thermal Interaction of Building Structure and Heating and Ventilation System.* PhD Thesis. University of Eindhoven, The Netherlands.

LBNL. 2003. *The RADIANCE 3.5 Synthetic Imaging System*. Building Technologies Department, Lawrence Berkeley National Laboratory, California, USA.

Liddament, M. 2004. *Why CO_2? Air Infiltration Review, Volume 18, No 1, December 1996*, World Wide Web Edition © Oscar Faber PLC on behalf of the International Energy Agency, 1996. http://www.aivc.org/air/18_1/mwlco2.html

Sundell, J. 1982. *Guidelines for NORDIC Buildings Regulations regarding Indoor Air Quality.* Environment International, Volume 8(1).

7 CONCLUSIONS AND RECOMMENDATIONS

7.1 Conclusions

The main objective of this research was to provide practitioners with the means to address contaminant behaviour within the indoor environment at an appropriate level of confidence. To achieve this, modelling techniques applied to simulation of contaminants have been advanced. This approach treats contaminant behaviour at a bulk flow level using network flow modelling and at a higher resolution using CFD. The two solution methods have been combined and integrated with thermal modelling so as to provide a solution that both domains arrive upon iteratively.

This objective has been realised within the developments to the ESP-r whole building performance simulation program. The first part of the research was to integrate contaminant modelling within thermally integrated mass flow network simulation. This was done by developing a contaminants network solution which is dependent upon a thermally coupled network mass flow algorithm. Thermal integration is important because, as was shown in chapter 4, air flow prediction can be seriously compromised if thermal effects are not considered. The importance of thermal coupling cannot be overstated because of the current trend for less mechanisation of HVAC and building ventilation systems and a move towards natural and mixed mode ventilation regimes. These types of ventilation systems inherently depend upon indoor – outdoor temperature differences and accurate modelling of this is normally outside the scope and capability of temperature scheduling as employed by most standalone network mass flow simulation software.

Furthermore, whereas previously thermal comfort and energy efficiency were the main focus, the science of air quality in terms of the chemical build up of indoor air pollutants seems to be gaining importance as the effects of 'traditional' and the more recent organic chemicals are coming to light. The theory for prediction of bulk flow of contaminants is well defined and tools exist for stand alone air flow and contaminant prediction. The first part of the research built upon currently implemented algorithms and included a facility for the dynamic uptake of contaminant mass flows from knowledge of bulk air flow using a thermally coupled mass flow network. This is described in chapter 3. Chapter 3 also details various capabilities and implementation details.

The basic contaminant mass flow prediction model was enhanced by the implementation of filter efficiencies for the various flow paths in the model, first order chemical reaction simulation and various source and sink algorithms for the contaminants. One particular source model is of interest in that it is a good example of inter-module information transfer. This is the personal CO_2 generation source model. Within any ESP-r model there exists information about occupants in terms of their metabolic rates for each thermal zone. The personal CO_2 generation source model infers CO_2 mass injection from the metabolic rates. Hence the user does not need to input CO_2 source strengths separately within the contaminants module. This is a typical example of how information given to a simulation tool in one context can be used in another and could be the way forward for development of easy to use and intelligent programs.

Typical air flow capacitances are much lower than building fabric thermal capacitances and changes in the air flow patterns have a more rapid effect on the performance of a building than changes in thermal boundary conditions. For this reason the contaminant module was designed to run at a much shorter time step than the building thermal module. This is considered in Chapter 3.

In view of the interest on mean age of air and the use of CO_2 concentration measurement as a means of ascertaining staleness of air, an air flow controller was developed. The controller controls air flow components (e.g. windows, doors, fans etc.) depending upon the concentration of CO_2 (or any other contaminant) in a room. Using this controller a study was done for a public house in England and it was seen that typical ventilation rates may not be adequate to dilute contaminants to an appreciable level and ventilation levels may need to be increased. This has implication on the thermal performance of buildings and the two opposing factors, adequate indoor air quality and adequate thermal performance, need to be considered together in order to determine optimal design functions and working conditions for ventilation plant.

The validity of ESP-r and its CFD module are well documented so only validation of the new developments is presented in this thesis. The simulation approach is validated in chapter 4 for network air flow and in chapter 5 for CFD. Three generally accepted validation methodologies are used i.e. analytical verification, inter-model comparison and empirical confirmation. Results obtained from the various test models simulated show good correlation between the different solutions. The analytical models used were, as expected, very simple and the results obtained corresponded almost exactly with simulated results. This was evident from less than 0.5% error between the two which was obtained for all configurations and was independent of the conformation of the problem. Further testing was done using time steps of different magnitudes and it was confirmed that the numerical solution approached the analytical solution as the time step was decreased. Inter-model validation efforts were also promising. The computer tool of choice was CONTAM which was used because of ease of procurement, good documentation and user friendliness. It was ensured that ESP-r and CONTAM models that were used corresponded exactly with each other by removing differences between climatic conditions, internal temperatures, air flow rates etc. Much of the ESP-r contaminants bulk prediction facility is based upon CONTAM theory. Therefore good agreement between the two was expected.

Comparison of empirical results with simulation was done to ASTM standards. The experimental building had also been modelled using COMIS and so it was also possible to compare ESP-r results against modelled results as well as empirical results. As in the inter-model comparisons similar airflow conditions were imposed using fans modelled as constant mass flow components. Other network components were also similar in dimensions and behaviour. ASTM criteria were seen to be satisfied most of the time. It seems that the ASTM standard used may be too stringent possibly because it is relatively recent and not extensively applied and therefore not much feedback has been given on it.

Furthermore the few applications for it that have been reported do not completely satisfy it either.

Micro-climatic appraisal of contaminant distribution is made possible by using computational fluid dynamics. CFD boundary conditions are defined dynamically from the contaminants network and not statically as in the traditional approach to the problem. This caters to the varying concentration loads over the course of a simulation and is considered to be more realistic. For the purpose of contaminant modelling the whole idea of network mass flow and CFD conflation has been revisited. The work done regarding this translates into a mutual solution approach so that, using the same boundary conditions, both network mass flow and CFD reach a solution that simultaneously satisfies both. This solution evolves within a thermally coupled environment in order to take into account all important interactions within the building. This is done by passing critical parameters between the two domains after each has converged. The purpose of this is to progressively improve the solution. Mutual convergence is assumed when the difference between the current values and the previously determined values diminishes below a predefined tolerance. A number of conflation methods and associated advantages and disadvantages were studied and one of these was chosen to be used as default. This method passes pressures from domain flow (*dfs*) to network flow (*mfs*) and passes mass flows the other way. This approach was validated using standalone CFD. Air flow within the standalone CFD model was governed by wind pressures as predicted from the ESP-r network mass flow model. Air flow within the conflated ESP-r was governed by network flow predicted mass flow rates which in turn were dependent upon wind conditions. Validation results were satisfactory with most results to within a tolerance of 5% or better.

The importance of including dynamic thermal simulation within the context of the contaminant prediction facility is also made evident in Chapter 6. A public house in England is modelled as a case study. It was seen that indoor CO_2 concentrations rose to more than allowable limits for parts of the building. This resulted in accumulation of contaminants and stale air causing low air quality and associated problems. The problem was alleviated by using a ventilation system designed with the knowledge of both thermal and contaminant behaviour. The second case study involving a manager's office showed how contaminant levels may become dangerously high when occupancy design conditions are exceeded and how contaminant based control can be used to improve air quality in such situations. Another interesting case study was that of the Canadian three storey building with an atrium. This building is exceptionally sensitive to thermal loading (primarily due to occupancy) and air flow is predominantly buoyancy driven. Due to this reason both stand alone CFD and stand alone network flow have their limitations for this type of study. The approach used was the conflated CFD and network flow approach (both being integrated within a thermal model).

There are issues relating to accessibility of the models and results. These form barriers to the further adoption of simulation in the building design profession. All the developments and research activities described in this thesis have been made accessible within the ESP-r simulation environment. Menu driven interfaces have been developed to support contaminant definition. The conflation mechanism is made semi-automatic with user interaction kept to essential minimum. When mapping from network flow to contaminants to computational fluid dynamics the user does not need to repeat inputs of data, the process has been made as effortless and user friendly as possible. Effort has also been made to make the contaminants file as human readable as possible. The contents of this file are described in appendix CTM. This is a quality control measure so that information held in this file can be scrutinised with a text editor as well as through the ESP-r interface.

The final outcome of the work allows a user to define contaminants and map the time varying inter-zonal contaminant distribution (using mass flow network) as well as intra-zonal distribution (using CFD). Results predicted from the solution methods are thermally coupled and fully conflated with each other. Contaminant behaviour is emulated in detail using time varying external concentrations, source and sink models, chemical reaction information and filtration of contaminant at various flow paths.

7.2 Recommendations for Future Work

Although this thesis has described the research leading to a prediction model for contaminant transport and distribution much work still remains to be done. Some recommendations are given here and these can be the subject of further research and development activities.

7.2.1 Theoretical Improvements for Particulate Matter

Particulate Matter (PM) behaves differently from gases on a microscopic scale although much of their macroscopic behaviour is analogous to gases. From a physical point of view PM cannot be approximated by the ideal gas theory. Hence there needs to be some means of addressing the different behaviour of PM which needs to include some of the typical PM characteristics (e.g. sorption, desorption, coagulation and other such characteristics expounded in chapter 1).

7.2.2 Transport Delays

The network air flow algorithm works in such a way that air is transported through it instantaneously. Whereas this restriction has no impact on bulk air flow predictions it does have implications for contaminant modelling. In studies of time dependent features such as the time for concentration to reach critical values in a room it is important to consider transport delays during modelling. The currently implemented approach does not allow for this and could give inaccurate results where time governance is important (e.g. in a long duct). Implementation of a model that takes into account time delays for transport of contaminants would be a useful feature within the contaminant prediction capability.

7.2.3 Contaminant and Related Information Procurement

It seems that information related to contaminants is not readily available. This problem is compounded with the fact that there are numerous indoor air pollutants many of which have been identified in very recent times and so it has not been possible to gather a lot of information about these. For example valuable information about chemical reaction parameters for numerous reactions could not be found or was difficult to find. Similarly, listings of emission strengths of various contaminants from different sources is not exhaustive. Although detailed source and sink models were readily available it was difficult to get physical parameters for most contaminants to fit those models. It can be appreciated that such a task is daunting but it would be convenient to collect all contaminants related information within a contaminants database which could be easily accessible for modelling (and other) purposes.

7.2.4 Filter Efficiencies

Presently, constant values for filter efficiencies are being used for the purposes of modelling filters. Even though different efficiencies can be assigned to the same network flow component for different contaminants, it would be more accurate to employ filter algorithms to model filter efficiencies. Thus taking into account filter efficiencies as a function of filter age, amount of contaminant residing on the filter, air velocity and other relevant parameters.

7.2.5 Temporal Definition of Ambient Concentration

ESP-r can presently associate 24 hourly values to ambient concentration of a contaminant. Where this is better than just one constant value it is not advisable to use for situations where ambient concentration of a contaminant varies appreciably during one hour. This could be true for certain very short lived gases and vapours. A facility that temporally defines ambient concentration of contaminants at a resolution comparable to the time step would be a desirable and useful feature in future versions of contaminant modelling.

7.2.6 Occupant Exposure

It would be interesting to be able to predict occupant exposure within buildings. This could be done by describing an exposure algorithm. Occupancy for different building parts and different times could again come from the general description of the building use.

7.2.7 Solution Optimisation

The air flow mass matrix as formulated in chapter 3 is sparse and there exist techniques to invert such matrices that are more efficient than the Gaussian elimination technique used currently. Some of the calculation methods such as iterative bi-conjugate gradient method, iterative successive over-relaxation method and the LU decomposition method have been reported by Dols and Walton (2002) and individual merits and demerits discussed. It would be interesting to carry out a similar exercise for the developed approach within ESP-r. Again it is a relatively easy task to do because there are some generic and specialist matrix inversion and decomposition methods within the program source code and these could be adapted for the task. However, a model with 28 nodes and 2 contaminants was tested and simulation time was not significantly increased compared to modelling without contaminants, so this is not considered to be important.

7.2.8 CFD Solution Process

A number of improvements could be made to enhance the stability and efficiency of the CFD solution process and to encourage convergence. Techniques such as residual tracking for converging / oscillating solutions and rewinding to initial conditions following the initiation of divergence could be introduced. Dynamic adjustment of under relaxation factors could be investigated for problematic simulations. More efficient equation solvers could be employed. Techniques that adapt governing parameters could be invoked to reduce number of iterations required to achieve convergence. It may be possible to develop algorithms that have the capacity to learn the relationships between solver parameters, convergence potential and rate to assist this.

7.3 References

Dols, W. S., Walton, G. N. 2002. *CONTAMW 2.0 User Manual*. *Multizone Airflow and Contaminant Transport Analysis Software.* NIST. USA.

APPENDIX AS1

Analytical Solution to Project Model Test 1

The following list of symbols is used with the same meanings in analytical solution appendices AS1 to AS3. When a symbol is subscripted by the word *air* the property is for air otherwise it is for contaminant e.g. m_2 would mean mass of contaminant in node 2 whereas m_{air2} would mean the air mass in node 2. For some of the models analysed only one node of interest was present and in those cases subscripts are dropped. Subscripts are also dropped if the property has the same numerical value for all nodes.

C	Concentration of contaminant (kg/kg)
C_{amb}	Ambient concentration of contaminant (kg/kg)
C_n	Concentration of contaminant at node *n* (kg/kg)
k	Decay or rate constant of contaminant (s^{-1})
k_n	Decay or rate constant of contaminant at node *n* (s^{-1})
m	Mass of contaminant (kg)
m_n	Mass of contaminant at node *n* (kg)
m_{air}	Mass of air (kg)
$m_{air\,n}$	Mass of air at node *n* (kg)
$\dot{m}_{air}$	Mass flow rate of air (kg/s)
$\dot{m}_{air\,n-p}$	Mass flow rate of air from node *n* to node *p* (kg/s)
R_i	Rate of increase of contaminant (kg/s)
R_o	Rate of decrease of contaminant (kg/s)
$R_{i\,n}$	Rate of increase of contaminant inside node *n* (kg/s)
$R_{o\,n}$	Rate of decrease of contaminant inside node *n* (kg/s)
t	Time (s)
τ	Time Constant (s) (reciprocal of *k*)
ΔT	Time step (s)

ϵ Error in mass (kg)

Additional symbols are defined where they are first introduced.

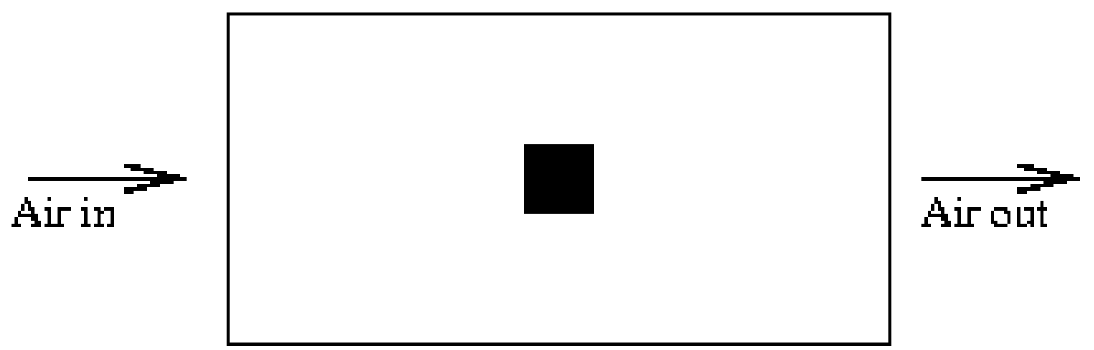

Fig AS1.1 Schematic for airflow for internal node in Test 1

Figure AS1.1 shows a schematic arrangement of air passage for the single zone test mode test1. The rate of change of contaminant inside the node is given by

$$\frac{dm}{dt}=R_i-R_o$$

The solution to the above equation is standard and is quoted below[12]:

$$m=C_{amb}m_{air}(1-e^{-kt}) \qquad \text{(AS 1-1)}$$

where k is the room contaminant mass decay constant given by $k=\frac{\dot{m}_{air}}{m_{air}}$

The reciprocal of k is the room time constant. Equation AS 1-1 can be written as shown below after dividing both sides by m_{air}, in order to get transient room contaminant concentration:

$$C=C_{amb}(1-e^{-kt}) \qquad \text{(AS 1-2)}$$

12 Differential Equations by Paul Blanchard, Robert L. Devaney, Glen R. Hall. Publication Details: Pacific Grove, CA : Brooks/Cole Pub. Co., © 1998

APPENDIX AS2

Analytical Solution to Project Model Test 2

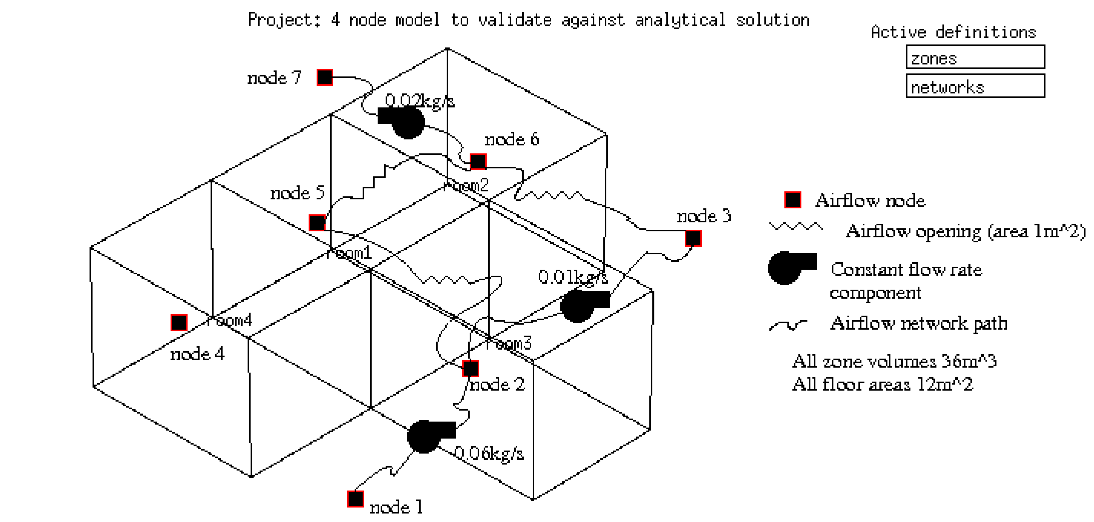

Figure AS 2.1 Airflow network for Test 2

The airflow network for Test2 is represented in figure AS 2.1. Solution for node 2 has the same form as that for the internal node in Test 1. Therefore equation AS 1-2 can be used with some modifications

$$C_2 = C_{amb}(1 - e^{-k_2 t}) \qquad \text{(AS 2-1)}$$

For node 5

$$\frac{dm_5}{dt} = R_{i5} - R_{o5} \qquad \text{(AS 2-2)}$$

Here according to the configuration of this particular model

$R_{i5} = \dot{m}_{air2-5} C_2$ and $R_{o5} = \frac{m_5}{m_{air5}} \dot{m}_{air2-5}$ [$\dot{m}_{air2-5}$ is the air flow rate from node 2 to 5]

Putting these and equation AS 2-1 in equation AS 2-2:

$$\frac{dm_5}{dt} = \dot{m}_{air2-5}\left[C_{amb}(1 - e^{-k_2 t})\right] - m_5 k_5 \qquad \text{(AS 2-3)}$$

Where $k_5 = \frac{\dot{m}_{air2-5}}{m_{air5}}$ [$\dot{m}_{air2-5}$ is the only flow into node 5]

This equation is of the form

$$\frac{dy}{dt}+Cy=A-Ae^{-Bt}$$ where

$$A=\dot{m}_{air2-5}C_{amb}\,,\ B=k_2\,,\ C=k_5\,,\ y=m_5$$

This equation can be put in the standard form[13]

$$\frac{dy}{dx}+yP(x)=f(x)$$ the solution for which is

$$y=e^{-\int P(x)dx}+e^{-\int P(x)dx}\int f(x)e^{-\int P(x)dx}dx$$

Hence the solution of equation AS 2-3 gives

$$m_5=De^{-k_5t}+C_{amb}m_{air5}-\dot{m}_{air2-5}C_{amb}t\,e^{-k_5t}+E \qquad \text{(AS 2-4)}$$

Where D and E are constants of integration. These can be found by putting the following initial and boundary conditions.

$$m_5|_{t=0}=0$$

$$m_5|_{t=\infty}=C_{amb}m_{air5}$$,and the limit

$$\lim_{t\to\infty}t\,e^{-t}=0$$

Solving for D and E

$$D=-C_{amb}m_{air5}\,,E=0$$

Furthermore from the configuration of the model as shown in figure AS2.1 it can be seen that the flow rates for nodes 2 and 5 are equal and because the rooms they represent have the same volume therefore $k_2=k_5=k$ (say). Therefore equation AS 2-3 reduces to

$$C_5=C_{amb}\left[1-e^{-k_5t}(1+kt)\right] \qquad \text{(AS 2-5)}$$

For node 6

$$\frac{dm_6}{dt}=R_{i6}-R_{o6}$$ where $R_{i6}=\dot{m}_{air5-6}C_5$ and $R_{o6}=\frac{m_6}{m_{air6}}\dot{m}_{air5-6}$

and by manipulation similar to that for node 5 it can be shown that

$$C_6=C_{amb}\left[1-e^{-k_6t}(1+kt+\frac{k^2t^2}{2})\right] \qquad \text{(AS 2-6)}$$

---

13 Differential Equations by Paul Blanchard, Robert L. Devaney, Glen R. Hall. Publication Details: Pacific Grove, CA : Brooks/Cole Pub. Co., © 1998

APPENDIX AS3

Error Estimation for Project Model Test 3

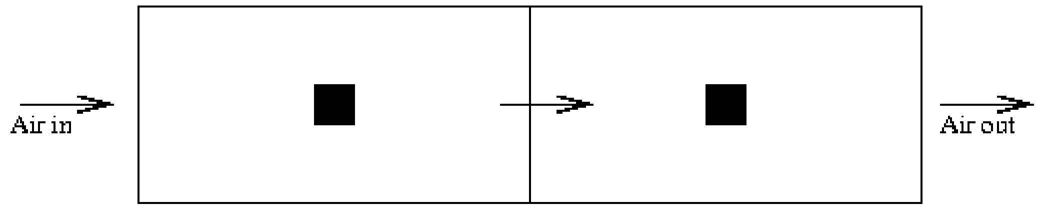

Figure AS 3.1 Schematic airflow network for Test3

Equations similar to the ones in appendices AS1 and AS2 can be shown to apply with no initial contaminant concentration. When this model is considered with non-zero initial concentration then it can be shown that if C_1^0 and C_2^0 represent the concentration at *t=0* for nodes *1* and *2* respectively, then

$$\frac{dm_1}{dt}=R_{i1}-R_{o1} \tag{AS 3-1}$$

Using a method similar to that in appendix AS1, it can be shown that the general solution for the above equation is given by

$$\frac{-1}{k}\ln(\dot{m}_{air}C_{amb}-m_1 k)=t+\ln D \tag{AS 3-2}$$

Here the subscripts for flow rate can be dropped because it is same for both the zones. In the above equation *D* is the constant of integration. The equation can be reduced to

$$m_1 k=\dot{m}_{air}C_{amb}-De^{-kt} \tag{AS 3-3}$$

The solution for Test 3 is now a matter of putting the initial conditions of contaminant concentration and solving to give

$$C_1=C_{amb}(1-e^{-k_1 t})+C_1^0 e^{-k_1 t} \tag{AS 3-4}$$

This equation gives contaminant concentration for zone 1. It can be multiplied with m_{air} to give contaminant mass for zone 1:

$$m_1=m_{air1}C_{amb}(1-e^{-k_1 t})+m_1^0 e^{-k_1 t} \tag{AS 3-5}$$

where m_1^0 is the initial mass of contaminant in node 1.

The matrix equation solved for Test 3 is quoted from chapter 3 (Equation 3-10)

$$(M-\zeta\,\Delta TK)X^*=MX+\Delta T\left[(1-\zeta)KX+V+G\right] \qquad \text{(AS 3-6)}$$

This equation can be reduced to algebraic form for zone 1, and for a Crank-Nicolson formulation (using * to represent future time row values) reduces to:

$$\left(m_1-\frac{1}{2}\Delta Tk_1\right)\frac{m_1^*}{m_{air1}}=m_1+\Delta T\left(\frac{1}{2}\dot{m}_{air}\frac{m_1}{m_{air1}}+\dot{m}_{air}C_{amb}\right) \qquad \text{(AS 3-7)}$$

Putting $m_1^*=m_1$ and $m_1=m_1^0$ and defining the room time constant $\tau=\frac{m_{air1}}{\dot{m}_{air}}$ this equation can be rearranged into

$$m_1=\left(1-\frac{\Delta T}{2\tau}\right)\left[1+\frac{\Delta T}{\tau}\left\{\frac{1}{2}+\frac{C_{amb}}{C_1^0}\right\}\right]m_1^0 \qquad \text{(AS 3-8)}$$

The error ϵ is defined as the difference of mass calculated from equation AS 3-5 and that calculated from equation AS 3-8. These equations were used to calculate error from the analytical results for validation test 3 as time step ΔT was varied. Results were similar to those obtained by actually running the program at different time steps and are shown in figure 4.6.

APPENDIX ATR

CFD results from Canadian Conference Building

The following images show how the temperature of the ground level room in the Canadian building with atrium of chapter 6 varied between 0800 and 1230. It was assumed that a meeting was being held in that room. The occupancy was 14 people from 0800 to 0900 which doubled after that. After 1200 it was assumed that there were no people in the room. Lighting was at 30W/m² and typical office equipment such as laptops etc. was also modelled. The images show how the temperature changed in the room at different times. It was seen that after an initial high temperature in the vicinity of people and equipment the temperature dropped and was maintained at this temperature until the occupied period. After which the temperature dropped to the ambient. The initial fall in temperature was a result of the ventilation system driving more air into the room because of increased temperature. The final fall in temperature was because the internal gains associated with people and equipment was not present after 1200. A detailed appraisal of the room was only possible by using the CFD and network mass flow conflated approach as developed in this thesis.

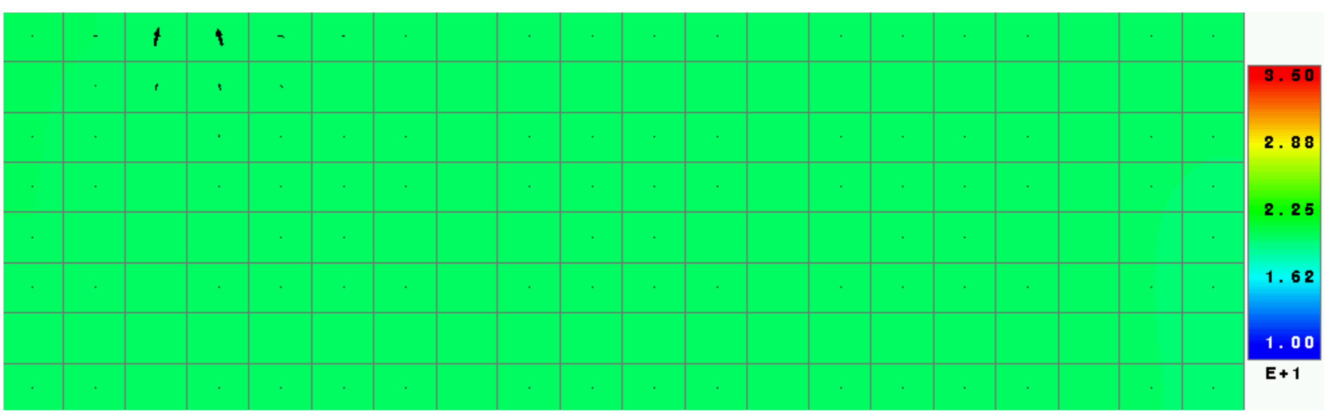

Figure ATR.1 Temperature at 0806

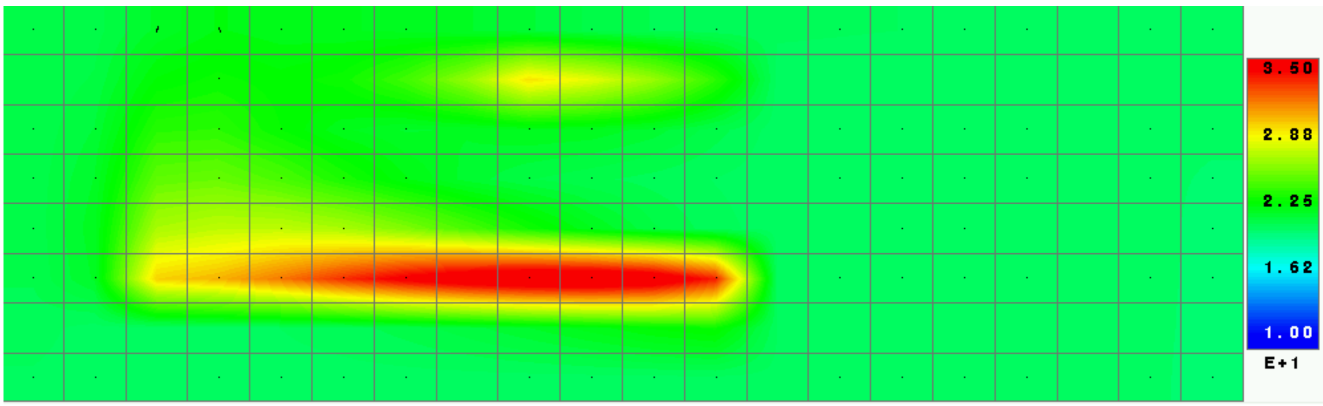

Figure ATR.2 Temperature at 0812

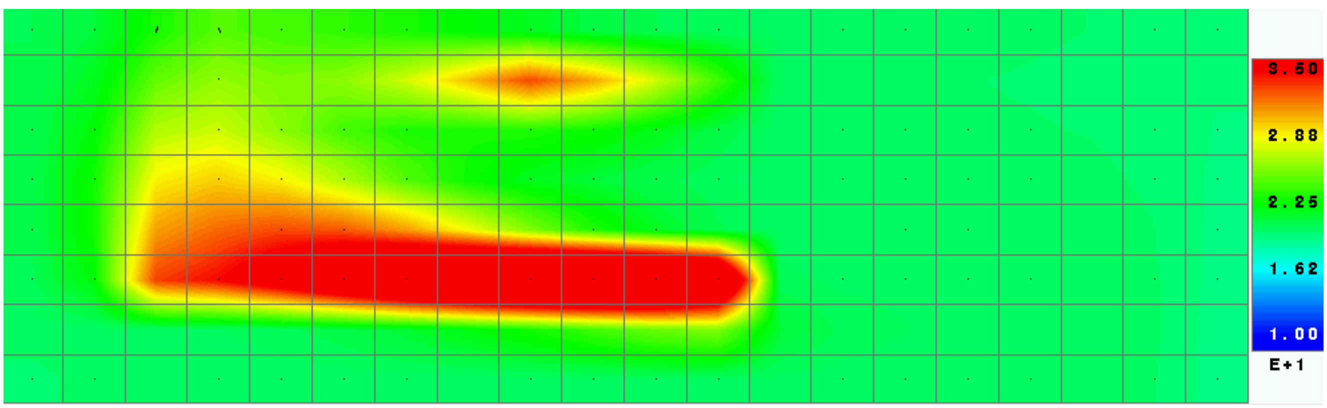

Figure ATR.3 Temperature at 0818

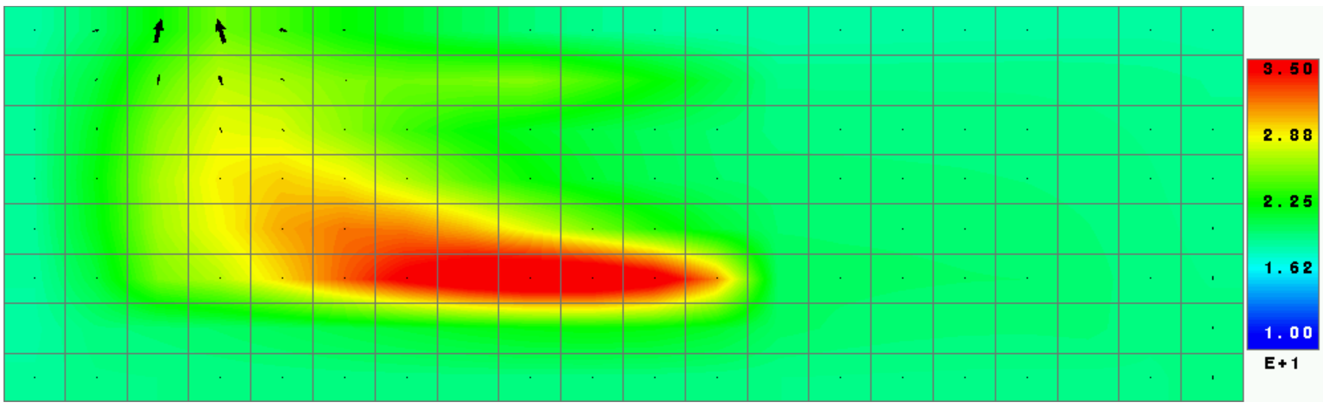

Figure ATR.4 Temperature at 0830

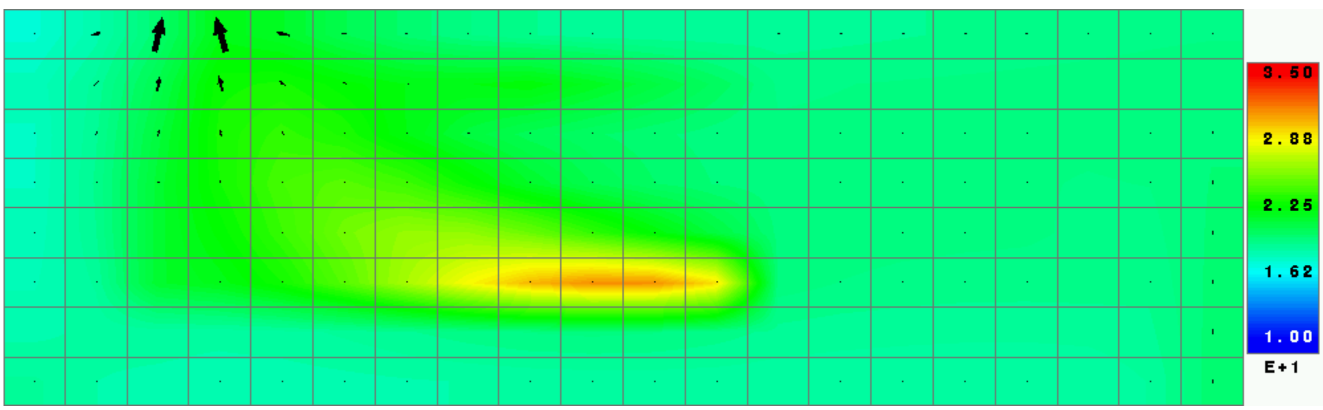

Figure ATR.5 Temperature at 0842

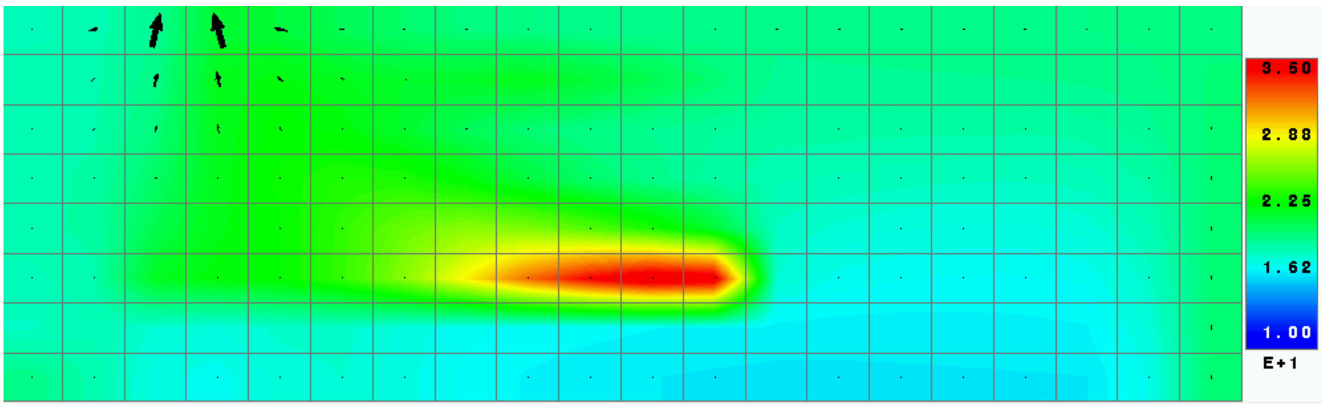

Figure ATR.6 Temperature at 0900

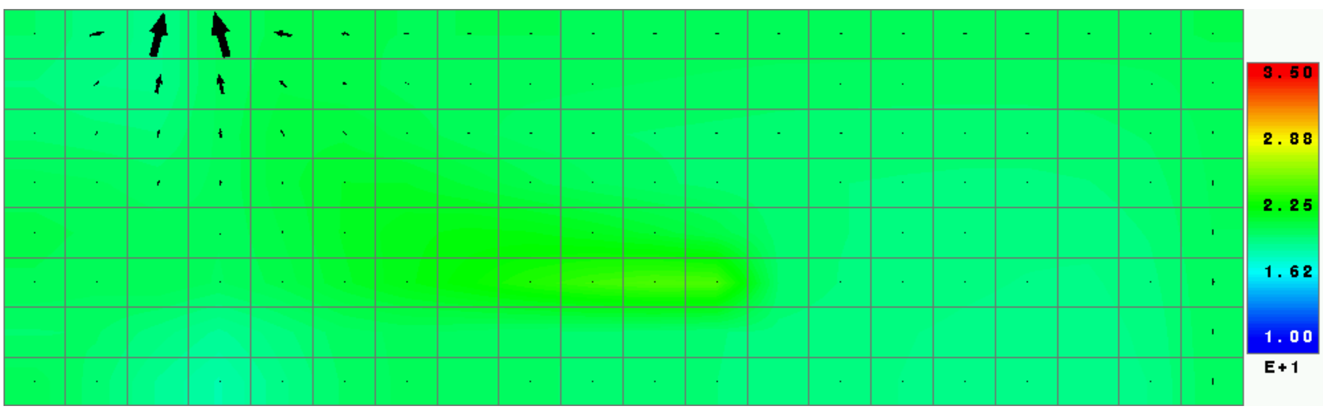

Figure ATR.7 Temperature at 1206

APPENDIX CAS

Comparison of COMIS and ESP-r with empirical

CAS.0 Introduction

This Appendix contains comparison of COMIS and ESP-r results against empirically collected data. The data was originally collected in an IEA exercise (Bossaer et al 1999). Modelling using COMIS was also done within the original research exercise. For validation and comparison purposes an ESP-r model was created details of which can be found in Chapter 4. Comparison of the two software against empirical measurements was based on ASTM D5157-97 which is a guide for statistical evaluation of indoor air quality models.

CAS.1 Results

Table CAS.1 is an extension to table 4.5 and gives a complete list of results obtained from the comparison. The different ASTM criteria are as follows

Parameter	***Synopsis***	***Prescribed Range***
r	Correlation coefficient	0.9 to 1.0 or -0.9 to -1.0
a	Intercept on vertical axis of line of regression	25% or less of average measured concentration
b	Slope of line of regression	Between 0.75 and 1.25
NMSE	Normalized mean square error	0.25 or lower
FB	Normalized or fractional bias	0.25 or lower
FS	Similar index of bias based on variance	0.5 or lower

(Below) Table CAS.1 ASTM D5157 criteria for different zones of the modelled flat

	BED1		***Prescribed results***
	COMIS	***ESP-r***	
r	0.97	0.98	0.9 or more
a	-96	-53	±52 or less
b	1.51	1.08	0.75 to 1.25
NMSE	0.83	0.24	0.25 or less
FB	0.05	-0.20	0.25 or less
FS	0.20	0.09	0.5 or less

	BED2		***Prescribed results***
	COMIS	***ESP-r***	
r	0.99	0.99	0.9 or more
a	29	-120	±108 or less
b	1.29	1.25	0.75 to 1.25
NMSE	0.14	0.21	0.25 or less
FB	0.31	-0.03	0.25 or less
FS	0.53	0.46	0.5 or less
	LIVING		***Prescribed results***
	COMIS	***ESP-r***	
r	0.98	1.00	0.9 or more
a	-145	-38	±43 or less
b	1.64	1.07	0.75 to 1.25
NMSE	0.16	0.16	0.25 or less
FB	-0.21	-0.16	0.25 or less
FS	0.02	0.32	0.5 or less
	HALL		***Prescribed results***
	COMIS	***ESP-r***	
r	0.97	1.00	0.9 or more
a	-24	-80	±57 or less
b	1.42	1.17	0.75 to 1.25
NMSE	0.20	0.46	0.25 or less
FB	0.27	-0.20	0.25 or less
FS	0.87	0.42	0.5 or less
	KITCHEN		***Prescribed results***
	COMIS	***ESP-r***	
r	0.97	1.00	0.9 or more
a	-145	-25	±41 or less
b	1.63	1.04	0.75 to 1.25
NMSE	0.28	0.26	0.25 or less
FB	-0.28	-0.12	0.25 or less
FS	-0.06	0.29	0.5 or less

	BATH		*Prescribed results*
	COMIS	***ESP-r***	
r	0.99	0.99	0.9 or more
a	-22	-64	±56 or less
b	1.41	1.13	0.75 to 1.25
NMSE	0.15	0.47	0.25 or less
FB	0.27	-0.18	0.25 or less
FS	0.71	0.34	0.5 or less
	TOILET		***Prescribed results***
	COMIS	***ESP-r***	
r	0.99	0.99	0.9 or more
a	-13	-31	±56 or less
b	1.40	1.05	0.75 to 1.25
NMSE	0.15	0.30	0.25 or less
FB	0.29	-0.09	0.25 or less
FS	0.74	0.17	0.5 or less

CAS.1 References

Bossaer A., Ducarme D., Wouters P., Vandaele L. 1999. *An example of model evaluation by experimental comparison: pollutant spread in an apartment.* Energy and Buildings 30, 1999.

APPENDIX CCS

Comparison of Conflated and Standalone CFD

CCS.0 Introduction

Complete results from the validation study using mass flow network and CFD conflation approach within ESP-r and standalone CFD using FLUENT (FLUENT 2003) are given in table CCS.1. Mass flow rates for the three air flow paths are given for hourly intervals for 9^{th} June. The climate file used is the an example year for Kew, UK (ESRU 2005). The external temperatures though are modified and set to the constant value of 20^0C in order to equalise the ESP-r model and the FLUENT model. Both models consisted of 1080 hexahedral grid cells measuring 0.3 by 0.35 by 0.4 m each. A standard $k-\epsilon$ two equation turbulence model with Yuan et al (1993) wall functions was used in both software. Similar initialisations of the various solution parameters (velocity, momentum, pressure, kinetic energy etc.) were done and segregated solvers were used. Under relaxation factors and solution convergence criteria were also kept invariant as far as possible. The SIMPLEC (van Doormal and Raithby 1984) pressure correction method was used in both models. The walls of the CFD domain were modelled as thermally specified boundary condition. These were described using the Dirichlet boundary specification and a constant temperature of 20^0C was used in both cases. The difference between the two CFD models was the mass flow type boundary conditions: the FLUENT model had constant pressure type boundary conditions with the pressures calculated for the room configuration and defined from hourly values of wind direction and speed from the ESP-r climate file. Using treatment for correcting wind pressure for terrain, wall orientation, vertical height and effect of surrounding buildings described in Clarke (2001) the pressures were estimated for the FLUENT boundary conditions. Mass flow boundary conditions on the other hand were described as velocity type boundary conditions for the ESP-r conflated mass flow network and CFD solver. This was necessary because of the conflation requirement of mass flow definition from the mass flow network. A complete description of the model used is given in section 5.4.

Table CCS.1 (below) Mass flow rates predicted for model described in Section 5.3 using thermally coupled mass flow network (mfs), thermally coupled mass flow network and CFD solver using pressure feed back conflation (mfs-dfs) and standalone CFD solver (FLUENT)

Time	***Mass flow rates (kg/s)***	***mfs***	***mfs-dfs***	***FLUENT***
0030	west_out -> CFD_room	-0.0717	-0.0717	-0.0733
	top_out -> CFD_room	0.1461	0.1461	0.1317
	CFD_room -> east_out	0.0717	0.0717	0.0743

Time	*Mass flow rates (kg/s)*	*mfs*	*mfs-dfs*	*FLUENT*
0130	west_out -> CFD_room	0.0227	0.0230	0.0220
	top_out -> CFD_room	0.0225	0.0232	0.0220
	CFD_room -> east_out	0.0493	0.0495	0.0497
0230	west_out -> CFD_room	0.0070	0.0070	0.0073
	top_out -> CFD_room	0.0082	0.0082	0.0074
	CFD_room -> east_out	0.0153	0.0154	0.0140
0330	west_out -> CFD_room	0.0132	0.0133	0.0122
	top_out -> CFD_room	0.0421	0.0419	0.0415
	CFD_room -> east_out	0.0522	0.0515	0.0531
0430	west_out -> CFD_room	0.0752	0.0770	0.0764
	top_out -> CFD_room	-0.0075	-0.0072	-0.0068
	CFD_room -> east_out	-0.0583	-0.0588	-0.0601
0530	west_out -> CFD_room	0.0117	0.0119	0.0112
	top_out -> CFD_room	-0.0047	-0.0047	-0.0050
	CFD_room -> east_out	0.0100	0.0104	0.0108
0630	west_out -> CFD_room	0.0280	0.0279	0.0264
	top_out -> CFD_room	-0.0183	-0.0183	-0.0172
	CFD_room -> east_out	0.0096	0.0111	0.0097
0730	west_out -> CFD_room	0.0070	0.0069	0.0071
	top_out -> CFD_room	0.0081	0.0081	0.0077
	CFD_room -> east_out	0.0151	0.0152	0.0140
0830	west_out -> CFD_room	0.0069	0.0069	0.0071
	top_out -> CFD_room	0.0081	0.0081	0.0075
	CFD_room -> east_out	0.0151	0.0151	0.0140
0930	west_out -> CFD_room	0.0768	0.0767	0.0776
	top_out -> CFD_room	-0.0572	-0.0575	-0.0570
	CFD_room -> east_out	0.0190	0.0191	0.0204
1030	west_out -> CFD_room	-0.0209	-0.0209	-0.0218
	top_out -> CFD_room	0.0829	0.0829	0.0811
	CFD_room -> east_out	0.0618	0.0619	0.0595

Time	*Mass flow rates (kg/s)*	*mfs*	*mfs-dfs*	*FLUENT*
1130	west_out -> CFD_room	0.0340	0.0339	0.0357
	top_out -> CFD_room	0.0397	0.0396	0.0378
	CFD_room -> east_out	0.0748	0.0750	0.0764
1230	west_out -> CFD_room	0.1346	0.1345	0.1310
	top_out -> CFD_room	-0.1007	-0.1009	-0.1030
	CFD_room -> east_out	0.0335	0.0337	0.0325
1330	west_out -> CFD_room	0.1234	0.1233	0.1306
	top_out -> CFD_room	-0.0386	-0.0390	-0.0374
	CFD_room -> east_out	0.0846	0.0846	0.0875
1430	west_out -> CFD_room	0.1233	0.1233	0.1307
	top_out -> CFD_room	-0.0377	-0.0381	-0.0380
	CFD_room -> east_out	0.0842	0.0842	0.0829
1530	west_out -> CFD_room	0.1234	0.1233	0.1239
	top_out -> CFD_room	-0.0387	-0.0391	-0.0378
	CFD_room -> east_out	0.0846	0.0846	0.0836
1630	west_out -> CFD_room	0.1811	0.1811	0.1851
	top_out -> CFD_room	-0.1355	-0.1356	-0.1441
	CFD_room -> east_out	0.0448	0.0450	0.0470
1730	west_out -> CFD_room	0.1708	0.1707	0.1760
	top_out -> CFD_room	-0.0536	-0.0534	-0.0560
	CFD_room -> east_out	0.1171	0.1172	0.1122
1830	west_out -> CFD_room	0.0752	0.0752	0.0779
	top_out -> CFD_room	0.0878	0.0877	0.0812
	CFD_room -> east_out	0.1645	0.1645	0.1648
1930	west_out -> CFD_room	0.0592	0.0591	0.0580
	top_out -> CFD_room	0.0700	0.0689	0.6460
	CFD_room -> east_out	0.1300	0.1300	0.1282
2030	west_out -> CFD_room	0.0485	0.0484	0.0455
	top_out -> CFD_room	0.0565	0.0564	0.0546
	CFD_room -> east_out	0.1050	0.1050	0.1082

Time	*Mass flow rates (kg/s)*	*mfs*	*mfs-dfs*	*FLUENT*
2130	west_out -> CFD_room	0.0416	0.0416	0.0429
	top_out -> CFD_room	0.0486	0.0484	0.0455
	CFD_room -> east_out	0.0902	0.0903	0.0929
2230	west_out -> CFD_room	0.0347	0.0347	0.0358
	top_out -> CFD_room	0.0405	0.0405	0.0400
	CFD_room -> east_out	0.0754	0.0756	0.0769
2330	west_out -> CFD_room	0.0534	0.0534	0.0503
	top_out -> CFD_room	0.0623	0.0622	0.0605
	CFD_room -> east_out	0.1158	0.1158	0.1211

CCS.1 References

Clarke, J. 2001. *Energy Simulation in Building Design*. Butterworth-Heinemann, Oxford, UK. ISBN 0-7506-5082-6

ESRU 2005. *ESP-r Standard Distribution*. http://www.esru.strath.ac.uk

FLUENT. 2003. *FLUENT User's Manual*. Fluent Inc. http://www.fluent.com

van Doormal, J. P., Raithby, G. D. 1984. *Enhancements of the SIMPLE Method for Predicting Incompressible Fluid Flows.* Numerical Heat Transfer, Volume 7, pp. 147-163.

Yuan, X., Moser, A., Suter, P. 1993. *Wall Functions for Numerical Simulation of Turbulent Natural Convection Along Vertical Plates.* International Journal of Heat and Mass Transfer, 36 (18).

APPENDIX CTM

Sample ESP-r Contaminants Network File

CTM.1 File:

```
#ESP-r contaminant file
../nets/win100.afn #fluid flow file for which this file is defined
SECTION_1
#no. of contaminants,time steps/hour
    2     12
SECTION_2
#name and ambient concentrations (kg/kg) of contaminants
#(max conc, min conc, hour at which max conc occurs)
#followed by no. of source/sink models and model no.s
carb_diox
0.000480  0.000480  0.000480  0.000480  0.000480  0.000480  0.000480  0.000480  0.000480
 0.000480 0.000480 0.000480
0.000480  0.000480  0.000480  0.000480  0.000480  0.000480  0.000480  0.000480  0.000480
 0.000480 0.000480 0.000480
  4  1  2  3  4
VOC
0.000050  0.000050  0.000050  0.000050  0.000050  0.000050  0.000050  0.000050  0.000050
 0.000045 0.000045 0.000045
0.000045  0.000045  0.000045  0.000045  0.000045  0.000045  0.000045  0.000050  0.000050
 0.000050 0.000050 0.000050
  2  5  6
SECTION_3
#first order rate constants (if defined)
carb_diox          VOC                0.350E-013
VOC                carb_diox         -0.350E-013
SECTION_4
#node based information for contaminant
carb_diox
#node,node no.,initial conc.
toilet         1   0.000480
lounge         2   0.000480
conser         3   0.000480
conser_sun     4   0.000480
bar           12   0.000480
public        13   0.000480
VOC
#node,node no.,initial conc.
toilet         1  -1.000000
lounge         2  -1.000000
conser         3  -1.000000
conser_sun     4  -1.000000
bar           12  -1.000000
public        13  -1.000000
SECTION_5
#component based information
#all filter efficiencies other than nought are listed
   4 #no. of components having efficiency other than nought
```

```
#contaminant name and no.,component,filter efficiency
carb_diox     1 supply068    .15
carb_diox     1 supply056    .15
VOC           2 supply068    .10
VOC           2 supply056    .10
SECTION_6
#source and sink models
#number of sources and sinks
  6
# Source/sink name, number, type, supplementary data items
src_lounge     1  6 -1.00000 0.00 0.00 0.00 0.00 0.00 0.00 0.00 0.00
src_conser     2  6 -1.00000 0.00 0.00 0.00 0.00 0.00 0.00 0.00 0.00
src_c_sun      3  6 -1.00000 0.00 0.00 0.00 0.00 0.00 0.00 0.00 0.00
src_public     4  6 -1.00000 0.00 0.00 0.00 0.00 0.00 0.00 0.00 0.00
VOC_const      5  1 0.01
VOC_var        6  2 0.01 0.00006000
SECTION_7
#source/sink linkage with nodes
#node,node no.,no. of source/sink models linked,model no
toilet         1   0
lounge         2   1 1
conser         3   1 2
conser_sun     4   1 3
bar           12   1 5
public        13   2 4 6
```

CTM.2 Explanation:

The contaminants network file begins with the name and relative path of the associated mass flow network file. This is a quality control feature so that just one flow network file is referenced by one contaminants file and if the flow network file is changed then a warning is issued to the user to update the contaminants file accordingly.

Section 1 holds the number of contaminants in the model and the simulation time step for the contaminants. It is possible that the building side is run at a longer time step because building side thermal capacitances are higher than contaminant side concentration capacitances. In such a circumstance when contaminants are being solved more often than building thermal and mass flow, the same information from building and mass flow side is passed every time to the contaminant model. This is justifiable in that this is the best possible information available to the simulation engine at run time. For a better appraisal time step at which building simulation is run should be lowered to be the same as time step for contaminant simulation.

Section 2 holds information specific to the contaminant. Contaminant names are held here (carb_diox and VOC for this example) and so are 24 hourly values for ambient concentration. As in this example for carb_diox, it is possible that the ambient concentration is constant in which case the same value is held, for VOC different values are held for different times of day. Any source / sink models linked to a particular contaminant are also listed here. For the example shown there are four source / sink models (numbered 1 through 4) linked to contaminant carb_diox and two models (model number 5 and 6) linked to contaminant VOC.

Section 3 holds first order chemical reaction rate constants for the reaction between any two contaminants. A hypothetical reaction has been defined. By default a negative reaction rate is also defined for the reverse reaction. This facility corresponds to loss of mass of the reacting species to form the new contaminant.

Section 4 holds node based information. Air flow nodes are assumed to be previously defined in the air flow network file. The node name and number from the air flow network file are repeated here to make the file less terse. Initial concentrations of the contaminants in various nodes are then written out. If the initial concentration is to be taken from time varying ambient concentration (as is the case for VOC) a flag (-1) is displayed. The simulator is programmed to take initial concentration equal to the ambient at that time.

Section 5 holds component based information i.e. filter efficiency. The contaminant name is displayed first to show that a particular efficiency is to be used for that contaminant (different efficiencies can be defined for different contaminants for the same component). The contaminant number follows, followed by the name of the component and then the filter efficiency. Once again because of the deep coupling of the air flow and contaminant networks it is important that the contaminant network file holds the name of the air flow network file because the nodes and components that are defined in the air flow network file should be exactly the same in the contaminants network file.

Section 6 holds source and sink information. It holds the total number of sources and sinks in the model and supplementary data items. The number of supplementary data items is different for different source and sink algorithms. In the example shown src_lounge is the first source / sink. It is a type 6 source (personal CO_2 emission model) and may need up to 9 data items. The first item is -1 indicating that emission rates are to be taken from metabolic rates of occupants as defined in the zones operations files and for such a case the other 8 items for this source are not required.

Section 7 holds information about source / sink linkage with nodes. This information indicates the node with which the source / sink is associated. Node names and numbers are given followed by the total number of sources / sinks associated with that node. Hence there is no source / sink in node toilet and there are two sources in node public (models number 4 and 6).

APPENDIX TSN

Calculation of Schmidt Number

In order to make CFD contaminant prediction generic within ESP-r a dimensionless constant (the Schmidt number) needs to be specified for each contaminant. Previously this number had to be calculated external to the program, It has now been made possible to include calculation of the Schmidt number within ESP-r. The parameters required for this are molecular mass(g/mol), critical volume(cm^3/mol), critical temperature(K) and boiling point(K). This appendix shows how the Schmidt number can be calculated from these parameters.

TSN.0 Variable list for calculation of Schmidt Number:

A-G	=	constants (dimensionless)
D	=	diffusivity / diffusion coefficient of a binary mixture of species A & B also called mass diffusivity (m^2/s)
M	=	relative molecular weight (g/mol)
n	=	number of moles
P	=	absolute pressure (Pa)
R	=	universal gas constant (8.314 J/kg K)
r	=	distance between molecules (Å)
Sc	=	Schmidt number (Ratio of kinematic viscosity & molecular diffusivity)
T	=	absolute temperature (K)
T*	=	dimensionless temperature (dimensionless)
T_b	=	normal boiling point (at 1atm pressure) (K)
T_c	=	Critical temperature (K)
v	=	Volume of gas (m^3)
V_b	=	liquid molar volume at normal boiling point (cm^3/mol)
V_c	=	Critical volume (cm^3/mol)
Ω_D	=	collision integral for mass diffusion (dimensionless)
Ω_μ	=	collision integral for viscosity (dimensionless)
ε	=	characteristic energy of interaction (J)
κ	=	Boltzmann constant (1.38×10^{-23} J/K)
μ	=	absolute viscosity (1Poise=0.1Ns/m^2)

ρ	=	density (kg/m^3)
σ	=	characteristic length or collision diameter (Å)
υ	=	kinematic viscosity (m^2/s)
ψ	=	intermolecular potential energy function (J)

NOTE: Other subscripts used include A and B denoting the constituents of a binary gas mixture.

TSN.1 Calculation of Schmidt Number:

The Schmidt number can be calculated using the following relationship:

$$Sc = \frac{\nu}{D} \tag{TSN-1}$$

The Schmidt number can be computed by using known values of kinematic viscosity and mass diffusivity.

Kinematic and absolute viscosity are related by the formula

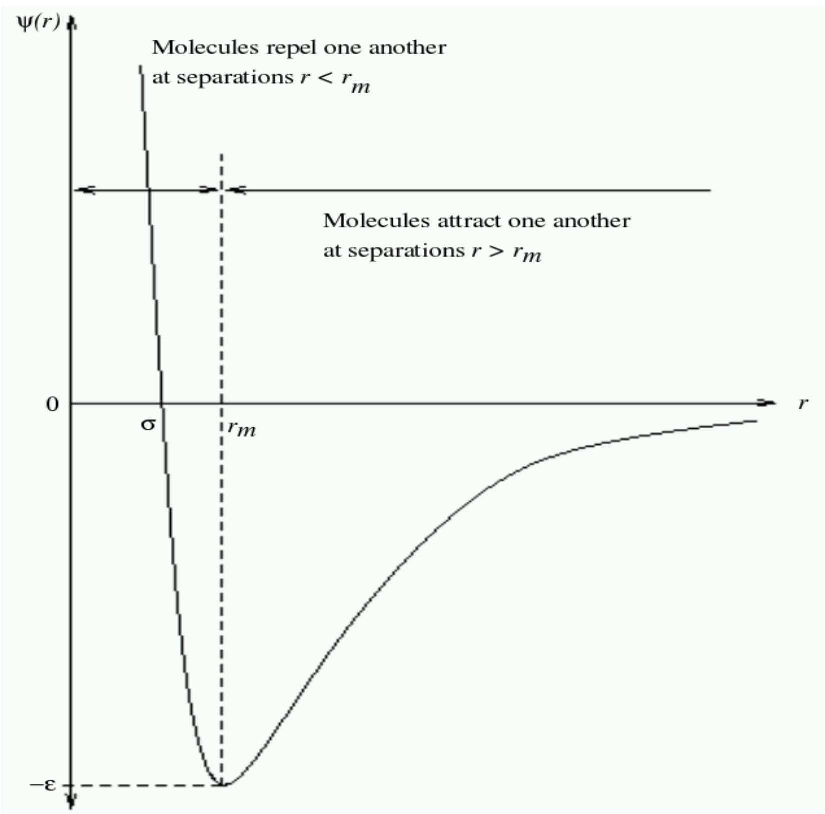

Figure TSN.1 Intermolecular Potential Function

$$\nu = \frac{\mu}{\rho} \tag{TSN-2}$$

If absolute viscosity and density are known then kinematic viscosity can be found.

TSN.2 Calculation of Absolute Viscosity:

Absolute viscosity for any gas can be computed by the method given by Reid et al (1987) and Bird et al (1960) which has been adopted below. Absolute viscosity can be calculated by the formula given by Chapman and Enskog:

$$\mu = 26.69 \times 10^{-6} \frac{\sqrt{MT}}{\sigma^2 \Omega_\mu} \tag{TSN-3}$$

In order to use this equation the collision diameter σ and collision integral Ω_μ must be found. In the derivation of equation (TSN-3) Ω_μ is obtained as a complex function of a dimensionless temperature T*. The functionality depends upon the intermolecular potential chosen. As shown in figure TSN-1 let ψ(*r*) be the potential energy of interaction between two molecules separated by distance *r*. At large separations ψ(*r*) is negative; the molecules attract each other[14]. At small distances repulsion occurs. The minimum in the ψ(*r*) versus *r* curve is termed the characteristic energy ε. For any potential curve the dimensionless temperature T* is related to ε as follows

$$T^* = \frac{K}{\epsilon} T \tag{TSN-4}$$

Referring again to figure S-1 the collision diameter σ is defined as the separation distance when ψ(*r*) = 0. The exact form of the function ψ(*r*) is not known but a fairly good empirical function is the Lennard-Jones potential equation

$$\psi(r) = 4\epsilon \left[\left(\frac{\sigma}{r} \right)^{12} - \left(\frac{\sigma}{r} \right)^{6} \right] \tag{TSN-5}$$

With this relationship for the intermolecular potential (Neufeld et al 1972) have proposed the following empirical equation for Ω_μ

$$\Omega_\mu = A(T^*)^{-B} + Ce^{-DT^*} + Ee^{-FT^*} \tag{TSN-6}$$

Where

$$A = 1.16145, B = 0.14874, C = 0.52487, D = 0.77320, E = 2.16178 \text{ and } F = 2.43787$$

Hence it is possible to calculate the viscosity of a gas given σ and ε/K. These values can be found in literature for many substances. A generic approach to finding these parameters is given by (Chung et al 1984) who have developed a method to calculate σ and ε/K from properties at the critical point namely T_c and V_c.

ε/K is calculated from

$$\frac{\epsilon}{K} = \frac{T_c}{1.2593} \tag{TSN-7}$$

14 The negative gradient of ψ(*r*) is the force of interaction.

and σ from

$$\sigma = 0.809\, V_c^{1/3} \tag{TSN-8}$$

Hence viscosity of a gas can be calculated by knowing either σ and ε/K or T_c and V_c

TSN.3 Calculation of Mass Diffusivity:

The mass diffusivity of a binary gas mixture is defined by Reid et al (1987)

$$D_{AB} = 0.00266 \frac{T^{3/2}}{PM_{AB}^{1/2}\sigma_{AB}^{2}\Omega_D} \tag{TSN-9}$$

Where

$$\sigma_{AB} = \frac{\sigma_A + \sigma_B}{2} \tag{TSN-10}$$

$$M_{AB} = 2\left(\frac{1}{M_A} + \frac{1}{M_B}\right)^{-1} \tag{TSN-11}$$

The value of Ω_D with the Lennard-Jones potential equation is given by Hirschfelder et al (1954)

$$\Omega_D = \frac{A}{T^{*B}} + \frac{C}{e^{DT^*}} + \frac{E}{e^{FT^*}} + \frac{G}{e^{HT^*}} \tag{TSN-12}$$

Where

$A = 1.06036, B = 0.15610, C = 0.19300, D = 0.47635, E = 1.03587, F = 1.52996,$

$G = 1.76474$ and $H = 3.89411$

The dimensionless temperature for a binary mixture is defined by

$$T^* = \frac{K}{\epsilon_{AB}} T \tag{TSN-13}$$

Where

$$\epsilon_{AB} = \left(\epsilon_A \epsilon_B\right)^{1/2} \tag{TSN-14}$$

The approach used is similar to Wilke and Lee (1955) who have rewritten equation (TSN-9) as

$$D_{AB} = \frac{[3.03 - (0.98/M_{AB}^{1/2})](10^{-3})T^{3/2}}{PM_{AB}^{1/2}\sigma_{AB}^{2}\Omega_D} \tag{TSN-15}$$

In conjunction with this equation, equation (TSN-10) and (TSN-11) are used to find the scaling parameters σ_{AB} and ε_{AB} /K where for each component the following relations are used

$$\sigma = 1.18\, V_b^{1/3} \qquad \text{(TSN-16)}$$

Reid et al (1987 pp 53) have given an empirical relationship giving V_b in terms of V_c

$$V_b = 0.285\, V_c^{1.048} \qquad \text{(TSN-17)}$$

this equation along with equation equation (TSN-16) can be solved to give

$$\sigma = 0.777\, V_c^{0.349} \qquad \text{(TSN-18)}$$

which contrasts with equation (TSN-8). Furthermore

$$\frac{\epsilon}{K} = 1.15\, T_b \qquad \text{(TSN-19)}$$

Hence it is possible to find diffusivity for any binary gas mixture given the normal (i.e. at atmospheric pressure) boiling point and critical molar volume.

TSN.4 Calculation of Density:

The density of any gas can be calculated from the standard gas equation

$$Pv = nRT \qquad \text{(TSN-20)}$$

Density can be expressed as

$$\rho = \frac{m}{v} = \frac{nM}{v} \qquad \text{(TSN-21)}$$

After a little rearranging of the above two equations density is given by

$$\rho = \frac{100\, PM}{RT} \qquad \text{(TSN-22)}$$

By knowing absolute viscosity and density, kinematic viscosity can be calculated using equation (TSN-2). Schmidt number can then be calculated using equation (TSN-1).

TSN.5 Turbulent Schmidt Number:

The calculation of turbulent Schmidt number is not straightforward and most of the time it has to be calculated from wind tunnel or CFD analyses. For most room ventilation purposes it can be taken to be equal to the turbulent Prandtl number (Gadgil et al 2000). This has a range 1.5 to 2.5 times the ordinary Schmidt number. Within the present implementation the turbulent Schmidt number is taken to be two times the ordinary Schmidt number although facility exists to change this.

TSN.6 References:

Bird, R. B., Stewart, W. E., Lightfoot, E. N. 1960. *Transport Phenomena*. Wiley International Edition. John Wiley and Sons, Inc.

Chung, T. H., Lee, L. L., Starling, K. E. 1984. *Applications of Kinetic Gas Theories and Multi-parameter correlation for Prediction of Dilute Gas Viscosity and Thermal Conductivity.* Industrial and Engineering Chemistry Fundamentals, 23:(1).

Gadgil, A. J., Finlayson, E. U., Fischer, M. L., Price, P. N., Thatcher, T. L., Craig, M. J., Hong, K. H., Housman, J., Schwalbe, C. A., Wilson, D., Wood, J. E., Sextro, R. G. 2000. *Pollutant Transport and Dispersion in Large Indoor Spaces: A Status Report for the Large Space Effort of the Interiors Project.* Environmental Energy Technologies Division, Indoor Environment Department. LBNL, Berkeley, USA.

Hirschfelder, J. O., Curtiss, C. F., Bird, R. B. 1954. *Molecular Theory of Gases and Liquids*. Wiley, New York.

Lide, D. R. 2003-2004 *CRC Handbook of Chemistry and Physics. 84th Edition.* CRC Press. ISBN 0-8493-0484-9

Neufeld, P. D., Janzen, A. R., Aziz, R. A. 1972. *Empirical Equations to Calculate 16 of the Transport Collision Integrals* $\Omega^{(l,s)^*}$ *for the Lennard-Jones (12-6) Potential.* Journal of Chemical Physics, 57:(1100).

Reid, R. C., Prausnitz, J. M., Poling, B. E. 1987. *The Properties of Gases and Liquids 4th Edition*. McGraw-Hill Inc. ISBN 0-07-051799-1

Wilke, C. R., Lee, C. Y. 1955. *Estimation of Diffusion Coefficients for Gases and Vapours.* Industrial and Engineering Chemistry, 47:1253 (1955)

GLOSSARY

Adaptive Conflation; Conflation in which one or both modules / programs that are being conflated are configured at run time adapting the algorithms or solution methods based on results.

Adsorption: See section 1.1.3

Air Flow Component: For the network mass flow model as implemented within ESP-r an air flow component is the connecting member for different air flow nodes. For example the air flow component between a room and a corridor may be a door.

Air Flow Connection: For the network mass flow model as implemented within ESP-r an air flow connection comprises the air flow component and air flow nodes that it connects.

Air Flow Node: For the network mass flow model as implemented within ESP-r an air flow node is a definite volume of air connected to other nodes via components.

Airflow Simulation: See flow network model.

Bi-directional Flow: An air flow component may be capable of allowing flow in both directions at the same time. A real world example could be a door in a warm room with colder climatic conditions. The door allows cold air to enter at the base and warmer air to exit from the top part of the door.

bld: ESP-r's building thermal module and solver.

bps: ESP-r's building, mass flow, CFD and plant integrated module and solver.

Building Energy Simulation BES: Simulation of the thermal domain using a computation tool (e.g. ESP-r) in the text this term does not refer to thermal loads due to ventilation air that is calculated using dynamic air flow simulation but may include scheduled and other simplistic ventilation schemes.

Building Related Illness BRI: Ailments associated with sick building syndrome such as headache, eye, nose or throat irritation, dizziness, nausea, fatigue.

Coagulation: See section 1.1.10

COMIS: A stand alone air flow network model based tool (Feustel 1997)

Computational Fluid Dynamics CFD: The process of solution of a fluid field using suitable algorithms to solve the equations of motion (Euler equations for inviscid and Navier-Stokes equations for viscid fluids).

Conflation: The process of integrating two (or more) solution algorithms / programs.

Consistency: Consistent numerical schemes produce systems of algebraic equations which can be demonstrated to be equivalent to the original governing equations as the discretization intervals for parameters of the numerical solution are reduced towards zero.

CONTAM: A stand alone air flow network model based tool. (Dols and Walton 2002)

Control: In building simulation, control normally refers to the process of imposing actuation of building plant components based on some sensed condition.

Convergence: The property of a numerical method to produce a solution which approaches the exact solution as the discretization parameters of the numerical solution are reduced towards zero.

Decipol: It is the pollution caused by one Olf ventilated by 10litre/sec of unpolluted air.

Deposition: See section 1.1.8

Desorption: See section 1.1.3

dfs: ESP-r's CFD module and solver.

Diffusion: See section 1.1.4

Discretization: The resolution of a parameter (variable) that is to be represented by a difference equation. The term is also used to refer to the division of a CFD domain into grids or cells.

Emission: See section 1.1.6

Environmental Tobacco Smoke ETS: The term is attributed to the chemicals given off during tobacco smoking that are generally distributed in the indoor environment.

ESP-r: A whole building performance simulation tool that is capable of running its different modules using internal coupling. (ESRU 2005)

External Coupling: Solution of two different equation set-ups (usually defining different physical processes within different executables) with some run time information exchange between the two set-ups. The two equation sets usually define different but linked physical phenomena.

Filtration: See section 1.1.2

Flow Domain: The aspect of building behaviour that has to do with air flow between the different parts of the building. In a more generic sense the term can also be applied to fluid flow between different parts of an energy system.

Flow Network Model: A modelling technique that assumes fluid flow through a network of nodes connected by components using a solution method similar to Newton-Raphson iteration. The technique allows air flow through buildings to be predicted.

FLUENT: A computational fluid dynamics software package (FLUENT 2003)

Identity Change: See section 1.1.5

Indoor Air Quality IAQ: The term deals with the content of interior air that could affect health and comfort of building occupants. IAQ can be compromised by microbial contaminants, chemicals, allergens and any mass or energy stress that can induce health effects.

Internal Coupling: Combination of two different solution techniques (usually defining different physical processes) within one executable, the solution techniques are usually solved separate from each other.

Jacobian: This is the matrix of all first order partial derivatives of a vector values function. Its importance lies in the fact that it represents the best linear approximation to a differentiable function at a given point.

Long Wave Radiation Exchange: Radiation exchange between elements of, for example, a room that are at relatively low temperatures as compared with short wave radiation that is produced by hot bodies e.g. the sun.

MERV: Maximum efficiency reporting value for a filter. It is a number from 1 to 16. The higher the number the more efficient the filter is at removing particles.

mfs: ESP-r's mass flow module and solver.

Multiple Chemical Sensitivity MCS: A chronic, recurring disease caused by a person's inability to tolerate an environmental chemical or class of foreign chemicals.

Olf: It is a unit to measure the scent of emission of people and objects. One olf is defined as the scent emission of an average person i.e. a sitting adult who takes 0.7 baths a day and whose skin has a total area of 1.8 square metres.

Partition Coefficient: The partition coefficient describes the relationship between the contaminant in the gas phase and concentration within a solid i.e. how easily does the contaminant diffuse from a solid surface as compared to the gas phase. It is a material property and obtained experimentally.

Personal Cloud Effect: The effect of personal movements indoors that usually contribute to greater exposure than would be present if the person was not moving.

Phase Change: See section 1.1.11

Plant: In building simulation terms, plant generally refers to HVAC and / or other environmental control systems associated with a building.

Positive Definite: A matrix A is positive definite if for all non-zero column vectors x $x^TAx>0$. A positive definite matrix is always non-singular.

prj: ESP-r's Project Manager – the model definition and editing module. Most of ESP-r is run using prj.

RADIANCE: A suite of computer tools for performing lighting simulation (LBNL 2003)

Radioactive Decay: See section 1.1.9

Response Factor Method: A mathematical technique that takes in account time varying responses of different functions usually using their Fourier series elements.

Resuspension: See section 1.1.7

Seasonal Affective Disorder SAD: Also known as winter depression this is an affective or mood disorder. Sufferers experience depression symptoms in the winter.

Sick Building Syndrome SBS: A combination of ailments associated with an individual's place of work or residence. In addition to other sources, indoor air pollution has been ascribed as a major contributor.

Smog: It is a kind of air pollution, usually resulting from the mixture of smoke and fog.

Stability: A stable numerical technique converges to the correct solution after the onset of errors due to round off errors etc. and may not exhibit wild oscillations and / or divergence.

Thermal Domain: The term generally encompasses all thermal processes (e.g. fabric conduction, surface convection, radiation exchanges) occurring within the modelled energy system.

Tight Building Syndrome TBS: A condition similar to sick building syndrome, but where most of the contribution to bad indoor air quality is because of lack of sufficient ventilation.

Transport: See section 1.1.1

Two way conflation: Conflation in which there is some form of feed back between the two modules or programs that are being conflated.

Zone: In building simulation terms a zone normally refers to a segregated space within a building (usually a room, part of a room or several rooms) that is assumed to have similar temperature, pressure and other physical properties.

GLO.1 References

Dols W. S., Walton G. N. 2002. *CONTAMW 2.0 User Manual Multizone Airflow and Contaminant Transport Analysis Software*. Building and Fire Research Laboratory. National Institute of Standards and Technology. U.S. Department of Commerce

ESRU. 2005. *The ESP-r System for Building Energy Simulation. User Guide Version 10 Series.* http://www.esru.strath.ac.uk

Feustel H., Smith B. V. 1997. *COMIS 3.0 – User's Guide*. Lawrence Berkeley National Laboratory. U. S.

FLUENT. 2003. *FLUENT User's Manual.* Fluent Inc. http://www.fluent.com

LBNL. 2003. *The RADIANCE 3.5 Synthetic Imaging System*. Building Technologies Department, Lawrence Berkeley National Laboratory, California, USA.